Trypanosoma cruzi: Where is it? Does it ever sleep? Why is a sterile outcome rarely achieved?

Alexander Ian Ward

November 2020

Thesis submitted to the University of London in fulfilment of the requirements for the degree of Doctor of Philosophy of the University of London

Supervisors (joint): Professor John M. Kelly and Dr Martin C. Taylor

Department of Infection Biology
London School of Hygiene and Tropical Medicine
University of London
United Kingdom

Funded by the Medical Research Council, UK

Declaration

I, Alexander Ian Ward, confirm that the work presented in this thesis is my own. Where information has been derived from other sources, I confirm that this has been indicated in the thesis.

Signed:

Alexander Ian Ward
January, 2021

Preface

This thesis is written as a research paper style thesis with adequate background information about each of the primary research papers and review to allow the reader to appreciate how the publications fit within the broader field of *Trypanosoma cruzi* research. This has been done in accordance with the research degree regulations of LSHTM 2020/2021. The 1st chapter provides a broad overview of *T. cruzi* epidemiology, clinical presentation of Chagas disease and the current status of drug and vaccine development. Chapter 2 is a joint-first author review published in *Parasite Immunology*, covering the most up-to-date thinking on how the parasite interacts with the host immune system at all infection stages. Chapter 3 provides an overview of the development of the parasite reporter strains used in the subsequent publications. Chapter 4 consists of work towards identifying the chronic stage localisation, both tissue and cellular, of this parasitic infection and is presented as a published first-author manuscript in *mBio*. Chapter 5 covers work, the aim of which was to identify a potential quiescent/dormant stage of the parasite life-cycle, presented as a first-author manuscript in *Open Biology*. Chapter 6 is based on work aimed at establishing why *T. cruzi* is able to persist in hosts that have generated a robust and well characterised immunological response. This chapter is presented as a first-author submitted manuscript. All published and submitted manuscripts are presented in this thesis after a chapter introduction, that will aid the reader in viewing the work within the context of the literature, and a summary that allows me to give my views and thoughts on the subjects outside of the word limits required by the publication process. Manuscripts are incorporated into this thesis as word documents. Figures and accompanying legends appear at the end of each text. The reader may find the published and submitted versions on-line if embedded figures within the main text are preferred.

Papers published or submitted during PhD studies:

1. Alexander I. Ward, Michael D. Lewis, Martin C. Taylor and John M. Kelly (submitted) Incomplete homing of protective T-cells facilitates *Trypanosoma cruzi* persistence in the mouse colon.
2. Alexander I. Ward, Francisco Olmo, Richard L. Atherton, Martin Taylor and John M. Kelly (2020) Trypanosoma cruzi amastigotes have a reduced rate of replication in the chronic stage. *Open Biology*. **10**, e200261. (Featured on front cover of issue).
3. Alexander I. Ward, Michael D. Lewis, Archie Khan, Conor J. McCann, Amanda F. Francisco, Shiromani Jayawardhana, Martin C. Taylor, John M. Kelly (2020) *in vivo* analysis of *Trypanosoma cruzi* persistence foci at single cell resolution. *mBio*. **11**, e01242-20.
4. Martin C. Taylor, Alexander I. Ward*, Francisco Olmo, Shiromani Jayawardhana, Amanda F. Francisco, Michael D. Lewis, John M. Kelly (2020) Intracellular DNA replication and differentiation of *Trypanosoma cruzi* is asynchronous within individual host cells *in vivo* at all stages of infection. *PLOS Neglected Tropical Diseases*. **14**, e0008007 *joint 1st author.
5. Damian Perez-Mazliah, Alexander I. Ward*, Michael D. Lewis (2020) Host-parasite dynamics in Chagas disease from systemic to hyper-local scales. *Parasite Immunology*. **2020**, e12786 *joint 1st author. (Featured on front cover of issue).
6. Martin C. Taylor, Alexander I. Ward, Francisco Olmo, Amanda F. Francisco, Shiromani Jayawardhana, Fernanda C. Costa, Michael D. Lewis and John M. Kelly (2020) Bioluminescent:fluorescent *Trypanosoma cruzi* reporter strains as tools to explore Chagas disease pathogenesis and drug activity. *Current Pharmaceutical Design* (in press).
7. Martin C. Taylor, Amanda F. Francisco, Shiromani Jayawardhana, Gurdip S. Mann, Alexander I. Ward, Francisco Olmo, Michael D. Lewis, John M. Kelly (2019) Exploiting genetically modified dual-reporter strains to monitor experimental *Trypanosoma cruzi* infections and host-parasite interactions. Karina Gomez and Carlos Andres Buscaglia (eds.), *T. cruzi* Infection: Methods and Protocols, Methods in Molecular Biology. **1955**, 147-163.

Abstract

Trypanosoma cruzi infection is responsible for Chagas disease, a condition that causes unacceptable morbidity and mortality throughout poorer populations of Latin America. Due to international migration, Chagas disease cases and asymptomatic *T. cruzi* infections are becoming a public health concern globally. At present there is no practical vaccine and the front-line drugs are rarely used due to low levels of diagnostic testing, long treatment regimens, unacceptable side effects and low efficacy.

Here, we have employed state-of-the-art bioluminescent-fluorescent parasite reporter cell lines in experimental murine models to investigate **parasite localisation in the chronic stage of infection, to assess if the recently reported dormant life-cycle stage can be demonstrated *in vivo*, and to better understand why infections are almost always life-long.**

In both the BALB/c and C3H/HeN murine models the gastrointestinal tract (GIT), specifically the colon and stomach, were confirmed to be primary sites of parasite persistence. In the colon, parasites were most commonly found in the circular smooth muscle layer, occupying the cytoplasm of the smooth muscle myocytes. The skeletal muscle in C3H/HeN, but not BALB/c mice, was identified as a key site of persistence, with the skeletal muscle fibres being the primary host cell type occupied. The skin in both models was shown to routinely harbour bioluminescent infection foci and therefore is likely to be a site of persistence, and critical to onward transmission. Infection in the acute stage is characterised by a large number of infected host cells, with rarely >50 amastigotes per cell. After transition to the chronic stage, even in reservoir sites such as the colon, the number of infected cells was extremely low. However, within these extremely rare infected myocytes, parasite numbers could be very high, up to 2000 in some cases.

To monitor the rate of parasite replication *in vivo*, we injected infected mice with the thymidine analogue EdU (5-Ethynyl-2-deoxyuridine). Incorporation of this analogue into parasite or host DNA identifies cells that are in S-phase during the period of exposure. This revealed that during the chronic stage of infection, there was a ~3-fold slow-down in the inferred rate of parasite replication, compared with the acute stage. Using a pulse-chase protocol we showed that long-term occupation of colonic wall myocytes is not a common feature of the chronic stage infection. We cannot exclude the possibility that parasites can enter a dormant state, but we found no definitive evidence for the existence of a truly dormant life-cycle stage in our *T. cruzi* infection model. Our interpretation of current data is that *T. cruzi* replication kinetics *in vivo* are more analogous to the

general slow-down described in *Leishmania*, rather than the definitive long-term cell cycle arrest seen in the *Plasmodium* hypnozoites or *Toxoplasma gondii* bradyzoites.

The technical approaches developed during this thesis allowed us, for the first time, to investigate the immunological context of large numbers of rare infected host cells in the colonic gut wall at late infection time-points. This revealed that a subset of infected host cells can act as a niche in which parasites are able to exist in large ‘mega-nests’ in the local absence of otherwise protective circulating T-cells. Investigating the molecular mechanisms responsible for this, and how they facilitate the long-term survival of the parasite, will be a focus of future work. We also found that serum antibody is incapable of maintaining the tight tissue load control characteristic of chronic infections, in the absence of circulating T-cells.

Acknowledgements

I would like to express my gratitude to John Kelly and the research group, whose support has allowed this PhD to be a truly scientifically fulfilling experience and more interesting than I could have hoped for. Their guidance throughout the four years have allowed me to present at multiple international conferences and publish first author papers in top journals on a variety of topics.

I would also like to thank my mother, father, brother and sister. All of whom have provided the most enjoyable and fun filled springboard into adult life I could ever have wished for. Without them, I would not have had the support required to complete something that requires so much time and energy.

Finally, I would like to thank my ~~wife~~ cat Sami, whom I have relied upon during the most difficult times of this process. Her love and encouragement have kept me on the path to completion when I would have otherwise abandoned my goals.

Table of Contents

Chapter 4 – Localisation of chronic stage *Trypanosoma cruzi* parasites in murine models

Chapter 5 – Replication kinetics of *Trypanosoma cruzi in vivo*

Chapter 6 – A hypothesis to explain long-term persistence in *Trypanosoma cruzi* infection

Chapter 7 – Discussion and future work

Appendix

List of Figures

List of abbreviations

Ab – Antibody

Ag – Antigen

APC – Antigen presenting cell

BALB/c – Immunocompetent mouse model

BCR – B-cell receptor

C3H/HeN or ‘C3H’– Immunocompetent mouse model

C57BL/6 or ‘Black 6’ – Immunocompetent mouse model

CB17-SCID – Commercially available murine model lacking functional T and B cells

CC – Chemokine

CCC – Chronic Chagasic cardiomyopathy

CD – Cluster of differentiation e.g. CD4, CD8, CD45

CLBr – CL Brener TcVI *T. cruzi* strain

CNS – Central nervous system

CSP – Circumsporoite protein

DAMP – Damage associated molecular pattern

D.C.’s – Dendritic cells

DLNs – Draining lymph nodes

DMSO – Dimethyl sulfoxide

DNA – Deoxyribose nucleic acid

DNA-PKcs – DNA-dependent protein kinase

DNDi – Drugs for Neglected Tropical Diseases *initiative*

DTH – Delayed-type hypersensitivity

DTU – Distinct typing unit

dpi – Days post-infection

EdU – 5-Ethynyl-2´-deoxyuridine

ELISA – Enzyme-link immunosorbent assay

FCS – Fetal calf serum

FMN – Flavin mononucleotide

GIT – Gastrointestinal Tract

GPI – Glucose Phosphate Isomerase

HRP – Horse radish peroxidase

IL – Interleukin e.g. IL-2, IL-12, IL-1β

MASPs – Mucin associated surface proteins

MHC – Major histocompatibility complex

NO – Nitric oxide

RNS – Reactive nitrogen species

MOA – Mode of action

PAMP – Pathogen associated molecular pattern

RBC – Red blood cell

PCR – Polymerase chain reaction

PRR – Pattern recognition receptor

ROS – Reactive oxygen species

SNP – Single Nucleotide Polymorphism

SylvioX10 – TcI *T. cruzi* strain

Tc-JR – Virulent *T. cruzi* strain

TcNTR-1 – *Trypanosoma cruzi* nitroreductase-1

TCR – T-cell receptor

T. cruzi – *Trypanosoma cruzi*

TCTs – Tissue cultured trypomastigotes

TGF-β – Transforming growth factor-Beta

Th1/Th2 – CD4+ helper T-cell type-1 and type-2 response

TLR – Toll-like receptor

TNF-α – Tumour necrosis factor alpha

TS – Tran-sialidase

V(D)J – Variable (Diversity) Junction

WHO – World Health Organisation

VSG – Variable surface glycoprotein

w.t. – Wild-type

1. Introduction

1.1 *Trypanosoma cruzi*: transmission and control

Endemic to the Americas for millions of years[1], *Trypanosoma cruzi*, the protozoan parasite that causes Chagas disease, is widely detected in diverse mammalian species across the region[2], making elimination impossible. Transmission to humans occurs when the *Triatominae* insect vector becomes established in the domestic environment, particularly in traditional housing built in rural areas. Night blood feeding on human occupants leaves parasite contaminated vector faeces on the skin. Infective stage parasites are then rubbed into the bite wound or a mucous membrane, leading to inoculation. Oral infection is also possible after the consumption of food or drink, commonly fruit juices, contaminated with vector faeces. Success in controlling the rate of new infections has been achieved by improving housing stock[3], making vector colonisation less likely, and routine insecticide spraying[4]. Approximately 6-7 million people are currently infected (WHO, 2020), mostly in the endemic regions (Figure 1).

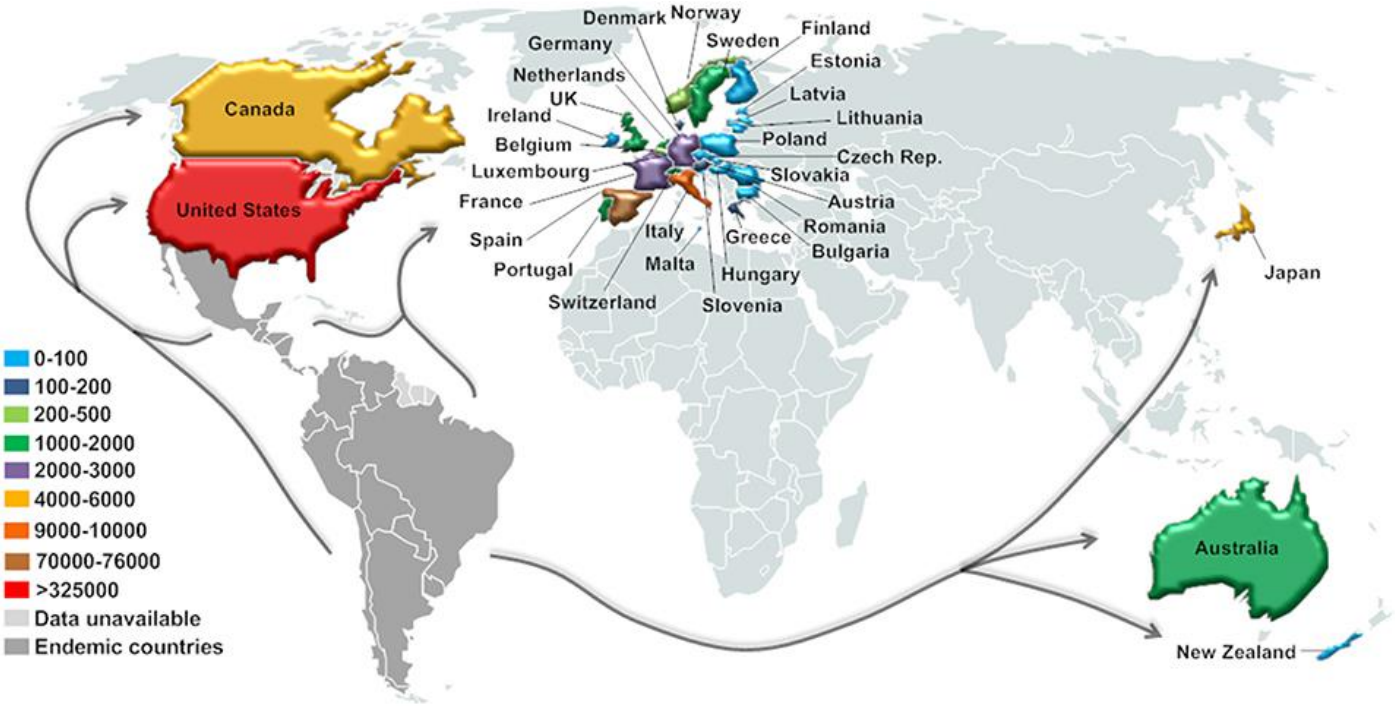

Figure 1 – Migration of people from the endemic countries in Latin America is leading to the global spread of infections and adds to the public health concerns of non-endemic countries. Figure taken from Lidani *et al* 2019[5].

Migration from endemic countries to North America, Europe, Japan and Australia has driven globalisation of the disease with transmission via the congenital or blood/organ transfusion/transplant routes possible outside the vector range. The current estimate of the global economic cost of Chagas disease is $7 billion per year[6]. Efforts to halt transmission have had

successes[7] but are incomplete. *T. cruzi* infection remains an uncontrolled threat with tens of millions at risk.

1.2 Chagas disease in the clinic

Acute infection in humans is asymptomatic or oligosymptomatic with fever, muscle stiffness, joint pain and headaches common (WHO, 2020). Parasite entry into the eye can lead to an obvious monocytic infiltration and swelling, referred to as Romana's sign or a 'Chagoma' if the swelling has taken place at the insect bite site. A small number of acute cases, particularly in children, can lead to complications including meningeal encephalitis, cardiac inflammation/dysfunction and death. It has been suggested that a more severe acute stage develops in orally transmitted cases[8], but this has been challenged in murine models[9]. Difference in infective load likely explains the discrepancy. Acute phase symptoms in human cases, if apparent, resolve over several weeks/months to be replaced by the intermediate stage.

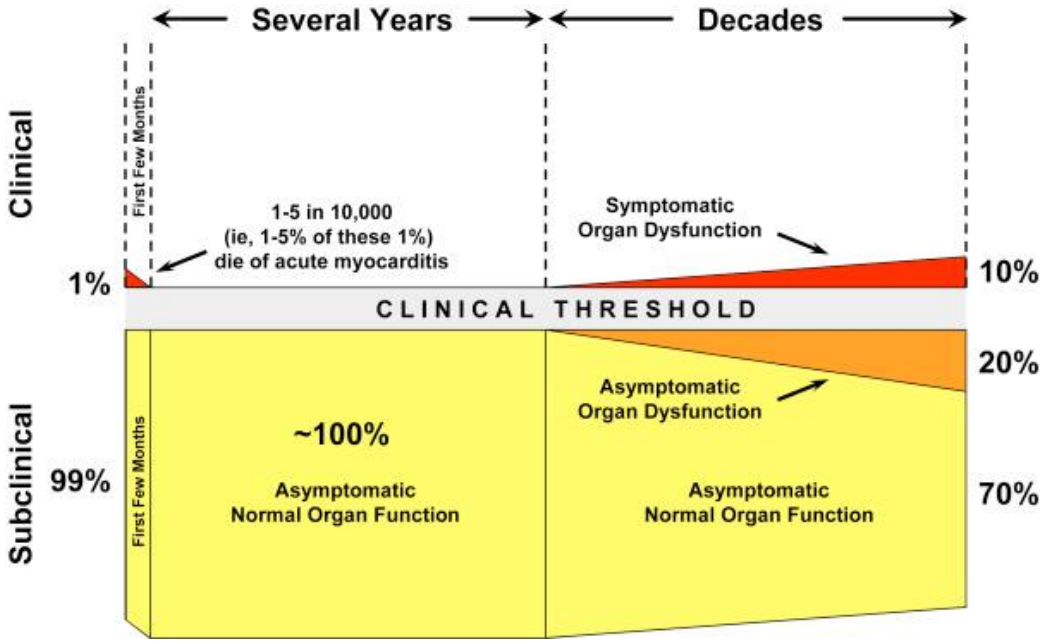

Figure 2 – Of the unknown number of new *T. cruzi* infections each year, the large majority will experience none or only mild symptoms over the first few weeks and months. A tiny minority, usually children, will experience severe cardiac or brain inflammation and a fraction of these individuals will die. In the decades following infection, an increasing proportion of cases will experience symptomatic cardiac disease, and for a sub-set, mortality. ~70% of human infections remain asymptomatic for life. Figure taken from Bonney and Engman, 2015[10].

This period is characterised by the absence of clinically recognisable pathology. In ~70% of cases, this situation continues until an unrelated mortality. In the remaining ~30% of cases, a spectrum of cardiac complications typical of Chagas disease develop at a rate of ~2% per year[11]. Chagasic cardiac disease can include arrythmias and infarctions. Dilated cardiomyopathy or congestive heart failure are prevalent at disease end-point[12]. The current consensus is that the cardiac

complications of Chagas disease are the result of inflammatory damage[13], although the details of how this relates to infection and a possible role of autoimmunity remain undefined[14].

In ~10% of cases, sometimes in conjunction with the cardiac symptoms, the digestive pathologies develop[15]. Digestive Chagas disease involves the hyperdilation of organs of the digestive tract, most commonly the colon and oesophagus. These pathologies are commonly referred to as 'mega-syndromes' and are responsible for significant morbidity and mortality. The mechanism that generates these complications is not well described but has been suggested to be the result of inflammatory damage combined with age-related loss of neurones in the gut wall[16].

Once the clinical pathologies have become established there is little evidence that drug treatment has much benefit (BENEFIT trial[17]). Treatment is essentially palliative and aims to improve the quality of life for patients[18]. Heart transplants have been conducted with some successes, but there are also issues with infection re-bound brought on by immune suppression[19]. Drug cure does appear to have a positive effect if done before the onset of clinical pathology[20] and is currently recommended by the WHO for all patients with positive serology. Despite this advice, ~1% of cases in the endemic regions are treated[21], due to a lack of diagnostic testing. In addition, there is reluctance to using poor-quality drugs to treat positive cases, the majority of whom will remain asymptomatic for life.

1.3 Drugs and clinical trials

There are two chemotherapy options available in the clinic, benznidazole (BZ) and nifurtimox, recently reviewed in Francisco *et al* 2020[22]. Both are heterocyclic pro-drugs activated by the parasite specific mitochondrial enzyme, type 1-nitroreductase (TcNTR-1)[23,24]. This enzyme catalyses the reduction of the nitro (NO_2) group on both drugs using flavin mononucleotide (FMN) as an electron donor. Downstream reductive metabolism yields a host of cytotoxic compounds with multiple targets[25]. The mode of action (MOA) for both drugs is poorly characterised, although DNA mutagenesis has been demonstrated in the case of BZ. Cross resistance to both drugs is easily generated *in vitro* by reduced expression of TcNTR-1[26]. Natural isolates show variable drug susceptibility[27], but no function-linked polymorphisms at the TcNTR-1 loci have been recorded. The mechanisms behind these resistance phenotypes could involve alternative catabolic pathways for the pro-drugs[28] generating less toxic metabolites, up-regulation of oxidative defence[29], enhanced DNA-repair pathways[30], or decreased drug up-take (Francisco Olmo, in preparation). Due to the low rates of usage and the fact that humans are a very minor component of the host range, selection of mutations for drug resistance is unlikely to occur at a parasite population level. Whether the acquisition of resistance mutations in individual patients is responsible for treatment

failures is currently unknown. The main issue with the current front-line compounds is the need for long treatment regimens, 30-60 days, combined with adverse side effects. Dermatitis, digestive tract intolerance, anorexia, sleeping disorders and headache are commonly reported side effects[31]. Less common, but more serious, is depression of the bone marrow leading to neutropenia[32]. Despite their well validated effect *in vitro* against multiple clinical isolates[33], outcomes in patients can be variable[34]. Nitroaromatic compounds other than BZ and nifurtimox have shown pre-clinical efficacy. The lead compound fexinidazole (Figure 3) out performs BZ in highly-sensitive bioluminescent mouse models[35]. This compound has already been licenced for treatment of the related kinetoplastid *T. brucei*[36]. A phase II clinical trial (*DNDi*, Fexinidazole for Chagas trial) is currently underway with results from Spain due in 2021.

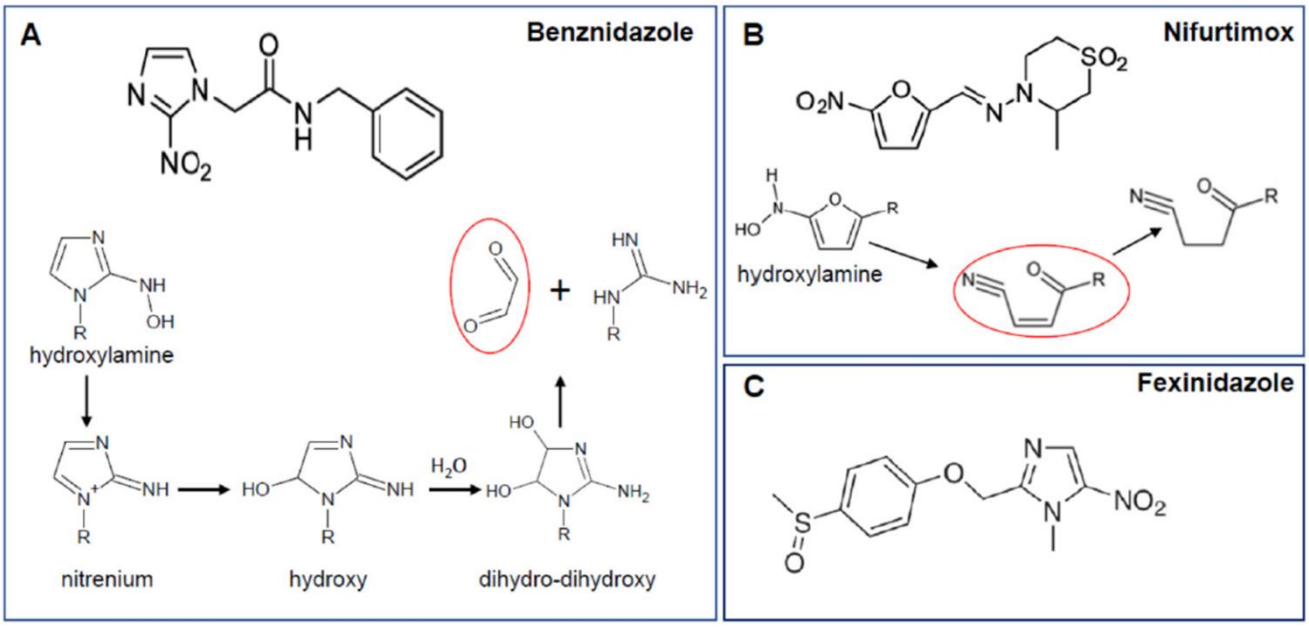

Figure 3 – A and B., The frontline drugs Benznidazole (BZ) and Nifurtimox with parts of their respective reductive metabolite processing indicated. **C.,** Fexinidazole, another nitroaromatic drug, currently undergoing clinical trials in humans as an anti-chagasic agent. Taken from Francisco *et al* 2020[22].

The repurposing of anti-fungal drugs has been attempted with the ergosterol inhibitor posaconazole, with significant knock-down of parasite load in mice, but not sterile cure[37]. Results in humans have been disappointing (STOP-CHAGAS trial[38]), highlighting the need for definitive pre-clinical cure rather than temporary reduction of parasite load. A related drug targeting the same lipid biosynthesis pathway has also had disappointing results in field trial[39]. The phase II (*DNDi*, BENDITA[40]) trial reduced the treatment regimen of BZ from 8 to 2 weeks, and the dosage from 300 to 100mg/day. The cure rate (~80%), as assessed by repeated PCR (polymerase chain reaction) of blood samples during follow-up, was similar to the standard treatment course but with fewer toxic effects. A shorter treatment regimen is desired to improve compliance in patients.

1.4 Cure vs. not cured

A major obstacle to better optimisation of front-line drugs and the testing of new compounds is the inability to rapidly determine cure of infection, reviewed in Machado-de-Assis *et al* 2012[41]. The most recent clinical trials testing new drugs and optimizing currently available compounds (above) have all used repeated rounds of PCR to distinguish cure vs. non-cure. Patient blood samples are assayed using the multi copy parasite minicircle mtDNA as a target[42]. The vast majority of patients enrolled on these trials are in the chronic stage of infection, a period when parasite numbers are extremely low and the infection focally distributed[43]. False negatives are a major problem[44]. An alternative method is assaying for reversion to serological negativity by ELISA. However, a significant time-lag exists between successful treatment and loss of serum antibodies in both murine models and humans[45], and evidence suggests not all positive cases can be detected by current serological methods[46]. Despite some recent progress[47], determining cure vs. treatment failure is still problematic in the clinic and in controlled trials. Current consensus states that infections can be more effectively cured in the acute stage[48], with current WHO guidance reflecting this. However, this has been challenged in murine models[49], where chronic infections, which have much lower parasite burdens, can be cured more easily.

1.5 Genetic organisation, diversity and evolution of *Trypanosoma cruzi*

T. cruzi is a member of the order kinetoplastida and forms part of the *Euglenozoa* phylum, which represents one of the earliest splits in the eukaryotic lineage. This order also contains the African trypanosome, *T. brucei*, and the *Leishmania* species, that are responsible for the human diseases sleeping sickness and leishmaniasis, respectively. The order is named after the morphological feature termed the ‘kinetoplast’, which consists of multiple copies of the mitochondrial genome (mtDNA) and associated proteins. Each parasite is endowed with a single mitochondrion. The mtDNA encodes several proteins essential for oxidative phosphorylation. These genes are expressed from maxicircles, circular copies of the mtDNA. Each transcribed mRNA product must be ‘edited’ through a series of enzymatic cleavage-ligations to produce the open reading frame mRNA for translation. The molecular machinery for this editing is directed by complementary guide RNA (gRNA). These guides are transcribed mostly from minicircles, which are catenated small circular DNA molecules that co-localise with the maxicircles. The selection pressures that have driven RNA editing in the kinetoplastid mitochondria are not known[50]. High minicircle copy numbers (in the 1000’s per parasite) are the basis for the highly sensitive PCR reactions used to determine cure in clinical trials (above). By microscopy (Chapter 4), the mtDNA appears as a 3D flattened disk of intense DNA stain, which in the amastigote is positioned adjacent to the more dimly stained nucleus.

Since the advent of wide spread sequencing, it has been clear that there is a huge amount of diversity within what is still classed a single species. Chromosomal polymorphism[51] and expanded families of genes[52], often in copy numbers of >2000, are hallmarks of the *T. cruzi* genome. From the whole sequences available to date (*UniPro*[53]), ~20,000 protein coding genes are predicted in a nuclear genome, which is ~40-50 Mb in size[51]. The largest of these duplicated families are the trans-sialidases (TS) that catalyse the removal of host sialic acid from the extracellular matrix and glycocalyx onto acceptor sites on the parasite membrane. Mucins and mucin associated surface proteins (MASPs) are the next largest gene families. Unlike in *T. brucei*[54] there is no evidence that these large families are mono-allelically expressed[55]. Their precise role is not fully determined but it is hypothesised that the selection of these large groups of surface expressed proteins has been driven by immunological pressure from the wide host range.

Genome expression in *T. cruzi* is also unusual, as in other kinetoplastids. Protein coding genes, transcribed by RNA polymerase II (pol II), are arranged in long poly-cistronic transcription units with start sites that lack the properties of classical pol II promoters[56]. Control of gene expression is predominantly at the mRNA level, with the polycistronic transcripts undergoing a process of trans-splicing in which a short splice-leader sequence is added to the 5'-end of each mRNA protein coding sequence[57]. This occurs in concert with polyadenylation, prior to the export of the mRNA from the nucleus into the cytoplasm. The stability of individual mRNAs is usually mediated by sequences in the 3'-untranslated region (UTR) of the transcript[58].

At present, this species diversity is categorised into six distinct typing units (DTUs) (I, II, III, IV, V and VI), two of which (V and VI) are hybrids of the II and III lineages. These were originally defined on the basis of single nucleotide polymorphisms (SNPs) in 3 housekeeping genes; rDNA, Hsp60 and GPI (glucose phosphate isomerase)[59]. Strains in each DTU have been hypothetically linked to pathological, drug resistance and virulence phenotypes[60], although evidence for this remains non-definitive. *T. cruzi* has historically been described as a clonal species that experiences rare stochastic hybridization events reviewed in Messenger and Miles, 2015[61]. The 2 major hybridization events occurred ~60,000 years ago[62] and may even have been a single event followed by clonal divergence. The mechanism of genetic exchange is difficult to assess in natural transmission cycles but has been shown to take place *in vitro*[63]. Figure 4 shows the hypothesised fusion of epimastigotes of different clonal lineage followed by recombination and chromosomal loss, producing a diploid hybrid with allelic variants from both parents. It has been suggested that hybridization events do not just take place on evolutionary time-scales, but are also relevant to epidemiological surveillance and case detection by PCR[62].

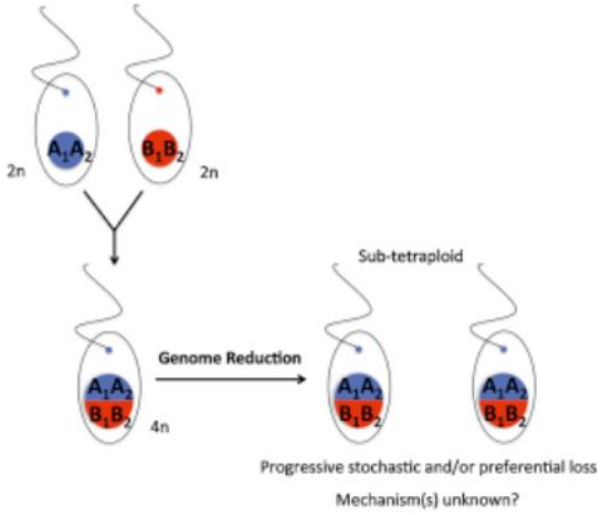

Figure 4 – Hypothesised mechanism of hybrid generation in *T. cruzi*. 2 epimastigotes in the *Triatomine* vector gut fuse to produce a 4 genome copy tetraploid cell. Subsequent loss of genetic material permits a return to the diploid state. Taken from Messanger and Miles 2015[62].

1.6 The life-cycle

The life-cycle of the parasite was pieced together soon after discovery of the pathogen[64]. Inoculation into a new mammalian host occurs on contact with the faeces of the vector as described above. The infecting life-cycle stage, the metacyclic trypomastigote, is fully differentiated in the vector midgut. This stage is replication arrested and specifically adapted for survival in complement active fluids and for initial host cell invasion. Entry into host cells has been widely investigated, reviewed in Epting *et al* 2010[65] and Maeda *et al* 2012[66]. Briefly, interaction between parasite and host glycocalyx reduces the motility of the trypomastigote[67]. Secreted pore-forming toxins 'wound' or 'puncture' the host plasma membrane causing an influx of extracellular Ca^{2+} down its biochemical gradient[68]. The ancient and ubiquitous membrane repair pathway[69] responds to local calcium increase by mobilising lysosomes to translocate from the peri-nuclear region and fuse with the plasma membrane stemming the breach. It is hypothesised that *T. cruzi* 'hijacks' the resulting endocytosis of the inserted lysosomal membrane for invasion. The exploitation of this pathway, which is conserved in all nucleated cells, likely contributes to the parasite's ability for promiscuous cell invasion. Trypomastigote cell entry ends in occupation of a parasitophorous vacuole (PV) within the cytoplasm, composed of lysosomal membrane. Rapid escape is triggered by increased H^+ concentration[70]. Differentiation into the non-motile intracellular life-cycle stage, the amastigote, begins in the PV and is completed following escape into the cytosol. Replication then occurs by asynchronous cell division[71]. At the chronic stage of infection, replication within host cells can generate up to 2000 parasites within a single cell, termed 'mega-nests'[72]. Differentiation into the replication arrested blood stage trypomastigote completes the process. Rupture/lysis of the host cell membrane releases motile, compliment resistant, trypomastigotes that disseminate in the lymph/blood and other tissue fluids invading further host

cells. Uptake in the insect blood meal occurs from the skin or blood stream, although the kinetics have not been defined.

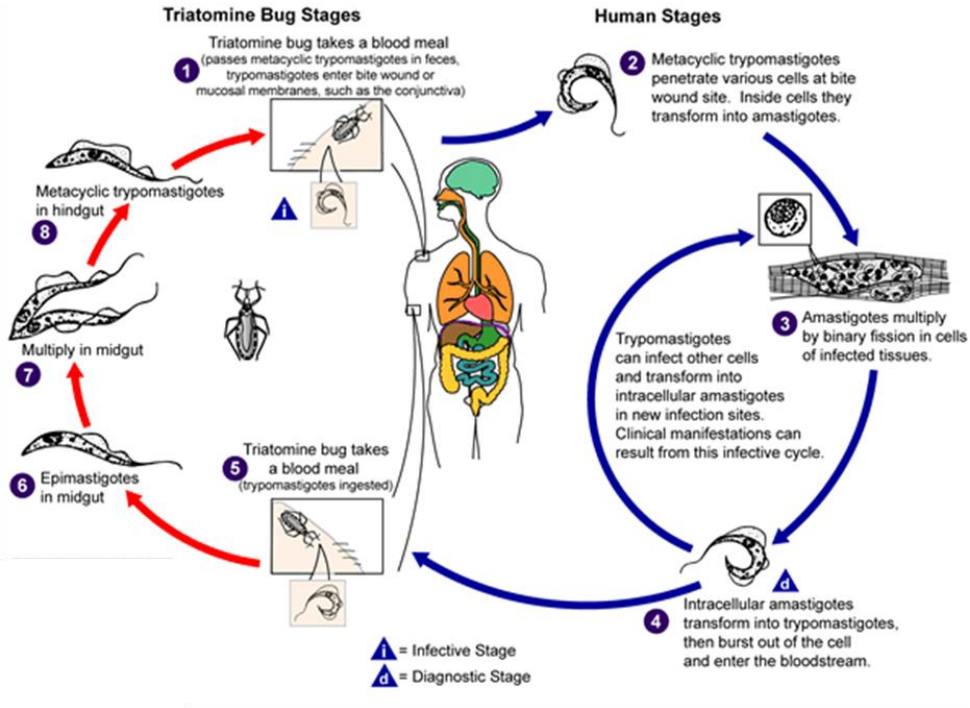

Figure 5 – All intracellular and extracellular stages of the *T. cruzi* life-cycle – Metacyclic trypomastigotes are inoculated into the host where they invade nucleated cells. Differentiation to the amastigote in the cytoplasm is followed by repeated cycles of parasite cell division. Differentiation into the motile blood stage trypomastigote, leads to the rupture of the plasma membrane and allows dissemination of the parasites. Most trypomastigotes will either enter new hosts cells or be cleared by the immune response. The uptake of trypomastigotes, or amastigotes, into the *Triatomine* vector triggers differentiation to the insect stage epimastigote. Epimastigotes go through several rounds of cell division, and then undergo differentiation ready for deposition in the faeces on to the next host. Most mammalian species can act as reservoirs for the infection, including humans and domestic animals. Taken from CDC[73].

The replication cycle is completed by the introduction of trypomastigotes, and possibly also amastigotes, into the gut of the insect vector. Differentiation into the replication-competent epimastigote leads to amplification of parasites numbers prior to deposition onto the next host.

References

1. Hamilton, P. B, Teixeira, M. G. and Stevens, J. R. The evolution of *Trypanosoma cruzi*: the 'bat seeding' hypothesis. *Trends Parasitol*. **28**, 136-41 (2012).
2. Xavier, S. C. el at. Lower richness of small wild mammal species and Chagas disease risk. *PLOS neg. Trop. Dis*. **6**, e1647 (2012).
3. Gaspe, M. S. et al. Urbanisation, risk stratification and house infestation with a major vector of Chagas disease in an endemic municipality of the Argentine Chaco. *Parasites & Vectors*. **13**, 316 (2020).

4. Samuels, A. M. et al. Epidemiology of and impact of insecticide spraying on Chagas disease in communities in the Bolivian Chaco. *PLOS Negl. Trp. Dis*. doi.org/10.1371
5. Lidani, K. C. et al. Chagas disease: From discovery to a worldwide health problem. Lancet Infect. Dis. **13**, 342-348 (2013).
6. Lee, B. Y., Bacon, K. M., Bottazzi, M. E. and Hotez, P. J. Global economic burden of Chagas disease: a computational simulation model. *J. Immunol. Res*. **2015**, 489758 (2015).
7. Schofield, C. J. and Dias, J. C. The southern cone initiative against Chagas disease. *Adv. Parasitol*. **42**, 1-27 (1999).
8. Souza-Lima, R. C. et al. Outbreak of acute Chagas disease associated with oral transmission in the Rio Negro region, Brazilian Amazon*. Rev. Soc. Bras. Med. Trop*. **46**, 510-4 (2013).
9. Lewis, M. D., Francisco, A. F., Jayawardhana, S., Langston, H., Taylor, M. C. and Kelly, J. M. Imaging the development of chronic Chagas disease after oral transmission. Scientific Reports. **8**, 11292 (2018).
10. Bonney, K. M. and Engman, D. M. Autoimmune pathogenesis of Chagas heart disease. *Am. J. Pathol*. **185**, 1537-1547 (2015).
11. Sabino, E. C. et al. Ten-year incidence of Chagas cardiomyopathy amoung asymptomatic Trypanosoma cruzi-seropositive former blood donors. *Circulation*. **127**, 1105-15 (2013).
12. Nunes, M. C. et al. Chagas cardiomyopathy: an update of current clinical knowledge and management: a scientific statement from the American Heart Association. *Circulation*. **138**, e169-e209 (2018).
13. Kölliker-Frers, R. A. Chagas cardiomyopathy: role of sustained host-parasite interaction in systemic inflammatory burden. *IntechOpen* (2018).
14. Bona, E. D. et al. Autoimmunity in chronic Chagas disease: a road of multiple pathways to cardiomyopathy. *Front. Immunol*. **9**, 1842 (2018).
15. Matsuda, N. M., Miller, S. M. and Barbosa Evora, P. R. The chronic gastrointestinal manifestations of Chagas disease. *Clinics (Sao Paulo)*. **64**, 1219-1224 (2009).
16. Jabari, S., de Oliveira, E. C., Brehmer, A. and de Silveira, A. B. Chagasic megacolon: enteric neurones and relates structures. *Histochem. Cell Biol*. **142**, 235-244 (2014).
17. Morillo, C. A. et al. Randomized trial of benznidazole for chronic Chagas cardiomyopathy. *N. eng. J. med.* **373**, 1295-1306 (2015).
18. Viotti, R. et al. Towards a paradigm shift in the treatment of chronic Chagas disease. *Antimicrob. Agents Chemother*. **58**, 635-9 (2014).
19. Gray, E. B. et al. Reactivation of Chagas disease among heart transplant recipients in the United States, 2012-2016. *Transpl. Infect Dis*. **20**, e 12996 (2018).

20. Viotti, R., Vigliano, C., Armenti, H. and Segura, E. Treatment of chronic Chagas disease with benznidazole: clinical and serological evolution of patients with long-term follow-up. *Am. Heart J*. **127**, 151-62 (1994).
21. Alonso-Padilla, J. Strategies to enhance access to diagnosis and treatment for Chagas disease patients in Latin America. *Expert Review of Anti-Infective Therapy*. **17**, 145-157 (2019).
22. Francisco, A. F. et al. Challenges in Chagas disease drug development. *Molecules*. **25**, 2799 (2020).
23. Wilkinson, S. R., Taylor, M. C., Horn, D., Kelly, J. M. and Cheeseman, I. A mechanism for cross-resistance to nifurtimox and benznidazole in trypanosomes. *PNAS*. **105**, 5022-5027 (2008).
24. Trochine, A., Creek, D. J., Faral-Tello, P., Barrett, M. P. and Robello, C. Benznidazole biotransformation and multiple targets in *Trypanosoma cruzi* revealed by metabolomics. *PLOS Neg. Trop. Dis*. **8**, e0002844 (2014).
25. Wilkinson, S. R., Bot, C., Kelly, J. M. and Hall, B. S. Trypanocidal activity of nitroaromatic prodrugs: current treatments and future perspectives. *Curr. Trop. Med. Chem*. **11**, 2072-2084 (2011).
26. Mejia, A. M. et al. Benznidazole-resistance in *Trypanosoma cruzi* is a readily acquired trait that can arise independently in a single population. *J. Infect. Dis*. **206**, 220-228 (2012).
27. Teston, A. P. et al*. in vivo* susceptibility to benznidazole of *Trypanosoma cruzi* strains from the western Brazilian Amazon. *Trop. Med. and Int. Heal.* **18**, 85–95 (2013).
28. Murta, M. A. et al. Depletion of genes encoding old yellow enzyme (TcOYE), a NAD(P)H flavin oxidoreductase, associates with *in vitro*-induced beznidazole resistance in *Trypanosoma cruzi*. *Mol. Biochem. Parasitol*. **148**, 151-162 (2006).
29. Nogueira, F. B., Krieger, M.A., Nirdé, P., Goldenberg, S., Romanha, A. J. and Murta, S. M. Increased expression of iron-containing superoxide dismutase-A (TcFeSOD-A) enzyme in *Trypanosoma cruzi* population with *in vitro*-induced resistance to benznidazole. *Acta. Trop*. **100**, 119-132 (2006).
30. Rajao, M. A. Unveiling benznidazoles mechanism of action through the upregulation of DNA-repair pathways. *Env. and Mol. Mut*. **55**, 309-321 (2014).
31. Viotti, R. et al. Side effects of benznidazole as treatment in chronic Chagas disease: fears and realities. *Expert Rev. Anti Infect. Ther*. **7**, 157-63 (2009).
32. Crespillo-Andujar, C., Roobles, M. C., Norman, R. F. and Perez-Molina, J. A. Severe immune thrombocytopaenia in a patient taking benznidazole for chronic Chagas disease. *BMJ Case Report*. e223788 (2018).

33. Sanchez-Valdez, F. J., Padilla, A., Wang, W., Orr, D. and Tarleton, R. L. Spontaneous dormancy protects *Trypanosoma cruzi* during extended drug exposure. *eLife*. **7**, e34039 (2018).
34. Bustamante, J. M. and Tarleton, R. L. Methodological advances in drug discovery for Chagas disease*. Expert Opin. Drug Discov*. **6**, 653-661 (2011).
35. Francisco, A. F. et al. Nitroheterocyclic drugs cure experimental *Trypanosoma cruzi* infections more effectively in the chronic stage than in the acute stage. *Nat. Sci. Reports*. **6**, e35351 (2016).
36. Mesu, V. K. et al. Oral fexinidazole for late-stage African *Trypanosoma brucei gambiense* trypanosomiasis: a pivotal multiple centre, randomised, non-inferiority trial. *Lancet*. **391**, 144-154 (2018).
37. Francisco, A. F., Lewis, M.D., Jayawardhana, S., Taylor, M. C., Chatelain, E. and Kelly, J. M. Limited ability of posaconazole to cure both acute and chronic *Trypanosoma cruzi* infection revealed by highly sensitive in vivo imaging. *mBio*. **59**, 4653-4661 (2015).
38. Morillo, C. A. et al. Benznidazole and posaconazole in eliminating parasites in asymptomatic *T. cruzi* carriers, the stop Chagas trial. *J. of the Amer. Col. of Cardiol*. **69**, 940-947 (2017).
49. Torrico, F. et al. Treatment of adult chronic indeterminate Chagas disease with benznidazole and three E1224 dosing regimens: a proof-of-concept, randomised, placebo-controlled trial. *Lancet Infect. Dis*. **18**, 418-430 (2018).
40. https://dndi.org/press-releases/2019/study-shows-dramatically-shorter-treatment-chagas-effective-and-safer/
41. Machado-do-Assis, G. F. et al. Post-therapeutic cure criteria in Chagas disease: conventional serology followed by supplementary serological, parasitological, and molecular test. *mBio*. **19**, 1283-1291 (2012).
42. Wei, B., Chen, L., Kibukawa, M., Kang, J., Waskin, H. and Marton, M. Development of a PCR assay to detect low level *Trypanosoma cruzi* in blood specimens collected with PAXgne blood DNA tubes for clinical trials treating Chagas disease. *PLOS neg. Trop. Dis*. **10**, e0005146 (2016).
43. Lewis, M. D. et al. Bioluminescence imaging of chronic *Trypanosoma cruzi* infections reveals tissue-specific parasite dynamics and heart disease in the absence of locally persistent infection. *Cell Microbiol*. **16**, 1285-300 (2014).
44. Calver, C. M. Long term follow-up of *Trypanosoma cruzi* infection and Chagas disease manifestations in mice treated with benznidazole or posaconazole. *PLOS Neg. Trop. Dis*. **14**, e0008726 (2020).

45. Moscatelli, G. Longitudinal follow up of serological response in children treated for Chagas disease. *PLOS Neg. Trop. Dis*. **13**, e0007668 (2019).
46. Salomone, O. A. *Trypanosoma cruzi* in persons without serological evidence of disease, Argentina. *Emerg. Infect. Dis*. **9**, 1558-1562 (2003).
47. Ortega-Rodriguez, U. et al. Purification of glycosylphophatidylinsitol-anchored mucins from *Trypanosoma cruzi* trypomastigotes and synthesis of α-Gal-containing neoglycoproteins: application as biomarkers for reliable diagnosis and early assessment of chemotherapeutic outcomes of Chagas disease. *Methods Mol. Biol*. **1955**, 287-308 (2019).
48. Coura, J. R. and Castro, S. L. A critical review on Chagas disease chemotherapy. *Men. Inst. Oswaldo Cruz*. **97**, 3-24 (2002).
49. Francisco, A. F. et al. Nitroheterocyclic drugs cure experimental *Trypanosoma cruzi* infections more effectively in the chronic stage than in the acute stage. *Sci. Reports*. **6**, e35351 (2016).
50. Simpson, L., Thiemann, O. H., Savill, N. J., Alfonzo, J. D. and Maslov, D. A. Evolution of RNA editing in trypanosome mitochondria. *Proc. Natl. Acad. Sci. USA*. **97**, 6986-93 (2000).
51. Souza, R. T. et al. Genome size, karyotype polymorphism and chromosomal evolution in *Trypanosoma cruzi*. *PLOS one*. **6**, e23042 (2011).
52. De Pablos, L. M. and Osuna, A. Multigene families in *Trypanosoma cruzi* and their role in infectivity. *Infect. Immun*. **80**, 2258-2264 (2012).
53. https://www.uniprot.org/proteomes/UP000002296
54. Faria, J., Glover, L., Hutchinson, S., Boehm, C., Field, M. C. and Horn, D. Monoallelic expression and epigenetic inheritance sustained by a *Trypanosoma brucei* variant surface glycoprotein exclusion complex. *Nat. Commun*. **10**, e3023 (2019).
55. Buscaglia, C. A., Campo, V. A., Frasch, A. C. and Noia, J. M. *Trypanosoma cruzi* surface mucins: host-dependent coat diversity. *Nat. Rev. Microbiol*. **4**, 229-36 (2006).
56. Clayton, C. Regulation of gene expression in trypanosomatids: living with polycistronic transcription. *Open Biol*. **9**, e190072 (2019).
57. McCarthy-Burke, C., Taylor, Z. A. and Buck, G. A. Characterisation of the spliced leader genes and transcripts in *Trypanosoma cruzi*. *Gene*. **82**, 177-89 (1989).
58. Araujo, P. A. and Teixeira, S. M. Regulatory elements involved in the post-translational control of stage-specific gene expression in *Trypanosoma cruzi* – a review. *Mem. Inst. Oswaldo Cruz*. **106**, 257-266 (2011).
59. Lewis, M. D., Llewellyn, M. S., Yeo, M., Acosta, N., Gaunt, M. W. and Miles, M. A. Recent, independent and anthropogenic origins of *Trypanosoma cruzi* hybrids. *PLOS Neg. Trop. Dis*. **5**, e1363 (2011).

60. Junior, P. A. *et al*. Experimental and clinical treatment of Chagas disease: a review. *Am. J. Trop. Med*. Hyg. **97**, 1289-1303 (2017).
61. Messenger, L. A. and MIlEs, M. A. Evidence and importance of genetic exchange among field populations of *Trypanosoma cruzi*. *Acta. Trop*. **151**, 150-155 (2015).
62. Lewis, M. D., Llewellyn, M. S., Yeo, M., Acosta, N., Gaunt, M. W. Miles, M. A. Recent, independent and anthropogenic origins of *Trypanosoma cruzi* hybrids. *PLOS Neg. Trop. Dis*. **5**, e1363 (2011).
63. Gaunt, M. W. Mechanism of genetic exchange in American trypanosomes. *Nature*. **421**, 936-9 (2003).
64. Carlos, C. Nova entidade morbida do homen. Brazil-Medico, *Rio de Janeiro*. **24**, 43-45 (1910).
65. Epting, C. L., Coates, B. M. and Engman, D. M. Molecular mechanisms of host cell invasion by *Trypanosoma cruzi*. *Exp. Parasitol*. **126**, 283-91 (2010).
66. Maeda, F. Y., Cortez, C. and Yoshida, N. Cell signalling during *Trypanosoma cruzi* invasion. *Front. Immunol*. **3**, 361 (2012).
67. Yoshida, N. Molecular basis of mammalian cell invasion by *Trypanosoma cruzi*. *Annals of the Brazilian academy of sciences*. **78**, 87-111 (2006).
68. Martins, N. O. Molecular characterisation of a novel family of *Trypanosoma cruzi* surface membrane proteins (TcSMP) involved in mammalian host cell invasion*. PLOS Neg. Trop. Dis*. **9**, e0004216 (2015).
69. Cooper, S. T. and McNeil, P. L. Membrane repair: mechanisms and pathophysiology. *Physiol. Rev*. **95**, 1205-1240 (2015).
70. Ley, V., Robbins, E. S., Nussenzweig, V. and Andrews, N. W. The exit of *Trypanosoma cruzi* from the phagosome is inhibited by raising the pH of the acidic compartments. *J. Exp. Med*. **17**, 401-13 (1990).
71. Taylor, M. C. et al. Intracellular DNA replication and differentiation of *Trypanosoma cruzi* is asynchronous within individual host cells in vivo at all stages of infection. *PLOS neg. Trop. Dis*. **14**, e0008007 (2020).
72. Ward, A. W. et al. *in vivo* analysis of *Trypanosoma cruzi* persistence foci at singl-cell resolution. *mBio*. **11**, e01242-20 (2020).
73. https://www.cdc.gov/parasites/chagas/biology.html

2. Immunology of *Trypanosoma cruzi* infection

2.1 Contribution to joint-first author review

As joint-first author, my contribution to the review in *Parasite Immunology* includes the innate detection and effectors sections, and the roles of T-cells in *T. cruzi*-host interaction. Since the publication of this manuscript I have generated new data which adds to the story (Chapter 6). I provide additional comment on the new data in section 2.3. Since I only edited and commented on the role of B-cells and serum antibody in parasite control, I also take the opportunity to comment more broadly on this topic in section 2.3.

See https://onlinelibrary.wiley.com/doi/abs/10.1111/pim.12786 for the on-line version.

2.2 –

London School of Hygiene & Tropical Medicine
Keppel Street, London WC1E 7HT

T: +44 (0)20 7299 4646
F: +44 (0)20 7299 4656
www.lshtm.ac.uk

RESEARCH PAPER COVER SHEET

Please note that a cover sheet must be completed for each research paper included within a thesis.

SECTION A – Student Details

Student ID Number	lsh1406159	**Title**	Mr
First Name(s)	Alexander		
Surname/Family Name	Ward		
Thesis Title	Trypanosoma cruzi: Where is it? Does it ever sleep? Why is a sterile outcome rarely achieved?		
Primary Supervisor	John Kelly		

If the Research Paper has previously been published please complete Section B, if not please move to Section C.

SECTION B – Paper already published

Where was the work published?	Parasite Immunology Review		
When was the work published?	13/08/2020		
If the work was published prior to registration for your research degree, give a brief rationale for its inclusion			
Have you retained the copyright for the work?*	**Yes**	Was the work subject to academic peer review?	**Yes**

*If yes, please attach evidence of retention. If no, or if the work is being included in its published format, please attach evidence of permission from the copyright holder (publisher or other author) to include this work.

SECTION C – Prepared for publication, but not yet published

Where is the work intended to be published?	
Please list the paper's authors in the intended authorship order:	
Stage of publication	Choose an item.

SECTION D – Multi-authored work

For multi-authored work, give full details of your role in the research included in the paper and in the preparation of the paper. (Attach a further sheet if necessary)	The initial brief from the journal was for an update on the state of knowledge for immune control of Tryapnsoma cruzi 'in the tissues'. I put together the sections on innate recognition, control and T-cells. I wrote the 1st draft of this section and provided confocal images for the relevant figures through an iterative process between the authors, we put together the final submitted version.

SECTION E

Student Signature	Alexander Ward
Date	13/08/2020

Supervisor Signature	John Kelly
Date	13/08/2020

Host-parasite dynamics in Chagas disease from systemic to hyper-local scales.

Damián Pérez-Mazliah[1*], Alexander I. Ward[2*] and Michael D. Lewis[2]

[*] Equal contribution

[1] York Biomedical Research Institute, Hull York Medical School, University of York, Heslington, York, YO10 5DD, UK

[2] Department of Infection Biology, Faculty of Infectious and Tropical Diseases, London School of Hygiene and Tropical Medicine, London, WC1E 7HT, UK

Disclosures:

None

Data availability statement:

Data sharing not applicable to this article as no datasets were generated or analysed during the current study

Abstract

Trypanosoma cruzi is a remarkably versatile parasite. It can parasitize almost any nucleated cell type and naturally infects hundreds of mammal species across much of the Americas. In humans it is the cause of Chagas disease, a set of mainly chronic conditions predominantly affecting the heart and gastrointestinal tract that can progress to become life threatening. Yet around two thirds of infected people are long-term asymptomatic carriers. Clinical outcomes depend on many factors, but the central determinant is the nature of the host-parasite interactions that play out over the years of chronic infection in diverse tissue environments. In this review, we aim to integrate recent developments in the understanding of the spatial and temporal dynamics of *T. cruzi* infections with established and emerging concepts in host immune responses in the corresponding phases and tissues.

Trypanosoma cruzi: A Formidable Foe

Trypanosoma cruzi, the causative agent of Chagas disease (American trypanosomiasis), is an extraordinarily versatile parasite. Its wild transmission cycles across the Americas are maintained by over 100 species of haematophagous triatomine bugs. Chagas disease is a zoonosis and *T. cruzi* infects diverse mammal reservoir species, including marsupials, bats, rodents, ungulates, carnivores (including domestic cats and dogs), armadillos, pilosans and primates (1). *T. cruzi* undergoes regulated morphological transitions involving at least four developmental forms, each with a distinctive biology e.g. cell structural features, modes of motility, surface protein coats (2) and metabolic programmes (3). The epimastigote form replicates in the vector's gut, then differentiates to a highly motile form, the metacyclic trypomastigote, which invades mammalian host cells after transmission. Potentially any nucleated cell type may be parasitized in any tissue the trypomastigote can reach (4-16). After invasion and escape from a parasitophorous vacuole into the cytosol, another transition occurs to the amastigote form, which replicates repeatedly and then differentiates to generate a population of pleomorphic tissue/bloodsteam form trypomastigotes. These are released into the extracellular space from where they may infect a new cell, in some cases after migration to the bloodstream. Alternatively, in the rare event they are taken up in a triatomine blood meal, they can complete the cycle by differentiating into epimastigotes.

Mounting evidence shows *T. cruzi*'s life cycle is considerably more complex than the textbook view. Findings include epimastigote-like forms in mammals, asynchronous replication and trypomastigogenesis, asymmetric divisions, reversible transitions and formation of apparently quiescent or dormant amastigotes (17-22). The morphological, antigenic and spatial variability, combined with active evasion strategies presents a formidable challenge to the mammalian immune system. Nevertheless, most infections resolve to a stable chronic equilibrium of parasite replication and suppression via a combination of sustained antibody and type 1 cellular responses. The majority of people (>95%) survive acute infection and progress to a chronic, asymptomatic phase. Chagas cardiomyopathy is then estimated to develop at a rate of ~2% per year (23).

Disorders of the gastrointestinal (GI) tract develop in a smaller proportion of cases, sometimes in combination with cardiac disease (24). Why Chagas pathology only affects a limited subset of tissues in only a specific subset of infected people is one of the longest-standing and most important unanswered questions in the field.

In this review, our aim is to integrate recent developments in the understanding of the spatial and temporal dynamics of *T. cruzi* infections with established and emerging concepts in host immune responses in the corresponding phases and tissues. The result is a view that parasite persistence occurs in a small number of privileged tissues alongside highly competent, *T. cruzi*-specific systemic responses, suggesting a substantial degree of compartmentalization, even within tissues. The low-level, yet perpetual chronic inflammation has the potential to become pathological, dependent on largely undefined host, parasite and environmental factors. Thus, progress in the development of anti-parasitic drugs, adjunct treatments, immunotherapies and vaccines is likely to require a much better understanding of the molecular and cellular determinants of *T. cruzi* persistence at the tissue-specific and even hyper-local, intra-tissue scale.

Advances in studies of tissue-specific infection dynamics

While *T. cruzi* must spend some time in extracellular environments of the blood and interstitial fluid to sustain infections and ensure transmission, it is predominantly an intracellular parasite of solid organs. Consequently, most of what is known of the cells and tissues targeted by *T. cruzi* comes from experimental animal studies. It is difficult to obtain robust data on tissue distribution in human patients, although post-mortem, transplant and biopsy results tend to be consistent with animal models. The mouse is the species of choice, but other rodents, rabbits, dogs and non-human primates have also demonstrated utility (25). Tissue-specific parasite loads can be measured by a range of direct and indirect methods (reviewed in (26). Developments in real-time bioluminescence imaging methods have underpinned much recent progress in understanding *T. cruzi* infection dynamics (4, 5, 27-31). These systems are based on transgenic parasites expressing luciferases, enabling analysis of light signals emitted by parasites in discrete anatomical locations. Major advantages include greatly reduced tissue sampling bias and the ability to monitor individual mice over time. Bioluminescence lacks the resolution necessary to visualise parasites at individual cell scale, but this can be achieved using parasites expressing fluorescent reporters (21, 32, 33), an approach that becomes particularly powerful when luciferase-fluorescence fusion proteins are employed (22, 34) (Figure 1). The possibility to integrate these imaging methods with analyses of concomitant immune responses (35) holds considerable promise for advancing our understanding of *T. cruzi* – host interactions.

Stage 1: *T. cruzi* systemic colonisation and innate responses

In vectorial transmission scenarios, infection results from contamination of the triatomine bite wound or of mucosal membranes with trypomastigotes present in the bug's faeces. Transmission may also occur orally, via contaminated food or drink, *in utero*, and by blood transfusion and organ transplant. Several mechanisms

of host cell invasion have been described and reviewed elsewhere (36). In humans, oedema with intense mononuclear infiltrate at the entry site in the skin (chagoma) or eye (Romaña's sign) indicate an initially very localised infection (37). However, the true extent of trypomastigote dissemination is not clear and surprisingly little is known at the cellular level about the actual sites of primary invasion and the first cycle of intracellular parasite replication, which lasts approximately one week. Experimental animal studies indicate that the route of inoculation is a key factor. Intra-peritoneal injection results in similar parasite numbers in diverse tissues after six days (38). Conversely, oral transmission results in highly localised infections in the stomach or nasomaxillary tissues (31, 38, 39) with initial infection of the local mucosal epithelium (40). Similarly, after conjunctival inoculation, parasites first invaded and replicated in the mucosal epithelium of the nasolacrimal ducts and nasal cavities (41).

At the end of the first intracellular cycle, trypomastigotes are released and the infection disseminates widely. *T. cruzi* is pan-tropic in the acute phase of infection (reviewed in (26). However, the relative intensity of infection in different cell or tissue types again varies depending on the inoculation route, inoculum size as well as intrinsic factors such as replication rate and capacity for dissemination. Sites reported to harbour the highest acute infection intensities include skeletal, smooth and cardiac muscle and adipose tissues. Some studies have described *T. cruzi* strains with an increased capacity to parasitize mononuclear phagocytes (13, 42, 43) or to cross the blood-brain barrier (12, 44, 45).

Sensors

The host response to *T. cruzi* primary infection is considered to be markedly delayed by comparison with model intra-cytosolic pathogens (46, 47). The main features of the immediate response are the induction of type I interferon signalling and recruitment of neutrophils, macrophages and Natural Killer (NK) cells (48). Ca^{2+} mobilization, associated with invasion of myeloid cells, can activate the transcription factor NFATc1, leading to interferon gamma (IFNγ) production by NK cells and dendritic cell (DC) maturation (49). *T. cruzi* also produces multiple B cell mitogens that directly trigger a robust T-independent B cell activation (50-52).

Few canonical pathogen associated molecular patterns (PAMPs) are conserved in *T. cruzi*. The best characterised innate pattern recognition receptors (PRRs) for *T. cruzi* PAMPS are Toll-like receptor (TLR) 2 and 9. These recognise, respectively, the glycophosphatidylinositol (GPI) anchor of parasite surface proteins and parasite genomic DNA, specifically unmethylated CpG motifs (53, 54). TLR2+9 double knockout mutant mice suffer higher, parasitaemias and significantly increased mortality rates (50% by day 50) compared to wild type controls (54). Mice lacking both MyD88 and TRIF, thus rendered incapable of any TLR-mediated responses, have uncontrolled parasitaemia and 100% mortality by 18 days of infection (55). This may be explained by the additional involvement of TLR4 and TLR7, recognising parasite glycoinositolphospholipids and RNA respectively (56-58).

Many *T. cruzi* surface proteins are extensively glycosylated (2) and several host galectins (a widely expressed family of carbohydrate-binding proteins) are able to bind them (59). Interactions involving several different galectins may actually help *T. cruzi* bind to and enter host tissues (60, 61), but this does not appear to directly trigger any anti-parasitic effector activity. As an occupant of the host cell cytoplasm, it is likely that *T. cruzi* triggers cytosolic sensors. The best known candidate systems centre on NOD-like receptors (NLR). Mice lacking the NOD1 receptor suffer 100% mortality to acute *T. cruzi* infection, although the mechanism explaining this remains obscure (62). Studies also support a parasite-suppressive role for the related receptor, NLRP3 and downstream components of the inflammasome complex that drives IL-1β and IL-18 secretion (63-65), although as with NOD1 it is not clear if this involves direct sensing of *T. cruzi in vivo*.

The majority of studies of innate immunity to *T. cruzi* have focussed on responses in myeloid cells, especially macrophages, yet these could represent only a minor subset of the parasite's early targets. Transcriptomic analysis of *in vitro* infected human fibroblasts revealed that inflammatory cytokine expression peaked 24 hr post-infection and the TLR-independent type I IFN response became the dominant signature by 72 hrs, which was suggested to promote, rather than inhibit, the infection (66). Trypomastigotes have a diverse secretome comprising proteins in native form and also as cargoes in shed extracellular vesicles (67-70). Important research questions to address include whether and at what point these are relevant for triggering PRRs *in vivo* and whether there are equivalent processes for intracellular amastigotes.

After the first cycle of replication ends, host cells rupture and trypomastigotes escape into the extracellular environment. At this point, trypomastigotes may invade local tissue cells, enter infiltrating leukocytes or migrate via the blood or lymphatics to other tissues. The factors governing the parasite's propensity to stay local or not remain obscure. Host cell rupture releases intracellular material rich in danger associated molecular patterns (DAMPs), further stimulating innate signalling via TLRs as well as, for example, degranulation of nearby mast cells and activation of myeloid cells. Recently, sensing of oxidised DNA in extracellular vesicles via cyclic GMP-AMP Synthase (cGAS) was identified as an important DAMP recognition mechanism for macrophage activation (71). As a eukaryote, *T. cruzi* has endogenous orthologues of many mammalian DAMPS, potentially blurring the boundaries between DAMPs and PAMPs. For example, recombinant *T. cruzi* High Mobility Group B (TcHMGB) protein can induce production of nitric oxide (NO) in macrophages *in vitro* and expression of genes encoding inflammatory cytokine genes *in vivo* (72).

Signal Mediators and Amplifiers

A plethora of cross-talking signalling pathways are activated downstream of the PAMP/DAMP sensors described above. Signalling converges on a set of transcription factors, (NF-κβ, AP-1, IRF3) which results in production of inflammatory cytokines (73-76). Critical amongst these are the IL-12 family, IFNγ and TNF-α, the canonical drivers of type 1 immune responses required to tackle intracellular infections. IL-12 is essential for the early activation of recruited natural killer cells and their production of IFN-γ; both these cytokines are indispensable for control of parasite loads and avoidance of acute mortality (77). TNF-α is also essential for

survival of the acute stage (78). IFNγ and TNF-α activate parasite destructive effector mechanisms via autocrine and paracrine signalling. Beyond the canonical IL-12-IFNγ axis, signalling through the IL-1 receptor is essential for early (10 days p.i.) induction of myocarditis needed to control heart parasitism (65).

The local tissue response is amplified via chemokine-driven recruitment of inflammatory monocytes, macrophages, neutrophils and, eventually, antigen (Ag) specific $CD4^+$ helper T and $CD8^+$ cytotoxic T lymphocytes (Th and CTL) to the site of infection (79). Microvascular plasma leakage into parasitized tissues is promoted further by activation of mast cells and the kallikrein-kinin system (KKS), via a mechanism involving cruzipain, a parasite-derived cysteine protease (80). The resulting tissue oedema and upregulation of associated receptors on cardiomyocytes may increase specific susceptibility to heart invasion as the infection progresses (81).

Innate effectors and their evasion

The infection, cell necrosis and associated inflammatory signalling result in the activation of a range of innate effector mechanisms. There is some evidence from analysis of Beclin-1-deficient mice that host cell autophagy can provide some marginal early restraint on parasite replication (82). Epimastigotes are complement-sensitive but trypomastigotes have effective molecular mechanisms providing resistance to complement-mediated lysis (83). Infiltrating NK cells, in addition to being major producers of IFNγ, may have direct parasiticidal effects involving release of cytotoxic granules (84).

An unusual population of innate-like CD8+ T cells with activation characteristics of (e.g. production of granzyme A and IFNγ) expands in the thymus of *T. cruzi*-infected mice. These cells appear to be driven by antigen-independent mechanisms and adoptive transfer experiments of thymocytes from infected mice suggest they might provide protection from otherwise lethal challenge (85); however, the underlying mechanisms conferring this protection remain to be elucidated.

Reactive oxygen and nitrogen species (ROS, RNS) are principal effectors for *T. cruzi* control. These are generated by IFNγ/TNF-α-activated macrophages and via diverse other mechanisms in non-phagocytes and extracellular compartments (86). They are a significant cause of collateral damage in infected tissues, but high levels are necessary because *T. cruzi* has an extensive and highly effective anti-oxidant defence system (86, 87). ROS can even promote *T. cruzi* replication, by a mechanism proposed to depend on the increased availability of intracellular Fe^{2+} ions that the parasite can utilise (88). Nitric oxide (NO) is directly parasiticidal *in vitro* (89) and inducible NO synthase (iNOS) is essential for *in vivo* parasite control in some models (62, 77, 90), although not in others (63, 91).

Despite the plethora of innate responses, the overall effectiveness of *T. cruzi*'s evasion mechanisms renders it debatable whether they actually have any meaningful impact on most infections apart from the induction and conditioning of the adaptive response (see below). Indeed, *T. cruzi* infections are 100% lethal in mice

that are genetically incapable of mounting adaptive responses (SCID, RAG, nude) (92-94) and bioluminescence imaging studies show that parasite growth in such mice is close to exponential (4).

Stage 2: Adaptive responses take control

The infection usually peaks, in terms of total parasite numbers and the extent of tissue dissemination, at a point between 2 and 3 weeks post-infection. Over the following weeks, parasite loads are reduced by several orders of magnitude by a highly adaptive immune response. Although they are ultimately thought to be non-sterilizing in virtually all cases (95), it is worth reviewing the key features at the systemic level before we consider the tissue-specific host-parasite dynamics at play in the chronic phase. We also refer readers to more in-depth reviews of adaptive immunity in Chagas disease (46, 96, 97).

T and B cell activation

T. cruzi cycles between the cytosolic and extracellular compartments and, accordingly, its control is critically dependent on the generation and deployment of Ag-specific CTL to infected tissues and antibody production by B cells. This is evidenced by relevant gene disruption and antibody-mediated depletion experiments in mice (98-102). Mature DCs in the spleen and lymph nodes draining infected tissues, conditioned by the inflammatory environment, activate parasite Ag-specific $CD8^+$ and $CD4^+$ T cells from the naïve pools (47, 103). Activated T cells then migrate to sites of infection to exert effector mechanisms or in some cases begin differentiation to memory subsets (102, 104). A number of factors may impinge on the quality and magnitude of the T cell response, including parasite-driven immature thymocyte apoptosis (105) and direct and indirect modulation of DC-T cell interactions (106-109). In terms of antigen specificity, the murine T cell repertoire is focussed mainly on a small number of immunodominant epitopes from highly expressed surface proteins (110-112) but in humans there is evidence of a broader hierarchy (97, 113) and immunodominance appears not to directly contribute to chronicity.

The role of $CD4^+$ T cells is not well characterised, but the association between HIV infection and life-threatening acute *T. cruzi* relapse in humans (114) indicates they are critical for parasite control. Accordingly, mice that are specifically incapable of mounting $CD4^+$ T cell responses experience 100% acute lethality of *T. cruzi* infection (115). This has been linked to loss of support for parasite-specific $CD8^+$ T cell cytotoxicity against i.v. delivered splenocytes loaded with parasite antigens from the ASP-2 gene (99), but not in similar experiments using trans-sialidase peptides (116). This may reflect differing requirements for T cell help depending on immunodominance hierarchies (97). Nevertheless, the majority of $CD4^+$ T cells develop a protective Th1 profile and contribute further to the abundance of type 1 cytokines, particularly IFNγ (93, 117-119). Broader phenotypic diversity does develop alongside Th1 predominance, including minor Th17, Th1/Th17 intermediate and possibly Th2 subsets in some circumstances (118, 120-124). There is no clear consensus on the relevance of these to parasite control and immunopathogenesis, but this is an active area of research. The $CD4^+$ T cells that provide B cell help are termed follicular helper T cells (Tfh), and represent

a distinct $CD4^+$ T cell programme regulated by the master transcription factor Bcl6. Although activation of Tfh responses to *T. cruzi* infection has not been explored in detail, it is reasonable to hypothesize that they are required for the production of *T. cruzi*-specific antibodies and ultimate control of the infection. In line with this, IL-6, which supports Tfh differentiation (125, 126), is required for the control of parasitaemia and splenocyte recall response to parasite antigens (127), but not for T-cell independent polyclonal activation of B cell responses (51).

The initial B cell response in the spleen is estimated to be at least 10-fold higher as compared to LNs draining infected tissues (52) and a robust *T. cruzi*-specific antibody response is still generated there alongside the aforementioned polyclonal B cell activation and non-specific hyper-gammaglobulinaemia. The parasite-specific antibody response is presumably driven by B cell activation involving T cell collaboration because it is accompanied by a robust germinal centre B cell response and production of parasite-specific class-switched antibodies (52). The specific and non-specific splenic B cell responses appear to be either differentially regulated or carried out by different B cell compartments because only the latter depend on the cytokine B cell activating factor (BAFF) (128).

Activation of auto-reactive T and B cell clones, the latter leading to the production of autoantibodies, are well described phenomena during *T. cruzi* infection (129). Polyclonal B cell activation, host molecular mimicry by parasite proteins and bystander activation caused by tissue damage have been postulated as underlying mechanisms (129). There is broad evidence and consensus that parasite persistence is required to sustain these autoimmune responses (130-132). Nevertheless, the significance of autoantibodies and auto-reactive T cells for Chagas disease pathogenesis and the mechanisms involved in their production during *T. cruzi* infection remain major unresolved questions.

It has been suggested that the non-specific polyclonal B cell activation contributes to delay the generation of *T. cruzi*-specific B cell responses, thus contributing to parasite escape and establishment of chronic infections (133, 134). Polyclonal B cell activation is associated with rapid, innate-like production of IL-17 and IL-10 (135, 136) but the wider relevance is unclear as both protective (136-138) and deleterious (51, 52, 135) roles for such innate-like B cell responses have been documented in different models. The infection also causes a transient, yet marked loss of immature B cells in the bone marrow in experimental mouse models, possibly further compromising the response (139).

The kinetics of the adaptive response depend to some extent on the early parasite load (99) but in most cases it coincides with second or third intracellular cycle and is considered relatively delayed (47). Nevertheless, substantial immune memory can be generated quite rapidly: mice whose infections were cured by benznidazole anti-parasitic chemotherapy starting 4 or 14 days after infection were then able to restrict acute parasite loads in challenge infections by 85% and >99% respectively (35). Notably though, very few of these animals achieved sterile cure and they progressed to chronic phase infections that were comparable

to primary infections in naïve mice. This raises important questions about what is mediating memory responses to secondary infections, for example whether they are T cell-dependent or independent.

Adaptive effector mechanisms

Lymphocytes contribute to control of *T. cruzi* by production of type 1 cytokines that amplify the prior, innate ROS and RNS production in infected tissues. Their signature, direct effector mechanisms are also crucial. These include the principal CTL effector pathways, namely perforin-mediated delivery of granzymes and FasL-induced apoptosis. In particular, granzymes cause fatal oxidative damage to *T. cruzi*, which can be mitigated by ROS scavenging drugs or overexpression of parasite antioxidant genes (140). This may potentially be accelerated in humans by granulysin-mediated delivery of granzymes directly into intracellular parasites themselves (140). Mice do not have a granulysin gene but in most cases still achieve good control of parasite levels, so immune pressure may be more focussed on extracellular amastigotes after host cell apoptosis and on clearance of trypomastigotes. These canonical pathways are essential in some experimental models (140-142) but dispensible in others (98, 143). The difference is likely explained by other pathways providing sufficient compensatory effector capacity in lower parasite load or virulence scenarios.

T. cruzi-specific lytic and neutralizing antibodies are normally detected in humans and animal models (144-147). These are mostly produced in the spleen; antibody secretion by bone marrow cells obtained from acutely infected mice is below detection level (52). This suggests that either plasma cells generated in secondary lymphoid organs during acute *T. cruzi* infection are unable to migrate to the bone marrow, or that the bone marrow may not sustain plasma cell survival during the early phase of the infection, or that plasma cell homing in the bone marrow is somehow delayed during *T. cruzi* infection. Whether this is a temporary mechanism or extends throughout chronic infection, and whether it is a direct mechanism driven by presence of the parasite in the bone marrow, are unknown.

Antibodies target extracellular trypomastigotes but they may also have a role in binding amastigotes released from ruptured host cells, for example, downstream of CTL-mediated lysis. Opsonized parasites are efficiently taken up by tissue-resident macrophages, especially in highly-vascularised organs e.g. liver, lung, spleen (148, 149). It is not clear how a subset of trypomastigotes evade this fate to sustain chronic infections. Beyond their role as antibody producers, B cells are critically required for functional T cell responses to control *T. cruzi* infection (102, 150-152) and production of cytokines including IL-17 and IL-10 (135, 136).

Deactivating / Regulatory Mechanisms

The strong and sustained systemic inflammation, host cell lysis and tissue parasite killing in this control phase causes potentially dangerous levels of collateral tissue damage. Infections may become overtly symptomatic and in some cases fatal, particularly if the CNS is involved (153). Tissue-protective immune regulatory

pathways are therefore initiated to dampen the inflammatory response, to the benefit of the remaining parasites, which form the founding populations of the chronic infection reservoirs (Figure 3).

The factor with the strongest evidence for an important regulatory role is probably the cytokine IL-10. Early studies of IL-10 deficiency using high virulence Tulahuen strain parasites reported better control of acute *T. cruzi* parasitaemia at the expense of rapidly fatal (~2 weeks p.i.) pathogenic inflammation e.g. TNF-α-mediated toxic shock (154, 155). More recent studies point to additional complexity. Rôffe *et al* (2012) reported IL-10 was essential to protect against later mortality (3-6 weeks p.i.) associated with poor control of Colombiana strain tissue parasite loads and increased myocarditis intensity. In still lower virulence scenarios, the absence of IL-10 has been associated with reduced CTL effector function but without any increased mortality (156). Both $CD8^+$ and $CD4^+$ T cells are IL-10 sources and a high proportion simultaneously produce IFNγ (157), likely supported by IL-27 production (158) and potentially in direct response to parasite shed *trans*-sialidase (123). B cells also produce IL-10 (135) and overall IL-10 production is lower in B1 B cell-deficient mice early during infection (159). CD11b+ B1 B cells from asymptomatic, infected individuals show increased capacity to produce IL-10 compared to those with cardiac disease symptoms (138). In addition, recent data shows that when compared to non-infected donors, chronically *T. cruzi*-infected individuals with cardiac manifestations have an increased proportion of immature transitional $CD24^{high}CD38^{high}$ and naïve B cells able to produce IL-10 upon *in vitro* re-stimulation (160). This suggests B cell-intrinsic IL-10 signalling might be important to regulate the intense adaptive immune response, as is the case for other parasitic infections (161), but direct mechanistic evidence is required to support this hypothesis.

Transforming growth factor beta (TGF-β), another potent regulatory and tissue protective cytokine, can be activated from its latent form by a *T. cruzi* protease (cruzipain) *in vitro* (162). TGF-β signalling to T cells reduces the risk of late acute mortality and this appears to involve inhibition of cell proliferation rather than suppression of inflammatory cytokine production (106, 163). Other factors potentially contributing to early inhibition of adaptive immune effector responses include suppressor of cytokine signalling (SOCS) (164), regulatory $CD4^+$ T cells (Tregs) (106, 165) and induction of various regulatory/suppressive myeloid cell phenotypes, for example expression of iNOS-limiting arginase (109, 166, 167).

The overall result of these deactivating pathways is the avoidance of potentially life-threatening levels of inflammation and tissue damage at the expense of incomplete clearance of the infection (Figures 2 and 3). The situation at the tissue-specific level, however, is likely to be more complex because only a subset of tissues serve as privileged sites for *T. cruzi* persistence in the chronic phase (26).

Stage 3: The 1% and the chronic host-parasite equilibrium

In the chronic phase, blood parasitaemia is typically sub-patent and tissue parasite loads are between 0.1 and 1% of their levels in the acute phase (4, 29). Animal imaging studies (4) and serial analysis of patient

blood by PCR (168) show infection levels fluctuate over time, pointing to a dynamic equilibrium between intracellular parasite replication, antibody and effector T cell activity. The state of this equilibrium at the organismal level is the product of many discrete host-parasite interactions within and between multiple tissues (Figure 2). Over time, these interactions can become overtly pathological and subsets of infected people develop a spectrum of symptomatic forms of Chagas disease, as reviewed elsewhere (169).

Given the difficulty in sampling tissue parasites from humans, most of our knowledge on their tissue distribution comes from animal models. These indicate that chronic infection dynamics are shaped by the combination of *T. cruzi* strain and the host's genetic background. It appears that the GI tract, mainly the large intestine and stomach, is a universal site of continual parasite persistence in mice (29, 170, 171). The well-studied parasite strain CL Brener is also commonly detected in the skin of BALB/c mice (38) but only sporadically in other sites e.g. skeletal muscle, lung, adipose. More virulent parasite strains (e.g. Brazil, Colombiana, Tulahuen, VFRA) and certain mice (e.g. C3H) are associated with more disseminated infections, including heart and skeletal muscle localisation (29, 170-176). There have been few robust data on the relevant cell types within any of these chronically infected tissues, but recent *in vivo* imaging analysis at single cell resolution revealed smooth muscle cells as the most frequent targets in the colon (176).

A population of central memory T cells (T_{CM}) is detectable during the chronic phase of infection, which may stem from a lack of parasite antigen in lymph nodes draining non-parasitized organs (104, 177). These T_{CM} are maintained after benznidazole-mediated cure of chronic infection and provide protection against re-challenge after transfer into naïve mice (178). Homologous challenge infections, in drug-cured mice themselves, result in acute parasite loads less than 1% of those in primary infection controls and fully sterile protection is seen in around half of the animals (35). The determinants of both categories of protection remain to be defined, but it is likely critically dependent on the T_{CM} population. It is likewise an open question whether T_{CM}-derived effectors contribute to suppression of tissue parasite numbers during chronic infections, particularly in organs subject to cycles of episodic re-invasion and clearance.

The mechanisms of immune evasion sustaining the host-parasite equilibrium during perpetual chronic infection are not necessarily the same as those that prevent sterile clearance in the acute to chronic transition, which resemble a conserved host tissue-protective, anti-inflammatory programme. They are also harder to study, both from the parasite perspective, owing to the scarcity of *T. cruzi* foci in tissues, and from the host perspective because of the need for conditional intervention techniques that can be applied after acute infections have been brought under control. The essentiality of $CD8^+$ T cells for continued suppression of parasite numbers in the chronic phase is reasonably clear. Parasite loads rapidly rebound upon treatment with anti-CD8 antibodies, almost to the level seen with pan-adaptive immunosuppression using cyclophosphamide (175, 179), although depletion of $CD8^+$ NK cells and DCs may contribute to the relapse in addition to CTLs. Unlike in the acute phase, experimental anti-CD4 treatment has no effect on chronic parasite loads (179). Nevertheless, severe reactivation of Chagas disease in HIV co-infected patients

indicates $CD4^+$ T cells are vital for control and the frequent presentation of meningoencephalitis points to a specific role in protection against invasion of the CNS (114).

There are various non-exclusive hypotheses for how a small subpopulation of parasites reliably evades sterilisation in the face of the sustained adaptive immune pressure. However, in our view none currently has compelling evidence supporting a mechanistic explanation so this will remain an active area of investigation.

1. Antigenic diversity

African trypanosomes famously evade host immunity using a system of antigenic variation, involving tightly regulated mono-allelic expression and switching of variant surface glycoprotein genes (180) but this is not conserved in *T. cruzi*. The *T. cruzi* genome contains enormous repetitive arrays of surface protein genes and there is evidence that some of these gene families or sub-families are reserved for expression in specific life cycle stages (2, 181). Signatures of strong positive selection in surface gene families (182) indicate immune pressure for diversification of antigens. At the population level, simultaneous expression of massively diverse 'decoy' antigens may conceivably prevent T or B cell clones specific to any particular epitope from reaching sufficient frequency in infected tissues and/or effector capacity (83, 112, 181, 183) but direct evidence for this is lacking.

Very little is known about how variant copy expression may be controlled at the individual cell level i.e. amongst amastigotes and amongst trypomastigotes. Investigating this is difficult, because gene control is mainly post-transcriptional and suitable variant-specific monoclonal antibodies are lacking. Available evidence suggests that within a class of surface proteins, expression in individual parasites is not strictly mono-allelic. For example, trypomastigotes can co-express at least two members of the mucin (184) and GP85 families (183). The finding that a specific mucin-associated surface protein (MASP) peptide was only expressed in ~5% of parasites indicates that neither is expression totally promiscuous at the protein level (185). Mechanisms controlling the expression of parasite surface proteins may therefore vary between gene families or sub-families. *T. cruzi* may also regulate its antigenic repertoire expression between infection phases and between different host cell types. This requires much deeper analysis because currently there is insufficient data to rule out clonal antigenic variation as a mechanism contributing to perpetual immune evasion.

2. Parasite dormancy

Many pathogens use dormancy or metabolic quiescence as an immune evasion strategy (186, 187). At the population level, *T. cruzi* amastigotes can rapidly decrease their replication rate in response to changes in *in vitro* culture conditions but this is a function of a longer G_1 phase rather than exit from the cell cycle (188). Individual non-replicating amastigotes also occur spontaneously *in vitro* and are less susceptible to the anti-parasitic drug benznidazole (21). The frequency of 4-day replication arrested *in vitro* amastigotes has been

estimated to be approximately 0.1 – 6 %, depending on the parasite strain (189). The *in vivo* relevance of these phenomena remains almost completely unknown and will be hard to establish definitively, not least because neither amastigote DNA/kDNA replication, nor differentiation to constitutively non-replicating trypomastigotes is synchronised (22). Nevertheless, it is reasonable to suspect that slowly replicating or transiently arrested intracellular parasites could have a selective advantage under immunological pressure and play a role in sustaining chronic infections.

3. Cytokine-mediated suppression of type 1 responses

T. cruzi may continue to benefit from the above-mentioned conserved negative-feedback mechanisms that damp down the acute inflammatory response. However, administration of blocking antibodies targeting IL-10 signalling had no discernible effect on chronic *T. cruzi* infections (175). This is in stark contrast to the well-established role of IL-10 in promoting chronicity of infections with the related parasite *Leishmania* spp. (190), which predominantly infects professional antigen-presenting cells. Chemical inhibition of the TGF-beta type I receptor significantly alleviated cardiac pathology and function in chronically infected mice, but this was not associated with any change in heart parasite loads (191). It should be noted that parasite loads in the chronic phase are often close to the limit of detection, which means that in these types of intervention experiment it is relatively clear when immunity is compromised, but difficult to conclusively demonstrate a significant enhancement of infection control.

Cytokine gene expression in heart tissue from human patients with severe chronic Chagas cardiomyopathy remains strongly polarised to a type 1 profile (192). Type 2 cytokine (IL-4, IL-5, IL-13) expression is reported as undetectable (192) and while it is a feature of some animal models, this is apparently not at the expense of IFNγ production (170). Interestingly, helminth co-infection is associated with reduced control of *T. cruzi* in a subset of patients, potentially as a result of a modulation of the cytokine balance (193). Overall, cytokine-mediated suppression of anti-parasitic type 1 inflammation likely influences the host-parasite equilibrium and long-term disease progression, but there is little evidence that it explains *T. cruzi* chronicity.

4. Immunological exhaustion

T cell exhaustion is a feature of many infectious and non-infectious diseases that involve chronic antigen stimulation and this has been a recent focus of research in the Chagas disease field. Analysis of PBMCs from Chagas patients revealed increased frequencies of $CD4^+$ and $CD8^+$ T cells expressing exhaustion markers e.g. PD-1^+, CTLA4^+, TIM-3^+ (194-196). Experimental studies suggest the development of exhaustion characteristics may be promoted by suboptimal B cell (152), IL-17A (197) or IL-10 (198) immune responses. Nevertheless, in chronically infected children and mice, both effector and memory $CD8^+$ T cells retain cytotoxic capacity and there is little to no evidence of *functional* exhaustion (119, 152, 175, 178, 199). Infection chronicity may also promote dysregulation of the Tfh and B cell compartments, for example, distinct phenotypes and frequencies of these have been noted between symptomatic and asymptomatic *T. cruzi*-

infected individuals (200, 201). Whether these alterations reflect a process of B-cell exhaustion which negatively impacts parasite control remains to be further elucidated. In summary, while deterioration of lymphocyte functional capacity may potentially be associated with progression from asymptomatic to symptomatic disease states, via progressively loosened control of parasite loads, exhaustion does not seem to be a core reason for parasite persistence *per se*.

5. Local and hyper-local immune privilege

The realisation that long-term *T. cruzi* infections exhibit an unexpectedly high degree of spatio-temporal dynamism (4) indicates that host responses and evasion mechanisms, including those set out above, need to be studied more intensively at the tissue-specific level. Motile trypomastigotes probably traffic between tissues in both blood and lymph, but there is also evidence that a significant amount of parasite trafficking between tissues may occur inside $SLAMF1^{+}$ myeloid cells, akin to a Trojan horse strategy (202). Consequently, parasites from privileged reservoir sites, such as the digestive tract, may seed other, less permissive sites such as the heart, resulting in episodic cycles of re-invasion and locally sterilizing host responses (26) (Figure 2). Tissue-specific variability in permissiveness is consistent with divergent responses observed in different secondary lymphoid organs (203). Moreover, when chronically infected mice are immunosuppressed, the infection relapses first in the GI tract and then disseminates to other organs (29). Host microbiota may also play a role: its composition can be modulated by *T. cruzi* infection (204), but it is not yet known whether this in turn influences anti-parasite immunity in barrier tissues.

To keep up with the parasite, effector cells must be continually deployed to infection foci in many organs. There appears to be no problem with T cell homing and entry into infected tissues (205), which is dependent on expression of integrins including VLA-4 and LFA-1 (175, 206), and CXCR3 chemokine receptor signalling (207). After extravasation though, the distinct microenvironment of each organ potentially drives phenotypic changes to infiltrating cells and in some cases the effect may be tolerogenic and incompatible with local sterilisation. For example, skeletal muscle bulk CTLs recovered from early chronic phase mice produced less IFNγ and had greatly diminished cytotoxic activity compared to splenic CTLs (208). Similar results have been reported for cardiac muscle compared to blood (205). Intriguingly, splenic CTLs adoptively transferred from one chronically infected mouse to another retained a high IFNγ response phenotype if they migrated to spleen or lung tissue, but lost it if they migrated to skeletal muscle or liver (208). More recently, however, direct *ex vivo* analysis of parasite-specific CTLs without antigen re-stimulation showed cells from chronically infected skeletal muscle tissue had equal or even greater effector capacity (production of IFNγ, TNF-α, granzyme B) than spleen-derived cells (175). To our knowledge, detailed analysis of CTLs in smooth muscle has yet to be conducted.

There is thus likely to be further compartmentalisation of response and evasion dynamics at the intra-organ level, perhaps even down to the hyper-local scale of individual infected cells' microenvironments. For example, the muscular, neuronal and mucosal layers of the GI tract, a key site of *T. cruzi* persistence, have

distinct immunological microenvironments that respond differently to *Salmonella* infection (209). Recent work has highlighted differences in the cellular composition of perivascular and parenchymal inflammatory infiltrates in *T. cruzi*-infected skeletal muscle (172, 179). Large, apparently immunologically invisible parasite nests even occur immediately adjacent to severely inflamed blood vessels, which led these authors to suggest leukocytes might fail to migrate through the parenchyma to infected cells because chemoattractant signalling is too weak in low parasite load settings (172). Immune evasion may also operate at the level of physical interaction between T cells and parasite antigen presenting cells, for example via manipulation of MHC class I or II expression (107, 210-212) or by parasitism of muscle cells, which are poor activators of NF-κB upon *T. cruzi* infection (76) and, in the case of skeletal muscle, do not normally express MHC class I (213).

Conclusions

From its origins in ancient South American fauna, *T. cruzi* has spread to diverse mammalian orders across the Americas and become a widespread human pathogen. This reflects a remarkable adaptability to evade mammalian immune responses and maintain enzootic, zoonotic and anthroponotic transmission cycles. As we have set out, this involves sophisticated molecular mechanisms that allow *T. cruzi* to resist innate responses so that in the early stages of infection parasite loads are high and widely disseminated in blood and solid organs. The adaptive immune response, principally effected by CTLs and antibodies, is able to eliminate ~99% of the parasites. The infection then transitions to a permanent chronic phase in which parasites replicate, mainly within muscle cells in a small number of privileged tissues, in a dynamic equilibrium with host responses. The available evidence supports the existence of a complex set of molecular and cellular mediators that firstly, prevent complete sterile clearance at the acute to chronic transition and, secondly, ensure perpetual parasite persistence during the chronic phase. These include parasite-intrinsic evasion mechanisms, direct and indirect manipulation of host responses, and host-intrinsic deactivating feedback loops. Further complexity arises from *T. cruzi*'s cycling between intra and extra-cellular parasite forms and its trafficking between different organs, tissues and cells, each with specific immunological microenvironments of variable permissiveness.

Important advances in fundamental aspects of tissue level immunity have yet to be investigated in detail in the Chagas disease field, for example, defining relative contributions of tissue resident and inflammatory myeloid cells, innate lymphoid cell populations, tissue resident memory T cells and neuro-immune interactions. Further progress in understanding *T. cruzi*-host interactions and how they shape Chagas disease pathogenesis is also likely to come from more intensive research at the tissue-specific and even single cell scale. Some key questions include: (i) Why do some infected people remain asymptomatic carriers while others progress to life-threatening disease states? (ii) Does active infection support concomitant immunity to second infections? (iii) Do drug-cured patients have protective immunity to re-infection? (iv) Can vaccines be developed that provide sterile protection? (v) To what degree are the proposed mechanisms of

immune evasion actually enabling parasite persistence *in vivo* in different tissues? (vi) How do host-parasite interactions promote or limit *in utero* transmission? The difficulties of answering these questions and addressing the wider challenges in Chagas disease biomedicine are great; however, the massive unmet need for better treatments, prophylaxis and diagnostics requires us to overcome them.

Figures

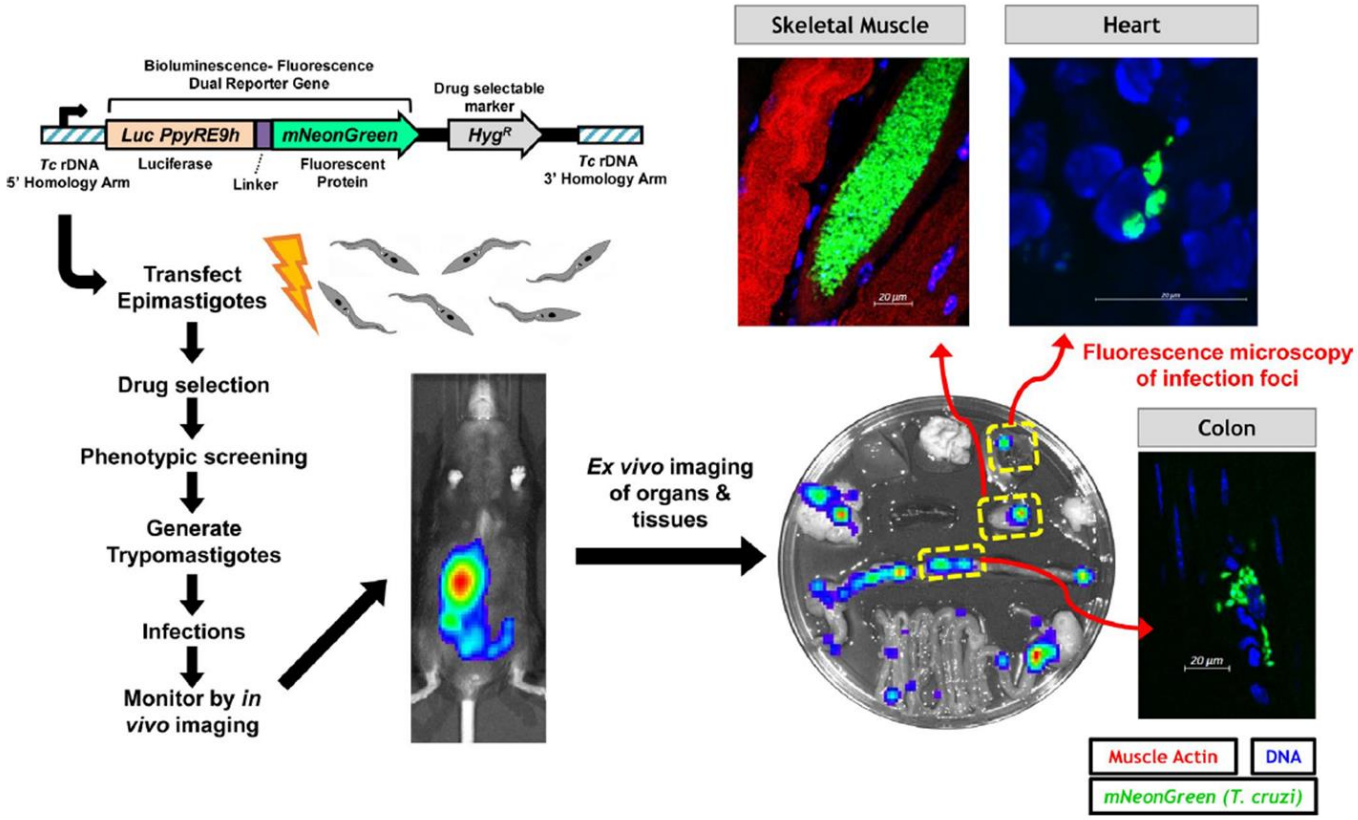

FIGURE 1 Visualization of *Trypanosoma cruzi* infection foci in vivo using bioluminescent-fluorescent dual reporter parasites

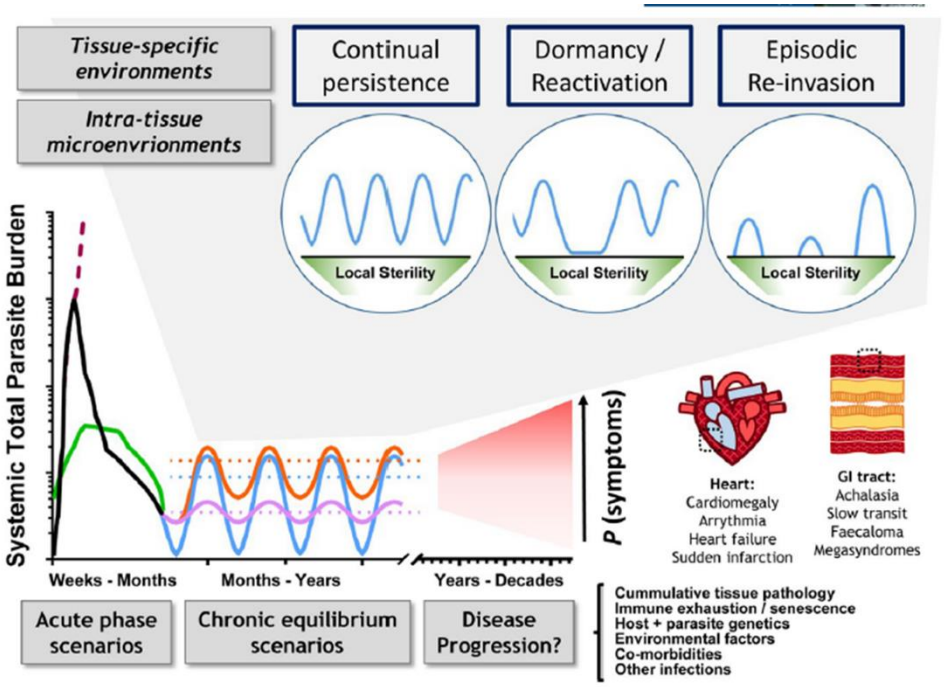

FIGURE 2 Overview of host-parasite interaction dynamics in *Trypanosoma cruzi* infections. Chart illustrates some alternative course of infection scenarios for acute and chronic phase total parasite burdens, feeding into potential clinical outcomes, which range from long-term non-progression to severe Chagas disease affecting the heart and/or gastrointestinal tract. The chronic equilibrium scenarios are the product of many temporally overlapping host-parasite interactions within and between the various organs targeted for infection by *T cruzi*. Three possible, non-mutually exclusive modes of persistence at the tissue or tissue sub-domain level are illustrated above the chart, continual persistence, dormancy/reactivation and episodic re-invasion.

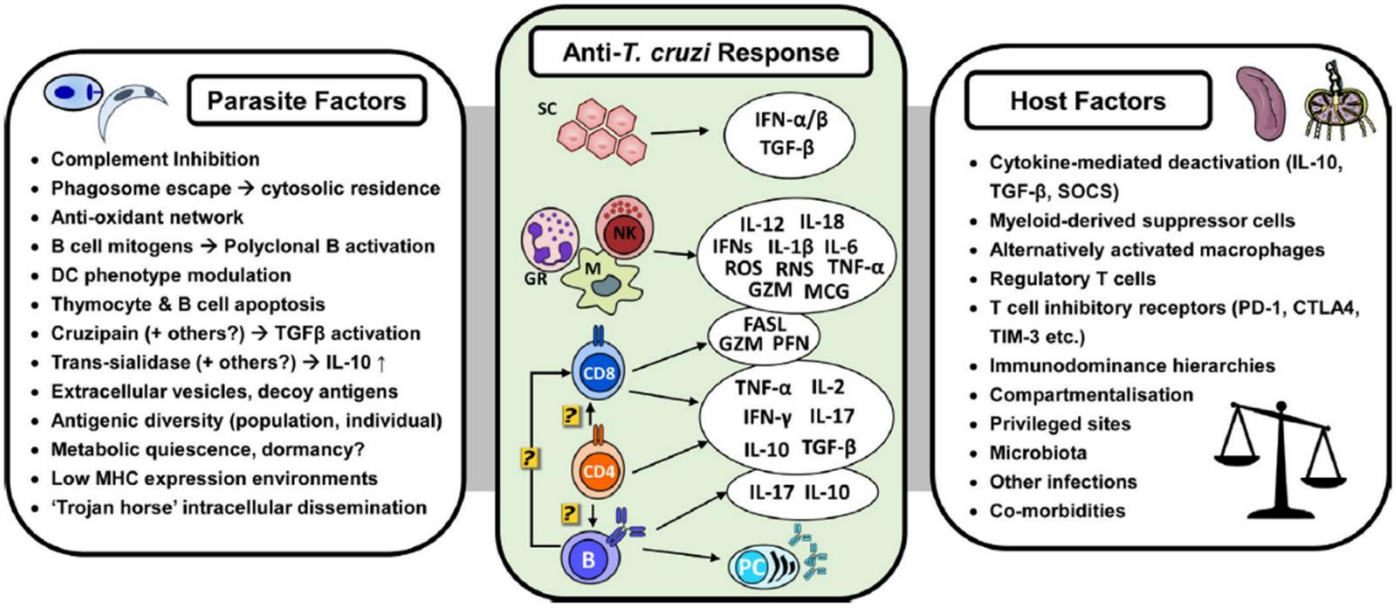

FIGURE 3 Overview of the principal cellular and molecular components of the immune response to *Trypanosoma cruzi* infection. Central panel shows key cell types, cytokines and effector molecules. B, B cell; CD4, helper T cell; CD8, cytotoxic T cell; GR, granulocytes; M, myeloid cells; NK, natural Killer cells; PC, plasma cell; SC, somatic cells. Left and right panels show parasite and host factors potentially contributing to infection chronicity.

References

1. Brenière SF, Waleckx E, Barnabé C. Over Six Thousand *Trypanosoma cruzi* Strains Classified into Discrete Typing Units (DTUs): Attempt at an Inventory. PLOS Neglected Tropical Diseases. 2016;10(8):e0004792.
2. Buscaglia CA, Campo VA, Frasch AC, Di Noia JM. *Trypanosoma cruzi* surface mucins: host-dependent coat diversity. Nature Reviews Microbiology. 2006;4(3):229 - 36.
3. Barisón MJ, Rapado LN, Merino EF, Pral EMF, Mantilla BS, Marchese L, et al. Metabolomic profiling reveals a finely tuned, starvation-induced metabolic switch in *Trypanosoma cruzi* epimastigotes. Journal of Biological Chemistry. 2017;292(21):8964-77.
4. Lewis MD, Francisco AF, Taylor MC, Burrell-Saward H, McLatchie AP, Miles MA, et al. Bioluminescence imaging of chronic *Trypanosoma cruzi* infections reveals tissue-specific parasite dynamics and heart disease in the absence of locally persistent infection. Cell Microbiol. 2014;16(9):1285-300.
5. Hyland KV, Asfaw SH, Olson CL, Daniels MD, Engman DM. Bioluminescent imaging of *Trypanosoma cruzi* infection. Int J Parasitol. 2008;38(12):1391-400.
6. Zhang L, Tarleton RL. Parasite Persistence Correlates with Disease Severity and Localization in Chronic Chagas' Disease. J Infect Dis. 1999;180(2):480-6.
7. Francisco AF, Lewis MD, Jayawardhana S, Taylor MC, Chatelain E, Kelly JM. The limited ability of posaconazole to cure both acute and chronic *Trypanosoma cruzi* infections revealed by highly sensitive in vivo imaging. Antimicrobial Agents and Chemotherapy. 2015;59(8):4653-61.
8. Lenzi HL, Oliveira DN, Lima MT, Gattass CR. *Trypanosoma cruzi*: Paninfectivity of CL Strain during Murine Acute Infection. Exp Parasitol. 1996;84(1):16-27.
9. Guarner J, Bartlett J, Zaki SR, Colley DG, Grijalva MJ, Powell MR. Mouse model for Chagas disease: immunohistochemical distribution of different stages of *Trypanosoma cruzi* in tissues throughout infection. The American Journal of Tropical Medicine and Hygiene. 2001;65(2):152-8.
10. Morocoima A, Rodríguez M, Herrera L, Urdaneta-Morales S. *Trypanosoma cruzi*: experimental parasitism of bone and cartilage. Parasitology Research. 2006;99(6):663-8.
11. Calabrese KS, Lagrange PH, da Costa SC. *Trypanosoma cruzi*: histopathology of endocrine system in immunocompromised mice. Int J Exp Pathol. 1994;75(6):453-62.
12. Postan M, Dvorak JA, McDaniel JP. Studies of *Trypanosoma cruzi* Clones in Inbred Mice: I. A Comparison of the Course of Infection of C3H/HEN- Mice with Two Clones Isolated from a Common Source. Am J Trop Med Hyg. 1983;32(3):497-506.
13. Melo R, Brener Z. Tissue tropism of different *Trypanosoma cruzi* strains. J Parasitol. 1978;64(3):475-82.
14. Buckner FS, Wilson AJ, Van Voorhis WC. Detection of Live *Trypanosoma cruzi* in Tissues of Infected Mice by Using Histochemical Stain for β-Galactosidase. Infection and Immunity. 1999;67(1):403-9.
15. Camandaroba E, Thé TS, Pessina DH, Andrade SG. *Trypanosoma cruzi*: clones isolated from the Colombian strain, reproduce the parental strain characteristics, with ubiquitous histotropism. International Journal of Experimental Pathology. 2006;87(3):209-17.
16. Gómez-Hernández C, Rezende-Oliveira K, Nascentes GAN, Batista LR, Kappel HB, Martinez-Ibarra JA, et al. Molecular characterization of *Trypanosoma cruzi* Mexican strains and their behavior in the mouse experimental model. Revista da Sociedade Brasileira de Medicina Tropical. 2011;44:684-90.
17. Almeida-de-Faria M, Freymüller E, Colli W, Alves MJM. *Trypanosoma cruzi*: Characterization of an Intracellular Epimastigote-like Form. Experimental Parasitology. 1999;92(4):263-74.
18. Tyler KM, Engman DM. The life cycle of *Trypanosoma cruzi* revisited. International Journal for Parasitology. 2001;31(5-6):472-80.
19. Kessler RL, Contreras VT, Marliére NP, Guarneri AA, Silva LHV, Mazzarotto GACA, et al. Recently differentiated epimastigotes from *Trypanosoma cruzi* are infective to the mammalian host. Molecular Microbiology. 2017;104(5):712-36.
20. Kurup Samarchith P, Tarleton Rick L. The *Trypanosoma cruzi* Flagellum Is Discarded via Asymmetric Cell Division following Invasion and Provides Early Targets for Protective CD8+ T Cells. Cell Host & Microbe. 2014;16(4):439-49.
21. Sánchez-Valdéz FJ, Padilla A, Wang W, Orr D, Tarleton RL. Spontaneous dormancy protects *Trypanosoma cruzi* during extended drug exposure. eLife. 2018;7:e34039.
22. Taylor MC, Ward A, Olmo F, Jayawardhana S, Francisco AF, Lewis MD, et al. Intracellular DNA replication and differentiation of *Trypanosoma cruzi* is asynchronous within individual host cells *in vivo* at all stages of infection. PLOS Neglected Tropical Diseases. 2020;14(3):e0008007.

23. Sabino EC, Ribeiro AL, Salemi VMC, Di Lorenzo Oliveira C, Antunes AP, Menezes MM, et al. Ten-Year Incidence of Chagas Cardiomyopathy Among Asymptomatic *Trypanosoma cruzi*–Seropositive Former Blood Donors. Circulation. 2013;127(10):1105-15.
24. Rassi Jr A, Rassi A, Marin-Neto JA. Chagas disease. Lancet. 2010;375(9723):1388-402.
25. Chatelain E, Konar N. Translational challenges of animal models in Chagas disease drug development: a review. Drug design, development and therapy. 2015;9:4807.
26. Lewis MD, Kelly JM. Putting Infection Dynamics at the Heart of Chagas Disease. Trends Parasitol. 2016;32(11):899-911.
27. Andriani G, Chessler A-DC, Courtemanche G, Burleigh BA, Rodriguez A. Activity *In Vivo* of Anti-*Trypanosoma cruzi* Compounds Selected from a High Throughput Screening. PLoS Negl Trop Dis. 2011;5(8):e1298.
28. Henriques C, Henriques-Pons A, Meuser-Batista M, Ribeiro AS, de Souza W. In vivo imaging of mice infected with bioluminescent *Trypanosoma cruzi* unveils novel sites of infection. Parasites & Vectors. 2014;7(1):1-15.
29. Lewis MD, Francisco AF, Taylor MC, Jayawardhana S, Kelly JM. Host and parasite genetics shape a link between *Trypanosoma cruzi* infection dynamics and chronic cardiomyopathy. Cell Microbiol. 2016;18(10):1429-43.
30. Silberstein E, Serna C, Fragoso SP, Nagarkatti R, Debrabant A. A novel nanoluciferase-based system to monitor *Trypanosoma cruzi* infection in mice by bioluminescence imaging. PLOS ONE. 2018;13(4):e0195879.
31. Silva-dos-Santos D, Barreto-de-Albuquerque J, Guerra B, Moreira OC, Berbert LR, Ramos MT, et al. Unraveling Chagas disease transmission through the oral route: Gateways to *Trypanosoma cruzi* infection and target tissues. PLoS Negl Trop Dis. 2017;11(4):e0005507.
32. Ferreira BL, Orikaza CM, Cordero EM, Mortara RA. *Trypanosoma cruzi*: single cell live imaging inside infected tissues. Cellular Microbiology. 2016;18(6):779-83.
33. Canavaci AMC, Bustamante JM, Padilla AM, Perez Brandan CM, Simpson LJ, Xu D, et al. *In Vitro* and *In Vivo* High-Throughput Assays for the Testing of Anti-*Trypanosoma cruzi* Compounds. PLoS Negl Trop Dis. 2010;4(7):e740.
34. Costa FC, Francisco AF, Jayawardhana S, Calderano SG, Lewis MD, Olmo F, et al. Expanding the toolbox for *Trypanosoma cruzi*: A parasite line incorporating a bioluminescence-fluorescence dual reporter and streamlined CRISPR/Cas9 functionality for rapid in vivo localisation and phenotyping. PLOS Neglected Tropical Diseases. 2018;12(4):e0006388.
35. Mann GS, Francisco AF, Jayawardhana S, Taylor MC, Lewis MD, Olmo F, et al. Drug-cured experimental *Trypanosoma cruzi* infections confer long-lasting and cross-strain protection. PLOS Neglected Tropical Diseases. 2020;14(4):e0007717.
36. Fernandes MC, Andrews NW. Host cell invasion by *Trypanosoma cruzi*: a unique strategy that promotes persistence. FEMS Microbiology Reviews. 2012;36(3):734-47.
37. Machado FS, Dutra WO, Esper L, Gollob KJ, Teixeira MM, Factor SM, et al. Current understanding of immunity to *Trypanosoma cruzi* infection and pathogenesis of Chagas disease. Seminars in Immunopathology. 2012;34(6):753-70.
38. Lewis MD, Francisco AF, Jayawardhana S, Langston H, Taylor MC, Kelly JM. Imaging the development of chronic Chagas disease after oral transmission. Scientific Reports. 2018;8(1):11292.
39. Shikanai-Yasuda MA, Carvalho NB. Oral Transmission of Chagas Disease. Clin Infect Dis. 2012;54(6):845-52.
40. Hoft DF, Farrar PL, Kratz-Owens K, Shaffer D. Gastric invasion by *Trypanosoma cruzi* and induction of protective mucosal immune responses. Infection and Immunity. 1996;64(9):3800-10.
41. Giddings OK, Eickhoff CS, Smith TJ, Bryant LA, Hoft DF. Anatomical Route of Invasion and Protective Mucosal Immunity in *Trypanosoma cruzi* Conjunctival Infection. Infection and Immunity. 2006;74(10):5549-60.
42. Andrade SG, Magalhães JB. Biodemes and zymodemes of *Trypanosoma cruzi* strains: correlations with clinical data and experimental pathology. Rev Soc Bras Med Tro. 1997;30:27-35.
43. Taliaferro WH, Tulo P. Connective Tissue Reactions in Normal and Immunized Mice to a Reticulotropic Strain of *Trypanosoma cruzi.* Journal of Infectious Diseases. 1955;96(3):199-226.
44. Zeledón R, Ponce C. Neurotropism in Costa Rican strains of *Trypanosoma cruzi*. J Parasitol. 1972;58(1):180-1.
45. Córdova E, Maiolo E, Corti M, Orduña T. Neurological manifestations of Chagas' disease. Neurological Research. 2010;32(3):238-44.

46. Tarleton RL. CD8+ T cells in *Trypanosoma cruzi* infection. Seminars in immunopathology. 2015;37(3):233-8.
47. Padilla AM, Simpson LJ, Tarleton RL. Insufficient TLR Activation Contributes to the Slow Development of CD8+ T Cell Responses in *Trypanosoma cruzi* Infection. The Journal of Immunology. 2009;183(2):1245-52.
48. Chessler A-DC, Unnikrishnan M, Bei AK, Daily JP, Burleigh BA. *Trypanosoma cruzi* Triggers an Early Type I IFN Response In Vivo at the Site of Intradermal Infection. The Journal of Immunology. 2009;182(4):2288-96.
49. Kayama H, Koga R, Atarashi K, Okuyama M, Kimura T, Mak TW, et al. NFATc1 Mediates Toll-Like Receptor-Independent Innate Immune Responses during *Trypanosoma cruzi* Infection. PLOS Pathogens. 2009;5(7):e1000514.
50. Reina-San-Martín B, Degrave W, Rougeot C, Cosson A, Chamond N, Cordeiro-da-Silva A, et al. A B-cell mitogen from a pathogenic trypanosome is a eukaryotic proline racemase. Nature Medicine. 2000;6(8):890--7.
51. Gao W, Wortis HH, Pereira MA. The *Trypanosoma cruzi* trans-sialidase is a T cell-independent B cell mitogen and an inducer of non-specific Ig secretion. International Immunology. 2002;14(3):299-308.
52. Bermejo DA, Amezcua Vesely MC, Khan M, Acosta Rodríguez EV, Montes CL, Merino MC, et al. *Trypanosoma cruzi* infection induces a massive extrafollicular and follicular splenic B-cell response which is a high source of non-parasite-specific antibodies. Immunology. 2011;132(1):123-33.
53. Campos MAS, Almeida IC, Takeuchi O, Akira S, Valente EP, Procópio DO, et al. Activation of Toll-Like Receptor-2 by Glycosylphosphatidylinositol Anchors from a Protozoan Parasite. The Journal of Immunology. 2001;167(1):416-23.
54. Bafica A, Santiago HC, Goldszmid R, Ropert C, Gazzinelli RT, Sher A. Cutting Edge: TLR9 and TLR2 Signaling Together Account for MyD88-Dependent Control of Parasitemia in *Trypanosoma cruzi* Infection. J Immunol. 2006;177(6):3515-9.
55. Koga R, Hamano S, Kuwata H, Atarashi K, Ogawa M, Hisaeda H, et al. TLR-Dependent Induction of IFN-beta Mediates Host Defense against *Trypanosoma cruzi*. J Immunol. 2006;177(10):7059-66.
56. Oliveira A-C, de Alencar BC, Tzelepis F, Klezewsky W, da Silva RN, Neves FS, et al. Impaired Innate Immunity in Tlr4$^{-/-}$ Mice but Preserved CD8+ T Cell Responses against *Trypanosoma cruzi* in Tlr4-, Tlr2-, Tlr9- or Myd88-Deficient Mice. PLOS Pathogens. 2010;6(4):e1000870.
57. Oliveira A-C, Peixoto JR, de Arruda LB, Campos MA, Gazzinelli RT, Golenbock DT, et al. Expression of Functional TLR4 Confers Proinflammatory Responsiveness to *Trypanosoma cruzi* Glycoinositolphospholipids and Higher Resistance to Infection with *T. cruzi*. The Journal of Immunology. 2004;173(9):5688.
58. Caetano BC, Carmo BB, Melo MB, Cerny A, dos Santos SL, Bartholomeu DC, et al. Requirement of UNC93B1 Reveals a Critical Role for TLR7 in Host Resistance to Primary Infection with *Trypanosoma cruzi*. The Journal of Immunology. 2011;187(4):1903-11.
59. Pineda MA, Cuervo H, Fresno M, Soto M, Bonay P. Lack of Galectin-3 Prevents Cardiac Fibrosis and Effective Immune Responses in a Murine Model of *Trypanosoma cruzi* Infection. The Journal of Infectious Diseases. 2015;212(7):1160-71.
60. Benatar AF, García GA, Bua J, Cerliani JP, Postan M, Tasso LM, et al. Galectin-1 Prevents Infection and Damage Induced by *Trypanosoma cruzi* on Cardiac Cells. PLoS Negl Trop Dis. 2015;9(10):e0004148.
61. Shi W, Xue C, Su XZ, Lu F. The roles of galectins in parasitic infections. Acta Trop. 2018;177:97-104.
62. Silva GK, Gutierrez FRS, Guedes PMM, Horta CV, Cunha LD, Mineo TWP, et al. Cutting Edge: Nucleotide-Binding Oligomerization Domain 1-Dependent Responses Account for Murine Resistance against *Trypanosoma cruzi* Infection. The Journal of Immunology. 2010;184(3):1148-52.
63. Gonçalves VM, Matteucci KC, Buzzo CL, Miollo BH, Ferrante D, Torrecilhas AC, et al. NLRP3 Controls *Trypanosoma cruzi* Infection through a Caspase-1-Dependent IL-1R-Independent NO Production. PLOS Neglected Tropical Diseases. 2013;7(10):e2469.
64. Paroli AF, Gonzalez PV, Díaz-Luján C, Onofrio LI, Arocena A, Cano RC, et al. NLRP3 Inflammasome and Caspase-1/11 Pathway Orchestrate Different Outcomes in the Host Protection Against *Trypanosoma cruzi* Acute Infection. Frontiers in Immunology. 2018;9(913).
65. Silva GK, Costa RS, Silveira TN, Caetano BC, Horta CV, Gutierrez FRS, et al. Apoptosis-Associated Speck–like Protein Containing a Caspase Recruitment Domain Inflammasomes Mediate IL-1β Response and Host Resistance to *Trypanosoma cruzi* Infection. The Journal of Immunology. 2013;191(6):3373-83.

66. Li Y, Shah-Simpson S, Okrah K, Belew AT, Choi J, Caradonna KL, et al. Transcriptome remodeling in *Trypanosoma cruzi* and human cells during intracellular infection. PLoS pathogens. 2016;12(4).
67. Bayer-Santos E, Gentil LG, Cordero EM, Correa PR, Silveira JF. Regulatory elements in the 3' untranslated region of the GP82 glycoprotein are responsible for its stage-specific expression in *Trypanosoma cruzi* metacyclic trypomastigotes. Acta Trop. 2012;123.
68. de Pablos Torró LM, Retana Moreira L, Osuna A. Extracellular Vesicles in Chagas Disease: A New Passenger for an Old Disease. Frontiers in Microbiology. 2018;9(1190).
69. Ribeiro KS, Vasconcellos CI, Soares RP, Mendes MT, Ellis CC, Aguilera-Flores M, et al. Proteomic analysis reveals different composition of extracellular vesicles released by two *Trypanosoma cruzi* strains associated with their distinct interaction with host cells. Journal of Extracellular Vesicles. 2018;7(1):1463779.
70. Caeiro LD, Alba-Soto CD, Rizzi M, Solana ME, Rodriguez G, Chidichimo AM, et al. The protein family TcTASV-C is a novel *Trypanosoma cruzi* virulence factor secreted in extracellular vesicles by trypomastigotes and highly expressed in bloodstream forms. PLOS Neglected Tropical Diseases. 2018;12(5):e0006475.
71. Choudhuri S, Garg NJ. PARP1-cGAS-NF-κB pathway of proinflammatory macrophage activation by extracellular vesicles released during *Trypanosoma cruzi* infection and Chagas disease. PLOS Pathogens. 2020;16(4):e1008474.
72. Cribb P, Perdomo V, Alonso VL, Manarin R, Barrios-Payán J, Marquina-Castillo B, et al. *Trypanosoma cruzi* High Mobility Group B (TcHMGB) can act as an inflammatory mediator on mammalian cells. PLOS Neglected Tropical Diseases. 2017;11(2):e0005350.
73. Huang H, Petkova SB, Cohen AW, Bouzahzah B, Chan J, Zhou J-n, et al. Activation of Transcription Factors AP-1 and NF-κB in Murine Chagasic Myocarditis. Infection and Immunity. 2003;71(5):2859-67.
74. Chessler A-DC, Ferreira LRP, Chang T-H, Fitzgerald KA, Burleigh BA. A Novel IFN Regulatory Factor 3-Dependent Pathway Activated by Trypanosomes Triggers IFN-β in Macrophages and Fibroblasts. The Journal of Immunology. 2008;181(11):7917-24.
75. Dias WB, Fajardo FD, Graça-Souza AV, Freire-de-Lima L, Vieira F, Girard MF, et al. Endothelial cell signalling induced by trans-sialidase from *Trypanosoma cruzi*. Cellular Microbiology. 2008;10(1):88-99.
76. Hall BS, Tam W, Sen R, Pereira MEA. Cell-specific Activation of Nuclear Factor-κB by the Parasite *Trypanosoma cruzi* Promotes Resistance to Intracellular Infection. Molecular Biology of the Cell. 2000;11(1):153-60.
77. Michailowsky V, Silva NM, Rocha CD, Vieira LQ, Lannes-Vieira J, Gazzinelli RT. Pivotal Role of Interleukin-12 and Interferon-γ Axis in Controlling Tissue Parasitism and Inflammation in the Heart and Central Nervous System during *Trypanosoma cruzi* Infection. The American Journal of Pathology. 2001;159(5):1723-33.
78. Castaños-Velez E, Maerlan S, Osorio LM, Åberg F, Biberfeld P, Örn A, et al. *Trypanosoma cruzi* Infection in Tumor Necrosis Factor Receptor p55-Deficient Mice. Infection and Immunity. 1998;66(6):2960-8.
79. McGovern KE, Wilson EH. Role of chemokines and trafficking of immune cells in parasitic infections. Current immunology reviews. 2013;9(3):157-68.
80. Scharfstein J. Subverting bradykinin-evoked inflammation by co-opting the contact system: lessons from survival strategies of *Trypanosoma cruzi*. Current Opinion in Hematology. 2018;25(5):347-57.
81. Nascimento CR, Andrade D, Carvalho-Pinto CE, Serra RR, Vellasco L, Brasil G, et al. Mast Cell Coupling to the Kallikrein–Kinin System Fuels Intracardiac Parasitism and Worsens Heart Pathology in Experimental Chagas Disease. Frontiers in Immunology. 2017;8(840).
82. Casassa AF, Vanrell MC, Colombo MI, Gottlieb RA, Romano PS. Autophagy plays a protective role against *Trypanosoma cruzi* infection in mice. Virulence. 2019;10(1):151-65.
83. Cardoso MS, Reis-Cunha JL, Bartholomeu DC. Evasion of the Immune Response by *Trypanosoma cruzi* during Acute Infection. Frontiers in Immunology. 2016;6(659).
84. Lieke T, Graefe SEB, Klauenberg U, Fleischer B, Jacobs T. NK Cells Contribute to the Control of *Trypanosoma cruzi* Infection by Killing Free Parasites by Perforin-Independent Mechanisms. Infection and Immunity. 2004;72(12):6817-25.
85. Baez NS, Cerbán F, Savid-Frontera C, Hodge DL, Tosello J, Acosta-Rodriguez E, et al. Thymic expression of IL-4 and IL-15 after systemic inflammatory or infectious Th1 disease processes induce the acquisition of "innate" characteristics during CD8+ T cell development. PLOS Pathogens. 2019;15(1):e1007456.

86. Mesías AC, Garg NJ, Zago MP. Redox Balance Keepers and Possible Cell Functions Managed by Redox Homeostasis in *Trypanosoma cruzi*. Frontiers in Cellular and Infection Microbiology. 2019;9(435).
87. Arantes RME, Marche HHF, Bahia MT, Cunha FQ, Rossi MA, Silva JS. Interferon-γ-Induced Nitric Oxide Causes Intrinsic Intestinal Denervation in *Trypanosoma cruzi*-Infected Mice. Am J Pathol. 2004;164(4):1361-8.
88. Paiva CN, Feijó DF, Dutra FF, Carneiro VC, Freitas GB, Alves LS, et al. Oxidative stress fuels *Trypanosoma cruzi* infection in mice. The Journal of Clinical Investigation. 2012;122(7):2531-42.
89. Vespa GN, Cunha FQ, Silva JS. Nitric oxide is involved in control of *Trypanosoma cruzi*-induced parasitemia and directly kills the parasite *in vitro*. Infection and Immunity. 1994;62(11):5177.
90. Hölscher C, Köhler G, Müller U, Mossmann H, Schaub GA, Brombacher F. Defective Nitric Oxide Effector Functions Lead to Extreme Susceptibility of *Trypanosoma cruzi*-Infected Mice Deficient in Gamma Interferon Receptor or Inducible Nitric Oxide Synthase. Infection and Immunity. 1998;66(3):1208.
91. Cummings KL, Tarleton RL. Inducible Nitric Oxide Synthase Is Not Essential for Control of *Trypanosoma cruzi* Infection in Mice. Infection and Immunity. 2004;72(7):4081.
92. Doyle PS, Zhou YM, Engel JC, McKerrow JH. A Cysteine Protease Inhibitor Cures Chagas Disease in an Immunodeficient-Mouse Model of Infection. Antimicrobial Agents and Chemotherapy. 2007;51(11):3932.
93. Hoft DF, Schnapp AR, Eickhoff CS, Roodman ST. Involvement of CD4+ Th1 Cells in Systemic Immunity Protective against Primary and Secondary Challenges with *Trypanosoma cruzi*. Infection and Immunity. 2000;68(1):197.
94. Trischmann T, Tanowitz H, Wittner M, Bloom B. *Trypanosoma cruzi*: Role of the immune response in the natural resistance of inbred strains of mice. Experimental Parasitology. 1978;45(2):160-8.
95. Francolino SS, Antunes AF, Talice R, Rosa R, Selanikio J, Rezende JMd, et al. New evidence of spontaneous cure in human Chagas' disease. Revista da Sociedade Brasileira de Medicina Tropical. 2003;36:103-7.
96. Acevedo GR, Girard MC, Gómez KA. The Unsolved Jigsaw Puzzle of the Immune Response in Chagas Disease. Frontiers in Immunology. 2018;9(1929).
97. Acosta Rodríguez EV, Araujo Furlan CL, Fiocca Vernengo F, Montes CL, Gruppi A. Understanding CD8+ T Cell Immunity to *Trypanosoma cruzi* and How to Improve It. Trends in Parasitology. 2019;35(11):899-917.
98. Kumar S, Tarleton RL. The relative contribution of antibody production and CD8+ T cell function to immune control of *Trypanosoma cruzi*. Parasite immunology. 1998;20(5):207--16.
99. Tzelepis F, Persechini PM, Rodrigues MM. Modulation of CD4+ T Cell-Dependent Specific Cytotoxic CD8+ T Cells Differentiation and Proliferation by the Timing of Increase in the Pathogen Load. PLOS ONE. 2007;2(4):e393.
100. Tarleton R, Koller B, Latour A, Postan M. Susceptibility of β 2-microglobulin-deficient mice to *Trypanosoma cruzi* infection. Nature. 1992;356(6367):338-40.
101. Tarleton RL, Sun J, Zhang L, Postan M. Depletion of T-cell subpopulations results in exacerbation of myocarditis and parasitism in experimental Chagas' disease. Infection and immunity. 1994;62(5):1820-9.
102. Cardillo F, Postol E, Nihei J, Aroeira LS, Nomizo A, Mengel J. B cells modulate T cells so as to favour T helper type 1 and CD8+ T cell responses in the acute phase of *Trypanosoma cruzi* infection. Immunology. 2007;122(4):584--95.
103. Dominguez MR, Ersching J, Lemos R, Machado AV, Bruna-Romero O, Rodrigues MM, et al. Re-circulation of lymphocytes mediated by sphingosine-1-phosphate receptor-1 contributes to resistance against experimental infection with the protozoan parasite *Trypanosoma cruzi*. Vaccine. 2012;30(18):2882-91.
104. Bixby LM, Tarleton RL. Stable CD8+ T cell memory during persistent *Trypanosoma cruzi* infection. The Journal of Immunology. 2008;181(4):2644-50.
105. Mucci J, Hidalgo A, Mocetti E, Argibay PF, Leguizamón MS, Campetella O. Thymocyte depletion in *Trypanosoma cruzi* infection is mediated by trans-sialidase-induced apoptosis on nurse cells complex. Proceedings of the National Academy of Sciences. 2002;99(6):3896-901.
106. Ersching J, Basso AS, Kalich VLG, Bortoluci KR, Rodrigues MM. A Human Trypanosome Suppresses CD8+ T Cell Priming by Dendritic Cells through the Induction of Immune Regulatory CD4+ Foxp3+ T Cells. PLOS Pathogens. 2016;12(6):e1005698.
107. Overtvelt LV, Andrieu M, Verhasselt V, Connan F, Choppin J, Vercruysse V, et al. *Trypanosoma cruzi* down-regulates lipopolysaccharide-induced MHC class I on human dendritic cells and impairs antigen presentation to specific CD8+ T lymphocytes. International Immunology. 2002;14(10):1135-44.

108. Poncini CV, Soto CDA, Batalla E, Solana ME, González Cappa SM. *Trypanosoma cruzi* Induces Regulatory Dendritic Cells In Vitro. Infection and Immunity. 2008;76(6):2633-41.
109. Poncini CV, Ilarregui JM, Batalla EI, Engels S, Cerliani JP, Cucher MA, et al. *Trypanosoma cruzi* infection imparts a regulatory program in dendritic cells and T cells via galectin-1–dependent mechanisms. The Journal of Immunology. 2015;195(7):3311-24.
110. Martin DL, Weatherly DB, Laucella SA, Cabinian MA, Crim MT, Sullivan S, et al. CD8+ T-Cell Responses to *Trypanosoma cruzi* Are Highly Focused on Strain-Variant trans-Sialidase Epitopes. PLoS Pathogens. 2006;2(8):e77.
111. Tzelepis F, de Alencar BC, Penido ML, Claser C, Machado AV, Bruna-Romero O, et al. Infection with *Trypanosoma cruzi* restricts the repertoire of parasite-specific CD8+ T cells leading to immunodominance. The Journal of Immunology. 2008;180(3):1737-48.
112. Rosenberg CS, Zhang W, Bustamante JM, Tarleton RL. Long-term immunity to *Trypanosoma cruzi* in the absence of immunodominant trans-sialidase-specific CD8+ T cells. Infection and immunity. 2016;84(9):2627-38.
113. Alvarez MG, Postan M, Weatherly DB, Albareda MC, Sidney J, Sette A, et al. HLA Class I-T cell epitopes from trans-sialidase proteins reveal functionally distinct subsets of CD8+ T cells in chronic Chagas disease. PLoS Negl Trop Dis. 2008;2(9):e288.
114. Pinazo M-J, Espinosa G, Cortes-Lletget C, Posada EdJ, Aldasoro E, Oliveira I, et al. Immunosuppression and Chagas Disease: A Management Challenge. PLoS Negl Trop Dis. 2013;7(1):e1965.
115. Tarleton RL, Grusby MJ, Postan M, Glimcher LH. *Trypanosoma cruzi* infection in MHC-deficient mice: further evidence for the role of both class I- and class II-restricted T cells in immune resistance and disease. Int Immunol. 1996;8(1):13-22.
116. Padilla A, Xu D, Martin D, Tarleton R. Limited Role for CD4+ T-Cell Help in the Initial Priming of *Trypanosoma cruzi*-Specific CD8+ T Cells. Infection and Immunity. 2007;75(1):231.
117. Gomes JAS, Bahia-Oliveira LMG, Rocha MOC, Martins-Filho OA, Gazzinelli G, Correa-Oliveira R. Evidence that Development of Severe Cardiomyopathy in Human Chagas' Disease Is Due to a Th1-Specific Immune Response. Infection and Immunity. 2003;71(3):1185-93.
118. Guo S, Cobb D, Smeltz RB. T-bet Inhibits the In Vivo Differentiation of Parasite-Specific CD4+ Th17 Cells in a T Cell-Intrinsic Manner. The Journal of Immunology. 2009;182(10):6179-86.
119. Albareda MC, De Rissio AM, Tomas G, Serjan A, Alvarez MG, Viotti R, et al. Polyfunctional T Cell Responses in Children in Early Stages of Chronic *Trypanosoma cruzi* Infection Contrast with Monofunctional Responses of Long-term Infected Adults. PLoS Negl Trop Dis. 2013;7(12):e2575.
120. Bonney KM, Taylor JM, Daniels MD, Epting CL, Engman DM. Heat-Killed *Trypanosoma cruzi* Induces Acute Cardiac Damage and Polyantigenic Autoimmunity. PLOS ONE. 2011;6(1):e14571.
121. Santamaría MH, Corral RS. Osteopontin-dependent regulation of Th1 and Th17 cytokine responses in *Trypanosoma cruzi*-infected C57BL/6 mice. Cytokine. 2013;61(2):491-8.
122. Guedes PMM, Gutierrez FRS, Silva GK, Dellalibera-Joviliano R, Rodrigues GJ, Bendhack LM, et al. Deficient regulatory T cell activity and low frequency of IL-17-producing T cells correlate with the extent of cardiomyopathy in human Chagas' disease. PLoS Neglected Tropical Diseases. 2012;6(4).
123. Díaz PR, Mucci J, Meira MA, Bogliotti Y, Musikant D, Leguizamón MS, et al. *Trypanosoma cruzi* trans-sialidase prevents elicitation of Th1 cell response via interleukin 10 and downregulates Th1 effector cells. Infection and immunity. 2015;83(5):2099-108.
124. Bryan MA, Guyach SE, Norris KA. Specific Humoral Immunity versus Polyclonal B Cell Activation in *Trypanosoma cruzi* Infection of Susceptible and Resistant Mice. PLoS neglected tropical diseases. 2010;4(7):e733.
125. Chavele K-M, Merry E, Ehrenstein MR. Cutting edge: circulating plasmablasts induce the differentiation of human T follicular helper cells via IL-6 production. The Journal of Immunology. 2015;194(6):2482-5.
126. Eto D, Lao C, DiToro D, Barnett B, Escobar TC, Kageyama R, et al. IL-21 and IL-6 are critical for different aspects of B cell immunity and redundantly induce optimal follicular helper CD4 T cell (Tfh) differentiation. PLOS One. 2011;6(3).
127. Gao W, Pereira MA. Interleukin-6 is required for parasite specific response and host resistance to *Trypanosoma cruzi*. International Journal for Parasitology. 2002;32:167--70.
128. Bermejo DA, Amezcua-Vesely MC, Montes CL, Merino MC, Gehrau RC, Cejas H, et al. BAFF Mediates Splenic B Cell Response and Antibody Production in Experimental Chagas Disease. PLOS Neglected Tropical Diseases. 2010;4(5):e679.

129. Bonney KM, Engman DM. Autoimmune Pathogenesis of Chagas Heart Disease: Looking Back, Looking Ahead. The American Journal of Pathology. 2015;185(6):1537-47.
130. Hyland KV, Leon JS, Daniels MD, Giafis N, Woods LM, Bahk TJ, et al. Modulation of Autoimmunity by Treatment of an Infectious Disease. Infection and Immunity. 2007;75(7):3641-50.
131. Viotti R, Alarcón de Noya B, Araujo-Jorge T, Grijalva MJ, Guhl F, López MC, et al. Towards a paradigm shift in the treatment of chronic Chagas disease. Antimicrob Agents Chemother. 2014;58(2):635-9.
132. Tarleton RL. Chagas disease: a role for autoimmunity? Trends Parasitol. 2003;19(10):447-51.
133. Minoprio P, Burlen O, Pereira P, Guilbert B, Andrade L, Hontebeyrie-Joskowicz M, et al. Most B Cells in Acute Trypanosoma cruzi Infection Lack Parasite Specificity. Scandinavian Journal of Immunology. 1988.
134. Acosta Rodriguez EV, Zuniga EI, Montes CL, Merino MC, Bermejo DA, Amezcua Vesely MC, et al. *Trypanosoma cruzi* Infection Beats the B-cell Compartment Favouring Parasite Establishment: Can we Strike First? Scandinavian Journal of Immunology. 2007;66(2-3):137-42.
135. Bryan MA, Norris KA. Genetic Immunization Converts the *Trypanosoma cruzi* B-Cell Mitogen Proline Racemase to an Effective Immunogen. Infection and immunity. 2010;78(2):810--22.
136. Bermejo DA, Jackson SW, Gorosito-Serran M, Acosta-Rodriguez EV, Amezcua-Vesely MC, Sather BD, et al. *Trypanosoma cruzi* trans-sialidase initiates a program independent of the transcription factors RORγt and Ahr that leads to IL-17 production by activated B cells. Nature Immunology. 2013;14(5):514-22.
137. Fares RCG, Correa-Oliveira R, de Arajo FF, Keesen TSL, Chaves AT, Fiuza JA, et al. Identification of phenotypic markers of B cells from patients with Chagas disease. Parasite immunology. 2013;35(7-8):214--23.
138. Passos LSA, Magalhães LMD, Soares RP, Marques AF, Alves MLR, Giunchetti RC, et al. Activation of Human CD11b+ B1 B-Cells by *Trypanosoma cruzi*-Derived Proteins Is Associated With Protective Immune Response in Human Chagas Disease. Frontiers in Immunology. 2019;9(3015).
139. Zuniga E, Acosta-Rodriguez E, Merino MC, Montes C, Gruppi A. Depletion of immature B cells during *Trypanosoma cruzi* infection: involvement of myeloid cells and the cyclooxygenase pathway. European Journal of Immunology. 2005;35(6):1849--58.
140. Dotiwala F, Mulik S, Polidoro RB, Ansara JA, Burleigh BA, Walch M, et al. Killer lymphocytes use granulysin, perforin and granzymes to kill intracellular parasites. Nature medicine. 2016;22(2):210.
141. de Alencar BCG, Persechini PM, Haolla FA, de Oliveira G, Silverio JC, Lannes-Vieira J, et al. Perforin and Gamma Interferon Expression Are Required for CD4+ and CD8+ T-Cell-Dependent Protective Immunity against a Human Parasite, *Trypanosoma cruzi*, Elicited by Heterologous Plasmid DNA Prime-Recombinant Adenovirus 5 Boost Vaccination. Infection and Immunity. 2009;77(10):4383.
142. Müller U, Sobek V, Balkow S, Hölscher C, Müllbacher A, Museteanu C, et al. Concerted action of perforin and granzymes is critical for the elimination of *Trypanosoma cruzi* from mouse tissues, but prevention of early host death is in addition dependent onthe FasL/Fas pathway. European Journal of Immunology. 2003;33(1):70-8.
143. Silverio JC, De-Oliveira-Pinto LM, Da Silva AA, De Oliveira GM, Lannes-Vieira J. Perforin-expressing cytotoxic cells contribute to chronic cardiomyopathy in *Trypanosoma cruzi* infection. International Journal of Experimental Pathology. 2010;91(1):72-86.
144. Leguizamon MS, Campetella O, Russomando G, Almiron M, Guillen I. Antibodies inhibiting *Trypanosoma cruzi* trans-sialidaseactivity in sera from human infections. Journal of Infectious Diseases. 1994;170(6):1570--4.
145. Leguizamon MS, Campetella OE, Cappa SMG, Frasch ACC. Mice infected with *Trypanosoma cruzi* produce antibodies against the enzymatic domain of trans-sialidase that inhibit its activity. Infection and Immunity. 1994;62(8):3441--6.
146. Pereira-Chioccola VL, Schenkman S, Kloetzel JK. Sera from chronic chagasic patients and rodents infected with *Trypanosoma cruzi* inhibit trans-sialidase by recognizing its amino-terminal and catalytic domain. Infection and Immunity. 1994;62(7):2973--8.
147. Krettli AU, Brener Z. Resistance against *Trypanosoma cruzi* associated to anti-living trypomastigote antibodies. The Journal of Immunology. 1982.
148. Sardinha LR, Mosca T, Elias RM, do Nascimento RS, Gonçalves LA, Bucci DZ, et al. The Liver Plays a Major Role in Clearance and Destruction of Blood Trypomastigotes in *Trypanosoma cruzi* Chronically Infected Mice. PLoS Negl Trop Dis. 2010;4(1):e578.
149. Umekita LF, Mota I. How are antibodies involved in the protective mechanism of susceptible mice infected with *T. cruzi*? Brazilian Journal of Medical and Biological Research. 2000;33:253-8.

150. Fiocca Vernengo F, Beccaria CG, Araujo Furlan CL, Tosello Boari J, Almada L, Gorosito Serrán M, et al. CD8+ T Cell Immunity Is Compromised by Anti-CD20 Treatment and Rescued by Interleukin-17A. mBio. 2020;11(3):e00447-20.
151. Gorosito Serrán M, Tosello Boari J, Fiocca Vernengo F, Beccaría CG, Ramello MC, Bermejo DA, et al. Unconventional Pro-inflammatory CD4+ T Cell Response in B Cell-Deficient Mice Infected with *Trypanosoma cruzi*. Frontiers in Immunology. 2017;8(1548).
152. Sullivan NL, Eickhoff CS, Sagartz J, Hoft DF. Deficiency of Antigen-Specific B Cells Results in Decreased *Trypanosoma cruzi* Systemic but Not Mucosal Immunity Due to CD8 T Cell Exhaustion. The Journal of Immunology. 2015;194(4):1806--18.
153. Rassi A, Marin-Neto JA. Chagas disease. Lancet. 2010;375.
154. Hölscher C, Mohrs M, Dai WJ, Köhler G, Ryffel B, Schaub GA, et al. Tumor necrosis factor alpha-mediated toxic shock in *Trypanosoma cruzi*-infected interleukin 10-deficient mice. Infection and immunity. 2000;68(7):4075-83.
155. Hunter CA, Ellis-Neyes LA, Slifer T, Kanaly S, Grünig G, Fort M, et al. IL-10 is required to prevent immune hyperactivity during infection with *Trypanosoma cruzi*. The Journal of Immunology. 1997;158(7):3311-6.
156. Pino-Martínez AM, Miranda CG, Batalla EI, González-Cappa SM, Alba Soto CD. IL-10 participates in the expansion and functional activation of CD8+ T cells during acute infection with *Trypanosoma cruzi*. Journal of Leukocyte Biology. 2019;105(1):163-75.
157. Roffê E, Rothfuchs AG, Santiago HC, Marino APMP, Ribeiro-Gomes FL, Eckhaus M, et al. IL-10 Limits Parasite Burden and Protects against Fatal Myocarditis in a Mouse Model of *Trypanosoma cruzi* Infection. J Immunol. 2012;188(2):649-60.
158. Medina TS, Oliveira GG, Silva MC, David BA, Silva GK, Fonseca DM, et al. Ebi3 prevents *Trypanosoma cruzi*-induced myocarditis by dampening IFN-γ-driven inflammation. Frontiers in Immunology. 2017;8:1213.
159. Minoprio P, El Cheikh MC, Murphy E, Hontebeyrie-Joskowicz M, Coffman R, Coutinho A, et al. Xid-associated resistance to experimental Chagas' disease is IFN-gamma dependent. The Journal of Immunology. 1993;151(8):4200-8.
160. Girard MC, Acevedo GR, Ossowski MS, Alcaráz PB, Fernández M, Hernández Y, et al. Altered frequency of CD24high CD38high transitional B cells in patients with cardiac involvement of chronic Chagas disease. bioRxiv. 2019:684589.
161. Guthmiller JJ, Graham AC, Zander RA, Pope RL, Butler NS. Cutting Edge: IL-10 Is Essential for the Generation of Germinal Center B Cell Responses and Anti-*Plasmodium* Humoral Immunity. The Journal of Immunology. 2017;198(2):617-22.
162. Ferrão PM, d'Avila-Levy CM, Araujo-Jorge TC, Degrave WM, Gonçalves AdS, Garzoni LR, et al. Cruzipain Activates Latent TGF-β from Host Cells during *T. cruzi* Invasion. PLOS ONE. 2015;10(5):e0124832.
163. Martin DL, Postan M, Lucas P, Gress R, Tarleton RL. TGF-β regulates pathology but not tissue CD8+ T cell dysfunction during experimental *Trypanosoma cruzi* infection. European Journal of Immunology. 2007;37(10):2764-71.
164. Esper L, Roman-Campos D, Lara A, Brant F, Castro LL, Barroso A, et al. Role of SOCS2 in Modulating Heart Damage and Function in a Murine Model of Acute Chagas Disease. The American Journal of Pathology. 2012;181(1):130-40.
165. Araujo Furlan CL, Tosello Boari J, Rodriguez C, Canale FP, Fiocca Vernengo F, Boccardo S, et al. Limited Foxp3+ Regulatory T Cells Response During Acute *Trypanosoma cruzi* Infection Is Required to Allow the Emergence of Robust Parasite-Specific CD8+ T Cell Immunity. Frontiers in immunology. 2018;9:2555.
166. Fresno M, Gironès N. Regulatory Lymphoid and Myeloid Cells Determine the Cardiac Immunopathogenesis of *Trypanosoma cruzi* Infection. Frontiers in Microbiology. 2018;9(351).
167. Carbajosa S, Rodríguez-Angulo HO, Gea S, Chillón-Marinas C, Poveda C, Maza MC, et al. L-arginine supplementation reduces mortality and improves disease outcome in mice infected with *Trypanosoma cruzi*. PLoS Negl Trop Dis. 2018;12(1):e0006179.
168. Parrado R, Ramirez JC, de la Barra A, Alonso-Vega C, Juiz N, Ortiz L, et al. Usefulness of Serial Blood Sampling and PCR Replicates for Treatment Monitoring of Patients with Chronic Chagas Disease. Antimicrobial Agents and Chemotherapy. 2019;63(2):e01191-18.
169. Bonney KM, Luthringer DJ, Kim SA, Garg NJ, Engman DM. Pathology and Pathogenesis of Chagas Heart Disease. Annual Review of Pathology: Mechanisms of Disease. 2019;14(1):421-47.

170. Santi-Rocca J, Fernandez-Cortes F, Chillón-Marinas C, González-Rubio M-L, Martin D, Gironès N, et al. A multi-parametric analysis of *Trypanosoma cruzi* infection: common pathophysiologic patterns beyond extreme heterogeneity of host responses. Scientific Reports. 2017;7(1):1-12.
171. Silberstein E, Serna C, Fragoso SP, Nagarkatti R, Debrabant A. A novel nanoluciferase-based system to monitor *Trypanosoma cruzi* infection in mice by bioluminescence imaging. PLoS ONE. 2018;13(4).
172. Roffê E, Marino APMP, Weaver J, Wan W, de Araújo FF, Hoffman V, et al. *Trypanosoma cruzi* Causes Paralyzing Systemic Necrotizing Vasculitis Driven by Pathogen-Specific Type I Immunity in Mice. Infection and Immunity. 2016;84(4):1123-36.
173. Cummings KL, Tarleton RL. Rapid quantitation of *Trypanosoma cruzi* in host tissue by real-time PCR. Mol Biochem Parasitol. 2003;129(1):53-9.
174. Pereira IR, Vilar-Pereira G, Marques V, da Silva AA, Caetano B, Moreira OC, et al. A Human Type 5 Adenovirus-Based *Trypanosoma cruzi* Therapeutic Vaccine Re-programs Immune Response and Reverses Chronic Cardiomyopathy. PLoS Pathog. 2015;11(1):e1004594.
175. Pack AD, Collins MH, Rosenberg CS, Tarleton RL. Highly competent, non-exhausted CD8+ T cells continue to tightly control pathogen load throughout chronic *Trypanosoma cruzi* infection. PLOS Pathogens. 2018;14(11):e1007410.
176. Ward AI, Lewis MD, Khan AA, McCann CJ, Francisco AF, Jayawardhana S, et al. *In Vivo* Analysis of *Trypanosoma cruzi* Persistence Foci at Single-Cell Resolution. mBio. 2020;11(4):e01242-20.
177. Fiuza JA, Fujiwara RT, Gomes JAS, Rocha MOdC, Chaves AT, de Araújo FF, et al. Profile of Central and Effector Memory T Cells in the Progression of Chronic Human Chagas Disease. PLOS Neglected Tropical Diseases. 2009;3(9):e512.
178. Bustamante JM, Bixby LM, Tarleton RL. Drug-induced cure drives conversion to a stable and protective CD8+ T central memory response in chronic Chagas disease. Nat Med. 2008;14(5):542-50.
179. Weaver JD, Hoffman VJ, Roffe E, Murphy PM. Low-level parasite Persistence drives vasculitis and myositis in skeletal muscle of mice chronically infected with *Trypanosoma cruzi*. Infection and immunity. 2019;87(6):e00081-19.
180. Horn D. Antigenic variation in African trypanosomes. Molecular and Biochemical Parasitology. 2014;195(2):123-9.
181. Nakayasu ES, Sobreira TJ, Torres R, Ganiko L, Oliveira PS, Marques AF, et al. Improved proteomic approach for the discovery of potential vaccine targets in *Trypanosoma cruzi*. Journal of proteome research. 2012;11(1):237-46.
182. Llewellyn MS, Messenger LA, Luquetti AO, Garcia L, Torrico F, Tavares SB, et al. Deep sequencing of the *Trypanosoma cruzi* GP63 surface proteases reveals diversity and diversifying selection among chronic and congenital Chagas disease patients. PLoS Negl Trop Dis. 2015;9(4).
183. Kahn SJ, Wleklinski M. The surface glycoproteins of *Trypanosoma cruzi* encode a superfamily of variant T cell epitopes. The Journal of Immunology. 1997;159(9):4444.
184. Buscaglia CA, Campo VA, Di Noia JM, Torrecilhas AC, De Marchi CR, Ferguson MA, et al. The surface coat of the mammal-dwelling infective trypomastigote stage of *Trypanosoma cruzi* is formed by highly diverse immunogenic mucins. Journal of Biological Chemistry. 2004;279(16):15860-9.
185. Bartholomeu DC, Cerqueira GC, Leao ACA, daRocha WD, Pais FS, Macedo C, et al. Genomic organization and expression profile of the mucin-associated surface protein (masp) family of the human pathogen *Trypanosoma cruzi*. Nucleic Acids Research. 2009;37(10):3407-17.
186. Barrett MP, Kyle DE, Sibley LD, Radke JB, Tarleton RL. Protozoan persister-like cells and drug treatment failure. Nature Reviews Microbiology. 2019;17(10):607-20.
187. Fisher RA, Gollan B, Helaine S. Persistent bacterial infections and persister cells. Nature Reviews Microbiology. 2017;15(8):453-64.
188. Dumoulin PC, Burleigh BA. Stress-induced proliferation and cell cycle plasticity of intracellular *Trypanosoma cruzi* Amastigotes. MBio. 2018;9(4):e00673-18.
189. Resende BC, Oliveira ACS, Guañabens ACP, Repolês BM, Santana V, Hiraiwa PM, et al. The Influence of Recombinational Processes to Induce Dormancy in *Trypanosoma cruzi*. Frontiers in Cellular and Infection Microbiology. 2020;10:5.
190. Nylén S, Sacks D. Interleukin-10 and the pathogenesis of human visceral leishmaniasis. Trends in immunology. 2007;28(9):378-84.
191. Ferreira RR, da Silva Abreu R, Vilar-Pereira G, Degrave W, Meuser-Batista M, Ferreira NVC, et al. TGF-β inhibitor therapy decreases fibrosis and stimulates cardiac improvement in a pre-clinical study of chronic Chagas' heart disease. PLoS neglected tropical diseases. 2019;13(7):e0007602.

192. Nogueira LG, Santos RHB, Fiorelli AI, Mairena EC, Benvenuti LA, Bocchi EA, et al. Myocardial gene expression of T-bet, GATA-3, Ror-t, FoxP3, and hallmark cytokines in chronic Chagas disease cardiomyopathy: an essentially unopposed TH1-type response. Mediators of Inflammation. 2014;2014.
193. Salvador F, Sulleiro E, Sánchez-Montalvá A, Martínez-Gallo M, Carrillo E, Molina I. Impact of Helminth Infection on the Clinical and Microbiological Presentation of Chagas Diseases in Chronically Infected Patients. PLOS Neglected Tropical Diseases. 2016;10(4):e0004663.
194. Albareda MC, Olivera GC, Laucella SA, Alvarez MG, Fernandez ER, Lococo B, et al. Chronic human infection with *Trypanosoma cruzi* drives CD4+ T cells to immune senescence. The Journal of Immunology. 2009;183(6):4103-8.
195. Argüello RJ, Albareda MC, Alvarez MG, Bertocchi G, Armenti AH, Vigliano C, et al. Inhibitory receptors are expressed by *Trypanosoma cruzi*-specific effector T cells and in hearts of subjects with chronic Chagas disease. PloS one. 2012;7(5).
196. Pérez-Antón E, Egui A, Thomas MC, Simón M, Segovia M, López MC. Immunological exhaustion and functional profile of CD8+ T lymphocytes as cellular biomarkers of therapeutic efficacy in chronic Chagas disease patients. Acta tropica. 2020;202:105242.
197. Tosello Boari J, Araujo Furlan CL, Fiocca Vernengo F, Rodriguez C, Ramello MC, Amezcua Vesely MC, et al. IL-17RA-signaling modulates CD8+ T cell survival and exhaustion during *Trypanosoma cruzi* infection. Frontiers in immunology. 2018;9:2347.
198. Pino-Martínez AM, Miranda CG, Batalla EI, González-Cappa SM, Alba Soto CD. IL-10 participates in the expansion and functional activation of CD8+ T cells during acute infection with *Trypanosoma cruzi*. Journal of Leukocyte Biology. 2019;105(1):163-75.
199. Mateus J, Guerrero P, Lasso P, Cuervo C, González JM, Puerta CJ, et al. An animal model of acute and chronic Chagas disease with the reticulotropic Y strain of *Trypanosoma cruzi* that depicts the multifunctionality and dysfunctionality of T cells. Frontiers in immunology. 2019;10:918.
200. Quebrada Palacio LP, Fernández ER, Hernández-Vásquez Y, Petray PB, Postan M. Circulating T Follicular Helper Cell Abnormalities Associated to Different Clinical Forms of Chronic Chagas Disease. Frontiers in Cellular and Infection Microbiology. 2020;10(126).
201. Fernández ER, Olivera GC, Palacio LPQ, González MN, Hernandez-Vasquez Y, Sirena NM, et al. Altered distribution of peripheral blood memory B cells in humans chronically infected with *Trypanosoma cruzi*. PloS one. 2014;9(8).
202. Calderón J, Maganto-Garcia E, Punzón C, Carrión J, Terhorst C, Fresno M. The Receptor Slamf1 on the Surface of Myeloid Lineage Cells Controls Susceptibility to Infection by *Trypanosoma cruzi*. PLoS Pathog. 2012;8(7):e1002799.
203. de Meis J, Morrot A, Farias-de-Oliveira DA, Villa-Verde DMS, Savino W. Differential Regional Immune Response in Chagas Disease. PLOS Neglected Tropical Diseases. 2009;3(7):e417.
204. McCall L-I, Tripathi A, Vargas F, Knight R, Dorrestein PC, Siqueira-Neto JL. Experimental Chagas disease-induced perturbations of the fecal microbiome and metabolome. PLOS Neglected Tropical Diseases. 2018;12(3):e0006344.
205. Silverio JC, Pereira IR, Cipitelli MdC, Vinagre NF, Rodrigues MM, Gazzinelli RT, et al. CD8+ T-Cells Expressing Interferon Gamma or Perforin Play Antagonistic Roles in Heart Injury in Experimental *Trypanosoma Cruzi*-Elicited Cardiomyopathy. PLoS Pathog. 2012;8(4):e1002645.
206. Ferreira CP, Cariste LM, Santos Virgílio FD, Moraschi BF, Monteiro CB, Vieira Machado AM, et al. LFA-1 Mediates Cytotoxicity and Tissue Migration of Specific CD8+ T Cells after Heterologous Prime-Boost Vaccination against *Trypanosoma cruzi* Infection. Frontiers in Immunology. 2017;8(1291).
207. Pontes Ferreira C, Cariste LM, Ferri Moraschi B, Ferrarini Zanetti B, Won Han S, Araki Ribeiro D, et al. CXCR3 chemokine receptor guides *Trypanosoma cruzi*-specific T-cells triggered by DNA/adenovirus ASP2 vaccine to heart tissue after challenge. PLOS Neglected Tropical Diseases. 2019;13(7):e0007597.
208. Leavey JK, Tarleton RL. Cutting edge: dysfunctional CD8+ T cells reside in nonlymphoid tissues during chronic *Trypanosoma cruzi* infection. The Journal of Immunology. 2003;170(5):2264-8.
209. Gabanyi I, Muller Paul A, Feighery L, Oliveira Thiago Y, Costa-Pinto Frederico A, Mucida D. Neuro-immune Interactions Drive Tissue Programming in Intestinal Macrophages. Cell. 2016;164(3):378-91.
210. La Flamme AC, Kahn SJ, Rudensky AY, Van Voorhis WC. *Trypanosoma cruzi*-infected macrophages are defective in major histocompatibility complex class II antigen presentation. Eur J Immunol. 1997;27(12):3085-94.
211. Alba Soto CD, Mirkin GA, Solana ME, González Cappa SM. *Trypanosoma cruzi* Infection Modulates In Vivo Expression of Major Histocompatibility Complex Class II Molecules on Antigen-Presenting Cells and T-Cell Stimulatory Activity of Dendritic Cells in a Strain-Dependent Manner. Infection and Immunity. 2003;71(3):1194-9.

212. Camargo R, Faria LO, Kloss A, Favali CBF, Kuckelkorn U, Kloetzel P-M, et al. *Trypanosoma cruzi* Infection Down-Modulates the Immunoproteasome Biosynthesis and the MHC Class I Cell Surface Expression in HeLa Cells. PLOS ONE. 2014;9(4):e95977.
213. Lundberg IE, Grundtman C. Developments in the scientific and clinical understanding of inflammatory myopathies. Arthritis Research & Therapy. 2008;10(5):220.

2.3 *Trypanosoma cruzi*-host interaction, final thoughts

Innate and adaptive effector pathways – A major effector mechanism specifically associated with cytotoxic CD8+ T-cells (CTLs) is the recognition of a damaged or infected cell, followed by local permeabilization of the target membrane and introduction of granzymes. These granzymes cleave pro-caspases in the cytosol, triggering the apoptotic cascade to the detriment of the defective host cell and any microbial occupants[1]. In several mouse models, the key effector molecules of this pathway can be knocked out with no effect on proficiency of parasite control, and even in other models the effect is marginal[2]. 'The' major canonical, and protective, effector response is the delivery, probably very locally, of IFN-γ[3]. This cytokine upregulates the production of ROS and RNS not just in cells of the immune system, but in all somatic cells expressing the IFN-γ receptor[4]. These reactive effector molecules are generated by innate signalling during *T. cruzi* infection[5], and the protection provided by T-cells is likely in the form of upregulation of the pathways that are already producing these oxidative agents. In addition, the largely under-studied, not just in *T. cruzi* but across immunology, role of the terminally differentiated somatic cells that are all capable of pathogen recognition and response, may also be important. The molecular events within these cells, as explored in Chapter 6, could be fundamental to *T. cruzi* infection outcome.

Hyper-local immune privilege is potentially the most significant factor in parasite persistence – Since completing the data collection, analysis and interpretation presented in Chapter 6, I would now qualify the idea that the negative immune feedback mediated via IL-10, PD-1 and TGF-β is likely involved in parasite survival after resolution of the acute stage. The chapter will present an extended hypothesis in which survival of rare parasites is possible even with fully activated circulating, and tissue resident, T-cell effectors.

B-cells and antibody roles beyond the resolution of the acute stage – Parasite specific serum antibody undoubtedly contributes to optimal control of virulent acute stage infections, with multiple examples described in the above review. However, the data presented in Chapter 6 now suggests that serum antibody does not have a non-redundant role, at least in the absence of T cells in continued suppression of chronic stage parasite burden.

References

1. Barry, M. and Bleackley, R. C. Cytotoxic T lymphocytes: all roads lead to death. *Nat. Rev. Immunol*. **2**, 401-409 (2002).
2. Henriques-pons, A. et al. Evidence for a perforin-mediated mechanism controlling cardiac inflammation in *Trypanosoma cruzi* infection. *Int. J. Exp. Pathol*. **83**, 67-79 (2002).
3. Rodrigues, A. A. IFN-γ plays a unique role in protection against low virulent *Trypanosoma cruzi* strain. *PLOS Neg. Trop. Dis*. **6**, e1598 (2012).
4. Baht, M. Y. et al. Comprehensive network map of interferon gamma signalling. J. Cell Commun. Signal. 12, 745-751 (2018).
5. Rodrigues, M. M., Oliveira, A. C. and Bellio, M. The immune response to *Trypanosoma cruzi*: role of Toll-like receptors and perspectives for vaccine development. *J. Parasitol. Res*. **2012**, 507874 (2012).
6. de Almeida, E. A., Junior, A. N., Correia, D. and Shikanai-Yasuda, M. A. Co-infection *Trypanosoma cruzi*/HIV: systematic review (1980-2010). *Rev. Soc. Bras. Med. Trop*. **44**, 762-70 (2011).

2.4 Aims

The aims of this work were to utilise the recently available bioluminescent-fluorescent CL Brener reporter strains (Chapter 3) in mouse models to answer three unknowns currently inhibiting progress in our understanding and management of Chagas disease:

- **In which host cells and tissues do the extremely rare chronic stage parasites persist? (Chapter 4)**

- **Can these new reporters be used to identify/characterise the potentially quiescent/dormant stage of the parasite life-cycle recently hypothesised? (Chapter 5)**

- **Why is the parasite able to routinely establish life-long infections in hosts that generate specific, non-exhausted and highly effective systemic immunological responses? (Chapter 6)**

The progress achieved in the direction of each of these is presented below in the form of 3 published (Chapter 4 and 5) or submitted (Chapter 6) first-author manuscripts. My overarching conclusions are reserved until after the reader has been exposed to each of the manuscripts and will come as a general discussion in Chapter 7.

3. Materials and Methods

3.1 Background to the CL Brener Luc::mNEON reporter stain

Multiple attempts to stably transfect *T. cruzi*, with the luciferase gene isolated from the firefly *Photinus pyralis*, and employ these reporters *in vivo* for drug treatment assays have been published[1,2,3,4]. Although useful for assaying the acute stage *in vivo* parasite load and the kinetics of drug activity at this time point, none of these reporters were detectable after suppression of acute parasitaemia and establishment of the chronic stage. The ability to identify chronic stage parasites *in* and *ex vivo* by bioluminescence has been made possible by the introduction of mutations into the w.t. luciferase gene generating a far-red shifted photon output[5]. The increased wavelength improves tissue penetrance and reduces absorption by haemoglobin. Both *T. brucei*[6] and *T. cruzi*[7] are capable of integrating and expressing red-shifted luciferase from highly active rRNA loci. Serval strains of bioluminescent *T. cruzi* have now been developed[8]. Shown in (Figure 12) is a cartoon of the integration of this gene.

Figure 12 – Integration of the red-shifted luciferase gene into an rRNA loci. LucPpyRE9h, red-shifted luciferase gene. Neo^R, neomycin phosphotransferase gene. gGAPDH gene fragments from the *T. cruzi* genome are included as intergenic and 3'UTR regions. The rDNA promotor and 3' rDNA spacer sequences were taken from the published CL Brener genome and used as targets. Taken from Lewis et.al, 2014[7].

A critical additional improvement of the utility of these reporters was the addition of a gene, plus amino acid linker, coding for the intrinsically fluorescent mNeonGreen protein[9]. The resulting 'dual-expressing' reporters parasite cell lines are bioluminescent *in vivo* and *ex vivo* when the red-shifted luciferase enzyme has access to ATP and the injected luciferin substrate. Once histologically processed, individual parasites are identifiable as a result of their stable expression of the fixable mNeonGreen protein. Shown in (Figure 13) is a cartoon describing the insertion of the mNeonGreen protein coding sequence into a red-shifted luciferase transgene already integrated into a rRNA locus the CL Brener genome.

The DTU type VI CL Brener (CLBr) duel expressing (CL Luc::mNeonGreen) clone is employed in all three of the following chapters of this thesis. In addition, a DTU type I mono-functional JR strain parasite expressing the far-red shifted luciferase (TcI-JR *Luc*) gene only is used in Chapter 4.

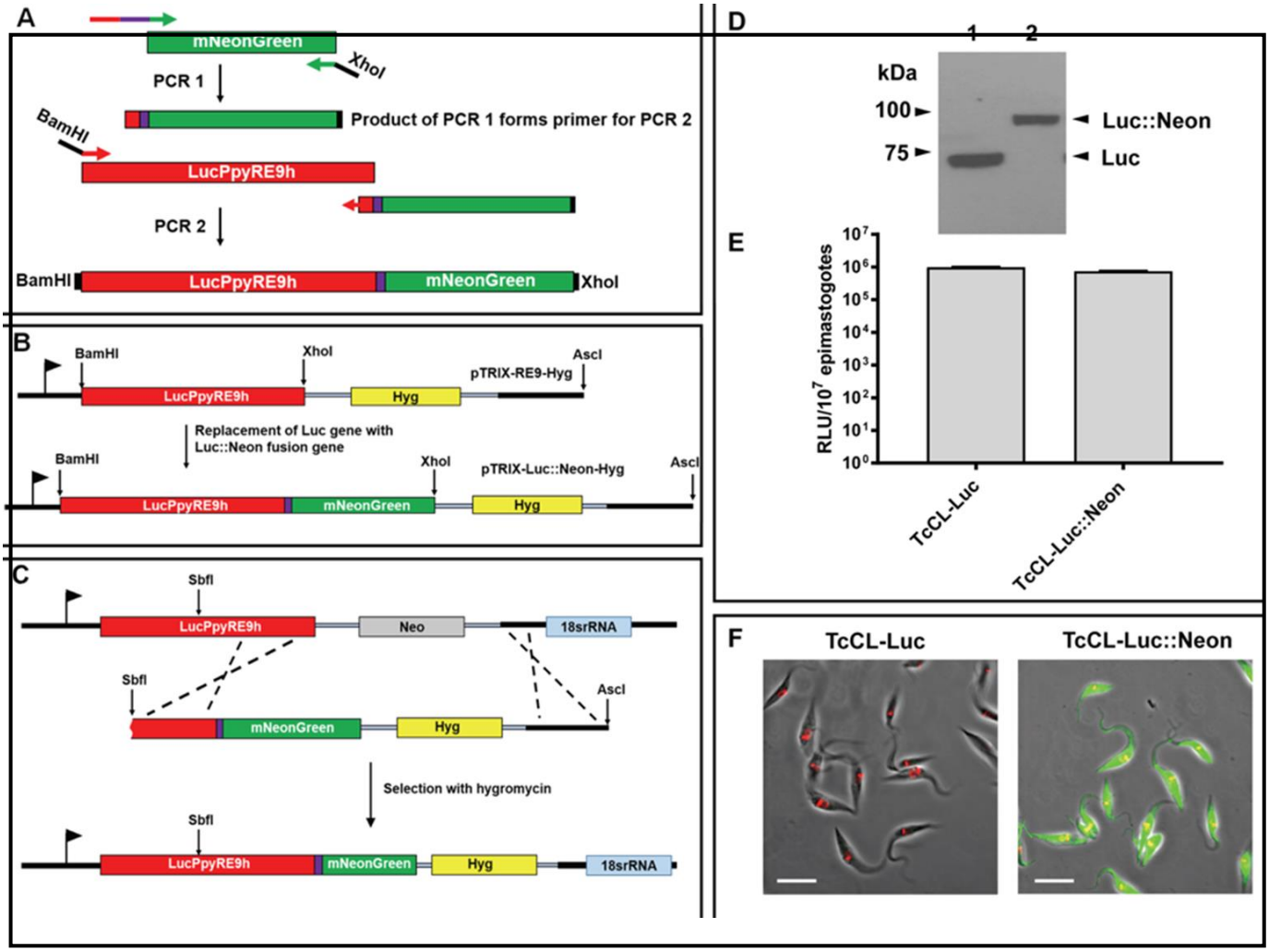

Figure 13 – Insertion of the mNeonGreen protein plus amino acid linker sequences immediately downstream of a previously integrated LucPpyRE9h, red-shifted luciferase gene. The high level expression of the resulting dual functional gene, driven by an RNA polymerase I promotor (flag), results in covalently linked bioluminescent and fluorescent protein sequences. Hyg, hygromycin resistance gene. Taken from Costa et.al, 2018[9].

3.2 Workflow overview

In the following chapters, parasites constitutively expressing the CL Luc::mNeonGreen reporter were combined with *in vivo* injection of the thymidine analogue EdU (5-Ethynyl-2´-deoxyuridine), extensive immunohistochemistry and novel tissue processing protocols. Since the materials and methods sections in each publication adequately cover how these techniques were employed, repetition is avoided here, and instead a workflow overview is provided (Figure 14). Additional pilot data are described at the beginning of chapters 4 and 5. The layout of the visceral organs in all *ex vivo* bioluminescence images is consistent throughout this thesis and is shown in Figure 14c.

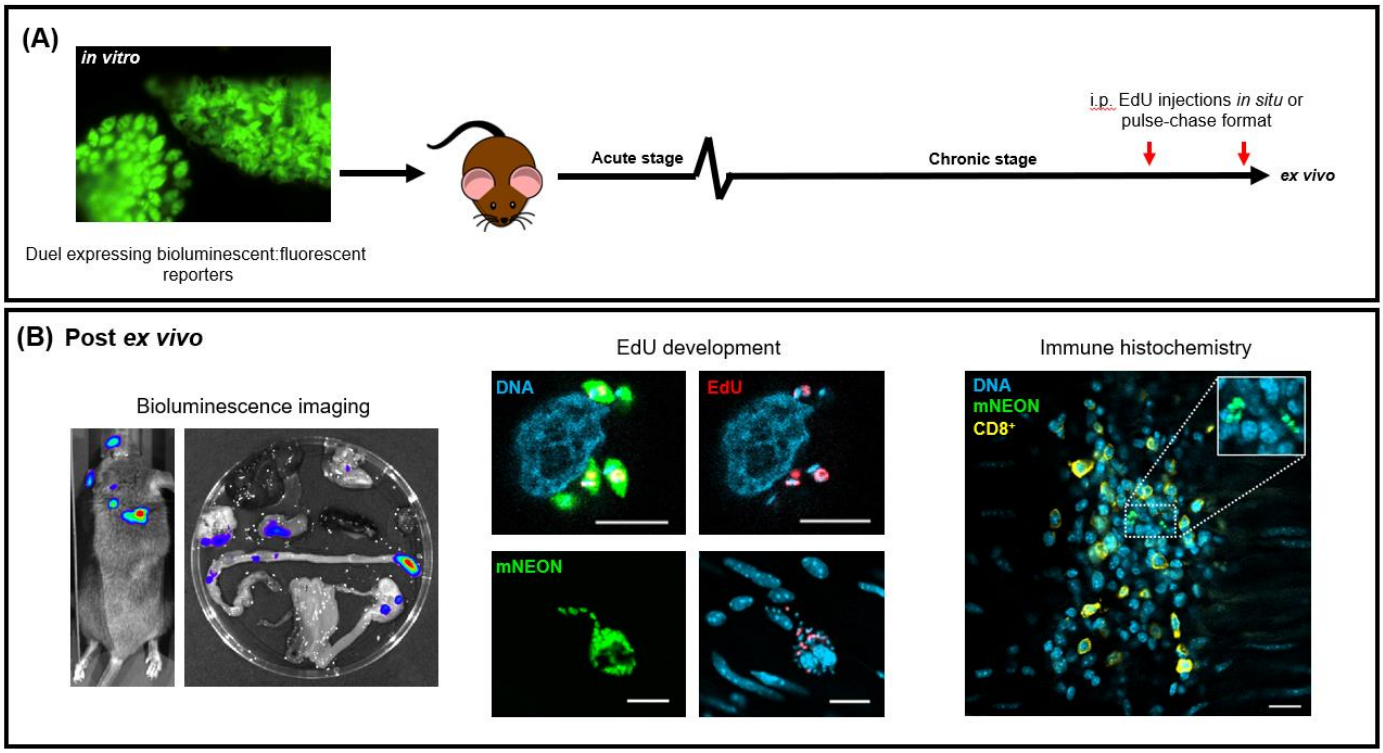

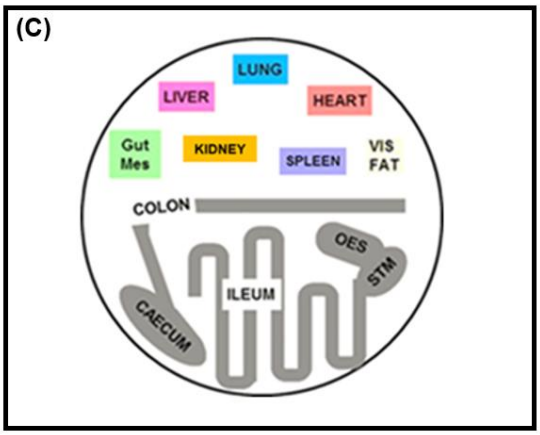

Figure 14 – A and B., Workflow overview showing the infection of mouse models with the CL Luc:mNeonGreen bioluminescent-fluorescent reporter, the *in vivo* i.p. injection of EdU either as an *in situ* or pulse-chase protocol, and the processing and immunohistochemical staining of the tissue (principally the colon) for imaging. **C.,** A cartoon showing the layout of the visceral organs used throughout this thesis and in the published or submitted papers.

References

1. Hyland, K. V., Asfaw, S. H., Olson, C. L., Daniels, M. D. and Engman, D. M. Bioluminescence imaging of *Trypanosoma cruzi* infection. *Int. J. Parasitol*. **38**, 1391-1400 (2008).
2. Canavaci, A. M. et al. *in vitro* and *in vivo* high-throughput assays for the testing of anti-*Trypanosoma cruzi* compounds. *PLOS Neg. Trop. Dis*. **13**, e740 (2010).
3. Andriani, G., Chessler, A. C., Courtemanche, G., Burleigh, B. A. and Rodriguez, A. Activity *in vivo* of anti-*Trypanosoma cruzi* compounds selected from a high throughput screening. *PLOS neg. Trop. Dis*. **8**, e3293 (2014).
4. Sanchez-Valdez, F. J., Padilla, A., Wang, W., Orr, D. and Tarleton, R. L. Spontaneous dormancy protects *Trypanosoma cruzi* during extended drug exposure. *eLife*. **7**, e34039 (2018).

5. Branchini, B. R. et al. Red-emitting luciferases for bioluminescence reporter and imaging applications. *Anal. Biochem*. **396**, 290-297 (2010).
6. McLatchie, A. P. et al. Highly sensitive *in vivo* imaging of *Trypanosoma brucei* expressing 'red-shifted' luciferase. *PLOS Neg. Trop. Dis*. **7**, e2571 (2013).
7. Lewis, M. D. et al. Bioluminescence imaging of chronic *Trypanosoma cruzi* infections reveals tissue-specific parasite dynamics and heart disease in the absence of locally persistent infection. *Cell Microbiol*. **16**, 1285-300 (2014).
8. Lewis, M. D., Fransisco, A. F., Taylor, M. C., Jayawardhana, S. and Kelly, J. M. Host and parasite genetics shape a link between *Trypanosoma cruzi* infection dynamics and chronic cardiomyopathy. Cell Microbiol. 18, 1429-1443 (2016).
9. Costa, F. C. et al. Expanding the toolbox for *Trypanosoma cruzi*: a parasite line incorporating a bioluminescent-flourescent dual reporter and streamlines CRISPR/Cas9 functionality for rapid *in vivo* localisation and phenotyping. *PLOS Neg. Trop. Dis*. **12**, e0006388 (2018).

4. Localisation of *Trypanosoma cruzi* in the chronic stage

4.1 The autoimmune hypothesis

Unlike other parasitic infections caused by *Trypanosoma brucei*, *Toxoplasma gondii* and *Plasmodium* species, the pathologies associated with *T. cruzi* infection develop at time-points when parasite numbers are extremely low[1]. A link between acute phase severity and progression of disease at later time-points has been hypothesised[2], but remains unresolved. The inability to routinely find parasites in infected humans and animal models after the resolution of parasitaemia[3] has been taken to suggest that infections are either cleared to sterility, or that the numbers of persisting parasites are so low that they are secondary to autoimmune damage. This 'autoimmune hypothesis', which stated that the chronic pathology was driven by immune activity against host targets triggered by, but not driven by, infection with the parasite, has been reviewed multiple times over past decades[4,5,6]. Self-reactive antibodies (Ab) and T-cells have long been identified in Chagas disease patients[7]. However, a direct link between these adaptive effectors and pathology is lacking[8]. Current dogma states that although autoreactivity may synergise with parasite targeted Ab and T-cells to promote cardiac damage, the continued presence of the parasite *is* required to drive the disease. This was summed up by Tarleton *et al* 2001[9] who states that, 'the persistence of *Trypanosoma cruzi* at specific sites in the infected host results in chronic inflammatory reactivity', and this is responsible for disease progression. Evidence supporting this hypothesis has come from improved detection technology[10,11], which is able to detect the rare parasites missed in earlier studies. Early[12,13] but not late (BENEFIT trial[14]) treatment with front-line drugs can slow progression of the cardiac disease.

4.2 Wide dissemination in the absence of adaptive effectors

Characterising parasite distribution, and dynamics, at the tissue/single cell level at chronic time-points is essential to better understand how pathology relates to infection and to better target new drugs. This has been recently reviewed[15]. Briefly, the earliest attempts to identify organs harbouring infection[16] involved creating histological sections from human tissue sourced from those who had succumbed to the disease. 'Nests' or 'pseudocysts' of amastigotes are sometimes visible as tightly packed clusters inside fixed host cells. Access to human tissue samples has been by necessity limited to patients who died during acute infection (Chagas, 1916[17]), or from chronic pathologies[18] or heart transplants. Animal models, most commonly the mouse, have been employed to better understand the organ/tissue distribution of *T. cruzi* infection and correlate well

with data collected in humans[19]. It is now widely accepted that in acute stage infection, or in instances of immunosuppression[20], the parasite is widely disseminated. It has been demonstrated *in vitro* that strains of all the *T. cruzi* lineages (DTU's) readily infect a large variety of cultured mammalian cells[21]. The parasite is assumed to have the capacity to invade any nucleated cell. Almost all organs and tissues have been described to harbour acute stage parasites across the diversity of mouse models and strain isolates. Tissues that have been reported to harbour high acute stage parasite loads include skeletal muscle[22], cardiac muscle[23], smooth muscle[24] and adipose tissue[25]. Sites of lower recorded infection load include immunologically privileged sites: brain, ovaries, testes and bone/cartilage[26]. Whether parasite-driven tropism[27]; nutritional environment of the invaded cells[28] or differing host immunological pressure[29] determines these higher/lower acute stage loads is unknown.

4.3 Chronic infection dynamics

Parasitaemia decreases dramatically with the expansion and deployment of the adaptive immune effectors. Since the published review presented in Chapter 2 has covered this topic, here it is sufficient to say that depending on the acute infection model[30] multiple arms of the innate and adaptive immune response are required for optimal acute phase control. Using data from bioluminescent models[31], the drop in tissue load is in the order of 100 to 1000-fold in size and occurs across all organs and tissues. Using more conventional PCR based sampling and histology in other mouse models[32] and humans[33], the transition to the chronic stage is marked by a similar decrease in parasite numbers. Detection of trypomastigotes in the blood of infected mice and patients becomes difficult. However, sterile cure is rarely noted[31,34], and an acute-like parasitaemia returns with the onset of immune suppression, even decades after resolution of the acute stage[35].

A key unresolved question is where do the remaining parasites persist in the host during chronic infections? The relevance of data derived from human chagasic syndrome end-points is uncertain[36] and no systematic autopsies have been conducted on intermediate stage patients who succumbed to other mortalities. Due to its importance in the morbidity and mortality associated with *T. cruzi* infection, the hearts of various parasite strain-mouse model combinations have been exhaustively examined by microscopy and sampled for *T. cruzi* DNA by PCR. Using these approaches, a direct correlation between end-point parasite presence and pathology has not been demonstrated. Even with highly sensitive molecular methods, parasites are not always detected in mouse hearts or in autopsies of human Chagas patients[37]. A recent review Lewis and Kelly, 2016[15], drawing on data from bioluminescent murine models, proposed a new hypothesis for the generation of cardiac pathology. It proposed that parasites periodically reinvade the heart form

other more permissive tissue sites, and that the resulting inflammatory responses drive the development of cardiac fibrotic damage, which accumulates over time.

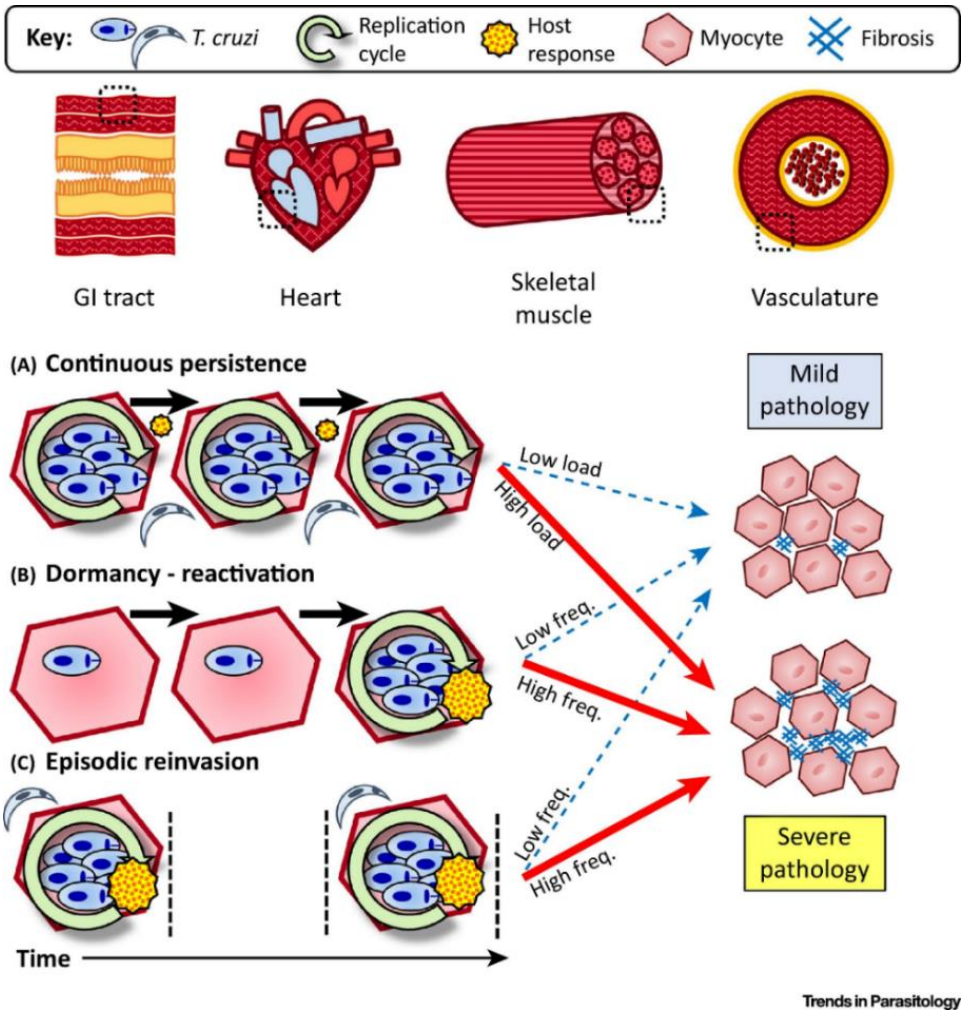

Figure 6 – Three non-mutually exclusive hypothesis for continued parasite persistence in patients and murine models. Taken from Lewis and Kelly, 2016[15].

The frequency of these events played out over >100-day infections in mice, and decades in humans, determines disease outcome. The symptoms observed in the clinic are therefore a cumulation of these repeated inflammatory events. Three mechanisms for tissue occupation have been proposed: (i) continuous replication and presence balanced by the local immune response, (ii) periodic activation of dormant parasites undetectable by bioluminescence imaging or PCR, and (iii) repeated re-invasion which promotes a sterilising immune response. Each mechanism is not mutually exclusive and is likely to be influenced by both parasite and host genetics[29]. Chapter 5 is concerned with the existence of a potentially dormant or quiescent life-cycle stage, so comment is reserved here. The current PCR, histology and bioluminescence data from both mice and man suggest the heart is not a site of continuous high load persistence and may routinely be cleared to sterility before being reseeded from other sites.

4.4 Localisation of the immuno-permissive sites

All currently available methodologies have been deployed in mouse models to identify these 'sites of persistence', from which the heart is repeatedly seeded. The skeletal muscle has been described in multiple models, and using multiple assays, as harbouring chronic stage parasites[38,39]. No evidence exists for the persistence of parasites at this site in humans. Smooth muscle tissue in the vascular system has been shown to harbour chronic parasites[24], again with no human data available for comparison. Adipose tissue has been described as a site of chronic stage occupation[34] and certainly harbours intense concentrations in mice lacking functional T and B cells. In the more disseminated infection associated with the C3H/HeN model, the visceral adipose tissue[29] is frequently found to contain bioluminescence signal. In the other host models, signal was more infrequent, or rarely found. Infection of cells of the central and peripheral nervous system has been recorded in humans during the acute stage and in reactivated infections[40], and a single report[41] from mice suggests this could be a site occupied during the chronic stage. The clinical features of both the cardiac and the digestive pathology involve the loss and damage of neuronal cells[42]. Whether this is the result of bystander immunological destruction or specific invasion of these cell types is unknown. The rationale behind the work presented in this chapter was to better define these chronic stage permissive sites at the level of the single-cell using state-of-the-art reporters in mouse models.

4.5 Background to publication

The gastrointestinal tract is a chronic persistence site – Despite significant effort, as referenced above, the localisation of chronic *T. cruzi* infection at the tissue and cellular level remains undefined. The development of the highly sensitive red-shifted luciferase reporter cell lines has allowed for the non-bias assessment of animal wide parasite persistence in the chronic stage, for the first time. This system circumvents the issue of sample bias that limits PCR and histological methods. Prior to this current project, the TcVI-CL *Luc* (CL Brener *red-shifted luciferase*) strain had been utilised. Identification of the gastrointestinal tract (GIT) as a site of relative higher parasite load >300dpi in the BALB/c model was published in 2014[31]. The other visceral organs were more sporadically bioluminescence positive at end-point. This relative restriction was abolished in immunosuppressed animals[31], which returned to an acute-like dissemination of infection. A 2016[29] study confirmed that higher GIT loads, specifically in the stomach, colon and caecum, were also a feature of both the C3H/HeN and the C57BL/6 mouse models. The level of restriction of infection to the GIT can be ordered BALB/c > C57BL/6 > C3H/HeN. Bioluminescent versions of the TcI-JR and TcX10/6 stains allowed comparison with TcVI-CLBr in all 3 murine hosts. All parasite strains were persistent in the GIT during chronic

infections, with the ability to disseminate to the 'systemic' organs ordered from TcI-JR > TcI-X10/6 > TcVI-CL. These papers, and some preliminary data that showed the skin in the BALB/c model as an additional site of higher chronic tissue loads[43], informed the hypothesis described above[15]. This hypothesis suggests that chagasic heart pathology is not the result of intense and persistent infection of this organ, as had been suggested, but the result of repeated invasions from more immunotolerant sites such as the GIT.

Pilot data using the CL Brener bioluminescent:fluorescent reporter – The completion of the first bioluminescent:fluorescent reporter (CLBr Luc:mNeonGreen)[44] opened the possibility that the cell types occupied by chronic stage parasites could be defined for the first time. The aim of the work presented in the *mBio* publication (below) was:

1: To fully exploit the highly-sensitive bioluminescent and fluorescent properties of the CL Luc:mNeonGreen reporter in both the BALB/c and C3H/HeN models. These were chosen as they represent opposite ends of the spectrum of ability to restrict infection to the GIT, which correlates directly with cardiac fibrosis at end-point[15].

2: To identify the host cell types occupied by the parasites at time-points >100dpi.

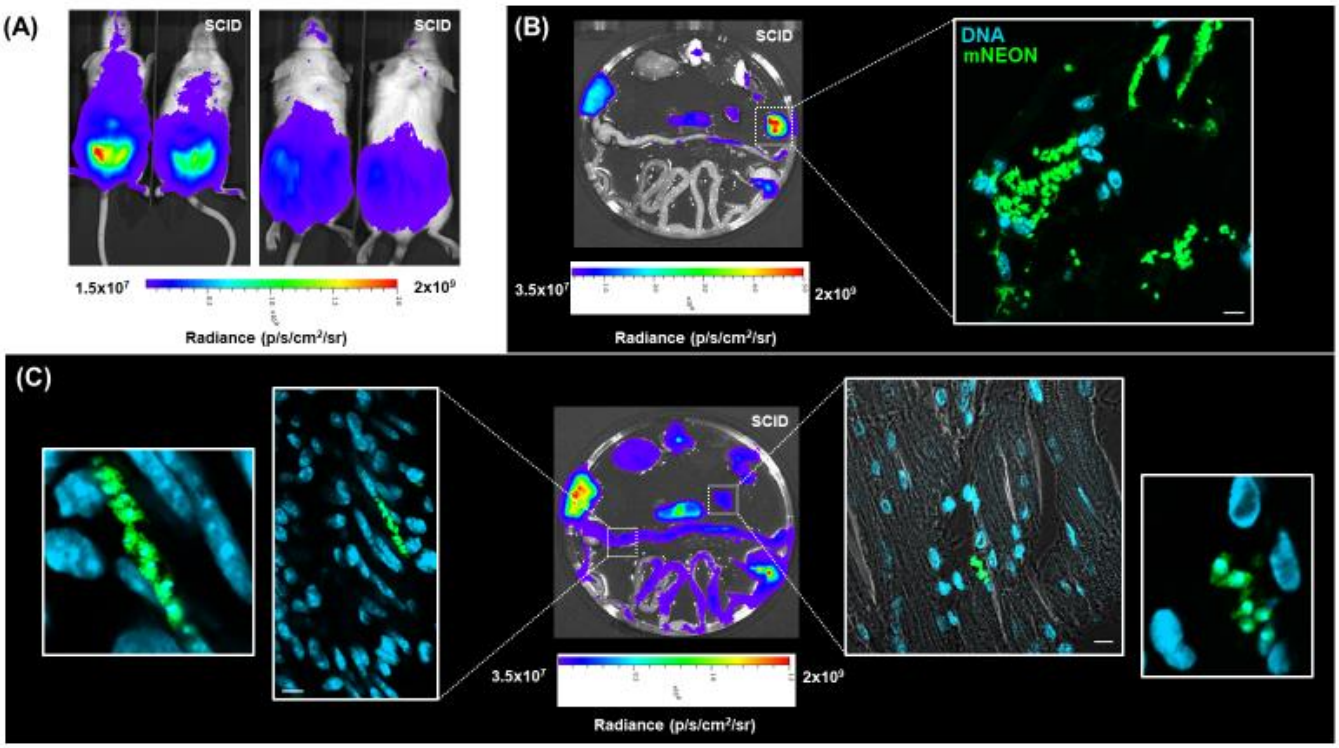

Figure 14 – Representative bioluminescent and fluorescent images from a CB17 SCID mouse 15dpi. **A.,** *in vivo* imaging reveals animal wide signal with the highest intensities around the site of the i.p. inoculation. **B.,** When visceral organs are imaged *ex vivo* the adipose tissues had the highest radiance (p/s/cm^2/sr) output. Fluorescent mNeonGreen+ parasites are evident in large numbers throughout histological sections. **C.,** Removal of the adipose tissue allows the software to match less intense regions of photon output with the log10 scale pseudocolour heatmap. Histological sections from the heart routinely show infected host cells containing mNeonGreen+ parasites but not at the intensities of the adipose tissue. mNeonGreen+ parasites imaged in a colon section is also shown.

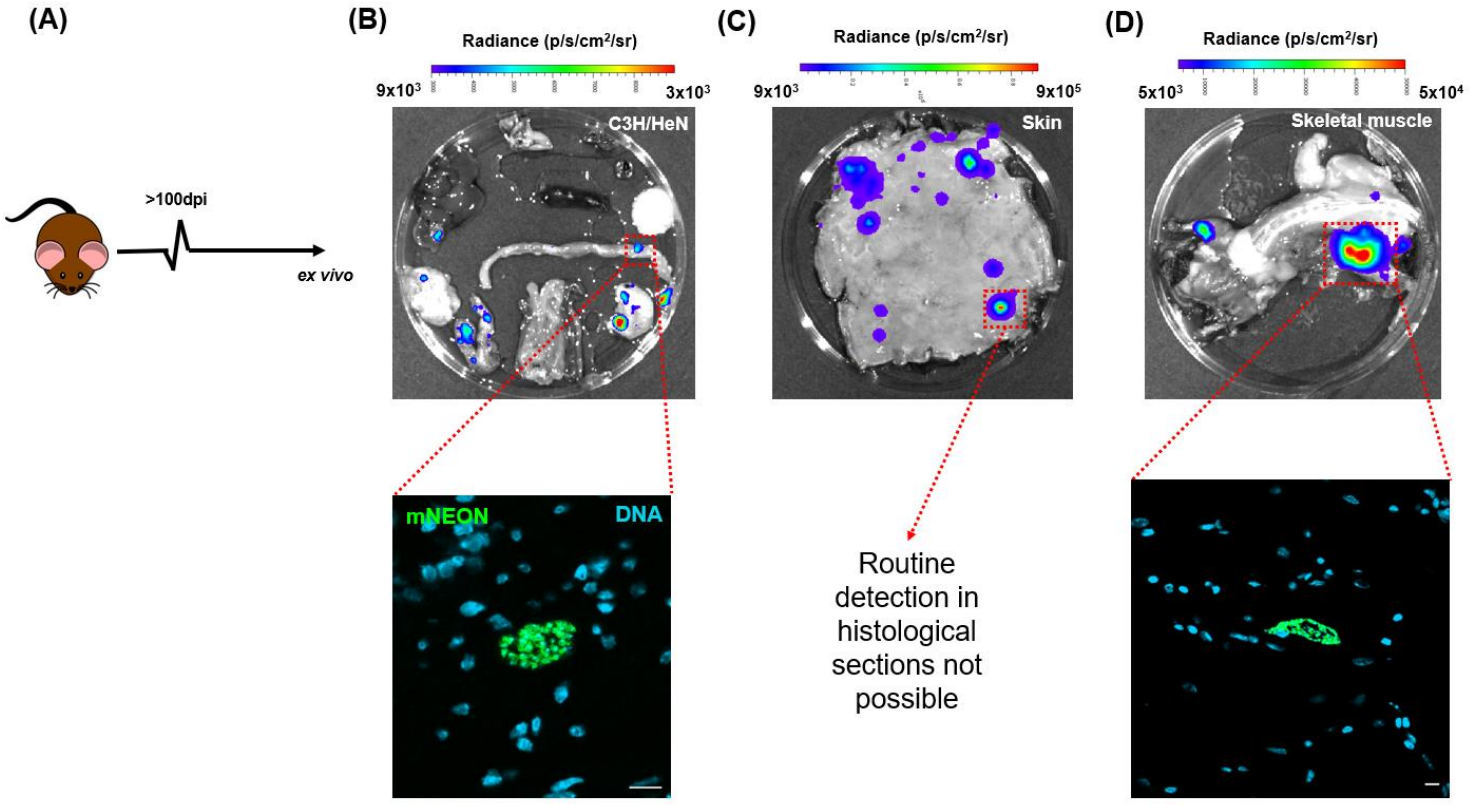

Figure 15 – A., Cartoon showing >100dpi *ex vivo* analysis of the *T. cruzi* CL Luc:mNeonGreen infected C3H/HeN model. Representative bioluminescence images for the visceral organs **(B)**, skin **(C)** and skeletal muscle **(D)**. Fluorescent parasites fixed in tissue sections from both the GIT and the skeletal muscle can be imaged after laborious and time-consuming searching. Routine detection in skin biopsies is not possible.

As a pilot to establish how easily the CL Luc:mNeonGreen reporter could be identified in processed tissues, and to assess the quality of the images that could be generated, CB17-SCID mice were infected. Through a natural mutation in the DNA-dependent protein kinase, catalytic subunit (DNA-PKcs) gene, which is essential for V(D)J recombination, these animals lack functional T and B lymphocytes (*TACONIC* website). The germ-line encoded innate compartment is unaffected. Animals were infected with 10,000 *in vitro* tissue cultured trypomastigotes (TCTs) and culled 15 days post inoculation (Figure 14). *In vivo* and *ex vivo* imaging, tissue processing and confocal image generation methodology are described in the published paper (below) and were unaltered from this pilot. Bioluminescence signal was strongest from the adipose tissue. Only after removal of this tissue from the dish was the IVIS software able to produce a pseudocolour Log10 scale heatmap for the other organs due to the high-level signal from the adipose tissue swamping the other signals. Fluorescent mNeonGreen+ parasites were easily identified, and in extremely high numbers, in the adipose tissue. Even in organs with relatively low signal, i.e. colon and heart, fluorescent parasites were routinely detectable and easily imaged. The picture quality was excellent and encouraged us to pilot a chronically infected animal to determine if parasites could be routinely imaged at this key time period (Figure 15).

Whole mounting the colonic gut wall, a key technical advance – The immunocompetent C3H/HeN model was selected for infection with the *T. cruzi* CL Luc:mNeonGreen clone. Tissue was exercised >100dpi and histologically sectioned and fixed in paraffin. An advantage of this method was the preservation of the distinct morphological layers of the GIT. The major disadvantage was the time required to find chronic stage parasites. Despite exhaustive searches of several hundred 10µm thick sections from the GIT, heart and spleen, many of which had been selected based on positive bioluminescence signal, the number of parasite-infected cells found was very low. Additionally, since individual amastigotes are ~5 µm in diameter larger clusters or 'nests' of parasites were inevitably sliced and placed on different slides.

To overcome these limitations, we focused on the colon, a region already well defined as harbouring higher infection loads into the chronic stage. In collaboration with Dr Connor McCann of UCL Institute of Child Health, we developed a novel protocol that produced colonic gut wall whole mounts suitable for confocal imaging. The production of these whole mounts is described in the paper below and has allowed us now to search much larger volumes of material in a shorter time. This made it practical, for the first time, to detect multiple extremely rare infected cells at a persistence site. This advance also made possible the work presented in Chapters 5 and 6.

References

1. Tiexeira, A. R., Hecht, M. M., Guimaro, M. C. Sousa, A. O. and Nitz, N. Pathologies of Chagas disease: parasite persistence and autoimmunity. *Clin. Microbiol. Rev*. **24**, 592-630 (2011).
2. Claudio, R. F., Lima, M. R., Grisotto, M. G. and Alvarez, J. m. Influence of acute-phase parasite load on pathology, parasitism, and activation of the immune system at late chronic phase of Chagas disease. *Infect. and Immunol*. **67**, 308-318 (1999).
3. D'Avila, D. A., Galvao, L. M., Sousa, G. R., Britto, C., Moreira, O. C. and Chiari, E. Monitoring the parasite load in chronic Chagas disease patients: comparison between blood culture and quantitative real time PCR. *PLOS one*. **13**, e0208133 (2018).
4. KIerszenbaum, F. Chagas disease and autoimmunity. *mBio*. **12**, 210–223 (1999).
5. Kierszenbaum, F. Views on the autoimmunity hypothesis for Chagas disease pathogenesis. *FEMS Immunol. And Med. Microbiol*. **37**, 1-11 (2003).
6. De Bona, E. et al. Autoimmuity in chronic Chagas disease: a road of multiple pathways to cardiomyopathy. *Front. Immunol*. **9**, e1842 (2018).
7. Giromes, N., Cuervo, H. and Fresno, M. *Trypanosoma cruzi*-induced molecular mimicry and Chagas disease. *Curr. Topics in microbiol. and Immunol*. **296**, 89-123 (2005).

8. Soares, M. B., Pontes-de-Carvalho, L. and Ribeiro-de-Santos, R. The pathogenesis of Chagas disease: when autoimmune and parasite-specific immune responses meet. *An. Acad. Bras. Clin*. **73**, 548-559 (2001).
9. Tarleton, R. l. Parasite persistence in the aetiology of Chagas disease. *Int. J. Parasitol*. **31**, 550-4(2001).
10. Lewis, M. D. et al. Bioluminescence imaging of chronic *Trypanosoma cruzi* infections reveals tissue-specific parasite dynamics and heart disease in the absence of locally persistent infection. *Cell Microbiol*. **16**, 1285-1300 (2014).
11. Salomone, O. A. et al. *Trypanosoma cruzi* in persons without serological evidence of disease, Argentina. *Emerg. Infect. Dis*. **9**, 1558-1562 (2003).
12. Viotti, R., Vigliano, C. and Segura, E. Treatment of chronic Chagas disease with benznidazole: clinical and serologic evolution of patients with long-term follow-up. *Am. Heart J*. **127**, 151-62 (1994).
13. Francisco, A. F. Jayawardhana, S., Taylor, M. C, Lewis, M. D. Kelly, J. M. Assessing the effectiveness of curative benznidazole treatment in preventing chronic cardiac pathology in experimental models of Chagas disease. *mBio*. 62, e00832-18 (2018).
14. Percoul, B. et al. The BENEFIT trial: where do we go from here? *PLOS Neg. Trop. Dis*. **10**, e0004343 (2016).
15. Lewis, M. D. and Kelly, J. M. Putting infection dynamics at the heart of Chagas disease. *Trends in Parasitol*. **32**, 899-911 (2016).
16. Laranja, F. S., Dias, E., Nobrega, G. and Miranda, A. Chagas disease. *Circulation*. **14**, 1035-1060 (1956).
17. Chagas, C. Agradecimento ao banquete oferecido por um grupo de colegas, amigos e admiradores, quando de seu regresso da Argentina, onde representou o Brasil no congresso médico, realizado em setembro. *Discursos e conferências*. *Rio de Janeiro*. 3-13 (1916).
18. Benvenuti, L. A., Roggerio, A., Nishiva, A. S., Campos, S. V., Fiorelli, A. I. Levi, J. E. *Trypanosoma cruzi* persistence in the native heart is associated with high-grade myocarditis, but not with Chagas disease reactivation after heart transplantation. *J. Heart Lung Transplant*. **33**, 698-703 (2014).
19. Zingales, B. Drug discovery for Chagas disease should consider *Trypanosoma cruzi* strain diversity. *Mem. Inst. Oswaldo Cruz*. **109**, 828-833 (2014).
20. Pinazo, M. et al. Immunosuppression and Chagas disease: a management challenge. *PLOS Neg. Trop. Dis*. **7**, e1965 (2013).

21. Duran-Rehbein, G., Vargas-Zambrano, J. C., Cuellar, A., Puerta, C. J. and Gonzalez, J. M. Mammalian cellular culture models of *Trypanosoma cruzi* infection: a review of the published literature. *Parasite*. **21**, e38 (2014).
22. Cummings, K. L. and Tarleton, R. L. Rapid quantitation of *Trypanosoma cruzi* in host tissue by real-time PCR. Mol. *Biochem. Parasitol*. **129**, 53-9 (2003).
23. Guarner, J. et al. Mouse model for Chagas disease: immunohistochemical distribution of different stages of *Trypanosoma cruzi* in tissues throughout infection. *The Am. J. of Trop. Med. and Hyg*. **65**, 152-158 (2001).
24. Hassan, G. S. et al. *Trypanosoma cruzi* infection induces proliferation of vascular smooth muscle cells. *Infect. Immun*. **74**, 152-159 (2006).
25. Versiani, A. Evidence for *Trypanosoma cruzi* in adipose tissue in human chronic Chagas disease pathology. *Microbes and Infections*. **12**, 1002-1005 (2011).
26. Morocoima, A., Rodriguez, M., Herrera, L. and Urdaneta-Morales, S. *Trypanosoma cruzi*: experimental parasitism of bone and cartilage. *Parasitol. Res*. **99**, 663-8 (2006).
27. Andrade, L. O. et al. Differential tissue tropism of *Trypanosoma cruzi* strains: an *in vitro* study. *Men. Inst. Oswaldo Cruz*. **105**, 834-837 (2010).
28. Taylor, M. C. and Kelly, J. M. Iron metabolism in trypanosomatids, and its crucial role in infection. *Parasitology*. **137**, 899-917 (2010).
29. Lewis, M. D., Francisco, A. F., Taylor, M. C., Jayawardhana, S. and Kelly, J. M. Host and parasite genetics shape a link between *Trypanosoma cruzi* infection dynamics and chronic cardiomyopathy. *Cell Microbiol*. **18**, 1429-1443 (2016).
30. Perez-Mazliah, D., Ward, A. I. and Lewis, M. D. Host-parasite dynamics in Chagas disease from systemic to hyper-local scales. *Para. Immunol. Rev*. **2020**, e12786 (2020).
31. Lewis, M. D. et al. Bioluminescence imaging of chronic *Trypanosoma cruzi* infections reveals tissue-specific parasite dynamics and heart disease in the absence of locally persistent infection. *Cell Microbiol*. **16**, 1285-300 (2014).
32. Kirchhoff, L. V., Votava, J. R., Ochs, D. E. and Moser, D. R. Comparison of PCR and microscopic methods for detecting *Trypanosoma cruzi*. *J. Clin. Microbiol*. **34**, 1175-1996 (1996).
33. Vergara, C. et al. Detection of *Trypanosoma cruzi* by PCR in adults with chronic Chagas disease treated with nifurtimox. *PLOS one*. **14**, e0221100 (2019).
34. Pack, A. D., Collins, M. H., Rosenberg, C. S. and Tarleton, R. L. High competent, non-exhausted CD8+ T cells continue to tightly control pathogen load throughout chronic *Trypanosoma cruzi* infection. *PLOS Pathog*. **14**, e1007410 (2018).

35. Burgos, L. G., Ortiz, B. D., Ojeda, A. and Melo, M. Reactivation of Chagas disease by immunosuppressive therapy in a patient with systemic lupus erythromatosus: report of an exceptional case. *Am. J. Dermatopathol*. **34**, 84-9 (2012).
36. Jones, E. M., Colley, D. G., Tostes, S., Lopes, E. R., Vnencak-Jones, C. L. and McCurley, T. L. Amplification of a *Trypanosoma cruzi* DNA sequence from inflammatory lesions in human chagasic cardiomyopathy. *Am. J. Trop. Med. Hyg*. **48**, 348-348 (1993).
37. Burgos, J. M. et al. Molecular identification of *Trypanosoma cruzi* discrete typing units in end-stage chronic Chagas heart disease and reactivation after heart transplantation. *Clin. Infect. Dis*. **51**, 485-95 (2010).
38. Bustamante, J. M., Bixby, L. M. and Tarleton, R. L. Drug-induced cure drives conversion to a stable and protective CD8+ T central memory response in chronic Chagas disease. *Nat. Med.* **14**, 542-550 (2008).
39. Weaver, J. D., Hoffman, V. J., Roffe, E. and Murphy, P. M. Low-level parasite persistence drives vasculitis and myosistis in skeletal muscle of mice chronically infected with *Trypanosoma cruzi*. *Infect. Immun*. **87**, e00081-19 (2019).
40. Cordova, E., Boschi, A., Ambrosioni, J., Cudos, C. and Corti, M. Reactivation of Chagas disease with central nervous system involvement in HIV-infected patients in Argentina, 1992-2007. *Int. J. Infect. Dis*. **12**, 587-92 (2008).
41. Buckner, F. S., Wilson, A. J. and Voorhis, W. C. Detection of live *Trypanosoma cruzi* in tissues of infected mice by using histochemical stain for β-galactosidase. *Infect. Immun*. **67**, 403-409 (1999).
42. Bonney, K. M. and Engman, D. M. Chagas heart disease pathogenesis: one mechanism or many? *Curr. Mol. Med*. **8**, 510-518 (2008).
43. Lewis, M. D., Francisco, M. D., Jayawardhana, S., Langston, H., Taylor, M. C. Kelly, J. M. Imaging the development of chronic Chagas disease after oral transmission. *Sci. Reports*. **8**, e11292 (2018).
44. Costa, F. C. et al. Expanding the toolbox for *Trypanosoma cruzi*: a parasite line incorporating a bioluminescent-flourescent dual reporter and streamlines CRISPR/Cas9 functionality for rapid *in vivo* localisation and phenotyping. *PLOS Neg. Trop. Dis*. **12**, e0006388 (2018).

Dr Connor McCann – https://www.ucl.ac.uk/child-health/people/iris-profile-conor-mccann

4.6 –

LONDON SCHOOL of HYGIENE &TROPICAL MEDICINE

London School of Hygiene & Tropical Medicine
Keppel Street, London WC1E 7HT
T: +44 (0)20 7299 4646
F: +44 (0)20 7299 4656
www.lshtm.ac.uk

RESEARCH PAPER COVER SHEET

Please note that a cover sheet must be completed for each research paper included within a thesis.

SECTION A – Student Details

Student ID Number	lsh1406159	**Title**	Mr
First Name(s)	Alexander		
Surname/Family Name	Ward		
Thesis Title	Trypanosoma cruzi: Where is it? Does it ever sleep? Why is a sterile outcome rarely achieved?		
Primary Supervisor	John Kelly		

If the Research Paper has previously been published please complete Section B, if not please move to Section C.

SECTION B – Paper already published

Where was the work published?	mBio		
When was the work published?	July 2020		
If the work was published prior to registration for your research degree, give a brief rationale for its inclusion			
Have you retained the copyright for the work?*	Yes	Was the work subject to academic peer review?	Yes

*If yes, please attach evidence of retention. If no, or if the work is being included in its published format, please attach evidence of permission from the copyright holder (publisher or other author) to include this work.

SECTION C – Prepared for publication, but not yet published

Where is the work intended to be published?	
Please list the paper's authors in the intended authorship order:	
Stage of publication	Choose an item.

SECTION D – Multi-authored work

For multi-authored work, give full details of your role in the research included in the paper and in the preparation of the paper. (Attach a further sheet if necessary)	Training and guidance in animal work provided by co-authors Amanda F. Francisco and Shiromani Jayawardhana. Whole monting imaging method for T. cruzi infected mouse model developed by Connor McCann (NIH) and Archie Khan, Michael Lewis and myself at (LSHTM). Figure 6 data collection and presentation done by Michael Lewis and Archie Khan. All the other data were generated by myself. I wrote the first draft of the paper Final edit done by John Kelly.

SECTION E

Student Signature	Alexander Ward
Date	09/07/2020

Supervisor Signature	John Kelly
Date	10/07/2020

see https://mbio.asm.org/content/11/4/e01242-20 for the on-line version.

In vivo analysis of *Trypanosoma cruzi* persistence foci at single cell resolution

Alexander I. Ward,[a] Michael D. Lewis,[a] Archie Khan,[a] Conor J. McCann,[b] Amanda F. Francisco,[a] Shiromani Jayawardhana,[a] Martin C. Taylor,[a] John M. Kelly[a#]

[a]Department of Infection Biology, London School of Hygiene and Tropical Medicine, London, UK

[b]Stem Cells and Regenerative Medicine, Great Ormond Street Institute of Child Health, University College London, London, UK

Running Head: Parasite persistence in chronic Chagas disease

[#]Address correspondence to John M. Kelly, john.kelly@lshtm.ac.uk

Word counts

Abstract: 247

Text: 5000

ABSTRACT Infections with *Trypanosoma cruzi* are usually life-long despite generating a strong adaptive immune response. Identifying the sites of parasite persistence is therefore crucial to understand how *T. cruzi* avoids immune-mediated destruction. However, this is a major technical challenge because the parasite burden during chronic infections is extremely low. Here, we describe an integrated approach involving comprehensive tissue processing, *ex vivo* imaging, and confocal microscopy, which has allowed us to visualise infected host cells in murine tissue, with exquisite sensitivity. Using bioluminescence-guided tissue sampling, with a detection level of <20 parasites, we show that in the colon, smooth muscle myocytes in the circular muscle layer are the most common infected host cell type. Typically, during chronic infections, the entire colon of a mouse contains only a few hundred parasites, often concentrated in a small number of cells containing >200 parasites, that we term mega-nests. In contrast, during the acute stage, when the total parasite burden is considerably higher and many cells are infected, nests containing >50 parasites are rarely found. In C3H/HeN mice, but not BALB/c, we identified skeletal muscle as a major site of persistence during the chronic stage, with most parasites found in large mega-nests within the muscle fibres. Finally, we report that parasites are also frequently found in the skin during chronic murine infections, often in multiple infection foci. In addition to being a site of parasite persistence, this anatomical reservoir could play an important role in insect-mediated transmission, and have implications for drug development.

IMPORTANCE *Trypanosoma cruzi* causes Chagas disease, the most important parasitic infection in Latin America. Major pathologies include severe damage to the heart and digestive tract, although symptoms do not usually appear until decades after infection. Research has been hampered by the complex nature of the disease and technical difficulties in locating the extremely low number of parasites. Here, using highly sensitive imaging technology, we reveal the sites of parasite persistence during chronic stage infections of experimental mice at single-cell resolution. We show that parasites are frequently located in smooth muscle cells in the circular muscle layer of the colon, and that skeletal muscle cells and the skin can also be important reservoirs. This information provides a framework for investigating how the parasite is able to survive as a life-long infection, despite a vigorous immune response. It also informs drug-development strategies by identifying tissue sites that must be accessed to achieve a curative outcome.

KEY WORDS: *Trypanosoma cruzi*, Chagas disease, chronic persistence, murine imaging, colon, skeletal muscle, skin

INTRODUCTION

The intracellular protozoan parasite *Trypanosoma cruzi* is the etiological agent of Chagas disease, and can infect a wide variety of mammalian hosts. Transmission to humans is mainly via the hematophagous triatomine insect vector, which deposits infected faeces on the skin after a blood-meal, with the parasite then introduced through the bite wound or mucous membranes. Oral, congenital and blood transfusion are other important transmission routes. 6-7 million people in Latin America are infected with *T. cruzi* (1), and as a result of migration, there are now hundreds of thousands of infected individuals in non-endemic regions, particularly the USA and Europe (2, 3).

In humans, infection normally results in mild symptoms, which can include fever and muscle pain, although in children the outcome can be more serious. Within 6 weeks, this acute phase is usually resolved by a vigorous CD8+ T cell response (4, 5), and in most cases, the infection progresses to a life-long asymptomatic chronic stage, where the parasite burden is extremely low and no apparent pathology is observed. However, in ~30% of individuals, the infection manifests as a symptomatic chronic condition, although this can take many years to develop. The associated cardiac dysfunction, including dilated cardiomyopathy and heart failure, is a major cause of morbidity and mortality (6, 7). In addition, ~10% of those infected display digestive pathologies, such as megacolon and megaoesophagus, which on occasions can occur in parallel with cardiac disease. There is no vaccine against *T. cruzi* infection, and the current frontline drugs, benznidazole and nifurtimox, have limited efficacy, require long treatment regimens, and can result in severe side effects (8, 9). The global effort to discover new drugs for Chagas disease involves not-for-profit drug development consortia, as well as the academic and commercial sectors (10, 11). Progress would benefit considerably from a better understanding of parasite biology and disease pathogenesis.

One of the major challenges in Chagas disease research is to determine how *T. cruzi* survives as a life-long infection, despite eliciting a vigorous immune response which is able to reduce the parasite burden by >99%. Exhaustion of the parasite-specific CD8+ T cell response does not appear to be the reason (12). Alternative explanations include the possibility that *T. cruzi* is able to persist in immune-tolerant tissue sites (13), and the potential for the parasite to assume a non-dividing dormant form that does not trigger an overt immune response (14). Attempts to investigate these issues in humans have been limited by the long-term and complex nature of the disease, and by difficulties in monitoring tissue infection dynamics during the chronic stage. By necessity, most information on the sites of parasite location in humans has come from autopsy and transplant studies (15), and the significance of these data to patients in the asymptomatic chronic stage is unclear. Bioluminescence imaging of animal models has therefore been adapted as an approach to explore aspects of host:parasite interaction, disease pathology and drug-development (16-18). Our previous work has exploited highly sensitive *in vivo* imaging to monitor mice infected with bioluminescent *T. cruzi* that express a red-shifted luciferase (19-21). These experiments have shown that mice are useful predictive models for human infections in terms of infection dynamics (21, 22), drug-sensitivity (23) and the spectrum of cardiac pathology (24). We have also demonstrated that *T. cruzi* infection is pan-tropic during the acute stage, and that the adaptive immune response results in a 100 to 1000-fold reduction in the whole animal

parasite burden as infections transition to the chronic phase, a process initiated 2-3 weeks post infection. The gastrointestinal (GI) tract, particularly the colon and/or stomach, was found to be a major site of parasite persistence during chronic stage infections, but it has not so far been possible to identify the infected host cell types in these complex tissues. The immune-mediated restriction to the GI tract was not absolute, with both host and parasite genetics impacting on the extent to which the infection could disseminate to a range of other organs and tissues (22). The severity of chronic cardiac pathology in different mouse strains was associated with the ability of parasites to spread beyond the permissive niche provided by the GI tract, and with the incidence of cardiac infection. This led us to propose a model in which the development of chagasic cardiac pathology, was linked with the frequency of the localised inflammatory immune responses stimulated by periodic trafficking of parasites into the heart (13).

More detailed information on the precise sites of parasite survival during chronic infections will provide new insights into disease pathogenesis, and aid the design of both immunotherapeutic and chemotherapeutic strategies. The scarcity of parasites during the chronic stage has made addressing this issue a major challenge, with PCR-based approaches being both uninformative with respect to host cell types, and unreliable because of the highly focal and dynamic character of infections (20, 23). To resolve this, we constructed *T. cruzi* reporter strains engineered to express a fusion protein that was both bioluminescent and fluorescent (25). This allowed individual infected host cells to be visualised routinely within chronically infected mouse tissue. The bioluminescent component facilitates the localisation of infection foci within *ex vivo* tissue samples, and fluorescence then enables histological sections to be rapidly scanned to identify infected cells (26). The utility of this approach has been further extended by using EdU labelling and TUNEL assays to explore the replicative status of parasites *in situ*.

Here, we describe how these enhanced imaging procedures, coupled with modifications to tissue processing, have allowed us to identify the sites of parasite persistence during chronic murine infections. We reveal that the circular muscle layer is the major reservoir of infection in the colon, that skeletal muscle can be an important site of persistence, although this phenomenon appears to be strain-specific, and that the skin can harbour multiple infection foci.

RESULTS

Locating the sites of *T. cruzi* persistence within the external wall of the colon during chronic murine infections. In multiple murine models, with a variety of parasite strains, bioluminescence imaging has revealed that the GI tract, particularly the large intestine and stomach, is a major site of parasite persistence during chronic *T. cruzi* infection (20, 22). However, our understanding of how this impacts on pathogenesis has been complicated by the difficultly in precisely locating, and then visualising, parasite infected cells. To resolve these technical issues, we infected mice with the *T. cruzi* CL-Luc::Neon line that constitutively expresses a reporter fusion protein that is both bioluminescent and fluorescent (25), and adapted our dissection procedures to allow a more detailed assessment of parasite location (Materials and Methods). At various periods post-infection, the colon of each mouse was removed, pinned luminal side up, and peeled

into two distinct sections (Fig. 1a and b) - the mucosal layers consisting of (i) thick mucosal, muscularis mucosa, and submucosal tissue, and (ii) the muscular coat, including the longitudinal and circular smooth muscle layers, the enteric neuronal network, at the level of the myenteric plexus, intramuscular neurons and extrinsic nerve fibres. The resulting external gut wall mount is thin enough, and sufficiently robust, to allow the full length of the colon to be viewed in its entirety at a 3-dimensional level by confocal laser scanning microscopy. Using this approach, each bioluminescent focus in live peeled tissue from chronically infected mice could be correlated with fluorescent parasites in individual infected host cells (Fig. 1c and d). The resulting images revealed that the limit of detection achievable by bioluminescence imaging is less than 20 parasites. This level of sensitivity, in an *ex vivo* context, confirms the utility of this model for studies on infection dynamics (22), and drug and vaccine efficacy (24, 27, 28). In infected host cells, the number of parasites could be determined with precision using full-thickness serial Z-stacking (Fig. 1e, Fig. S1). This allowed us to establish that the total number of parasites persisting in the external colonic wall (tunica muscularis) of a chronically infected mouse is typically in the range of a few hundred (697 $\pm$ 217, n=16), although this number can be higher if the tissue contains one or more “mega-nests” (Fig. 1c, highlighted in yellow, as example).

When we compared parasite distribution in the external gut wall during acute and chronic murine infections, the most striking difference was the presence in the chronic stage of some host cells that were infected with >200 parasites (Fig. 2). The existence of these mega-nests resulted in a major alteration in parasite number distribution at the level of single infected host cells (Fig. 1, Fig. 2b-d). In acute infections, parasites were spread between many more host cells, with the average parasite content per cell remaining relatively low (Mouse M1=6.5, M2=6.7, M3=6.5, M4=4.6, M5=19.7, mean=9.4; $1.15<\mu<16.46$, 95% confidence interval) (Fig. 2a, c and d). In the chronic stage, the situation was different. Of the total parasite number in the smooth muscle, more than half were present in mega-nests of >200 (marked by a dashed red line, Fig. 2c), although most infected cells (>90%) contained fewer than 50 parasites. Nest size could extend to >1000 parasites. The number per infected cell was determined by Z-stacking, which could be done with accuracy, even at this level of parasite burden (for details, see Fig. S1). In the chronic stage, fully developed trypomastigotes were not apparent in any of the infected cells examined during this study. In contrast, fully developed flagellated trypomastigotes were routinely observed in nests during the acute stage (Fig. 2e, as example). We did not find a single mega-nest in external colonic wall tissue derived from any animal during an acute stage infection, with 63 parasites being the maximum. Both of these findings could indicate faster replication and differentiation rates during the acute stage as the parasite attempts to more rapidly disseminate at the beginning of an infection. As a corollary to this, it may be that a slower growth rate during the chronic stage also benefits the parasite by reducing the immunological footprint of the infection. It will be important to explore this further.

To more accurately determine the specific location of parasites within the colon of chronically infected mice, we made histological sections of paraffin embedded whole colon tissue derived from both C3H/HeN and BALB/c mice infected with the CL Brener dual reporter strain. Using bioluminescence-guided sampling and

confocal imaging, we exhaustively searched the tissue sections for fluorescent parasites (>100 sections per mouse). Bioluminescent foci could be well correlated with individual infected host cells, or small numbers of infected cells in close proximity (Fig. 3b, Fig. S2). Infected cells were most commonly located in the circular muscle layer, and only infrequently in the longitudinal muscle, or, despite its relatively larger size/volume, the mucosal layer (Fig. 2, Fig. 3b and c, Fig. S2). No infections of the columnar epithelial cells in the mucosal layer were detected in any mouse. We therefore conclude that in the colon, smooth muscle tissue is the major, although not the exclusive site of parasite persistence during chronic infection. Consistent with the whole mount imaging results (Fig. 2c), there was high variability in the number of *T. cruzi* per infected cell in the colonic tissue, ranging from single parasites to nests of >200, but no obvious correlation between the parasite burden per cell and the location of the infected cells within the various tissue layers. In the whole tissue mounts, based on the bioluminescence profile, there was a tendency for the proximal region of the colon to be more highly infected than the mid and distal regions, although this did not reach statistical significance (Wilcoxon rank sum test) (Fig. 4a).

To identify the major cell type(s) which act as parasite hosts during chronic infections of the GI tract, we single-stained whole mounted external colonic wall sections with specific antibodies against SMA-α (smooth muscle actin-α), β-tubulin-3 (a marker for neurons), and CD45 (a broad range marker of all nucleated hematopoietic cells) (Materials and Methods). These experiments showed that smooth muscle myocytes were the predominant host cell type (Fig. 4b and c), with a minority of infected cells stained with the neuronal or leukocyte marker. Interestingly, mega-nests, cells infected with >200 parasites, were refractive to staining (Fig. 4b). In the case of the cytoplasmic markers SMA-α and β-tubulin-3, this could reflect that their levels are considerably reduced because almost all of the cytoplasm is filled with parasites.

Assessing skeletal muscle and the skin as sites of parasite persistence during chronic stage murine infections. For this study, BALB/c and C3H/HeN mice were chronically infected with *T. cruzi* CL-Luc::Neon (25), and the dissection procedures used for *ex vivo* imaging (Fig. 5a) were further modified to extend the range of tissue sites that could be assessed (Materials and Methods). Total removal of the skin and fur from the carcass allowed the whole of the skeletal muscle system to be exposed and imaged (Fig. 5b and d). The skin could also be placed fur side down and imaged in its entirety after the removal of adipose tissue. All adipose tissue harvested during the dissection process was combined to be imaged separately.

Each C3H/HeN mouse registered a bioluminescence signal in the skeletal muscle during chronic stage infections (n=16) (Fig. 5c). It could be inferred from the bioluminescence intensity that the parasite burden in this strain was significantly higher in skeletal muscle than in other organs or tissues, including the GI tract and lungs (*p*-value <0.001, Wilcoxon signed rank test) (Fig. 5b and c). As previously reported (22), parasite burden and dissemination during chronic stage infections is more extensive in C3H/HeN mice than in other mouse models. In line with this, we did not routinely detect highly bioluminescent foci in the skeletal muscle of BALB/c mice (Figure 5b and c). In addition, the adipose samples of the BALB/c mice were consistently close to background levels, whereas with the C3H/HeN mice, more than half displayed a detectable signal

(>2SDs above background radiance) (Fig. 5c). Following bioluminescence-guided excision (Fig. 5d), infected foci from C3H/HeN skeletal muscle were subjected to histological sectioning and examined by confocal microscopy, with parasites detected on the basis of green fluorescence. Consistent with the external colonic wall data (Fig. 1), strong bioluminescent foci corresponded with large mega-nests constituted by many hundreds of parasites (Fig. 5d). Co-staining of these skeletal muscle sections with anti-actin-α antibodies revealed that the mega-nests were internal to the muscle fibres. Therefore, skeletal muscle represents an important site of parasite persistence in chronically infected C3H/HeN mice, but not in BALB/c.

Previous studies have shown evidence of *T. cruzi* infection foci localised to skin samples (20, 22). However, the extent to which the skin could act as a potential reservoir site has not been evaluated systematically. To investigate this, we infected C3H/HeN and BALB/c mice with the bioluminescent *T. cruzi* lines JR (DTU I) or CLBR (DTU VI), and employed a modified dissection protocol that allowed near-complete skins from infected mice to be subjected to *ex vivo* imaging after removal of subcutaneous adipose tissue (Materials and Methods) (Fig. 6a). Depending on the infection model, between 80% and 90% of mice had at least one discernible focus of skin infection (Fig. 6b). For all four parasite:mouse strain combinations, we observed a wide range of skin parasitism patterns, as judged by both the number and the intensity of the bioluminescent foci (Fig. 6a and b). There was some evidence that C3H/HeN mice had more CL Brener skin parasites than BALB/c mice (Fig. 6b and c). Infections with the CL Brener strain produced more discrete foci and a higher inferred parasite load than JR infections, although some of this effect could be attributed to lower luciferase expression levels in the JR strain (22). Skin imaging was conducted after removal of subcutaneous adipose tissue by dissection, strongly suggesting that the majority of parasites were resident in the dermis. To visualise parasites at the cellular level, bioluminescence positive biopsies were processed for thin section fluorescence imaging from infections with parasites expressing the bioluminescent:fluorescent fusion protein (n~300 sections from 5 mice). Visualisation of infected cells in the skin biopsies was more challenging than for other tissues because of technical difficulties in generating longitudinal sections. Only a single, apparently multinucleated infected cell was identified (Fig. 6d), containing approximately 30 parasites and located within 150 µm of the epidermis. Parasites in this anatomical location could have a role in disease transmission.

DISCUSSION

Chronic Chagas disease in humans is characterised by long-term parasite persistence at levels that are difficult to monitor with accuracy, even using highly sensitive PCR-based techniques. This has been a complicating factor in diagnosis, and in monitoring therapeutic cure during clinical trials (29, 30). Additionally, it has not been possible to identify the main tissues and/or organs that function as sites of parasite persistence in an immunological environment that otherwise tightly controls the infection. Information on the systemic parasite load and location throughout the infection would provide a better understanding of disease progression and the determinants of the wide spectrum of symptoms that are characteristic of this chronic condition. Experimental animal models have proved to be invaluable experimental tools for providing data in these areas, particularly in combination with genetically modified parasite reporter strains. These systems can provide real-time readouts on infection dynamics (20, 22, 31), insights into tissue tropism (26), and

information on the influence of host and parasite genetics. The murine models used in the current study display a similar infection profile to that in humans, have proved to be predictive of drug efficacy, and display a spectrum of cardiac pathology that mirrors aspects of the human disease.

Here, we exploited parasites that express fusion proteins containing bioluminescent and fluorescent domains. Together with improved tissue preparation techniques, this has enabled us to achieve a limit of detection by *ex vivo* imaging that is less than 20 parasites (Fig. 2d and e). By facilitating the routine detection of parasites in their tissue context, at the level of individual host cells, these approaches have overcome a major barrier that has restricted progress in the investigation of chronic *T. cruzi* infections. Previous reports using bioluminescent parasites identified the GI tract as a major site of parasite persistence during the chronic stage (20, 22). However, these studies, which involved several mouse:parasite strain combinations, revealed few details on the nature of host cells, or on their precise location within tissue. In the colon, we have now shown that the circular smooth muscle coat is the predominant site of parasite persistence (Fig. 3) and that smooth muscle myocytes are the main infected host cell type. Enteric neurons can also be parasitized, but these infections are much less common (Fig. 4). The extent to which this apparent tropism is determined by a metabolic preference for the corresponding regions/cells, or by the immunological microenvironment is not known. Interestingly, external colonic wall resident CD45+ve hematopoietic cells were rarely infected (Fig. 4a), even though myeloid cells are well known targets during the acute stage infection in other sites such as the spleen or bone marrow. We also failed to find a single instance where parasites infected epithelial cells on the mucosal surface, suggesting that parasitized cells or trypomastigotes are unlikely to be shed into the lumen of the large intestine.

Experiments have shown that parasite survival in the colon during chronic infections reflects crucial differences between the immune environment of certain GI tract regions and systemic sites (22). Immunosuppression of infected mice leads to widespread parasite dissemination to other less permissive organs and tissues, including the heart. There is clearly a host genetic component to this immune restriction since the same parasite strains display a wider tissue distribution in C3H/HeN mice than in the BALB/c strain (Fig. 5c), a phenomenon which is associated with increased cardiac pathology (22). In the human population, this highlights that genetic diversity affecting the functioning of the immune system and its ability to restrict the tissue range of *T. cruzi* to reservoir sites could be a major determinant of Chagas disease pathology. Within C3H/HeN mice, skeletal muscle was also found to be an important site of persistence during the chronic stage, whereas in the BALB/c strain, parasites were far less evident in this location (Fig. 5c). Some *T. cruzi* strains have been reported to be myotropic in mice, with pathological outcomes that include paralyzing myositis and skeletal muscle vasculitis (32). Myocyte infections could also provide the parasite with access to myoglobin, a source of haem or iron that may contribute to a nutritional environment that is favourable for replication. The ability of high numbers of parasites to survive long-term in the skeletal muscle, compared to other sites, indicates that this tissue can function as a more immunologically permissive niche in the genetic background of the C3H/HeN mouse. Strikingly, myocytes in this tissue could contain several hundred parasites (Fig. 5d). We have previously suggested that the existence of large mega-nests such as

these could have implications for drug efficacy (26), with parasites in the centre of the nest having reduced drug exposure compared to those on the periphery, possibly contributing to treatment failure. This form of “herd-protection” may not be captured in the type of high-throughput *in vitro* screening assays that are a common feature of the drug development process. It will also be interesting to explore whether some parasites within these mega-nests adopt a metabolically quiescent state, analogous to the dormant phenotype recently reported (14).

Our study has also demonstrated that the skin is another location where *T. cruzi* can be frequently detected during chronic infections. In both C3H/HeN and BALB/c mice, infection levels of >80% were observed, although there was considerable variability in the level of infectivity in terms of the number of bioluminescent foci and the total parasite load. The extent of this only became apparent when the entire skin of the mouse was examined by *ex vivo* imaging with the fur side down (Fig. 6), presumably because bioluminescent signals at the levels displayed by the majority of foci are masked by the fur when monitored by *in vivo* imaging. Skin-localised parasites are a common and well characterised feature of many *Leishmania* species infections. More recently, it has also been reported that *Trypanosoma brucei,* can also be detected in the skin of both mice and humans, and that these parasites could have important roles in persistence and transmission (33, 34). Until now, descriptions of cutaneous *T. cruzi* have been restricted to intermittent (chagoma and Romaña's sign) or atypical manifestations of the acute stage (35), or to reactivation of chronic infections as a result of immunosuppression (36, 37). Parasites in the dermal layers (Fig. 6) have the potential to play a crucial role in transmission of Chagas disease since they would have ready access to the triatomine vector during a blood meal. The extent to which *T. cruzi* parasites are localised to the skin during human chronic infections will also be of interest, since this could impact on transmission dynamics, as has been suggested from the detailed spatial analysis of *Leishmania donovani* in the skin of infected mice (38). It will also be important to determine whether these skin-resident parasites are persistent at this location, or whether they represent a transient population that is constantly re-seeded from other permissive niches, such as the GI tract (13). Resolution of this question will help to inform drug-design by revealing whether the ability to access parasites in the dermal layers has to be a pre-requisite property of novel therapeutics. In murine models of *T. brucei* infection, adipose tissue also forms an important parasite reservoir (39). This was not the case with chronic *T. cruzi* infections of BALB/c mice (Fig. 5c), where parasites were largely absent from these tissue sites. Bioluminescent foci were detected in the adipose tissues in approximately half of the chronically infected C3H/HeN mice. However, rather than a specific tropism, this may simply reflect the immunological context in C3H/HeN mice, which allows more extensive parasite distribution than in other mouse models (22).

In summary, we have provided new data on the sites of parasite persistence in murine models of chronic Chagas disease. This provides a framework for identifying the immunological parameters that determine whether a specific tissue site can act as a permissive niche, and for investigating the extent to which the parasite itself has a direct role in the process.

MATERIALS AND METHODS

Ethics. Animal work was carried out under UK Home Office project licenses (PPL 70/8207 and P9AEE04E4) and approved by the LSHTM Animal Welfare and Ethical Review Board. Experiments were conducted in accordance with the UK Animals (Scientific Procedures) Act 1986.

Parasites, mice and infections. Two parasite reporter strains were used; the bioluminescent:fluorescent *T. cruzi* CL-Luc::Neon, a CL Brener clone (DTU VI) which expresses a fusion protein containing red-shifted luciferase linked to mNeonGreen (20, 25), and a JR clone (DTU I), which expresses red-shifted luciferase (19, 22). Epimastigotes were grown at 28°C in RPMI-1640 supplemented with 0.5% (w/v) tryptone, 20 mM HEPES pH 7.2, 30 mM haemin, 10% heat-inactivated fetal bovine serum (FBS), 2 mM sodium glutamate, 2 mM sodium pyruvate, 100 µg/ml streptomycin and 100 U/ml penicillin, with 150 µg/ml hygromycin (CL Brener) or 100 µg/ml G418 (JR) as selective drugs. Metacyclic trypomastigotes (MTs) were obtained by transfer to Graces-IH transformation medium (40). MTs were harvested after 4–7 days, when 70–90% of parasites had differentiated. Tissue culture trypomastigotes were obtained from infected MA104 cells grown at 37°C using Minimal Eagles medium supplemented with 10% heat-inactivated FBS.

BALB/c and C3H/HeN mice were purchased from Charles River (UK), and CB17 SCID mice were bred in-house. Animals were maintained under pathogen-free conditions in individually ventilated cages. They experienced a 12 h light/dark cycle and had access to food and water *ad libitum*. Female mice aged 8-12 weeks were used. SCID mice were infected with 1×10^4 *in vitro*-derived tissue culture trypomastigotes in 0.2 ml PBS via i.p. injection. Other mice were infected by i.p injection with 1×10^3 bloodstream trypomastigotes derived from parasitemic SCID mouse blood. Infection by the intravenous, subcutaneous or oral routes does not result in a different parasite distribution profile in tissues or organs (20, 31). All SCID mice developed fulminant infections and were euthanized at, or before, humane end-points by lethal injection with 0.1-0.2 ml Dolethal.

***Ex vivo* bioluminescence imaging.** For *ex vivo* imaging, mice were injected with 150 mg/kg d-luciferin i.p., then sacrificed by lethal i.p. injection 5 min later (20, 21). Mice were perfused with 10 ml 0.3 mg/ml d-luciferin in PBS via the heart. Organs and tissues were imaged using the IVIS Spectrum system (Caliper Life Science) and LivingImage 4.7.2 software. Firstly, heart, lungs, spleen, liver, GI tract, GI mesenteric tissue, kidneys and all visceral adipose tissue were transferred to a Petri dish in a standardized arrangement, soaked in 0.3 mg/ml d-luciferin in PBS and imaged using maximum detection settings (2 min exposure, large binning). Then, the skin was removed from the carcass and subcutaneous adipose tissue recovered (41) and added to the visceral fat creating a whole ‘adipose tissue’ sample, which was imaged in the same way. The skin was placed fur down, soaked in 0.3 mg/ml d-luciferin and imaged under the same conditions as the internal organs. The skeletal muscle was placed dorsal side up and soaked in 0.3 mg/ml d-luciferin and imaged, as above.

To assess infection intensities in *ex vivo* tissues, regions of interest (ROIs) were drawn to quantify bioluminescence expressed as radiance (photons/s/cm^2/sr). Because different tissue types have different background radiances, we normalized data from infected mice using matching tissues from uninfected controls (n=4) and used the fold-change in radiance, compared with the tissue-specific controls, as the final measure. Detection thresholds for *ex vivo* imaging were determined using the fold-change in radiance for ROIs from infected mice compared with matching empty ROIs in control mice of comparable age.

In some experiments, the colon was removed after standard imaging, an incision was made down the line of mesentery attachment, and the tissue pinned out under a dissection microscope. Using ultrafine tweezers, large sections of the smooth muscular coat from the other layers were peeled off, whilst the tissue remained bathed in 0.3 mg/ml d-luciferin (41). After imaging, luciferin was removed by 2x washing with PBS. Tissue was fixed with 4% paraformaldehyde for 45 min, followed by 2x washes with PBS (41). External colonic wall tissue was then whole mounted in Vectashield antifade mounting medium with DAPI (Vector Laboratories) and imaged as below.

Histological sections were created after bioluminescence-guided excision of infection foci from skeletal muscle and colon tissue (25, 26, 41). Biopsies were first incubated in 95% EtOH at 4^{o}C overnight, and then washed in 100% EtOH (4x10 min), followed by xylene (2x12 min). Samples were embedded by placing in melted paraffin wax (2x12 min). The wax was allowed to set and the embedded pieces were sectioned into 5-20 µm histological sections using a microtome. The sections were melted and paraffin dissolved in xylene for 30 s, then washed in 95% EtOH (3x1 min), followed by 3 washes in PBS. Sections were mounted in Vectashield and imaged using the Zeiss LSM880 confocal microscope. For precise counting of intracellular parasites, samples were imaged in 3-dimensions, with the appropriate scan zoom setting, and the files analysed using image J software (Fig. S1).

Antibody staining. Deparaffinized sections were incubated at 4^{o}C overnight in primary antibody diluted at 1:200 in PBS/0.5% FBS. Antibodies against β-tubulin-3 (Biolegend, Cat#802001), CD45 (Tonbo Biosciences, Cat#70-0451), smooth muscle actin (Sigma, Cat#A2547), and skeletal muscle actin (Thermo Fisher, Cat#MA5-12542) were used to stain for neuronal, nucleated hematopoietic, smooth muscle and skeletal muscle cells, respectively. Secondary antibodies (Thermo Fisher) diluted 1:500 in PBS were incubated on sections for 3 h at room temperature before mounting. Both primary and secondary antibodies were removed by 3x2 min washes in PBS. For staining of whole colon external wall sections, the tissue was submerged in the primary antibody dilution for 48 h at 4^{o}C, and then submerged in the secondary dilution at room temperature for 3 h before 3x2min washes in PBS.

Statistics

The Shapiro-Wilk test for normality, and the Wilcoxon rank sum non-parametric test were used to analyse the data presented in Fig. 4 and 5. Two-way ANOVA with Tukey's post hoc correction testing was used for Fig. 6. All tests were performed in GraphPad Prism v.8.

ACKNOWLEDGEMENTS

This work was supported by the following awards: UK Medical Research Council (MRC) Grants MR/T015969/1 to JMK and MR/R021430/1 to MDL, and MRC LID (DTP) Studentship MR/N013638/1 to AIW. The funders had no role in study design, data collection and interpretation, or the decision to submit the work for publication.

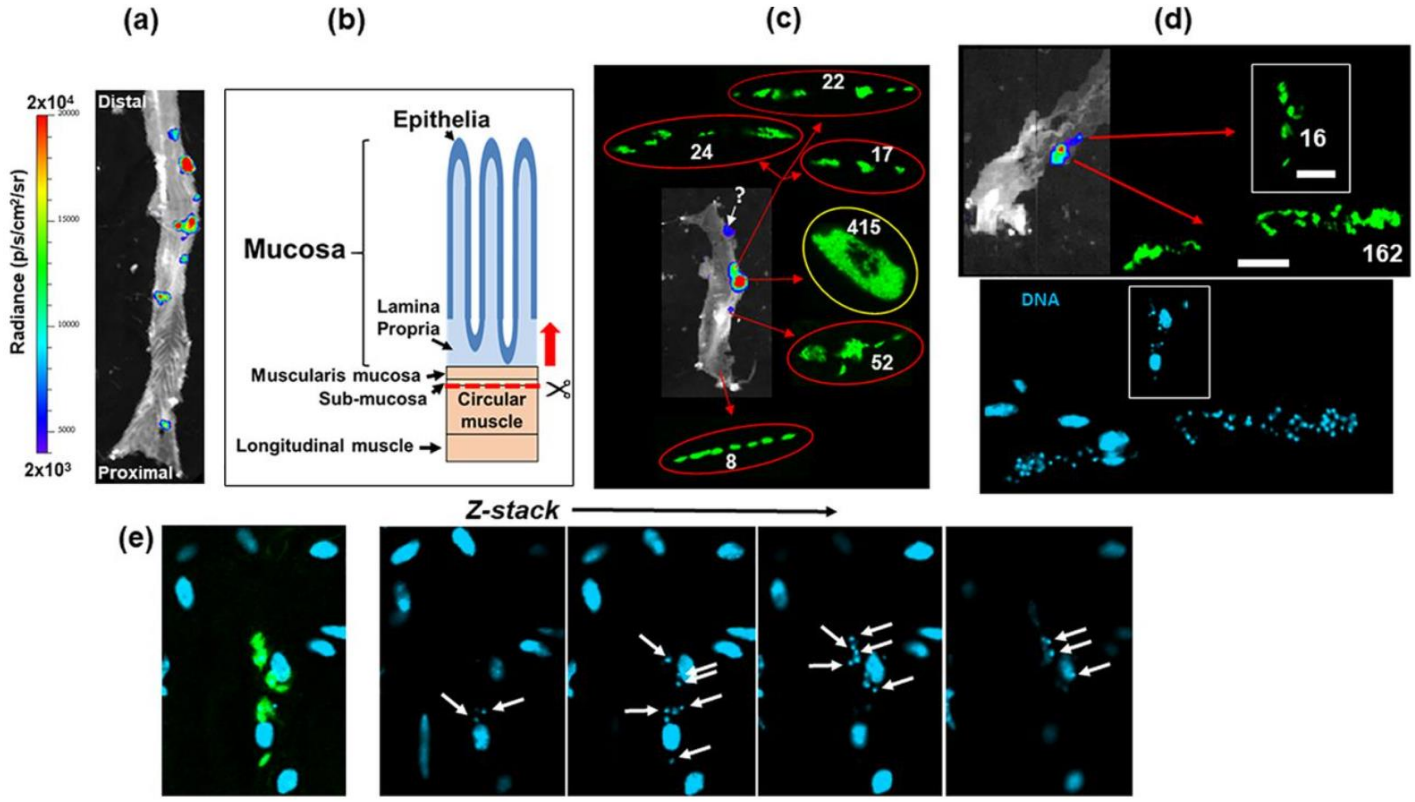

FIG 1 The limit of detection by *ex vivo* bioluminescence imaging of the murine colon is less than 20 parasites. (a) *Ex vivo* bioluminescence imaging of a section of the colon from a C3H/HeN mouse chronically infected (155 days post-infection) with *T. cruzi* CL-Luc::Neon (25), pinned luminal side up. The bioluminescence signal is on a linear scale pseudocolour heat map (same for all bioluminescence images in this figure). (b) Schematic showing the distinct layers of the GI tract (see also Fig. 3a). The dashed red line and arrow indicates the position above which tissue can be peeled off to leave the external colonic wall layers. (c) Bioluminescence image of a colonic wall section after peeling. The insets show the fluorescent parasites (green) detected after exhaustive 3-dimensional imaging of the tissue section (Materials and Methods), and the numbers detected. Parasites corresponding to one bioluminescent focus (marked by '?') could not subsequently be found, due to technical issues. (d) Upper image; an external colonic wall layer from a separate mouse showing the correlation of bioluminescence imaging and fluorescence (green), including an infection focus with 16 parasites (left) (white scale bars=20 µm). A vertical line was introduced into the colon *ex vivo* image by the IVIS software due to a pixel defect. Lower image; staining with DAPI identifies the location of parasite (small) and host cell (large) DNA. (e) Determination of parasite number. Serial Z-sections of the external colonic wall tissue containing the parasite nest shown in (d) indicate how 3-dimensional imaging can be used to calculate the number of parasites on the basis of DNA staining. See Fig. S1 for more detail.

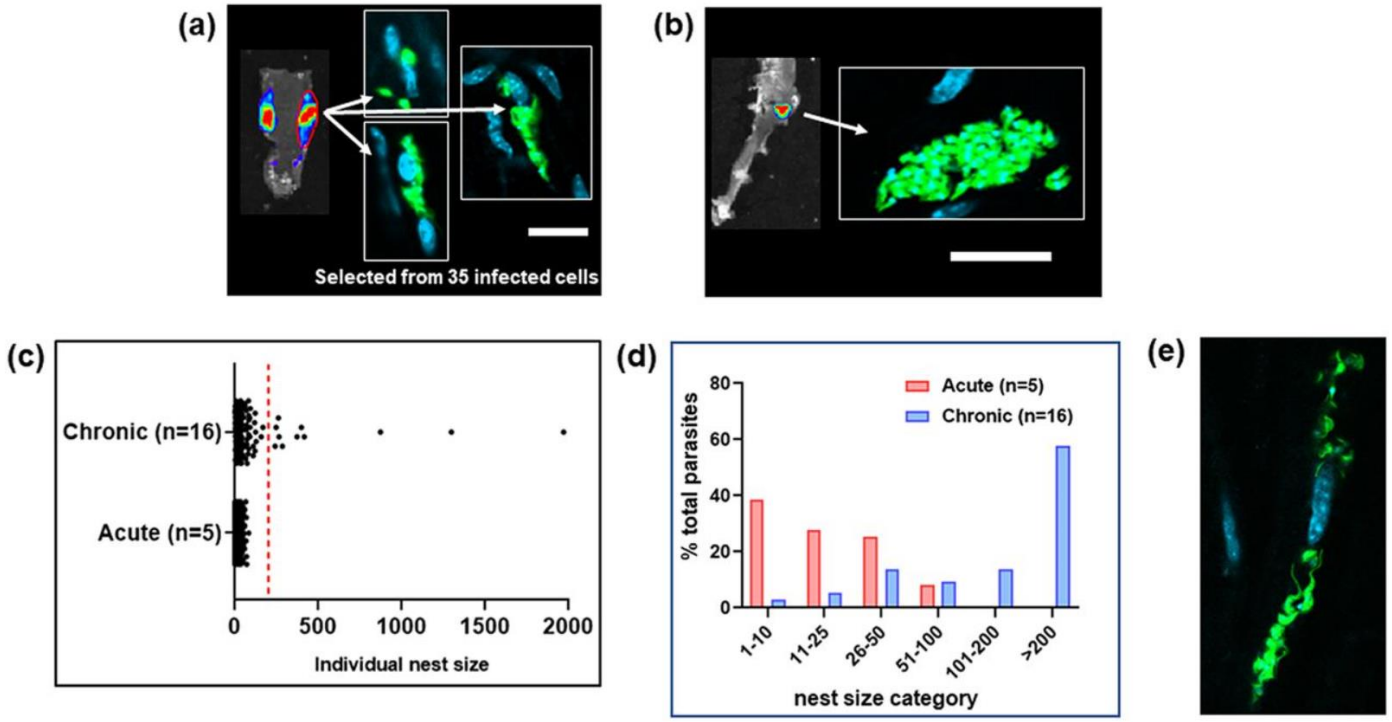

FIG 2 In the external colonic wall of chronic stage mice, cells infected with more than 200 parasites contain much of the *T. cruzi* population. (a) Bioluminescence imaging of peeled colon isolated from a C3H/HeN mouse 15 days post-infection (acute stage). After mounting, the region of interest (ROI) encompassed by the red line was exhaustively searched by confocal microscopy. 35 infected cells were found within the ROI, 3 of which are shown. Parasites, green. (b) Using the same approach, the external colonic wall from a chronically infected mouse (183 days post-infection) was assessed. The bioluminescent focus corresponded to a single highly infected host cell. White scale bars=20 µm. (c) Pooled data from *T. cruzi* infected cells in peeled colonic wall tissue muscle, isolated from 5 acutely and 16 chronically infected mice. Tissue was examined and the number of parasites per host cell established after the use of Z-stacking to provide a 3-dimensional image (Fig. S1). Each dot represents a single infected cell (acute stage, n=1198; chronic stage, n=140). Dots above the dashed red line indicate infected cells containing >200 parasites. (d) The same data set expressed as the % of the total parasites detected in the colons of mice in the acute (n=5) and chronic (n=16) stage of infection, by nest size category. (e) An infected cell in the peeled colon of a mouse in the acute stage (15 days post-infection) of infection in which the parasites have differentiated to flagellated trypomastigotes.

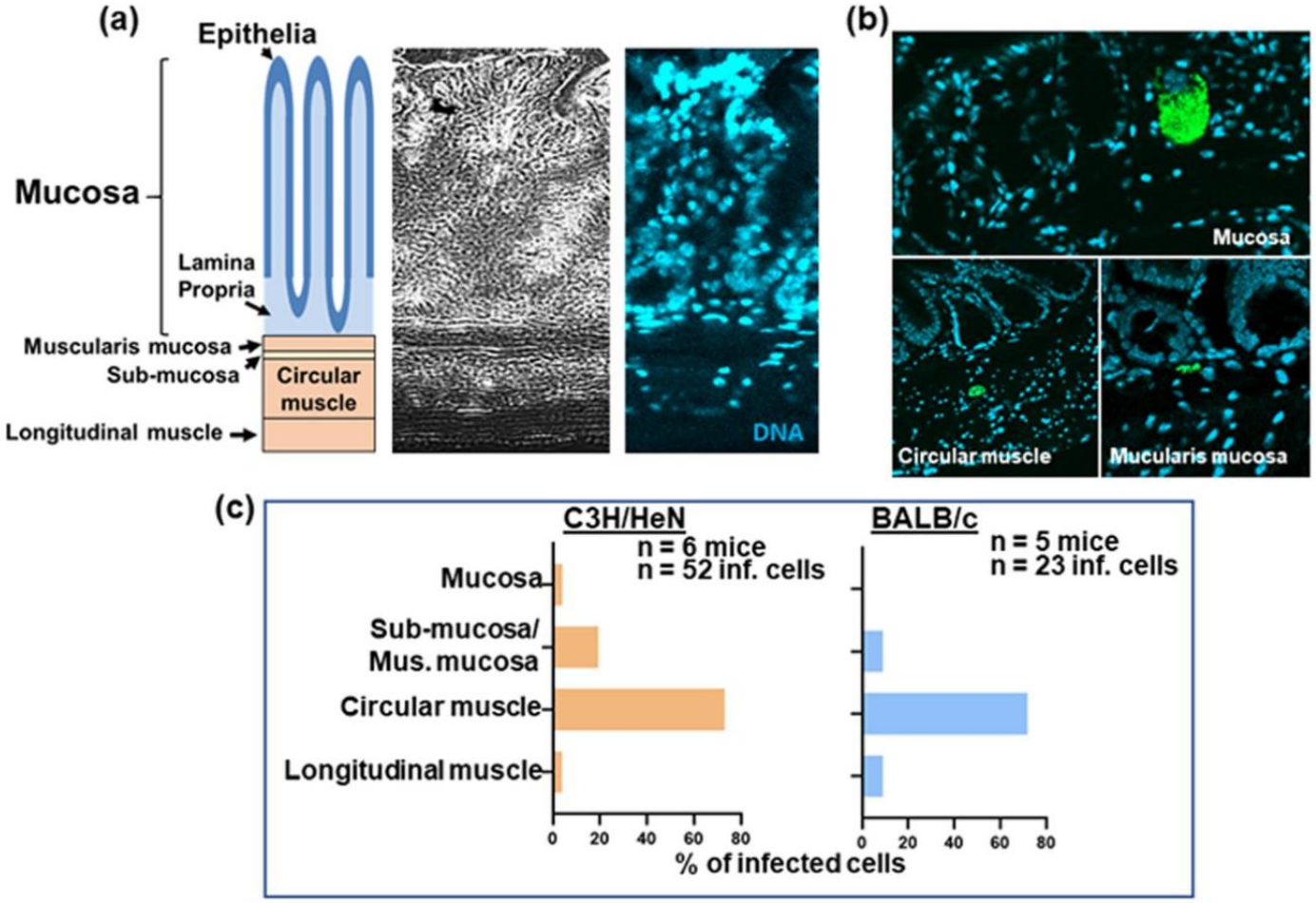

FIG 3 The majority of parasites in the colon of a chronically infected mouse are located in the circular muscle section. (a) Depiction of the layers of the GI tract, correlated with the phase (left) and DNA stained (DAPI) (right) images of the same tissue section. (b) Examples of host cells infected with fluorescent parasites (green) detected in different layers of the GI tract (see also Fig. S2). Infection foci were located by confocal imaging of fixed histological sections. (c) Summary of parasite location data obtained using histological sections from chronically infected C3H/HeN and BALB/c mice.

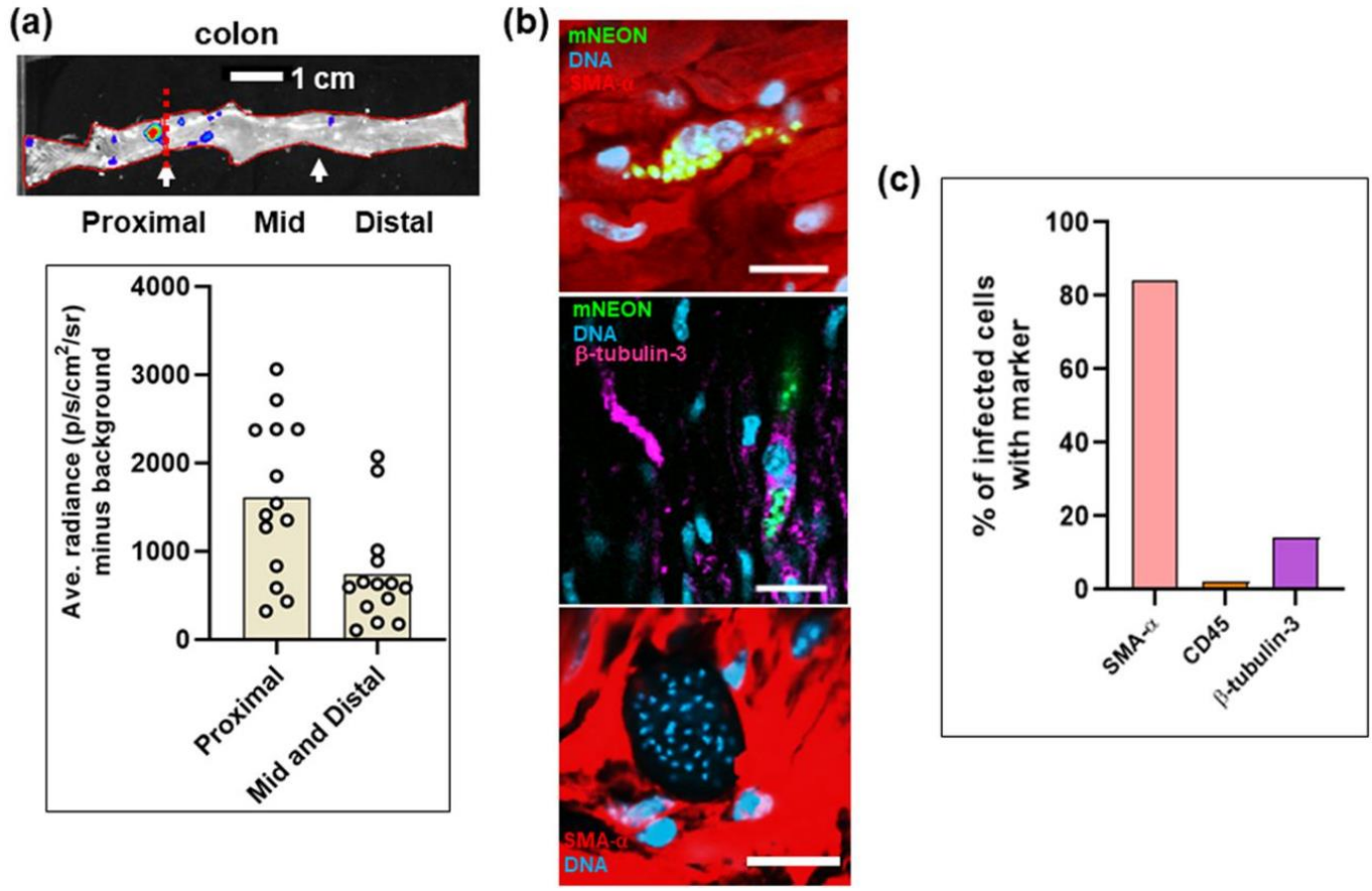

FIG 4 Smooth muscle cells are the predominant infected cell type in the GI tract of chronically infected mice. (a) Bioluminescence image of the large intestine of a chronically infected C3H/HeN mouse indicating the proximal, mid and distal regions, defined as the first, second and third segments measured using image J software. Data were analysed as described (Materials and Methods) (n=14) and are presented in the bar chart as the average radiance (p/s/cm^2/sr) minus the background. (b) Illustrative images taken with the mounted external colonic wall section, following staining with cell type specific antibodies (Materials and Methods). Upper, infected smooth muscle cell. Middle, infected neuronal cell. Lower, a large parasite nest, refractive to staining with any of the 3 markers. (c) Bar chart summarising distribution of infection by host cell type. External colonic wall sections were single-stained with

cell type specific antibodies. For smooth muscle (SMA-α; n=4 mice, 24 infected cells, 20+ve); for neuronal cells (β-tubulin-3; n=3 mice, 14 infected cells, 2+ve); for immune cells (CD45, n=8 mice, 61 infected cells, 1+ve).

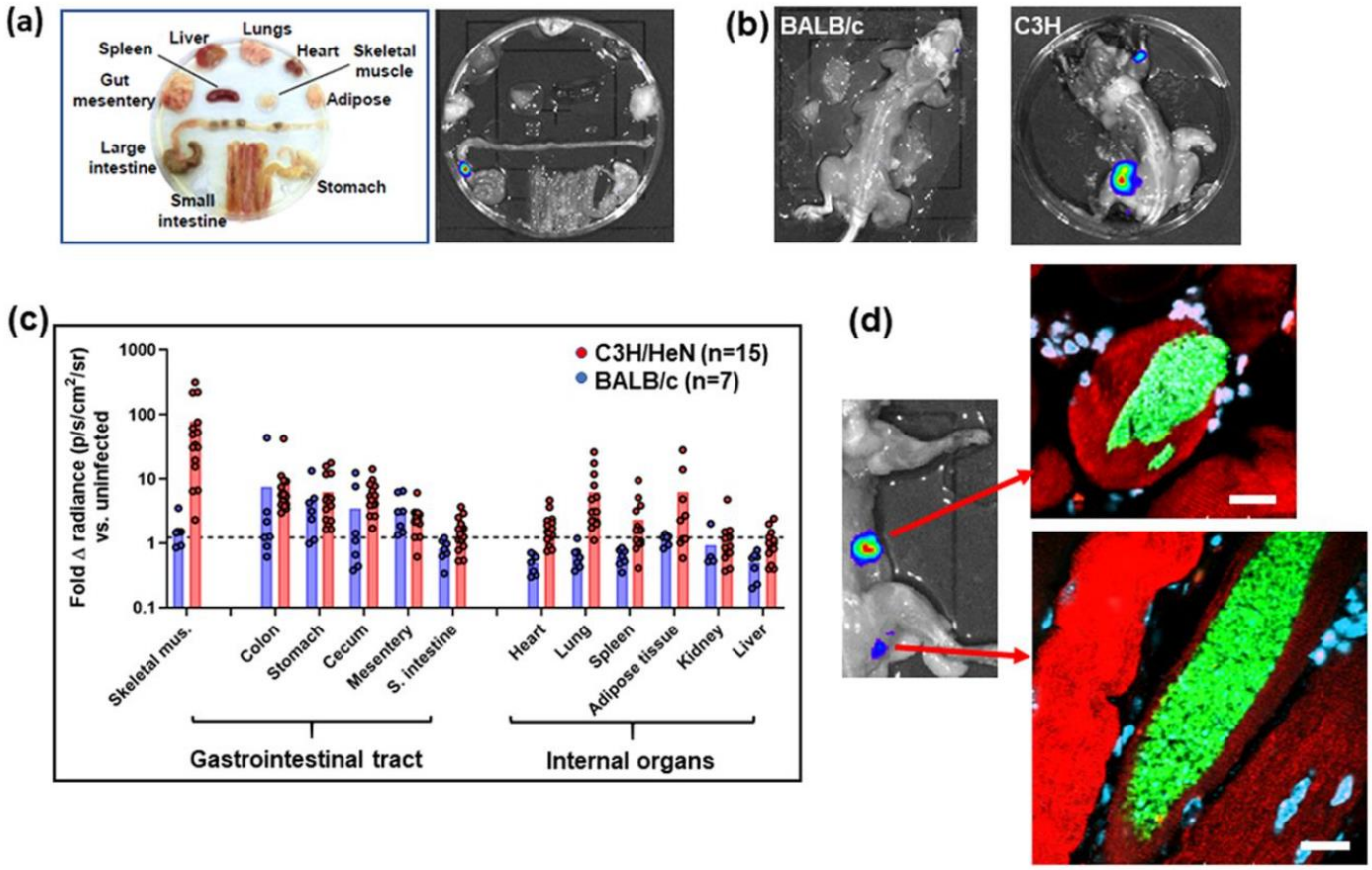

FIG 5 Skeletal muscle is a major site of parasite persistence during chronic *T. cruzi* infections in C3H/HeN mice, but not BALB/c. (a) *Ex vivo* imaging of organs and tissues from a BALB/c mouse chronically infected with bioluminescent *T. cruzi* CL Brener. (b) Dorsal bioluminescence imaging of chronically infected BALB/c and C3H/HeN mice following removal of internal organs, fur, skin and major adipose depots (Material and Methods). (c) Fold change in radiance (photons/s/cm^2/sr) established by *ex vivo* bioluminescence imaging of internal tissues and organs and skeletal muscle as imaged in (a) and (b). Dashed line indicates the detection threshold equal to the mean +2SDs of the bioluminescence background derived from corresponding empty regions of interest obtained in tissue from age-matched uninfected mice. For technical reasons, on a small number of occasions, data could not be acquired for tissue samples from some mice (eg adipose tissue). (d) Bioluminescent foci from skeletal muscle were excised, histological sections prepared, and then scanned by confocal microscopy (Materials and Methods). Sections were stained with specific markers for muscle (actin-α; red) and DNA (DAPI; blue/turquoise). Parasites can be identified by green fluorescence. White scale bars=20 µm.

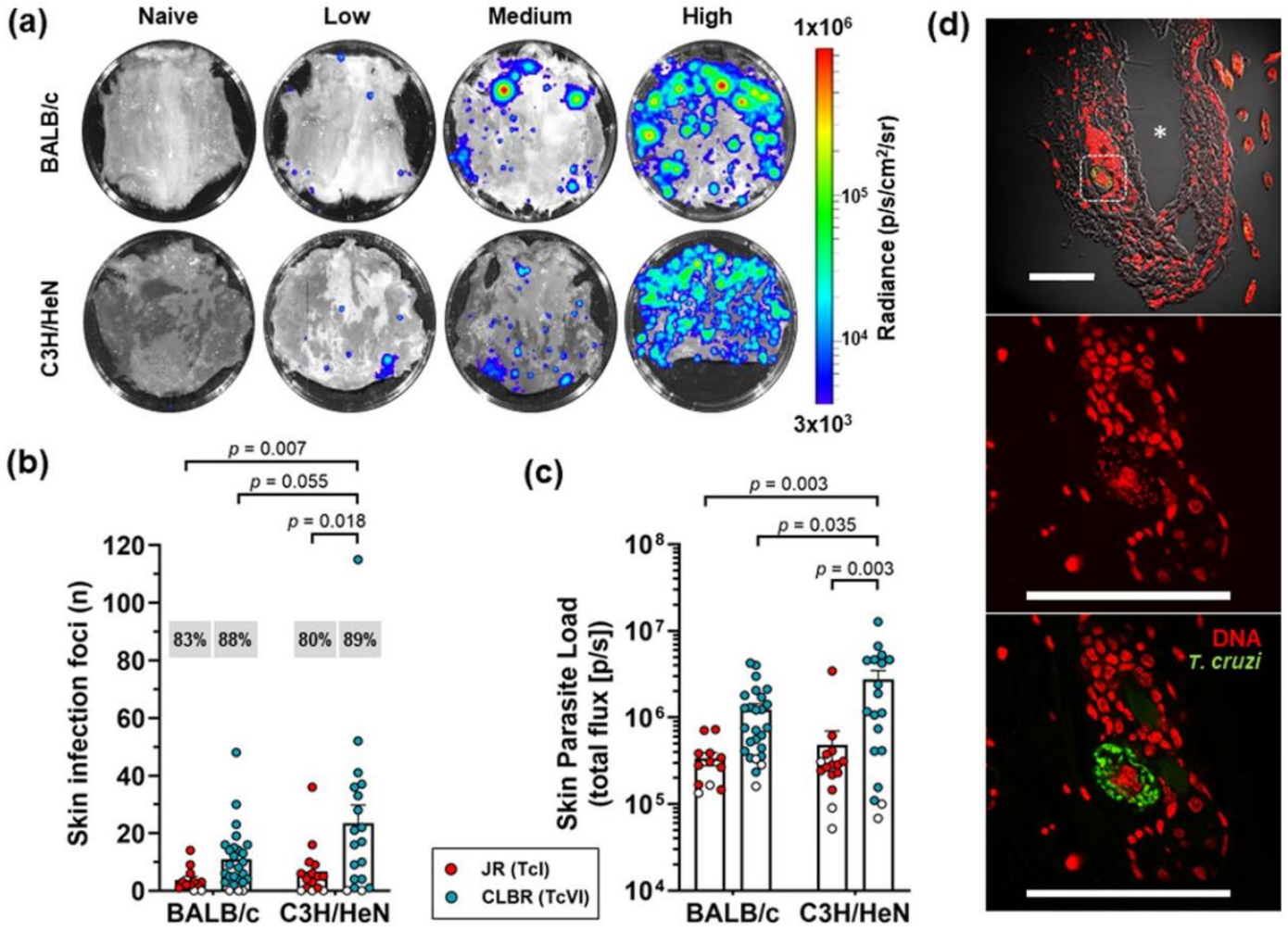

FIG 6 The skin is a major site of parasite persistence during chronic *T. cruzi* infections in mice. (a) *Ex vivo* bioluminescence imaging of skin (adipose tissue removed) from chronically infected BALB/c and C3H/HeN mice (>150 days post-infection) showing representative examples of low, medium and high parasite load. The bioluminescence signal is on a log10 scale pseudocolour heat map. (b and c) Quantification of the number of discrete infection foci (b) and the bioluminescence intensity for each skin (c). Data points are individual animals, with empty circles indicating skins having zero radiance above background. Mean values ±SEM are shown. Percentages in grey boxes (b) refer to the number of animals with at least one focus above the bioluminescence threshold. Infections with both *T. cruzi* CL Brener and JR bioluminescent strains were assessed (n=12-26 animals per combination, 3-4 independent experiments). Groups were compared by 2-way ANOVA. (d) Confocal micrographs showing fluorescent CL Brener parasites in an infected cell within the dermis of a BALB/c mouse 230 days post-infection (surface to the right). Upper image (200x). Asterisk indicates a gap resulting from a cutting artefact. Lower two images (630x) highlight the region in the white boxed area (above). White scale bars=100 µm.

SUPPLEMENTAL MATERIAL

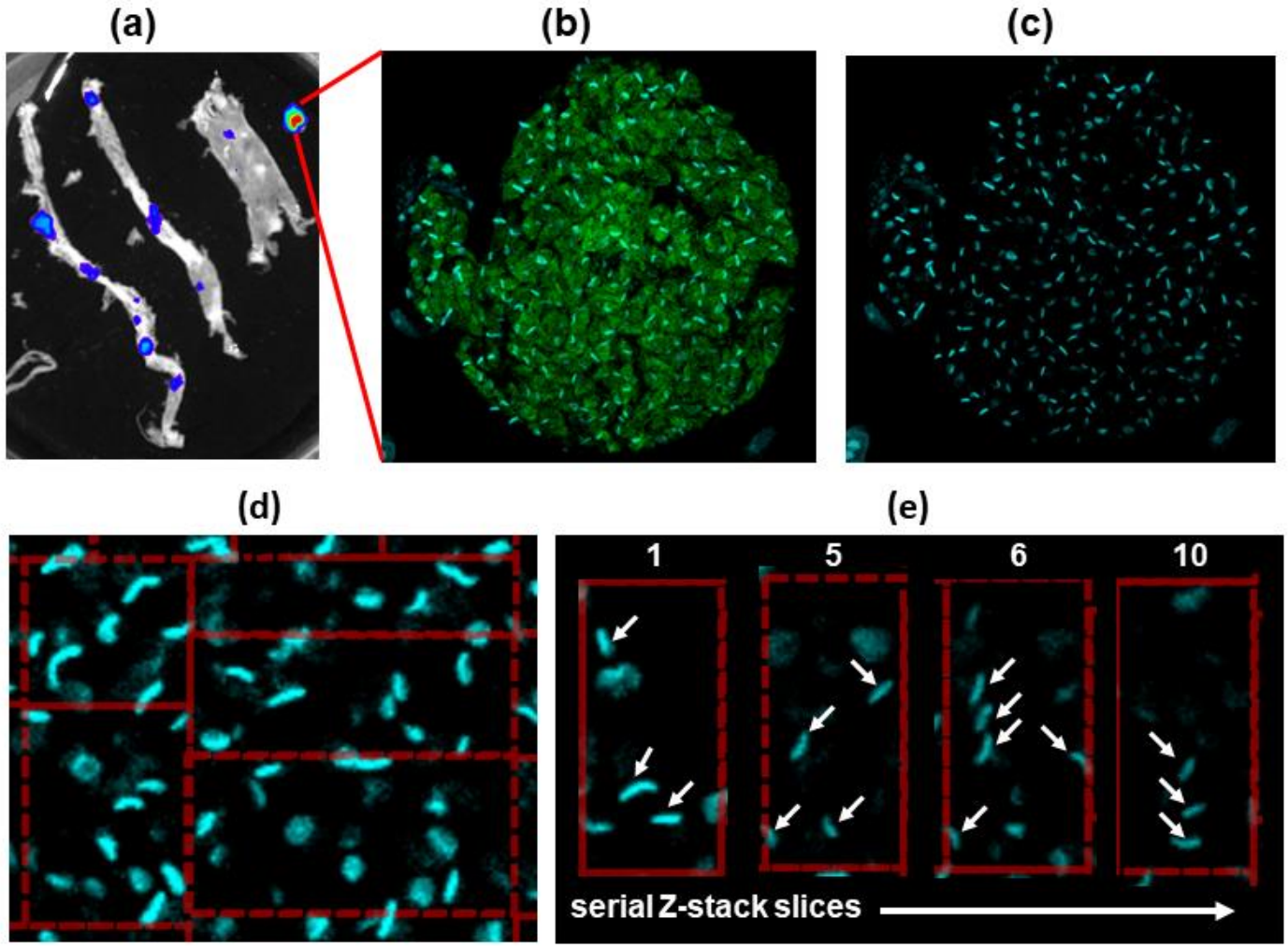

FIG S1 The determination of parasite numbers in highly infected host cells. (a) Bioluminescent image of a peeled large intestine from a C3H/HeN mouse chronically infected with *T. cruzi* CL-Luc::Neon. (b) The excised tissue was imaged by confocal microscopy (x100) to reveal a highly infected smooth muscle cell (parasites, green). (c) The same image showing DAPI staining (blue) to reveal DNA. (d) For Z-stack analysis, the image was split into grids using the ZEN software. Parasite load was determined from the number of discoid-shaped kinetoplasts. To facilitate accurate counting, the relatively faint staining of the nuclear genome can be reduced by adjusting the contrast. (e) A series of 4 representative Z-stacked images from a total of 13 slices taken to assess parasite number across the infected cell. A total of 60 parasites were assigned to this 3-dimensional grid. The total number of parasites in the nest was 1969.

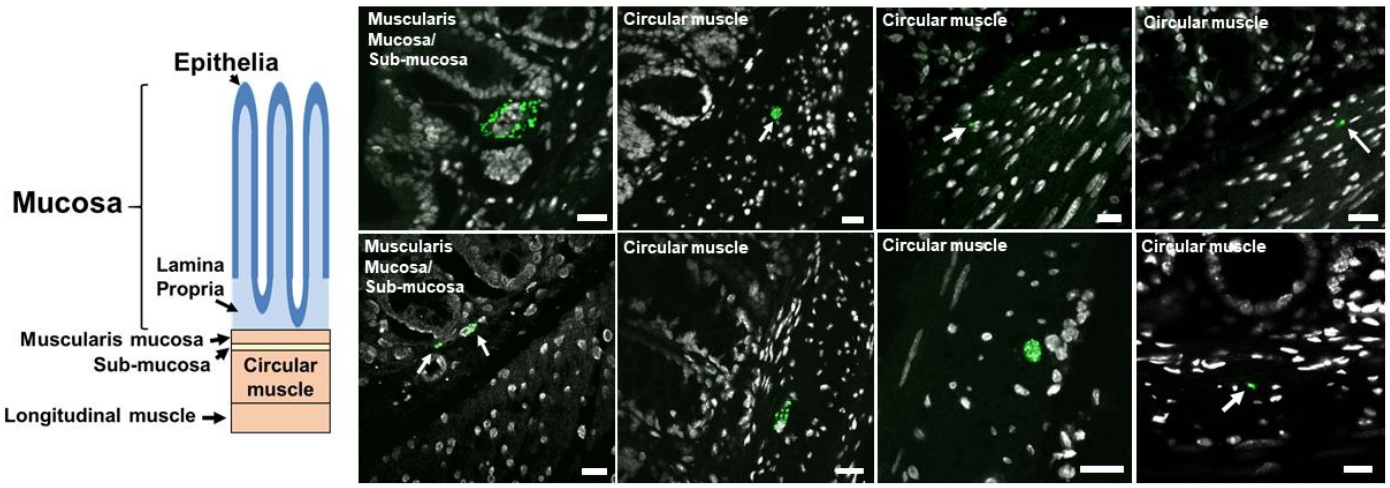

FIG S2 Location of parasites within the murine GI tract during chronic *T. cruzi* infection. C3H/HeN mice were chronically infected with *T. cruzi* CL-Luc::Neon and the colon was examined by confocal imaging of histological sections following DNA staining (DAPI - white) (Materials and Methods). Host cells infected with fluorescent parasites (green, indicated by white arrows) were detected in different layers of the GI tract, as indicated. White scale bars=20 µm.

REFERENCES

1. WHO. 2020. Chagas disease. www.who.int/news-room/fact-sheets/detail/chagas-disease-(american-trypanosomiasis).

2. Requena-Mendez A, Aldasoro E, de Lazzari E, Sicuri E, Brown M, Moore DA, Gascon J, Muñoz J. 2015. Prevalence of Chagas disease in Latin-American migrants living in Europe: a systematic review and meta-analysis. PLoS Negl Trop Dis 9:e0003540.

3. Bern C, Messenger LA, Whitman JD, Maguire JH. 2019. Chagas disease in the United States: a public health approach. Clin Microbiol Rev 33:e00023-19.

4. Cardillo F, de Pinho RT, Antas PR, Mengel J. 2015. Immunity and immune modulation in *Trypanosoma cruzi* infection. Pathog Dis 73:ftv082.

5. Tarleton RL. 2015. CD8+ T cells in *Trypanosoma cruzi* infection. Semin Immunopath 37:233-238.

6. Ribeiro AL, Nunes MP, Teixeira MM, Rocha MO. 2012. Diagnosis and management of Chagas disease and cardiomyopathy. Nature Rev Cardiol 9:576-589.

7. Cunha-Neto E, Chevillard C. 2014. Chagas disease cardiomyopathy: immunopathology and genetics. Mediat Inflamm 2014:683230.

8. Wilkinson SR, Kelly JM. 2009. Trypanocidal drugs: mechanisms, resistance and new targets. Exp Rev Molec Med 11:e31, 1-24.

9. Gaspar L, Moraes CB, Freitas-Junior LH, Ferrari S, Costantino L, Costi MP, Coron RP, Smith TK, Siqueira-Neto JL, McKerrow JH, Cordeiro-da-Silva A. 2015. Current and future chemotherapy for Chagas disease. Curr Med Chem 22:4293-4312.

10. Katsuno, K., Burrows, JN, Duncan K, Hooft van Huijsduijnen R, Kaneko T, Kita K, Mowbray CE, Schmatz D, Warner P, Slingsby BT. 2015. Hit and lead criteria in drug discovery for infectious diseases of the developing world. Nature Rev Drug Dis 14:751-758.
11. Chatelain E. 2016. Chagas disease research and development: Is there light at the end of the tunnel? Comput Struct Biotech J 15:98-103.
12. Pack AD, Collins MH, Rosenberg CS, Tarleton RL. 2018. Highly competent, non-exhausted CD8+ T cells continue to tightly control pathogen load throughout chronic *Trypanosoma cruzi* infection. PLoS Pathog 14:e1007410.
13. Lewis MD, Kelly JM. 2016. Putting *Trypanosoma cruzi* dynamics at the heart of Chagas disease. Trends Parasitol 32:899-911.
14. Sánchez-Valdéz FJ, Padilla A, Wang W, Orr D, Tarleton RL. 2018. Spontaneous dormancy protects *Trypanosoma cruzi* during extended drug exposure. Elife 7:e34039.
15. Duarte JG, Nascimento RD, Martins PR, d'Ávila Reis D. 2017. An autopsy-based study of *Trypanosoma cruzi* persistence in organs of chronic chagasic patients and its relevance for transplantation. Transpl Infect Dis 19:e12783.
16. Hyland KV, Asfaw SH, Olson CL, Daniels MD, Engman DM. 2008. Bioluminescent imaging of *Trypanosoma cruzi* infection. Int J Parasitol 38:1391–1400.
17. Silberstein E, Serna C, Fragoso SP, Nagarkatti R, Debrabant A. 2018. A novel nanoluciferase-based system to monitor *Trypanosoma cruzi* infection in mice by bioluminescence imaging. PLoS One 13:e0195879.
18. Calvet CM, Choi JY, Thomas D, Suzuki B, Hirata K, Lostracco-Johnson S, de Mesquita LB, Nogueira A, Meuser-Batista M, Silva TA, Siqueira-Neto JL, Roush WR, de Souza Pereira MC, McKerrow JH, Podust LM. 2017. 4-aminopyridyl-based lead compounds targeting CYP51 prevent spontaneous parasite relapse in a chronic model and improve cardiac pathology in an acute model of *Trypanosoma cruzi* infection. PLoS Negl Trop Dis 11:e0006132.
19. Branchini BR, Ablamsky DM, Davis AL, Southworth TL, Butler B, Fan F, Jathoul AP, Pule MA. 2010. Red-emitting luciferases for bioluminescence reporter and imaging applications. Anal Biochem 396:290-297.
20. Lewis MD, Fortes Francisco A, Taylor MC, Burrell-Saward H, McLatchie AP, Miles MA, Kelly JM. 2014. Bioluminescence imaging of chronic *Trypanosoma cruzi* infections reveals tissue-specific parasite dynamics and heart disease in the absence of locally persistent infection. Cell Microbiol 16:1285-1300.
21. Lewis MD, Fortes Francisco A, Taylor MC, Kelly JM. 2015. A new experimental model for assessing drug efficacy against *Trypanosoma cruzi* infection based on highly sensitive *in vivo* imaging. J Biomolec Screen 20:36-43.
22. Lewis MD, Fortes Francisco A, Taylor MC, Jayawardhana S, Kelly JM. 2016. Host and parasite genetics shape a link between *Trypanosoma cruzi* infection dynamics and chronic cardiomyopathy. Cell Microbiol 18:1429-1443.
23. Francisco AF, Lewis MD, Jayawardhana S, Taylor MC, Chatelain E, Kelly JM. 2015. The limited ability of posaconazole to cure both acute and chronic *Trypanosoma cruzi* infections revealed by highly sensitive *in vivo* imaging. Antimicrob Agents Chemother 59:4653-4661.

24. Francisco AF, Jayawardhana S, Taylor MC, Lewis MD, Kelly JM. 2018. Assessing the effectiveness of curative benznidazole treatment in preventing chronic cardiac pathology in experimental models of Chagas disease. Antimicrob Agents Chemother 62:e00832-18.
25. Costa FC, Francisco AF, Jayawardhana S, Calderano SG, Lewis MD, Olmo F, Beneke T, Gluenz E, Sunter J, Dean S, Kelly JM, Taylor MC. 2018. Expanding the toolbox for *Trypanosoma cruzi*: A parasite line incorporating a bioluminescence-fluorescence dual reporter and streamlined CRISPR/Cas9 functionality for rapid *in vivo* localisation and phenotyping. PLoS Negl Trop Dis 12:e0006388.
26. Taylor MC, Ward A, Olmo F, Jayawardhana S, Francisco AF, Lewis MD, Kelly JM. 2020. Intracellular DNA replication and differentiation of *Trypanosoma cruzi* is asynchronous within individual host cells *in vivo* at all stages of infection. PLoS Negl Trop Dis 14:e0008007.
27. Francisco AF, Jayawardhana S, Lewis MD, White KL, Shackleford DM, Chen G, Saunders J, Osuna-Cabello M, Read KD, Charman SA, Chatelain E, Kelly JM. 2016. Nitroheterocyclic drugs cure experimental *Trypanosoma cruzi* infections more effectively in the chronic stage than in the acute stage. Sci Rep 6:35351.
28. Mann GS, Francisco AF, Jayawardhana S, Taylor MC, Lewis MD, Olmo F, López-Camacho C, Oliveira de Freitas E, Leoratti FMS, Reyes-Sandoval A, Kelly JM. 2020. Drug-cured experimental *Trypanosoma cruzi* infections confer long-lasting and cross-strain protection. PLoS Negl Trop Dis 14:e0007717.
29. Molina I, Gómez i Prat J, Salvador F, Treviño B, Sulleiro E, Serre N, Pou D, Roure S, Cabezos J, Valerio L, Blanco-Grau A, Sánchez-Montalvá A, Vidal X, Pahissa A. 2014. Randomized trial of posaconazole and benznidazole for chronic Chagas disease. N Eng J Med 370:1899-1908.
30. Morillo CA, Marin-Neto JA, Avezum A, Sosa-Estani S, Rassi A Jr, Rosas F, Villena E, Quiroz R, Bonilla R, Britto C, Guhl F, Velazquez E, Bonilla L, Meeks B, Rao-Melacini P, Pogue J, Mattos A, Lazdins J, Rassi A, Connolly SJ, Yusuf S; BENEFIT Investigators. 2015. Randomized trial of benznidazole for chronic Chagas' cardiomyopathy. N Eng J Med 373:1295-1306.
31. Lewis MD, Francisco AF, Jayawardhana S, Langston H, Taylor MC, Kelly JM. 2018. Imaging the development of chronic Chagas disease after oral transmission. Sci Rep 8:11292.
32. Weaver JD, Hoffman VJ, Roffe E, Murphy PM. 2019. Low-level parasite persistence drives vasculitis and myositis in skeletal muscle of mice chronically infected with *Trypanosoma cruzi*. Infect Immun 87:e00081-19.
33. Capewell P, Cren-Travaillé C, Marchesi F, Johnston P, Clucas C, Benson RA, Gorman TA, Calvo-Alvarez E, Crouzols A, Jouvion G, Jamonneau V, Weir W, Stevenson ML, O'Neill K, Cooper A, Swar NK, Bucheton B, Ngoyi DM, Garside P, Rotureau B, MacLeod A. 2016. The skin is a significant but overlooked anatomical reservoir for vector-borne African trypanosomes. Elife 5:e17716.
34. Caljon G, Van Reet N, De Trez C, Vermeersch M, Pérez-Morga D, Van Den Abbeele J. 2016. The dermis as a delivery site of *Trypanosoma brucei* for tsetse flies. PLoS Pathog 12:e1005744.
35. Hemmige V, Tanowitz H, Sethi A. 2012. *Trypanosoma cruzi* infection: a review with emphasis on cutaneous manifestations. Int J Dermatol 51:501-508.
36. Gallerano V, Consigli J, Pereyra S, Gómez Zanni S, Danielo C, Gallerano RH, Guidi A. 2007. Chagas' disease reactivation with skin symptoms in a patient with kidney transplant. Int J Dermatol 46:607-610.
37. Riganti J, Guzzi Maqueda M, Baztan Piñero MC, Volonteri VI, Galimberti RL. 2012. Reactivation of Chagas' disease: cutaneous manifestations in two immunosuppressed patients. Int J Dermatol 51:829-834.

38. Doehl JSP, Bright Z, Dey S, Davies H, Magson J, Brown N, Romano A, Dalton JE, Pinto AI, Pitchford JW, Kaye PM. 2017. Skin parasite landscape determines host infectiousness in visceral leishmaniasis. Nat Commun 8:57.
39. Trindade S, Rijo-Ferreira F, Carvalho T, Pinto-Neves D, Guegan F, Aresta-Branco F, Bento F, Young SA, Pinto A, Van Den Abbeele J, Ribeiro RM, Dias S, Smith TK, Figueiredo LM. 2016. *Trypanosoma brucei* parasites occupy and functionally adapt to the adipose tissue in mice. Cell Host Microbe 19:837–848.
40. Isola EL, Lammel EM, González Cappa SM. 1986. *Trypanosoma cruzi:* differentiation after interaction of epimastigotes and *Triatoma infestans* intestinal homogenate. Exp Parasitol 62:329-335.
41. Taylor MC, Francisco AF, Jayawardhana S, Mann GS, Ward AI, Olmo F, Lewis MD, Kelly JM. 2019. Exploiting genetically modified dual-reporter strains to monitor experimental *Trypanosoma cruzi* Infections and host-parasite interactions. Methods Mol Biol 1955:147-163.

4.6 Chapter summary

As covered in the introduction to this chapter, prior to the development of bioluminescent-fluorescent strains, technical challenges precluded a single-cell level analysis of parasite localisation post suppression of the acute stage. This first publication draws on data from the *T. cruzi* CL Brener background reporter and 2 murine host models, BALB/c and C3H/HeN. Occupation of myocytes in both the skeletal muscle (C3H/HeN) and the colon (BALB/c and C3H) confirms earlier studies employing more traditional methodology that proposed these cell types as important reservoirs. The systematic characterisation of the skin as a reservoir site is new but not surprising, considering the vectoral nature of transmission. The host cell types occupied in this organ remain undefined, although the dermis, particularly in hairy mammals, does have smooth muscle myocytes attached to hair follicles in abundance. Future work, with further refined tissue processing methodology will be needed to confirm cell type occupation. The generation of new bioluminescent-fluorescent stains, beyond the hybrid DTU VI line, and the utilisation of additional animal models (rats and hamsters), will allow a more complete answer to the crucial question, **where does the parasite persist in the chronic stage?**

5. Replication kinetics of *Trypanosoma cruzi in vivo*

5.1 Evolution of the ‘persister’ phenotype

Well established in prokaryotes, both pathogenic and environmental, including the archaea[1,2,3], is the concept of a ‘persister’ phenotype linked to survival of cellular stress, including that induced by chemotherapeutic drugs[4]. Recently[5], this concept has been associated with treatment failure in neoplastic disease. The persister state is phenotypic, and separate from drug resistance conferred by mutations of the genome[6]. Cues for entry into the persistence state are all inducers of metabolic stress; nutrient starvation, switching of carbon source[7] and DNA damage[8]. An array of cellular sensors detect these stresses, TOR (target of rapamycin) and p53 orthologues, being the most famous signalling nodes for nutrient deficiency and genome damage, respectively. Why heterogeneity of the persistence phenotype exists within populations is unknown. Distinct microenvironments that are more ‘stressful’ than their surroundings and stochastic expression of persister promoting genes have been hypothesised[9]. The triggering of signalling pathways that promote the persister state, reviewed in Prax and Bertram 2014[10], lead to down regulation of protein synthesis, tRNA synthesis, DNA synthesis, Krebs cycle carbon flux and other biochemical pathways that produce reactive oxygen species (ROS). The reduction of these nutrient consuming-toxin releasing processes is combined with the up-regulation of protein misfolding chaperones[11], DNA-repair machinery[12], oxidative stress protective proteins[13] and anabolic maintenance of amino acid levels[14]. The combined effect allows for survival for prolonged periods in adverse environmental conditions at the expense of reproduction. Persister cells cause significant complications in the frontline clinical management of both prokaryotic pathogens[15] and tumours[16]. From a theoretic stand-point, all modern cellular life adopts ‘persister’-like characteristics when presented with cellular stress. The sensors, signalling pathways and effectors are among the most ancient and widespread molecular components of the cell[17].

5.2 Protozoan persisters and drug tolerance

As recently reviewed[18], all of the single-celled eukaryotic pathogens of man are well established to assume slow or no replication life-cycle stages. The infective stages of all are incapable of progressing through the cell cycle prior to contact with a suitable host. The terms ‘dormancy’, ‘quiescence’ and ‘persister’ are often used interchangeably. Here, these pathogens are described in terms of their *in vivo* replication kinetics and its relevance to current drug treatment challenges.

5.3 *Toxoplasma gondii*, the master of 'quiescence'

Sexual stages of the *T. gondii* life-cycle occur in the gastrointestinal tract (GIT) of the cat. Shed in the faeces are replication arrested oocysts, or 'sporocysts', that contaminate the environment. These are highly resistant to physical and chemical insult[19]. Once consumed by any warm-blooded animal, other than a *Felidae* (cat), the sporocysts rupture and release motile sporozoites in response to environmental change. Active invasion of the mucosal epithelium is followed by intracellular differentiation into the tachyozoite within a parasitophorous vacuole. Wide-spread dissemination is accomplished within circulating immune cells[20] or as free vacuole bound tachyzoites[21]. Crossing of the blood-brain or placental barrier and subsequent exponential replication within CNS neurones leads to pathology in the immunosuppressed host and in the unborn foetus (WHO, 2020). In immunocompetent hosts the deployment of parasite specific IFN-γ+ T-cells control tachyzoite numbers[22].

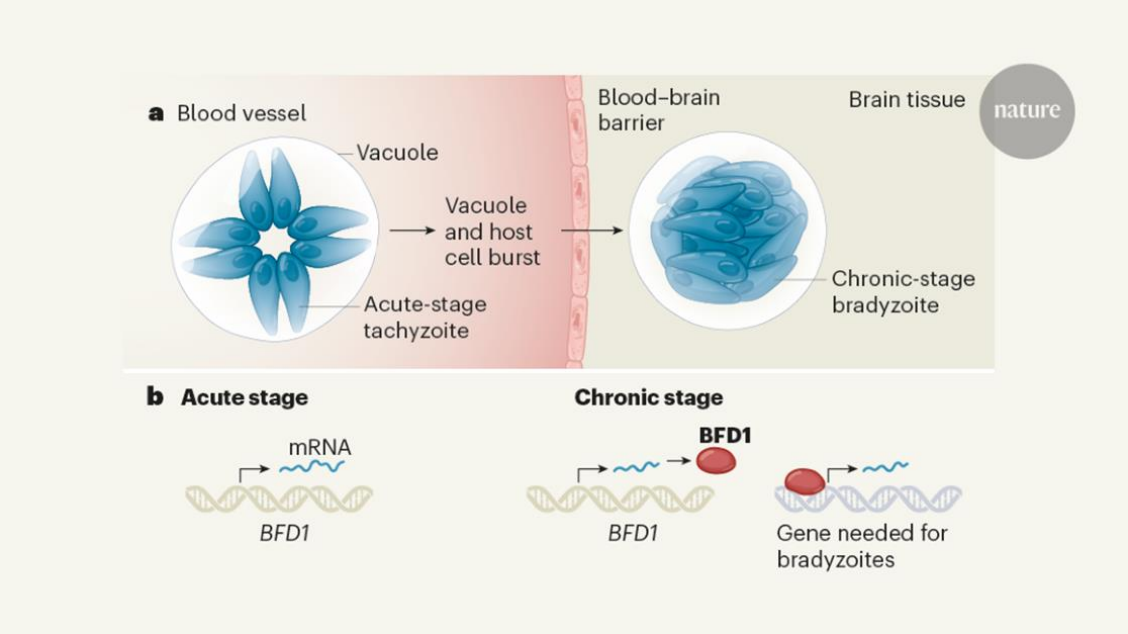

Figure 7 – Cartoon showing the link between translation and nuclear accumulation of the transcription factor bradyzoite formation deficient-1 (BFD-1) and the transition from the replicating tachyzoites to the dormant bradyzoites. While the tachyzoites are able to replicate intracellularly in multiple cell types[23], persistent bradyzoites are routinely found in the CNS and skeletal muscle fibres. Taken from Waldman *et al* 2020[24].

In direct response to oxidative stress directed and promoted by the adaptive immune response, parasites up-regulate translation of the 'master switch', Bradyzoite Formation Deficient-1 (BFD1) mRNA[24]. BFD1 nuclear translocation and binding to promotor targets up-regulates genes that transition metabolism into a definitively 'persister' state, the bradyzoite[25]. Secretion of an encapsulating cyst structure provides isolation away from, and protection from, the otherwise competent immune effectors[26]. Tissue cysts are found in both skeletal muscle cells and neurones, in which the parasite awaits consumption by a predatory cat. Whether cyst bradyzoites are slowly replicating or contain a sub-population that do not enter a new G1/S-phase of the cell cycle for

extended periods (months or years)[27], is academic to the existence of a truly metabolically dormant *in vivo T. gondii* life-cycle stage. This well validated state is resistant to all clinically available compounds[28] and perhaps represents one of the most extreme *in vivo* persisters.

5.4 The *Plasmodium* species hypnozoite

The morphological, metabolic and transcriptomic profile of the 'hypnozoite' life-cycle stage has been best characterised in *P. vivax*, but certainly exists in other species[29]. The evolutionary pressure for the development of this life-cycle stage almost invariably comes from the need, away from the territories on the equator, to persist in the host during dry periods in which mosquito numbers are low[30]. At the equator, where access to the vector and onward transmission opportunities are abundant all year-round *P. falciparum*, which does not enter a hypnozoite stage, is dominant[31]. The mechanism which decides whether individual sporozoites arriving in the liver differentiate into hypnozoites or amplify by replication through schizogony is unknown[32]. A master transcription factor that is sufficient and responsible for differentiation to the hypnozoite, analogous to BFD-1 in *T. gondii*, has not been identified[33]. The hypnozoite exhibits the hallmarks of the 'persister' state with reduced transcription[34], limited or no cell-cycling and up-regulation of genes involved in DNA-damage repair[35]. The hypnozoite expression profile is under epigenetic control of chromatin structure, which is key for long term maintenance of the transcriptome composition[36]. Although modulation of the hepatocyte does take place during the period of replicative inactivity[37], a protective cyst structure has not been described. The currently available options in the clinic able to treat this dormant liver stage in *Plasmodium* infections are limited[38].

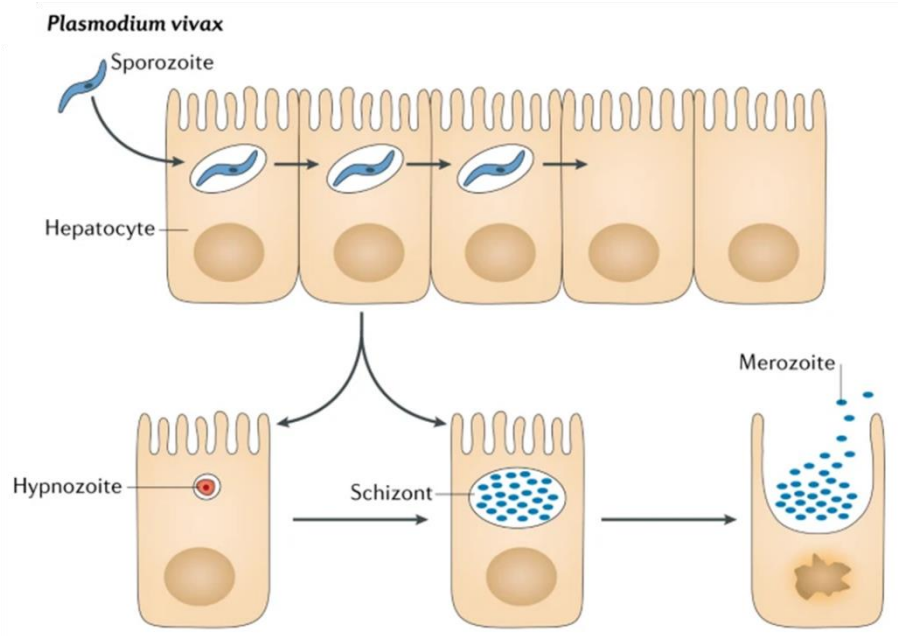

Figure 8 – Cartoon showing the developmental decision to either exist for extended time periods as a dormant or 'persister' hypnozoite or to undergo schizogony and amplification through replication. Taken from Barrett *et al* 2019[18].

5.5 Persistent leishmaniasis, slow but not no replication?

The various *Leishmania* species, kinetoplastids in the same class as *T. cruzi* and *T. brucei*, are transmitted between mammalian hosts by the bite of the sand-fly vector. At the bite site the recruitment of innate monocytes provides these parasites with their intracellular reservoir[39]. Clinically symptomatic cases range from localised lesions of the skin to visceral spread of the infection and mortality, depending on both parasite species and host genetic factors[40]. Many cases are asymptomatic[41] but retain onward vector transmission potential[42]. Some evidence suggests that the acute stage of the infection is characterised by rapid replication of the parasite in macrophages[43]. Deployment of the adaptive immune effectors, principally CD4+ IFN-γ$^+$ T-cells[44] to the lesion site controls *Leishmania* growth by lengthening the parasite cell-cycle and promoting destruction within the phagolysosomal system. Whether this reduced replication includes a sub-population of truly dormant non-replicating parasites, which has been suggested[43,45], is unknown.

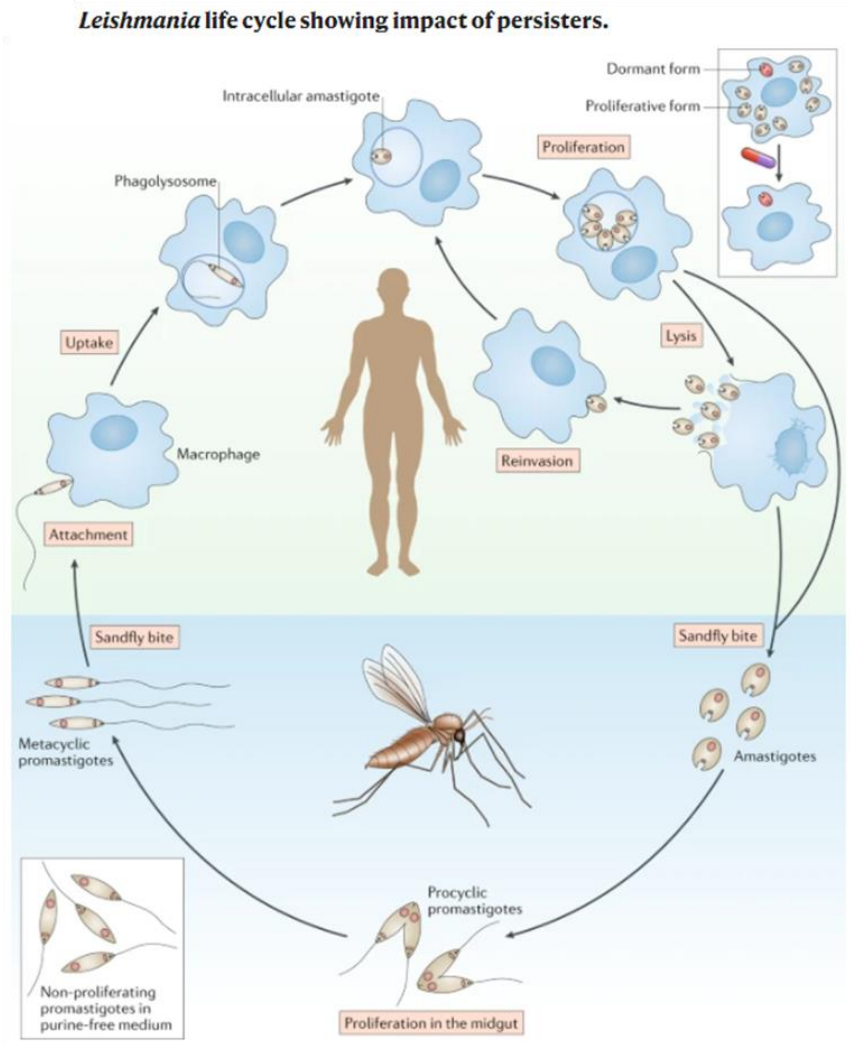

Figure 10 – The *Leishmania* species life-cycle. Included (top right) is the hypothesised existence of a dormant or persister form of the parasite that is more resistant to drug treatment but can reactivate once this cellular stress is removed. Taken from Barrett *et al* 2019[18].

When compared to *in vitro* axenically grown parasite cultures, *in vivo Leishmania* replication after deployment of T-cells *is* significantly reduced. Hallmarks of the persister phenotype have been described, including metabolic reprogramming triggered by amino acid restriction[46], upregulation of the misfolded protein response[47] and reduced flux through multiple biochemical pathways[45]. The poor quality of front-line drugs has been linked to their inability to kill chronic persister amastigotes[48].

5.6 *Plasmodium falciparum*: A drug treatment induced persister state?

P. falciparum has been described to enter temporary cell cycle arrest after exposure to front-line artemisinin-based therapies[49]. These morphologically altered ring-stage schizonts have been imaged within red blood cells post treatment *in vitro*. Interestingly pyrimethamine, an alternative to artemisinin, causes cell cycle arrest and the persister phenotype only in the subsequent round of schizogony after exposure[50], while some drugs fail to induce this arrested state. The metabolic status of these 'persister' cells is poorly defined, but reduced mRNA translation by cycloheximide antagonises the anti-malarial drug dihydroartemisinin (DHA)[51], potentially indicating that reduced protein synthesis promotes drug resistance. Phosphorylation of the translation initiator eIF2α has been demonstrated to prevent cell cycling in the replication arrested sporozoite[52], and could potentially be a molecular mechanism for entry into blood-stage dormancy. Outside of experiments exposing *P. falciparum* to anti-malarial drugs, no suggestion has yet been made for the spontaneous acquisition of this dormant life-cycle stage in natural *in vivo* infections.

Beyond the replication arrested stumpy form, no data currently exists to suggest that *T. brucei* is capable of entering a dormant/quiescent state.

5.7 *Trypanosoma cruzi* 'dormancy', an unresolved question

T. cruzi is able to enter the canonical persister phenotype in response to nutrient starvation in both the amastigote[53] and epimastigote[54] life-cycle stages *in vitro*. This status includes growth slow-down on nutrient withdrawal and accumulation in G_1, but not death. On exposure to sub-lethal benznidazole (BZ) concentrations, classical features of the persister state are evident. Once nutrient starvation was ended a return to pre-starvation growth was rapid. In the case of sub-lethal BZ treatment, the stall in G_1 continued for some time, the length being dependent on BZ concentration, until the resumption of pre-exposure growth rate. Since DNA damage is a key outcome of the downstream reduction of BZ, the time taken for repair pathways to complete their work may determine the prolongation of the persister phenotype.

The Sanchez-Valdez *et al*, 2018[55] study was the first to ascribe a definitively dormant phenotype to *T. cruzi*. This study injected the thymidine analogue EdU into an acute and chronic mouse model infected with fluorescent parasites and led to the inference that parasites that failed to incorporate the nucleotide were in a state of dormancy. Similar non-labelling cells were confirmed to be a feature of *in vitro* infections. Using a cytosolic labelling tracker dye, non-dividing (dye+) parasites were shown to differentiate, exit and then enter new host cells *in vitro*. These dye+ dormant parasites resisted 2-days of *in vivo* and up to 30-days *in vitro* treatment with BZ. I*n vitro* survival was not associated with the acquisition of resistance mutations. This first report on *in vivo* replication kinetics in *T. cruzi* firmly ascribes the ability to spontaneously enter a 'dormant', 'quiescent' or 'persister' phenotypic state that is pre-conditioned to be resistant to the front-line drug BZ. It is suggested that this is a major reason behind treatment failure in human cases.

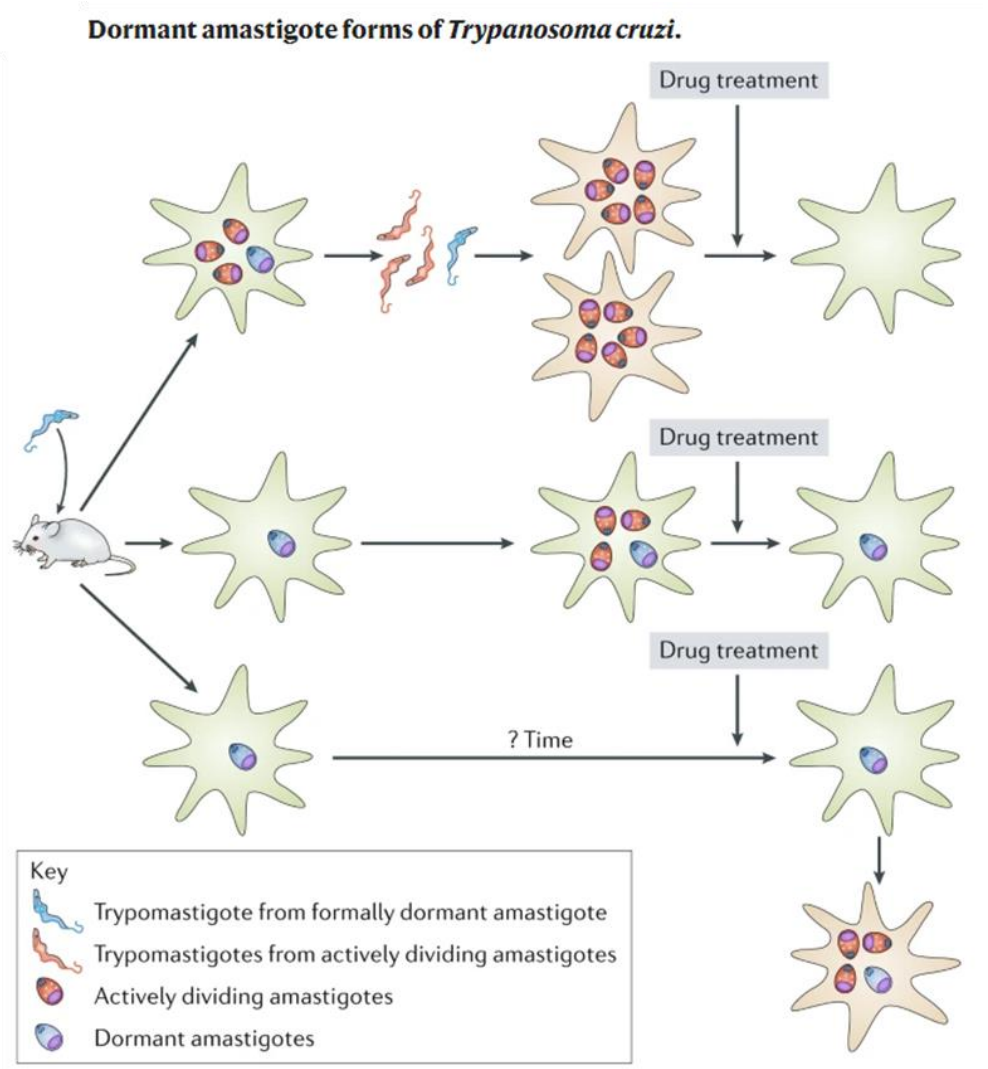

Figure 11 – Cartoon showing the hypothesised mechanism behind drug treatment resistance in *T. cruzi* initially published in Sanchéz *et al* 2018[55]. In the absence of drug treatment rare amastigotes spontaneously enter a non-replicating dormant state. Amastigotes can remain in this state for prolonged periods of time and are tolerant to drug treatment. Post treatment, dormant amastigotes are able to re-enter S-phase and resume amplification of the infection. Taken from Barrett *et al* 2019[18].

5.8 Background work

The rationale behind the work presented in this chapter was to further assess the existence of the dormant life-cycle stage using our *in vivo* infection model. This build on previous work that had already firmly established the asynchronous nature of *T. cruzi* replication *in vivo*[56(Appendix 1)].

Optimisation of EdU incorporation – Before the publication of the Sanchez *et al* 2018[55] study, *T. cruzi* replication kinetics *in vivo* and the potential existence of a 'dormant' life cycle stage were purely speculative. Researchers working on other eukaryotic parasites had made significant progress in this area (above). The following pilot work was carried out in preparation for exploiting EdU (5-Ethynyl-2´-deoxyuridine)[58] labelling as a marker for parasite replication in our *T. cruzi* CL Luc:mNeonGreen-C3H/HeN infection model. The aim was to assess whether the synthetic thymidine analogue EdU was able to be incorporated into *in vivo* replicating parasite DNA. For this piolet experiment, CB17-SCID mice were infected as described in Chapter 4.

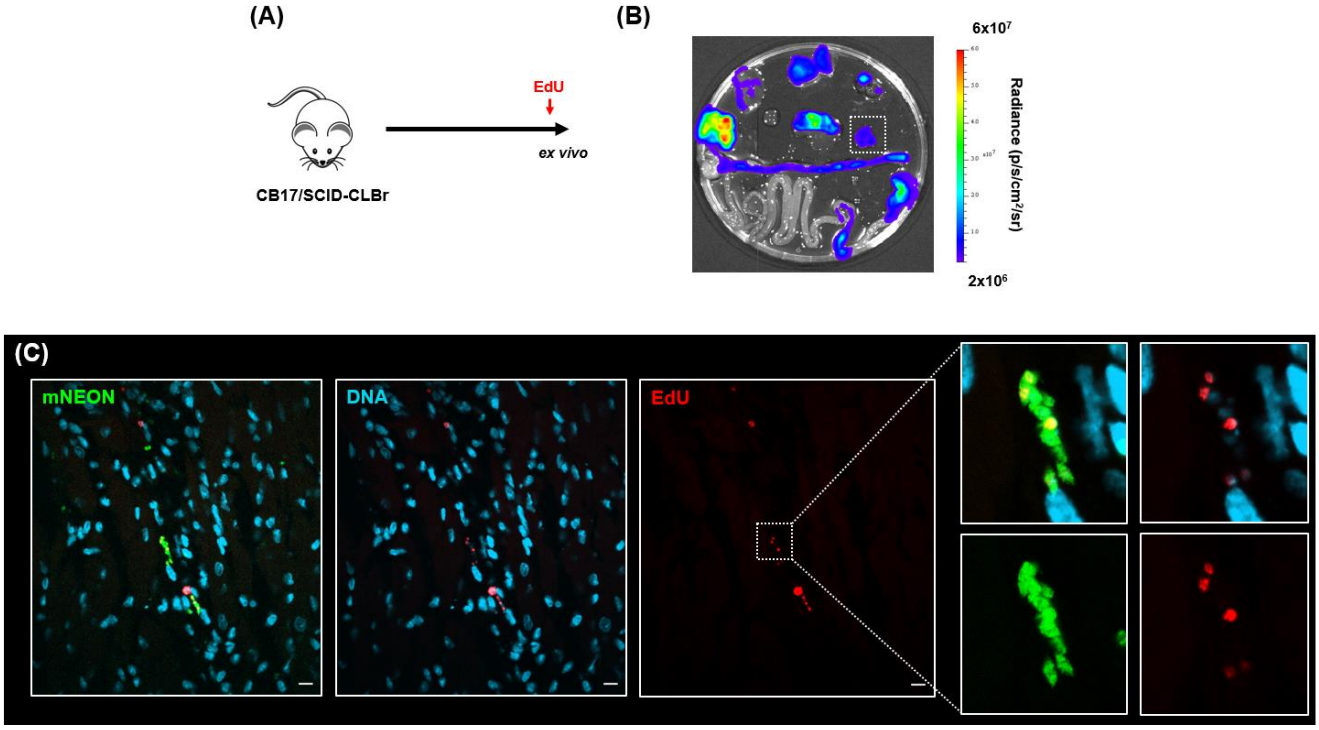

Figure 16 – A., Cartoon of pilot experiment protocol. A CB17-SCID animal infected with *T. cruzi* CLBr-Luc::mNeonGreen was subjected to *ex vivo* analysis 15dpi, following injection with a single shot of 12.5 mg/Kg EdU i.p. 6 hrs prior to cull. **B.,** A bioluminescent image, with adipose tissue removed, with the heart outlined by the white square (for organ identification see materials and methods, Chapter 3). **C.,** Histological section from the heart developed for EdU incorporation. A single host cell and several of the parasites have clearly incorporated the thymidine analogue.

This model allows quick imaging of many fluorescent parasites in fixed tissue sections. A single shot of 12.5 mg/Kg EdU was given 6 hrs before *ex vivo* analysis (Figure 16). The histological processing of tissue is described in Chapter 4. After Click-IT™-reaction development of 10 µm

thick sections, following the manufacturers protocol, EdU+ (red) parasites were easily detected within host cells that also contained EdU- cells. Host cell labelling was routinely identified in most tissues, particularly the mucosal barrier tissue of the GIT, and the spleen. This labelling provided validation that regions containing EdU- parasites had been exposed to the analogue *in vivo* and that the labelling reaction had been successful.

A second pilot experiment was done with immunocompetent BALB/c mice, a strain that is used routinely to assay drug efficacy[59]. Mice were culled 21dpi after either a 1xi.p. 12.5 mg/Kg shot 3-days prior to cull, or after 3xi.p. 12.5 mg/Kg shots administered each day over 3 days before *ex vivo* analysis (Figure 17).

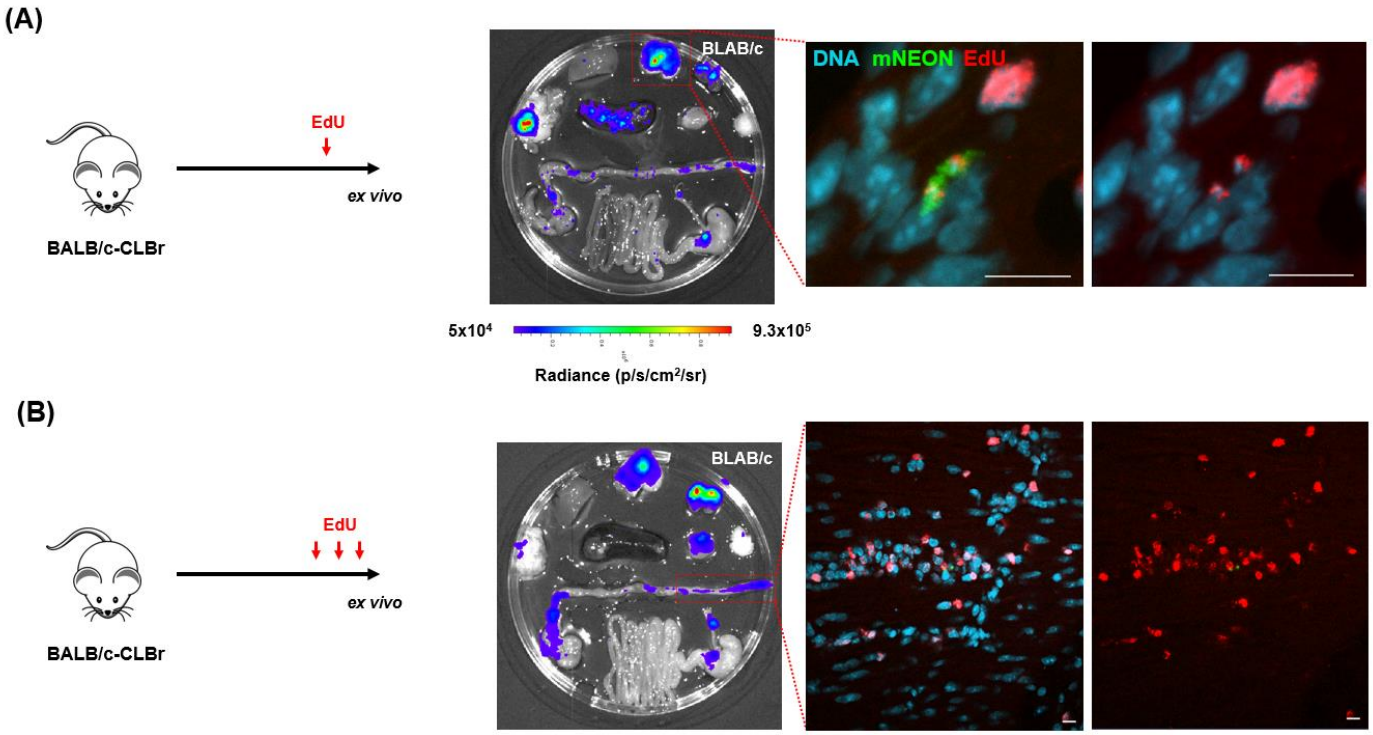

Figure 17 – A., Cartoon showing the acute stage (21dpi) BALB/c-*T. cruzi* CL Luc:mNeonGreen model injected with 1xi.p. 12.5 mg/Kg EdU 3-days prior to *ex vivo* analysis. Bioluminescence image of the visceral organs (for organ identification see cartoon in Materials and Methods, Chapter 3). Histological sections taken from heart tissue developed for EdU incorporation and stained with DNA labelling DAPI. **B.,** The same as in (A) for an animal that received 3xi.p. injections of 12.5 mg/Kg over the 3 days prior to *ex vivo* analysis. In this example the example histological section was taken from the colon. White scale bars = 10 µm.

Neither EdU regimen caused an obvious impact on infection distribution or bioluminescence intensity relative to untreated controls (not shown). Like in the SCID model, host cell labelling was evident in all organs of BALB/c mice that were examined (spleen, heart and colon), particularly in the colon epithelium. Parasites found in the colon in both the 1x and 3x EdU injected mice were identifiable as EdU+ or EdU-.

References

1. Wood, T. R., Knabel, S. J. and Kwan, B. W. Bacterial persister cell formation and dormancy. *Appl. Environ. Microbiol*. **79**, 7116-21 (2013).
2. Ficher, R. A., Gollan, B. and Helaine, S. Persistent bacterial infections and persister cells. *Nat. Rev. Microbiol*. **15**, 453-464 (2017).
3. Megaw, J. and GIllmore, B. F. Archaeal persisters: persister cell formation as a stress response in *Haloferax volcanii*. *Front. Microbiol*. **8**, e1589 (2017).
4. Hong-Geller, E. and NIcheva-Viteva, S. N. Targeting bacterial persistence to develop therapeutics against infections disease. *Drug discovery from molecules to medicine*. **Chapter 9**, 202-218 (2015).
5. Oren, Y. et al. Targetting the root of cancer persister cells using an expression barcode library. *Cancer Res.* **79**, Abstract 2101 (2019).
6. Grubaugh, N. D., Petrone, M. E. and Holmes, E. C. We shouldn't worry when a virus mutates during disease outbreaks. *Nat. Microbiol*. **5**, 529-530 (2020).
7. Amato, S. M. and Brynildsen, M. P. Nutrient transitions are a source of persisters in Escherichia coli biofilms. *Mol. Syst. Biol.* **12**, 882 (2016).
8. Podlesek, Z. and Bertok, D. Z. The DNA damage inducible SOS response is a key player in the generation of bacterial persister cells and population wide tolerance. *Front. Microbiol*. **11**, e1785 (2020).
9. Fasani, R. A. and Savageau, M. A. Molecular mechanisms of multiple toxin-antitoxin systems are coordinated to govern the persister phenotype. *PNAS*. **2013**, e2528-e2537 (2013).
10. Prax, M. and Bertram, R. Metabolic aspects of bacterial persisters. Front. *Cell Infect. Microbiol*. **4**, e148 (2014).
11. Leszczynska, D., Matuszewska, E., Kuczynska-Wisnik, D., Furmanek-Blaszk, B. and Laskowska, E. The formation of persister cells in stationary-phase cultures *of Escherichia Coli* is associated with aggregation of endogenous proteins. *PLOS one*. **8**, e54737 (2013).
12. Moka, W. W. and Brynildsena, M. P. Timing of DNA damage responses impacts persistence to fluoroquinolones. *PNAS*. **115**, e6301-e6309 (2018).
13. Wu, N. et al. Ranking of persister genes in the same *Escherichia coli* genetic background demonstrates varying importance of individual persister genes in tolerance to different antibiotics. *Front. Microbiol*. **6**, e1003 (2015).
14. Duan, X. et al. Mycobacterium lysine ε-aminotransferase is a novel alarmone metabolism related persister gene via dysregulating the intracellular amino acid level. *Sci. Reports*. **6**, e19695 (2016).

15. Fauvart, M., De Groote, V. N. and Michials, J. Role of persister cells in chronic infections: clinical relevance and perspectives on anti-persister therapies. *J. Med. Microbiol*. **6**, 699-709 (2011).
16. Mullard, A. Stemming the tide of drug resistance in cancer. *Nature rev*. **19**, e221 (2020).
17. Beauchamp, E. M. and Platanias, L. C. The evolution of the TOR pathway and its role in cancer. *Oncogene*. **32**, 3923-32 (2013).
18. Barrett, M. P., Kyle, D. E., Sibley, L. D., Radke, J. B. and Tarleton, R. L. Protozoan persister-like cells and drug treatment failure. *Nat. Rev. Microbiol*. **17**, 607-620 (2019).
19. David, W. F., Ferguson, D. J., Jiender, K. S., Pierre-Henri, P. D. and Dumetre, A. Structure, composition, and roles of the *Toxoplasma gondii* oocyst and sporocyst walls. *The Cell Surface*. **5**, e100016 (2019).
20. Courret, N., Darche, S., Sonigo, P., Milon, G., Buzoni-Gatel, M. D. and Tardieux, I. CD11c and CD11d expressing mouse leukocytes transport single *Toxoplasma gondii* tachyzoites to the brain. *Blood*. **107**, 309-16 (2006).
21. Konradt, C. et al. Endothelial cells are a replicative niche of entry of *Toxoplasma gondii* to the central nervous system. *Nat. Microbiol*. **15**, e16001 (2016).
22. Fisch, D., Clough, B. and Frickel, E. Human immunity to *Toxoplasma gondii*. *PLOS path*. **15**, e1008097 (2019).
23. Sweeney, K. R., Morrissette, N. S., LaChapelle, S. and Blader, I. J. Host cell invasion by *Toxoplasma gondii* is temporally regulated by the host microtubule cytoskeleton. *Eukaryot. Cell*. **9**, 1680-9 (2010).
24. Waldman, B. S., Schwarz, D., Wadsworth, M. H., Saeij, J. P., Shalek, A. K. and Lourido, S. Identification of a master regulator of differentiation in *Toxoplasma*. *Cell*. **180**, 359-372 (2020).
25. Sullivan Jr, W. J. and Jeffers, V. Mechanisms of *Toxoplasma gondii* persistence and latency*. FEMS Microbiol. Rev*. **36**, 717-33 (2012).
26. Watts, E. A., Dhara, A. and Sinai, A. P. *Toxoplasma gondii* tissue cyst purification using Percoll gradients. *Curr. Protoc. Microbiol*. **16**, 20C.2.1-20C.2.19 (2018).
27. Watts, E., Zhao, Y., Dhara, A., Eller, B., Patwardhan, A. Sinai, A. P. Novel approaches reveal that *Toxoplasma gondii* bradyzoites within tissue cysts are dynamic and replicating entities *in vivo*. *mBio*. **6**, e01155-15 (2015).
28. Alday, P. H. and Doggett, J. S. Drugs in development for toxoplasmosis: advances, challenges, and current status. *Drug Des. Devel. Ther*. **25**, 2730293 (2017).
29. Richter, J., Franken, G., Mehlhorn, H., Labisch, A. and Haussinger, D. What is the evidence for the existence of *Plasmodium ovale* hypnozoites? *Parasitol. Rev*. **107**, 1285-90 (2010).

30. Hulden, L. and Hulden, L. Activation of the hypnozoite: a part of *Plasmodium vivax* life cycle and survival. Malarai. Jour. **10**, e90 (2011).
31. Gething, P. W.et al. A new world malaria map: *Plasmodium falciparum* endemicity in 2010. *Malaria Jour*. **10**, e378 (2011).
32. Gupta, D. K. et al. The *Plasmodium* liver-specific protein 2 (LISP2) is an early marker of liver stage development. *eLife*. **16**, e43362 (2019).
33. Jeninga, M. D., Quinn, J. E. and Petter, M. ApiAP2 transcription factors in apicomplexan parasites*. Pathogens*. **8**, e47 (2019).
34, Bertchi, N. L. et al. Transcriptomic analysis reveals reduced transcriptional activity in the malaria parasite *Plasmodium cynomolgi* during progression into dormancy. *eLife*. **27**, e41081 (2018).
35. Voorberg-van der Wel, A. et al. A comparative transcriptomic analysis of replicating and dormant liver stages of the relapsing malaria parasite *Plasmodium cynomolgi*. *eLife*. **6**, e29605 (2017).
36. White, M. T. et al*. Plasmodium vivax* and *Plasmodium falciparum* infection dynamics: re-infections, recrudescence's and relapses. *Malar. J*. **17**, e170 (2018).
37. Agop-Nersesian, C., Niklaus, L., Wacker, R. and Heussler, V. T. Host cell cytosolic immune response during *Plasmodium* liver stage development*. FEMS Microbiol. Rev*. **42**, 324-334 (2018).
38. Campo, B., Vandal, O., Wesche, D. L. and Burrows, J. N. Killing the hypnozoite-drug discovery approaches to prevent relapse in *Plasmodium vivax*. *Pathog. Glob. Health*. **109**, 107-22 (2015).
39. Liu, D. and Uzonna, E. D. The early interaction of Leishmania with macrophages and dendritic cells and its influence on the host immune response. *Front. Cell Infect. Microbiol*. **12**, e83 (2012).
40. Blackwell, J. M., Fakiola, M. and Castellucci, L. C. Human genetics of *Leishmania* infection. *Human Genetics*. **139**, 813-819 (2020).
41. Shadab, M. et al. RNA-seq revealed expression of many novel genes associated with *Leishmania donovani* persistence and clearance in the host macrophages. *Front. Cell Infect. Microbiol*. **8**, e17 (2019).
42. Singh, O. P., Hasker, E., Sacks, D., Boelaert, M. Sundar, S. Asymptomatic *Leishmania* infection: a new challenge for *Leishmania* control. *Clin. Infect. Dis*. **58**, 1424-1429 (2014).
43. Mandell, M. A. and Beverley, S. M. Continual renewal and replication of persistent *Leishmania major* parasites in concomitantly immune hosts. *PNAS*. **144**, e801-e810 (2017).
44. Kumar, R. and Engwerda, C. Vaccines to prevent Leishmaniasis. *Clinic. and Transla. Immunol*. **3**, e13 (2014).

45. Kloehn, J., Saunders, E. C., O'Callaghan, S., Dagley, M. J. McConville, M. J. Characterisation of metabolically quiescent *Leishmania* parasites in murine lesions using heavy water labelling. *PLOS Patholg*. **11**, e1004683 (2015).
46. Martin, J. L. et al. Metabolic reprogramming during purine stress in the protozoan pathogen Leishmania donovani. *PLOS Pathog*. 10, e1003938 (2014).
47. Hombach-Barrigah, A. et al. *Leishmania* donovani 90kD heat shock protein – impact of phosphosites on parasite fitness, infectivity and casein kinase affinity. *Scientific Reports*. **9**, e5074 (2019).
48. Ponte-Sucre, A. et al. Drug resistance and treatment failure in leishmaniasis: a 21st century challenge. *PLOS Neg. Trop. Dis*. **11**, e0006052 (2017).
49. Teuscher, F., Chen, N., Kyle, D. E., Gratton, M. L. and Cheng, Q. Phenotypic challenges in artemisinin-resistant *Plasmodium falciparum* lines *in vitro*: evidence for decreased sensitivity to dormancy and growth inhibition. *Antimicrob. Agents Chemother*. **56**, 428-431 (2012).
50. Hott, A. et al. Artemisinin-resistant *Plasmodium falciparum* parasites exhibit altered patterns of development in infected erythrocytes. *Antimicrob. Agents Chemother*. **59**, 3156-3167 (2015).
51. Bridgeford, J. L. et al. Artemisinin kills malaria parasites by damaging proteins and inhibiting the proteasome*. Nature Commun*. **9**, e3801 (2018).
52. Holmes, M. J., Augusto, L. Zhang, M., Wek, R. C. and Sullivan, W. J. Translational control in the latency of apicomplexan parasites. *Trends. Parasitol*. **33**, 947-960 (2017).
53. Dumoulin, P. C. and Burleigh, B. A. Stress-induced proliferation and cell cycle plasticity of intracellular *Trypanosoma cruzi* amastigotes. *mBio*. **9**, e00673-18 (2018).
54. Barison, M. J. et al. Metabolomic profiling reveals a finely tuned, starvation-induced metabolic switch in *Trypanosoma cruzi* epimastigotes. *J. Biol. Chem*. **292**, 8964-8977 (2017).
55. Sanchez-Valdez, F. J., Padilla, A., Wang, W., Orr, D. and Tarleton, R. L. Spontaneous dormancy protects *Trypanosoma cruzi* during extended drug exposure. *eLife*. **7**, e34039 (2018).
56. Taylor, M. C. Intracellular replication and differentiation of Trypanosoma cruzi is asynchronous. *PLOS Neg. Trop. Dis*. **14**, e0008007 (2020). See appendix 1.
57. Ward, A. I. et al. *in vivo* analysis of *Trypanosoma cruzi* persistence foci at single-cell resolution. *mBio*. **11**, e01242-20 (2020).
58. Sailc, A. and Mitchison, T. J. A chemical method for fast and sensitive detection of DNA synthesis *in vivo*. *PNAS*. 7, 2415–2420 (2008).

59. Francisco, A. F., Lewis, M. D., Jayawardhana, S., Taylor, M. C., Chateliain, E. Kelly, J. M. Limited ability of posaconazole to cure both acute and chronic *Trypanosoma cruzi* infections revealed by highly sensitive *in vivo* imaging. *Antimicrob. Agents Chemother*. **59**, 4653-4661 (2015).

60. Lewis, M. D. et al. Bioluminescence imaging of chronic *Trypanosoma cruzi* infections reveals tissue-specific parasite dynamics and heart disease in the absence of locally persistent infection. *Cell Microbiol*. **16**, 1285-1300 (2014).

61. Mandyam, C. D., Harburg, G. C. and Eisch, A. J. Determination of key aspects of precursor cell proliferation, cell cycle length and kinetics in the adult mouse sub-granular zone. *Neuroscience*. **146**, 108-122 (2006).

62. Ward, A. I., Olmo, F., Atherton, R., Taylor, M. C. and Kelly, J. M. Trypanosoma cruzi amastigotes have reduced replication rate during chronic stage infections. *in press* with *Open Biology*.

5.9 –

LONDON SCHOOL of HYGIENE &TROPICAL MEDICINE

London School of Hygiene & Tropical Medicine
Keppel Street, London WC1E 7HT

T: +44 (0)20 7299 4646
F: +44 (0)20 7299 4656
www.lshtm.ac.uk

RESEARCH PAPER COVER SHEET

Please note that a cover sheet must be completed for each research paper included within a thesis.

SECTION A – Student Details

Student ID Number	lsh1406159	**Title**	Mr
First Name(s)	Alexander		
Surname/Family Name	Ward		
Thesis Title	Trypanosoma cruzi: Where is it? Does it ever sleep and why are infections life-long?		
Primary Supervisor	John Kelly		

If the Research Paper has previously been published please complete Section B, if not please move to Section C.

SECTION B – Paper already published

Where was the work published?	Open Biology		
When was the work published?	16/12/2020		
If the work was published prior to registration for your research degree, give a brief rationale for its inclusion			
Have you retained the copyright for the work?*	**Yes**	Was the work subject to academic peer review?	**Yes**

*If yes, please attach evidence of retention. If no, or if the work is being included in its published format, please attach evidence of permission from the copyright holder (publisher or other author) to include this work.

SECTION C – Prepared for publication, but not yet published

Where is the work intended to be published?	
Please list the paper's authors in the intended authorship order:	
Stage of publication	Choose an item.

SECTION D – Multi-authored work

For multi-authored work, give full details of your role in the research included in the paper and in the preparation of the paper. (Attach a further sheet if necessary)	I collected all data with the exception of the Cell Trace Violet numbers presented in figure 1. I wrote the full initial draft with all interpretion. John Kelly conducted the final edit and formating for submission.

SECTION E

Student Signature	Alexander I Ward
Date	16/12/2020

Supervisor Signature	John Kelly
Date	16/12/2020

See https://doi.org/10.1101/2020.08.04.236240 for the on-line version.

Trypanosoma cruzi amastigotes that persist in the colon during chronic stage murine infections have a reduced replication rate.

Alexander I. Ward, Francisco Olmo, Richard Atherton, Martin C. Taylor and John M. Kelly*

Department of Infection Biology,

London School of Hygiene and Tropical Medicine,

London, UK

*For correspondence john.kelly@lshtm.ac.uk

Abstract

Chronic *Trypanosoma cruzi* infections are typically life-long, with small numbers of parasites surviving in restricted tissue sites, which include the gastro-intestinal tract. There is considerable debate about the replicative status of these persistent parasites and whether there is a role for dormancy in long-term infection. Here, we investigated *T. cruzi* proliferation in the colon of chronically infected mice using 5-ethynyl-2'deoxyuridine incorporation into DNA to provide "snapshots" of parasite replication status. Highly sensitive imaging of the extremely rare infection foci, at single cell resolution, revealed that parasites are three times more likely to be in S-phase during the acute stage than during the chronic stage. By implication, chronic infections of the colon are associated with a reduced rate of parasite replication. Despite this, very few host cells survived infection for more than 14 days, suggesting that *T. cruzi* persistence continues to involve regular cycles of replication, host cell lysis and re-infection. We could find no evidence for wide-spread dormancy in parasites that persist in this tissue reservoir.

Key words:

Trypanosoma cruzi, chronic infection, dormancy, proliferation, replication

1. Introduction

Disease latency, mediated by a wide range of mechanisms, is a common feature of viral, bacterial and parasitic infections [1-3]. However, there can be long-term consequences for the host, which include relapse and/or inflammatory pathology. The terms “persistent”, “dormant” and “metabolically quiescent” are used, often interchangeably, to describe pathogens in this state. The phenomenon has evolved independently and frequently in different pathogen groups, presumably because it acts to enhance survival and transmission. The “persister” phenotype does not involve the acquisition of selected mutations, and is often associated with treatment failure, antibiotic tolerance being the best studied example [4,5]. In the case of Chagas disease, some form of dormancy or restricted replication has been widely postulated as a mechanism that might explain long-term parasite survival and the high rate of treatment failure [6].

Chagas disease is caused by the protozoan parasite *Trypanosoma cruzi*, which infects 6-7 million people, mainly in Latin America. Better drugs and innovative immunological interventions are urgently required. Human infection is normally initiated when faeces of the triatomine insect vector, contaminated with metacyclic trypomastigote forms of the parasite, come into contact with the bite wound, or when they are rubbed into mucous membranes. An acute parasitaemia develops, which can be asymptomatic, or manifest as generalised symptoms such as fever, headache and muscle pain. Suppression of the infection is then mediated by a CD8+ T cell mediated response which reduces parasite numbers to extremely low levels [7,8]. A subset of infected individuals (~30%) eventually develop the classical Chagasic cardiac and/or digestive symptoms, although this can be decades after the acute stage infection. Dilated cardiac myopathy and digestive megasyndromes are the most common morbidities, and can often be fatal [9,10]. It remains to be established how the parasite is able to persist long-term, albeit at very low levels, in the face of a robust adaptive immune response [11]. Furthermore, the reasons why treatment failures are a common outcome needs to be better understood at a mechanistic level to guide the design of improved chemotherapy [12]. In this context, the recent report of a non-proliferative form of *T. cruzi* that is refractory to treatment with the front-line drug benznidazole [13], could have important implications.

The ability of human parasites to enter a long-term quiescent state, in which both replication and metabolism are slowed, has been described in *Toxoplasma gondii* (the bradyzoite) [14] and some *Plasmodium* species

[3]. As with many prokaryotic pathogens [15,16], the ‘dormant’ state involves lower levels of DNA synthesis and transcription, down-regulation of energy catabolism, and activation of DNA damage/cellular stress responses. In *T. gondii*, a master transcription factor (BFD1), activated by stress response pathways, initiates the on-set of bradyzoite development [17]. The precise triggers that lead to differentiation into the quiescent hypnozoite liver stage in some *Plasmodium spp.* have been elusive [3]. Amongst eukaryotic pathogens, these examples represent one end of the “dormancy spectrum”, in which entry into a quiescent metabolic state is for extended periods. It has also been tentatively proposed that *Leishmania donovani* can enter a form of dormancy, although the mechanisms involved are unknown [18]. The situation in other *Leishmania spp.* is more definitive, with the identification of quiescent intracellular amastigotes which exhibit a slower metabolic flux and a reduced replication rate [19,20]. This stops short of full long-term dormancy in which parasites enter G0/G1 cell cycle arrest. *Plasmodium falciparum* blood stage schizonts can also enter a transient state of dormancy, induced by treatment with the front-line drug artemisinin [21,22]. This capacity to respond to stress by halting progress through the cell cycle exists in most cells that have DNA damage sensing machinery [23,24]. The existence of a dormant phenotype in the African trypanosome, *Trypanosoma brucei*, beyond the G0/G1 arrested stumpy form required for onward transmission [25] remains speculative.

Observations of both *in vitro* and *in vivo T. cruzi* infections identified a sub-population of non-dividing intracellular amastigotes that retained the ability to differentiate into flagellated trypomastigotes, which were then able to propagate the infection [13]. This phenomenon was defined as spontaneous dormancy on the basis of experiments that involved monitoring incorporation of the thymidine analogue 5-ethynyl-2’deoxyuridine (EdU) into replicating DNA, and use of the tracker dye CellTrace Violet (CTV) to mark non-dividing parasites. Whether this represents long-term metabolic quiescence analogous to that in *T. gondii* and *Plasmodium spp.,* a slow-replicating phenotype as in *Leishmania spp.*, or temporary arrest induced by stress, as exhibited by *P. falciparum* and all non-tumorous mammalian cells, is unresolved. In this latter context, the report that *T. cruzi* amastigotes have an intrinsic ability to reduce their replication rate by temporary cell cycle arrest in G1, as a response to stress, nutrient availability and drug treatment, may be of relevance [26]. It is not known whether these represent overlapping or distinct mechanisms for entering a quiescent state. This could have implications for drug design, immunological interventions, and our understanding of *T. cruzi* persistence.

Using highly sensitive bioluminescence and fluorescence imaging [27-29], we demonstrated that the gastrointestinal tract, specifically the colon and stomach, is a key site of *T. cruzi* persistence during chronic murine infections. Smooth muscle myocytes in the circular muscle layer of the colonic gut wall are the predominant host cell type. In the chronic stage, the entire colon typically contains only a few hundred parasites, often concentrated in a small number of cells that can contain >100 parasites. During the acute stage, however, when the parasite burden is considerably higher and many cells are infected, host cells containing >50 parasites are rarely found. Persistent parasites are also frequently detected in the skin during chronic infections, and in C3H/CeN mice, the skeletal muscle [29,30]. Further studies have also shown that parasite replication is asynchronous in individual host cells, a process that is independent of tissue location or disease stage, that replication of the nuclear and mitochondrial genomes is non-coordinated within the intracellular population, and that replicating amastigotes and non-replicating trypomastigotes can co-exist in the same cell [31].

We have developed tissue processing protocols and imaging procedures that allow us to routinely detect *T. cruzi* persistence foci during chronic murine infections at single cell resolution [28,29]. Here, we describe experiments which provide new insights into parasite persistence, and indicate that chronic infections are associated with a reduced rate of parasite replication.

2. Methods

2.1. Ethics statement

Animal work was performed under UK Home Office project licenses (PPL 70/8207 and P9AEE04E4) and approved by the LSHTM Animal Welfare and Ethical Review Board. All procedures were conducted in accordance with the UK Animals (Scientific Procedures) Act 1986 (ASPA).

2.2. Parasites, mice and cell lines

The *T. cruzi* bioluminescent:fluorescent lines CL Luc::mNeon or CL Luc::Scarlet [28] were used throughout. Epimastigotes were grown in RPMI-1640, supplemented with 10% foetal bovine serum (FBS, BioSera), hemin (17 µg ml^{-1}), trypticase (4.2 mg ml^{-1}), penicillin (100 U ml^{-1}) and streptomycin (100 µg ml^{-1}), at 28°C. Metacyclic trypomastigotes were generated by culturing epimastigotes to stationary phase. *In vitro* studies

were performed with the MA104 and Vero African green monkey kidney cell lines. *In vivo* experiments were carried out using female C3H/HeN mice, initially aged 8-12 weeks, purchased from Charles River (UK). Mice were maintained under specific pathogen-free conditions in individually ventilated cages, with a 12-hour light/dark cycle. They had access to food and water *ad libitum*.

2.3. CellTrace Violet *in vitro* assay

T. cruzi trypomastigotes were isolated by centrifugation and allowed to recover for 2 hours at 37ºC in high-glucose DMEM medium with 10% FBS, and then labelled with CTV fluorescent dye (Thermo Fisher Scientific), according to the manufacturer's protocol. Briefly, $2x10^6$ trypomastigotes were washed in PBS and then incubated for 20 minutes at 37°C in 10, 5, 2, or 1 µM CTV, protected from light. Unbound dye was quenched by the addition of one volume FBS and incubating for 5 minutes at 37°C. After washing (x2) in fresh complete medium, trypomastigotes were used for infection. Vero cells maintained in RPMI 10% FBS were trypsinized and seeded at 10^4 or 10^5 cells per well in 24-well plates containing cover slips, or in 8 well Ibidi µ-slides with a polymer coverslip, and allowed to attach for 6 hours before infection. Trypomastigotes were added at a multiplicity of infection (MOI) of 10:1 (parasite:host cell) and allowed to invade overnight (16-18 hours). Cultures were then washed with PBS (x3) to remove non-invading parasites, and infected cultures incubated in RPMI with 2% FCS. Coverslips were fixed at different timepoints by transfer into a plate containing 4% paraformaldeyde for 30 minutes, then stained and mounted for microscopy using Vectashield® with DAPI, or with propidium iodide following RNase treatment.

Images and videos were acquired using an inverted Nikon Eclipse microscope. The slide containing the infected cells was moved along the x-y plane through a 580 nm LED illumination. Images and videos were collected using a 16-bit, 1-megapixel Pike AVT (F-100B) CCD camera set in the detector plane. An Olympus LMPlanFLN 40x/1.20 objective was used to collect the exit wave leaving the specimen. Time-lapse imaging was performed by placing the chamber slide on the microscope surrounded by an environmental chamber (OKOLab cage incubator) maintaining the cells and the microscope at 37˚C and 5% CO_2. Video projections and Z-stack sequences were created using the deconvolution app in the Nikon imaging software.

2.4. *In vitro* parasite culturing and EdU labelling

Tissue culture trypomastigotes (TCTs) were derived after infecting MA104 cells with metacyclic trypomastigotes. MA104 cells were cultured in Minimum Essential Medium Eagle (MEM, Sigma-Aldrich.), supplemented with 5% FBS at 37^{o}C, in 5% CO_2. 24-well plates containing cover slips were seeded with 10^5 cells per well and left for 48 hours. After reaching 95-100% confluency, they were infected with TCTs at an MOI of 5:1 (parasite:host cell). 18 hours later, external parasites were removed by washing (x3), fresh supplemented MEM was added, and the infections allowed to proceed.

EdU (Sigma-Aldrich) in PBS was diluted to the appropriate concentration in supplemented MEM. The medium was removed, and the infected monolayer washed (x2), and fresh medium including EdU was added. After the appropriate incubation period, cells were washed (x3). For EdU toxicity studies, parasite growth in infected cells was assessed in 96-well plates, 3 days after EdU addition, by measuring mNeonGreen fluorescence in a FLUOstar Omega plate reader (BMG LABTECH). Background fluorescence was calculated using uninfected MA104 cells (n=6). For microscopy, cells in the 24-well plates were washed (x2) and incubated for 45 minutes in 4% paraformaldehyde diluted in PBS. Cover slips were then removed and washed (x2) in PBS. EdU incorporation was assessed using a Click-iT Plus EdU AlexaFluor 555 Imaging kit (Invitrogen), as per manufacturer's instructions, followed by washing (x2) with PBS, with coverslips then mounted in Vectashield. To allow precise counting of amastigotes, cells were imaged in 3-dimensions with a Zeiss LSM880 confocal microscope, using the Image Browser overlay function to add scale bars. Images were exported as .TIF files to generate figures.

2.5. *In vivo* infections

CB17 SCID mice were infected with $1x10^4$ *T. cruzi* CL Luc::mNeon TCTs and monitored by bioluminescence imaging [32]. At the peak of infection (approximately 18 days), when bloodstream trypomastigotes were visible by microscopy, the mouse was euthanised [33] and infected blood obtained by exsanguination. Trypomastigotes were washed in Dulbecco's Modified Eagle Medium, diluted to $5x10^3$ ml^{-1}, and CH3/HeN mice injected i.p. with $1x10^3$ trypomastigotes.

2.6. *In vivo* EdU labelling

The standard 1-day EdU treatment involved two i.p. injections (12.5 mg kg^{-1} EdU in PBS) delivered 6 hours apart. The second injection took place 18 hours prior to sacrifice. For the 3.5-day treatment, the daily injection protocol (above) was extended for 3 days, with a final single injection on day 4, followed 4 hours later with euthanisation and necropsy. For acute stage experiments, mice were 14-16 days post-infection when EdU was administered, and for the chronic stage, mice had been infected for >100 days. Organs and tissues were subjected to *ex vivo* imaging, bioluminescent foci from skeletal muscle and the colon were excised, and processed for histology [33]. Where indicated, whole colons were removed from the gastrointestinal tract, split longitudinally, pinned luminal side up, and the mucosal layer removed. Whole mounting of the entire external colonic gut wall was performed as described previously [29]. Parasites were identified by mNeonGreen fluorescence using confocal microscopy, and carefully removed, together with ~5mm^2 of surrounding tissue. Prior to a second mounting, tissue pieces were processed for EdU detection by incubation overnight at 4ºC in PBS containing 2.5% FBS and 0.5% triton-X (Sigma-Aldrich), and then washed in PBS (x2) [31]. Several tissue segments could be developed for visualisation using 500 □l of Click-iT reaction mix.

2.7. Statistics

All statistical analyses were performed in GraphPad PRISM v8.0 and STATA v16.0., and the data expressed as the mean ± standard deviation of mean (SD), unless otherwise stated. *In vitro* EdU toxicity was calculated as % growth relative to non-treated controls. The data were fitted with a sigmoidal function with variable slope and the absolute IC_{50} value calculated by solving the function for X when Y= 50%. All data were tested for normality and homogeneity of variance using Shapiro-Wilk's and Levene's tests, respectively. Statistical comparisons between samples to analyse *in situ* EdU incorporation were performed using one-way ANOVA with post-hoc Tukey's test for multiple comparisons. Data sets were analysed by non-parametric tests when variances were not homogenous. The % EdU incorporation in colon tissue sections vs. whole mount were compared using the Wilcoxon signed-rank test. The Kruskal-Wallis test was performed on the exposure data. Statistical significance was accepted where $p \leq 0.05$ (* $p \leq 0.05$, ** $p \leq 0.01$, *** $p \leq 0.001$, **** $p \leq 0.0001$).

3. Results

3.1. The CellTrace Violet tracker dye inhibits *T. cruzi* proliferation

We sought to explore parasite replication by using CTV, a tracker dye that has been employed as a marker for spontaneous dormancy in *T. cruzi* amastigotes [13]. This succinimidyl ester dye diffuses into cells, binds covalently to the amine groups of proteins, and becomes fluorescent following cleavage by intracellular esterases [34]. CTV fluorescence undergoes serial dilution with each round of parasite cell division, resulting in an inverse correlation between dye retention and proliferation rate. However, reports that CTV itself can inhibit cell division [35] prompted us to first investigate toxicity towards *T. cruzi.* Trypomastigotes were labelled by incubation for 20 minutes in 5 or 10 µM CTV (Methods), conditions that had been used previously to monitor parasite proliferation [13]. When these parasites were added to the Vero cell monolayer, we found they were 60% less infectious than trypomastigotes that had been incubated in the DMSO solvent alone (figure 1*a*). In the first 48 hours post-infection, there was then limited division of intracellular CTV+ve parasites, with most trypanosomes in a state of growth arrest (figure 1*b,c*). By 72 hours, replication had been more widely initiated, although the average number of amastigotes per infected cell was still significantly below that of the controls (figure 1*b*). Microscopy also revealed extensive heterogeneity in the intensity of CTV-staining within the *T. cruzi* population, with many parasites failing to replicate, particularly in the first 36-48 hours post-infection. At lower CTV concentrations (1 and 2 µM), growth inhibition was less evident and fewer parasites retained the dye at 5 days post-infection (figure 1*d*). Collectively, these experiments indicate that CTV is an inhibitor of trypomastigote infectivity and amastigote replication, and that the use of dye retention as a marker for dormancy and cell cycle arrest could lead to ambiguity. Furthermore, the heterogeneous nature of *T. cruzi* CTV-staining, even within individual host cells (figure 1*c,d*), could result in differential growth and development rates within the same intracellular parasite population. Prior to infection, we removed non-bound CTV by quenching with addition of bovine serum (Methods). Despite this, some dye was taken up by mammalian cells and retained in stained vesicles for several days (figure 1*d*, electronic supplementary material, Video 1). It was important to ensure co-localisation of blue (CTV), red (fluorescent parasites) and/or green (DAPI - DNA) staining to avoid the risk of confusing amastigotes and spherical CTV-containing vesicles, both of which appear motile in the highly dynamic cytoplasmic environment.

3.2. Continuous EdU exposure can inhibit amastigote replication *in vitro*

We then used the thymidine analogue EdU to monitor parasite proliferation. In *T. cruzi*, incorporation of EdU provides a readout on the replicative status of both nuclear and mitochondrial DNA (kDNA) [28,31]. However, the procedure has to be used with caution, since EdU exposure *in vitro* can be associated with toxicity. In cultured mammalian cells, this is characterised by genome instability, DNA damage and cell cycle arrest [36-38]. Short-term exposure at lower concentrations (<12 hours, <10 µM) appears to have less impact, and does not perturb cell cycle kinetics [39]. Toxicity against *T. cruzi in vitro* has also been shown to be dependent on exposure time; 4 hours had only minor inhibitory effects on intracellular amastigotes, even at 70 µM, whereas with 24 hours continuous exposure, the IC_{50} dropped to 70 nM [40]. In contrast, when infected cells were cultured for 72 hours in presence of 100 µM EdU, there was no reported inhibition of amastigote replication [13]. Given these conflicting observations, as a preliminary to *in vivo* studies, we assessed the *in vitro* kinetics and growth inhibitory effects of EdU on intracellular amastigotes of *T. cruzi* CL-Luc::Neon (a derivative of the CL Brener strain). This parasite reporter line expresses a fusion protein that is both bioluminescent and fluorescent [28]. After only 10 minutes exposure, amastigotes were clearly labelled, and it was possible to distinguish those that were EdU+ve from those that were EdU-ve (figure 2*a*). Similar heterogeneity, including differential labelling of nuclear and kDNA, was observed when infected cells were labelled for 1 or 6 hours at different EdU concentrations (figure 2*b,c*). This pattern results from asynchronous amastigote replication [31], with EdU negativity/positivity determined by the position of individual parasites within the cell cycle during the period of exposure. When we assessed the extent of EdU growth inhibition after 6 hours exposure, washing, and examination 3 days later, we established an IC_{50} of 1.67 µM, although the level of inhibition plateaued at 70% (figure 2*d*). These outcomes are therefore consistent with those reported by Sykes *et al*. [40].

3.3. Reduced numbers of *T. cruzi* in S-phase during chronic stage of infections

We next compared the dynamics of EdU incorporation by parasites during acute and chronic murine infections with the *T. cruzi* CL-Luc::Neon strain. The elimination half-life ($T_{1/2}$) of EdU in mice has not been determined, but with other thymidine analogues, the period is relatively short. For example, the bioavailability of bromodeoxyuridine (BrdU), a thymidine analogue also used in DNA labelling experiments, is less than 15 minutes [41]. Infected C3H/HeN mice were therefore given two EdU injections (each of 12.5 mg kg^{-1}), 6 hours apart (figure 3*a*), in an attempt to highlight a greater number of parasites where DNA replication was

underway. At any one time, as judged by *in vitro* experiments, approximately 25-30% of amastigotes will be in S-phase [26]. In the majority of cases, the external gut wall mount methodology [29] was used to process the resulting tissue samples. The protocol enables the muscular coat, including the longitudinal and circular smooth muscle layers, which contain the majority of colon-localised parasites during chronic stage infections, to be visualised in their entirety at a 3-dimensional level with single-cell resolution (Methods). Intracellular parasite numbers can be determined with accuracy by confocal microscopy using serial Z-stacking (electronic supplementary material, figure S1). On occasions, infected host cells in colonic tissue were also investigated by coupling *ex vivo* bioluminescence-guided excision and confocal microscopy (Methods) [31].

Colon samples were excised 18 hours after the second injection, and the incorporated EdU visualised (Methods). We observed significantly greater levels of parasite labelling in tissue obtained from acute stage mice than from those that were chronically infected (70% vs 20%) (figures 3,4; electronic supplementary material, figure S2). Therefore, during the acute stage, a greater fraction of the parasite population is replicating their nuclear and/or mitochondrial DNA at any specific time point. By inference, the amastigote replication rate must be slower during chronic infections, at least in this tissue location. There were no differences in the data derived from colonic tissue processed by the two differing methodologies (grey and yellow dots, figure 3*b*). We further observed that during the acute stage, there was a positive correlation between the number of parasites per infected cell and the percentage of parasites where DNA synthesis was ongoing (figure 4*a*,*b,c*). Large parasites nests were less common during the acute stage, with few instances where infected cells contained more than 50 parasites (figure 4). We did attempt to quantify, for comparative purposes, the relative level of EdU labelling in each parasite. However, since most images were taken with whole mounted tissue sections, the variable depths of parasites from the surface made this technically challenging. As judged by visual inspection, the majority of EdU+ve parasites in any one cell were labelled to a similar extent (figure 3*c,d,e;* electronic supplementary material, figure S2). Since smooth muscle cells, the most frequently infected cell type in the colon [29], are typically in a state of cell cycle arrest, the nuclei of host cells were generally unlabelled.

In chronically infected mice, only a minority of parasites incorporated EdU when the 1-day protocol was used (figure 3, electronic supplementary material, figure S2), and in ~20% of infected cells, none of the parasites

were labelled (figure *5a,b*). A similar level of heterogeneous incorporation was observed in skeletal muscle, another site of parasite persistence in chronically infected C3H/HeN mice, and a tissue where parasites are often found in large nests (electronic supplementary material, figure S3, as example). When labelling was extended over 3.5 days (a total of 7 injections) (figure 3*a*), there was a 2.3-fold increase in the number of labelled parasites, with approximately half of those in the colon being EdU+ve (figures 3*b*,5*c;* electronic supplementary material, figure S2). With this more prolonged protocol, every infected host cell that we examined contained at least one labelled parasite (figure 5*c*). However, the percentage of EdU+ve parasites within the population was still significantly lower than during the acute stage, when the 1-day labelling protocol was used (figure 3). In combination, these data indicate that during chronic infection of the colon, there is a general reduction in the number of parasites in S-phase. As judged by bioluminescence *ex vivo* imaging of organs and tissues, neither the 1-day nor the 3.5-day EdU injection protocols had any detectable effect on the levels of infection or on tissue-specific parasite dissemination (electronic supplementary material; figure S4).

3.4. Long-term infection of individual colonic smooth muscle cells is not common during the chronic stage

To further investigate parasite replication during chronic stage infections, we undertook experiments to assess the extent and stability of parasite labelling 7 and 14 days after EdU injection using the 1-day labelling protocol (figure 6*a*). When mice were examined by *ex vivo* bioluminescence imaging after 14 days, there had been no measurable impact on the parasite burden or tissue distribution (electronic supplementary material, figure S4). At 7-day post-injection point, EdU+ve parasites were still readily detectable, although there was a 4-fold decrease in their relative abundance within the population, and only ~40% of infected cells contained any labelled parasites (figure *6b,c,e,f*). By 14 days post-injection, out of the 87 infected cells detected in the colons of 8 mice, just 1 contained EdU+ve amastigotes (figure 6*d,e,g*). Using serial Z-stacking, we established that this infected cell contained 82 parasites, 42 of which were labelled. Given this profile, the most likely explanation is that this host cell had remained infected for at least 14 days, with the parasites in a state of low proliferation. The EdU+ve parasites cannot have undergone many replication cycles during this period, since the labelling intensity was similar to that in parasites examined 1 day post-injection. Furthermore, in dividing cells, incorporated nucleosides become undetectable after 2 to 5 generations,

assuming random segregation of daughter chromosomes [42,43]. It can be further inferred from the rarity of cells containing EdU+ve parasites (figure 6*d,g*), that long-term occupancy of individual colonic smooth muscle cells by *T. cruzi* is not a common feature of chronic stage infections, even though this tissue is a site of parasite persistence. In the vast majority of cases therefore, the normal infection cycle of parasite replication, host cell lysis, and re-infection appears to continue during the chronic stage, albeit at a reduced rate. Finally, the observation of multiple labelled amastigotes within a single host cell 14 days after injection (figure 6*d*) demonstrates that EdU is stable once it has been incorporated into the *T. cruzi* genome, and that it is not readily susceptible to removal by metabolic or DNA repair pathways. This stability has similarities with the situation in mice, where Merkel cells labelled during pregnancy remained EdU+ve in off-spring 9 months after birth [44].

4. Discussion

The report that *T. cruzi* can undergo a form of spontaneous dormancy has highlighted the possibility that the proliferation status of the parasite could have a role in long-term persistence and contribute to the high rate of treatment failure [13]. Improvements in tissue processing and imaging procedures [29] have allowed us to explore this further by providing a platform to investigate parasite replication in the colon of chronically infected mice, a tissue that supports long-term *T. cruzi* persistence at extremely low levels [27]. Our major finding is that during chronic infections, the proportion of intracellular parasites in S-phase is significantly lower than it is during the acute stage. In acute infections, 70% of parasites were EdU+ve after using the 1-day protocol, compared with 20% during the chronic stage (figure 3, 4; electronic supplementary material, figure S2). This is unlikely to reflect reduced EdU uptake or bioavailability during chronic infections, as the staining intensity of individual EdU+ve parasites was similar during both stages of the disease, with the only apparent difference being the proportion of amastigotes that were positive. The most parsimonious explanation is that *T. cruzi* amastigotes proliferate at a slower rate in the chronic stage, at least in this tissue location, and were therefore less likely to be replicating their DNA during the period of EdU exposure. It is implicit from this that *T. cruzi* amastigotes have the capability of responding to environmental signals that are specific to chronic and/or acute stage disease, such as nutrient availability or indicators of the immune response. In the latter case, the observation that immunosuppression rapidly reactivates the infection [30], suggests that the host response could be a driver for slow replication, either directly or indirectly. These

observations are in line with previous reports that amastigote replication and cell cycle kinetics can be subject to reversible stress-induced inhibition *in vitro* [26]. A response mechanism of this type could also account for the correlation between amastigote growth rate and nest size during acute infections (figure 4).

The heterogeneous nature of labelling during the chronic stage, with many parasites being EdU-ve (figure 3; electronic supplementary material, figure S2), should not be interpreted as being indicative of spontaneous dormancy. Rather, it provides further evidence that parasite replication within individual host cells is asynchronous [31]. The observation that some intracellular parasites do not incorporate EdU reflects that amastigotes exist in a range of replicative states within individual infected cells, an inference supported by the cumulative nature of EdU labelling. There are several possible fates for parasites labelled with EdU during chronic stage infections, as outlined in figure 7. Given our data, which show a steady reduction in the % EdU+ve parasites per infected cell over time (figure 6), continued growth of these amastigotes and dilution of the label below the level of detection (figure 7*c*) would appear to be the most likely outcome.

Although incorporation of EdU into replicating DNA is widely used in proliferation studies, it can lead to a DNA damage response and cell cycle arrest, [36-38]. With *T. cruzi,* the measurable effect of EdU toxicity is time-dependent [40], and here we showed that 6 hours exposure *in vitro* at 1-2 µM is sufficient to inhibit amastigote replication (figure 2*d*). Therefore, studies on *T. cruzi* proliferation, dormancy and persistence could be confounded if EdU exposure is continuous. In the case of *in vivo* administration, EdU toxicity should be less problematic, because of the short clearance time of thymidine analogues [41]. Consistent with this, we found no detectable impact of EdU exposure on parasite burden or tissue tropism in chronically infected mice (electronic supplementary material, figure S4). In these infection experiments, where incorporation was employed as an end-point assay, providing snapshots of DNA replication within the parasite population, EdU toxicity would not be expected to compromise the outcome. This contrasts with *in vitro* experiments where EdU exposure can be continuous, resulting in inter-strand cross-linking and double-strand breaks, which trigger DNA damage signalling and cell cycle arrest [37]. This is a ubiquitous response in all cells with DNA damage sensing machinery [45,46]. Spontaneous dormancy has been proposed as a mechanism that could account for parasite persistence after therapy [13,47]. However, in *T. cruzi,* the front-line drug benznidazole can cause mutagenesis, disruption to DNA-repair pathways, and chromosome instability [48,49]. Therefore,

an alternative explanation could be that benznidazole-induced DNA damage responses trigger cell cycle arrest and a transient dormant-like state, which protects some parasites from further drug-induced toxicity, ultimately leading to relapse after the successful completion of DNA repair.

Our findings do not exclude the possibility that some parasites might have the potential to enter a canonical dormant state at specific points in the life cycle. However, they more strongly suggest, that rather than being a discrete biological stage, a dormancy-like phenotype in *T. cruzi* might be better described as representing one end of the normal proliferation spectrum. The cell cycle plasticity necessary for this has already been reported in amastigotes [26]. Therefore, the reduced rate of *T. cruzi* replication during the chronic stage could be a phenomenon more analogous to the biochemical quiescence and reduced proliferation exhibited by *Leishmania* [19,20], than to the more definitive dormant state displayed by *T. gondii* and some *Plasmodium* species [3]. Resolving this question and understanding the mechanisms involved has particular importance for Chagas disease drug development strategies. As described in this paper (figures 1,2), there are limitations to the cell tracker dye and DNA labelling methodologies that have previously been applied to investigate *T. cruzi* proliferation and quiescence**.** Therefore, new approaches are urgently required.

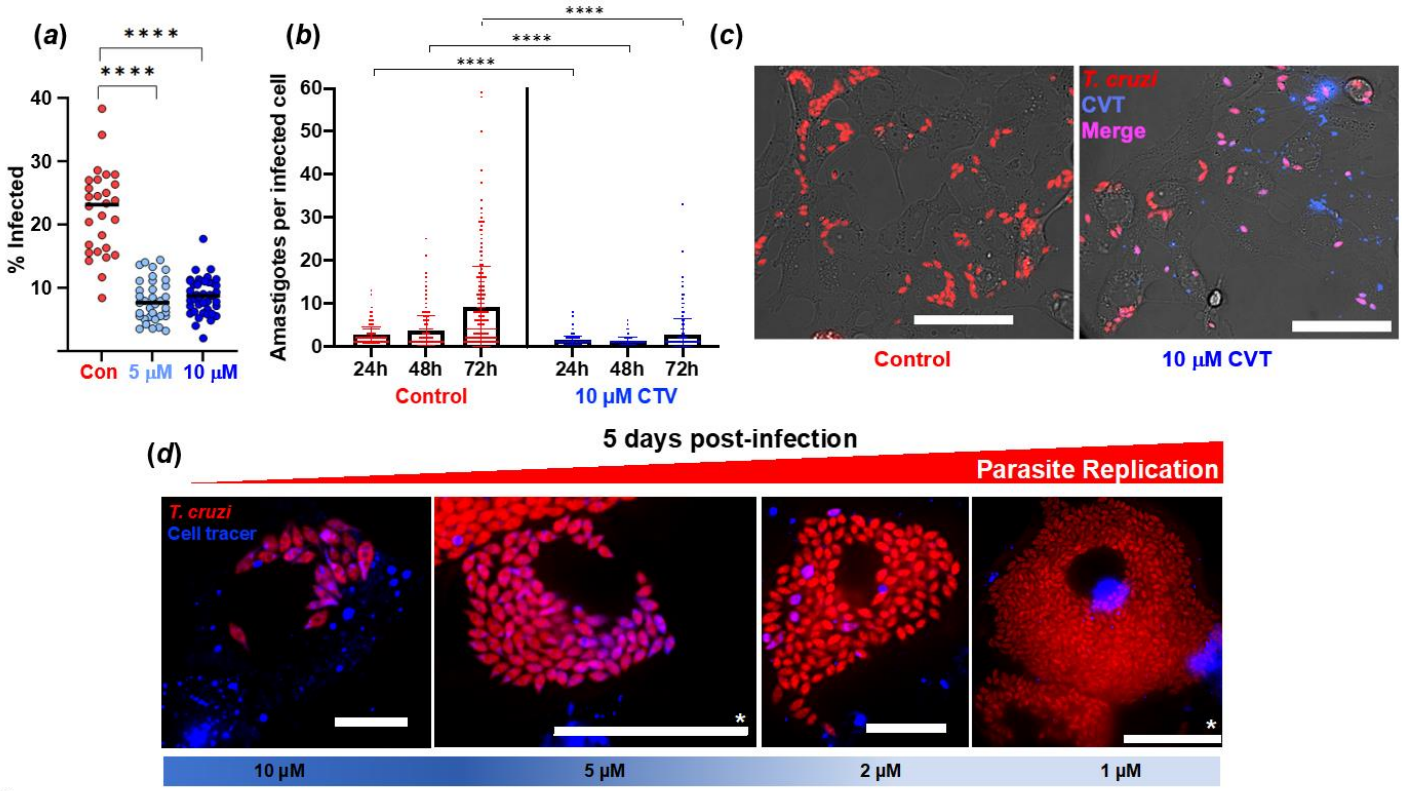

Fig. 1

Figure 1. CellTrace Violet (CTV) reduces *T. cruzi* infectivity and inhibits intracellular proliferation. (*a*) *T. cruzi* CLBr-Luc::Scarlet trypomastigotes were incubated with either 5 or 10 µM CTV for 20 minutes and used to infect Vero cell monolayers at an MOI of 10:1 (Methods). 18 hours later, infection efficiency was determined by inspecting a total of 2,203 (control), 3781 (5 µM), and 3,840 (10 µM) Vero cells (>300 infected cells in each case). Each data point corresponds a randomly acquired image and represents the mean percentage of cells infected. Differences between columns were analysed using a parametric one-way ANOVA with Tukey's post-hoc pair wise comparisons. **** $p \leq 0.0001$. (*b*) Vero cells infected with CTV-ve or CTV+ve trypomastigotes (as above) were incubated for the time periods indicated. The numbers of amastigotes per infected cell were then determined by analysing >300 infected cells per treatment. Error bars represent the standard deviation from the mean. Data were analysed using a Wilcoxon rank sum test. (*c*) Images of Vero cells 36 hours after infection with CTV-ve (control) or CTV+ve trypomastigotes. Red, fluorescent *T. cruzi* amastigotes. Fluorescent parasites containing the CTV tracer dye appear as purple on a red fluorescent background. Size bars=20 µM. (*d*) Images of Vero cells 5 days after infection with trypomastigotes that had been incubated with various concentrations of CTV, as indicated. Blue, intracellular vesicles containing CTV. See also electronic supplementary material, Video 1. Size bars=20 µM; those with *=50 µM

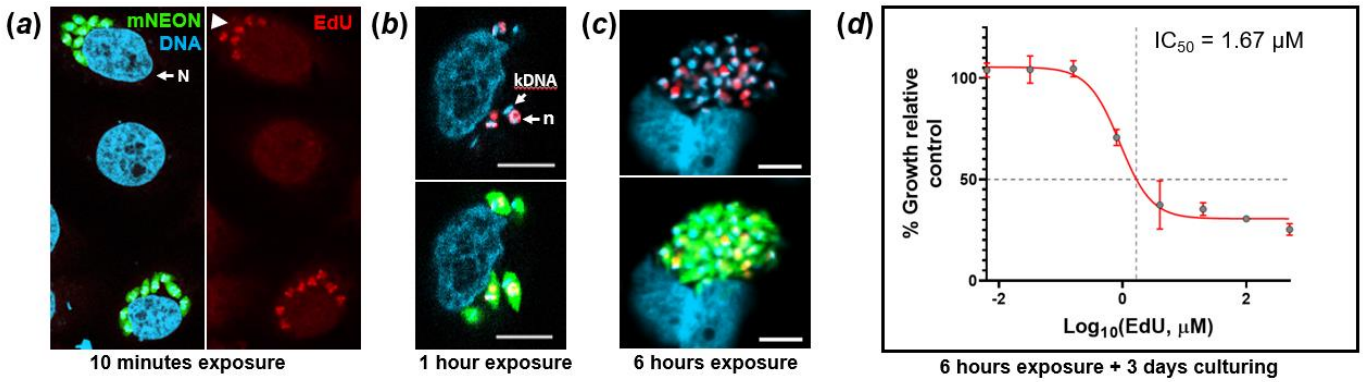

Figure 2. EdU incorporation by *T. cruzi* amastigotes *in vitro* is rapid, heterogeneous within the population, and can inhibit parasite growth. (*a*) *T. cruzi* CL-Luc::Neon trypomastigotes were used to infect MA104 cells at an MOI of 5:1 (Methods). 2 days later, cultures were exposed to EdU (50 µM) for 10 minutes, and then examined by confocal microscopy. The image shows adjacent infected cells where in one instance, all 8 amastigotes are EdU+ve, whereas in the other, 2/8 are EdU-ve (indicated by white arrowhead). N, host cell nucleus. (*b*) EdU labelling of amastigotes after 1 hour exposure (40 µM). kDNA, kinetoplast DNA; n, parasite nucleus. (*c*) EdU labelling of amastigotes after 6 hours exposure (10 µM). Scale bars=10 µm in all cases. (*d*) MA104 cells were infected with trypomastigotes, and 2 days later, the cultures were exposed for 6 hours to EdU at a range of concentrations, and then washed thoroughly. After a further 3 days incubation, amastigote growth was determined by assessing expression of the mNeonGreen reporter (Methods). The inhibition curve was plotted using PRISM graphpad to establish the concentration of EdU that conferred 50% growth inhibition compared to untreated controls. Data were derived from 5 replicates (CI_{95} 0.98 µM-4.83 µM).

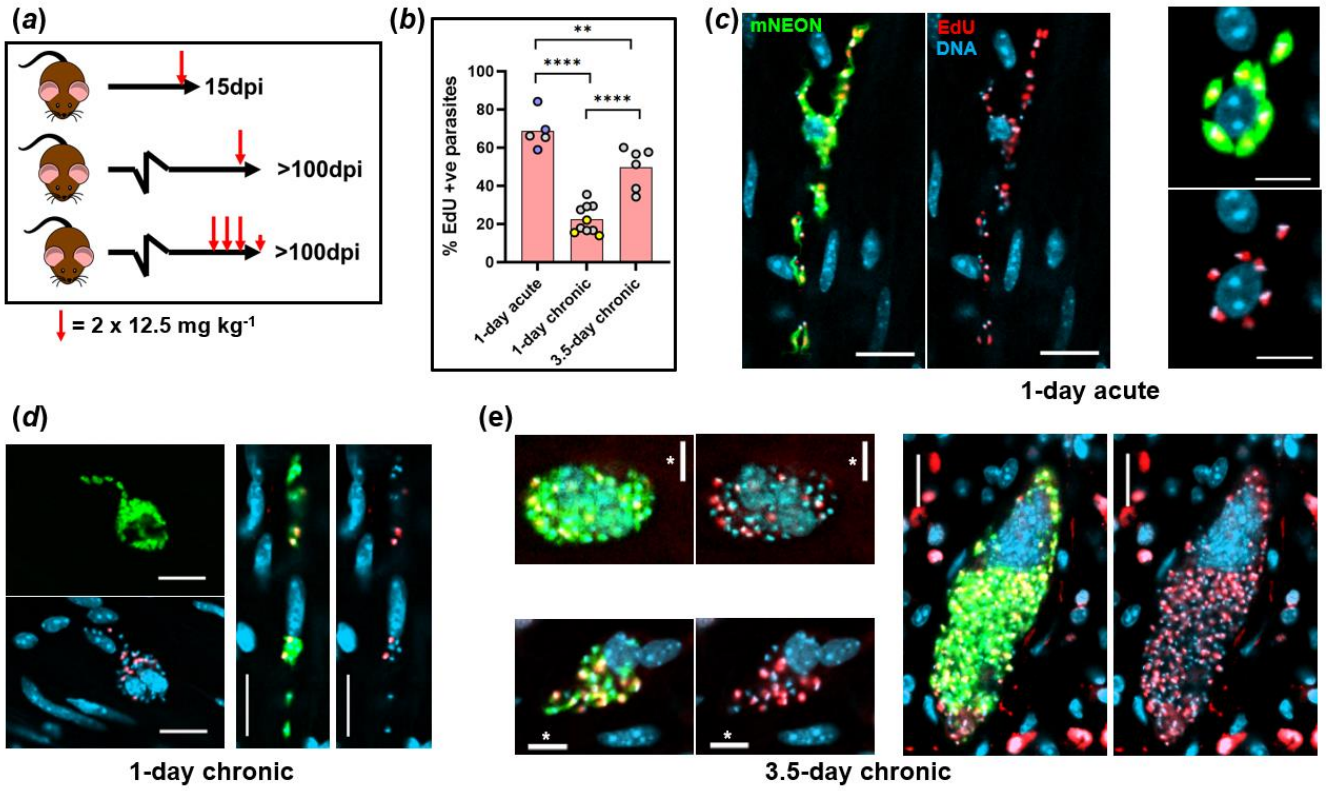

Figure 3. Intracellular *T. cruzi* replication, as inferred by EdU incorporation, is slower in the chronic stage than during acute infections. (*a*) Schematic showing experimental outline. C3H/HeN mice infected with *T. cruzi* CL-Luc::Neon were injected with EdU as indicated during the acute (15 days post-infection; dpi) or chronic stage (>100 dpi). Each larger red arrow indicates 2 i.p. injections separated by 6 hours. (*b*) Percentage of parasites that were EdU+ve under each treatment protocol. Colonic tissue was extracted from mice 18 hours after the second injection (1-day treatment) or 4 hours after the final injection (3.5-days treatment), and infected cells detected by *ex vivo* imaging and confocal microscopy (Methods) (electronic supplementary material, figure S1) [29]. Each data point represents a single mouse. Blue data points indicate mice aged ~150 days at the start of acute infection, and act as age-matched controls. In the chronically infected mice, yellow data points indicate colons processed by standard histological sectioning, and grey points highlight those processed through peeling away of the mucosal layer and whole mounting the remaining colonic gut wall (Methods). No significant differences were observed in the % EdU+ve parasites in colonic sections processed by each method (Wilcoxon rank sum test). For comparison of treatment conditions, statistical analysis was performed as described (Methods); **** $p \leq 0.0001$ and ** $p \leq 0.01$. (*c*) Representative images of infected colonic muscle cells from an acute stage mouse. Labelling: parasites, green; DNA, blue (DAPI staining); EdU, red. EdU labelling on a green background appears yellow. (*d* and *e*)

Images of infected colonic muscle tissue from chronically infected mice after EdU labelling using the 1-day and 3.5-day protocols, respectively (see also electronic supplementary material, figure S2). Scale bars=20 µm, except where indicated; *=10 µm.

(*a*)

	Acute		Chronic	
Nest size	Infected cells	Parasites	Infected cells	Parasites
1 - 10	750	2349	18	87
11 - 25	116	1738	16	270
25 - 50	44	1673	10	380
51 - 100	9	526	5	344
101 - 200	0	0	2	324
>201	0	0	4	2221

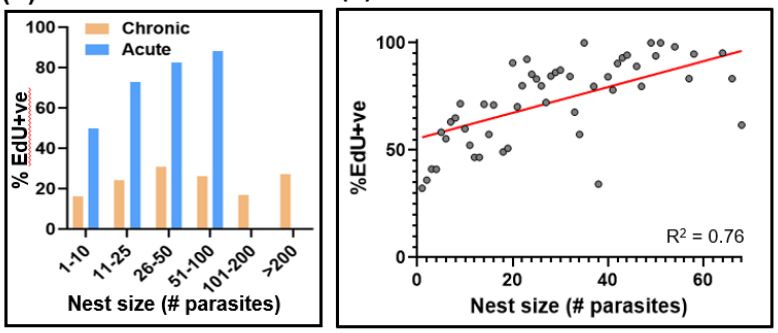

Figure 4. The inferred parasite replication rate is higher during the acute stage and correlates positively with nest size at this phase of the infection. (*a*) The number of infected cells (nests) detected in colonic gut wall tissue from mice in the acute (n=5) and chronic (n=7) stage, and the number of parasites found in each category. Tissue was processed using the colon peeling procedure (Methods). (*b*) Percentage EdU+ve parasites in infected cells during acute and chronic infections in relation to nest size. (*c*) Relating nest size to the % EdU+ve parasites during acute stage infection. Each point corresponds to a specific nest size (x-axis), and the corresponding %EdU+ve mean percentage value across all animals (y-axis). The R^2 value was determined by linear regression.

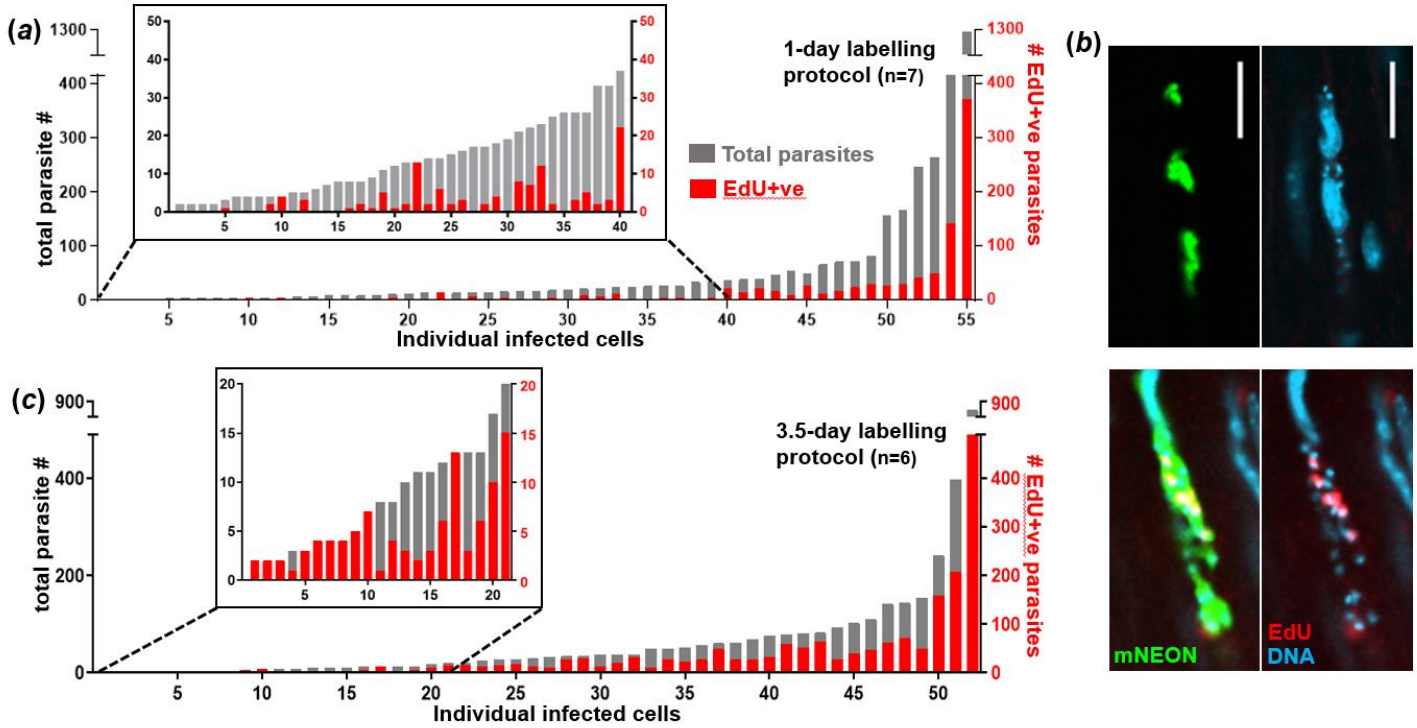

Figure 5. Increased chronic stage EdU incorporation by parasites with the 3.5-day protocol. (*a*) Level of EdU incorporation in the 55 infected cells detected in the whole mounted colonic gut walls from 7 chronic stage mice treated with the 1-day labelling protocol. The total parasite content (grey) and the number that were EdU+ve (red) are indicated. (*b*) Upper images; an infected cell containing no EdU+ve parasites after labelling with the 1-day protocol. Lower images; an infected cell from the same colonic tissue that contained EdU+ve parasites (see also electronic supplementary material, figure S2). Parasites, green. (*c*) EdU incorporation in 52 infected cells detected in 6 chronically infected mice treated with the 3.5-day labelling protocol. Every infected cell in the colonic gut walls of these mice contained at least 1 EdU+ve parasite. Raw data are available in Table S1.

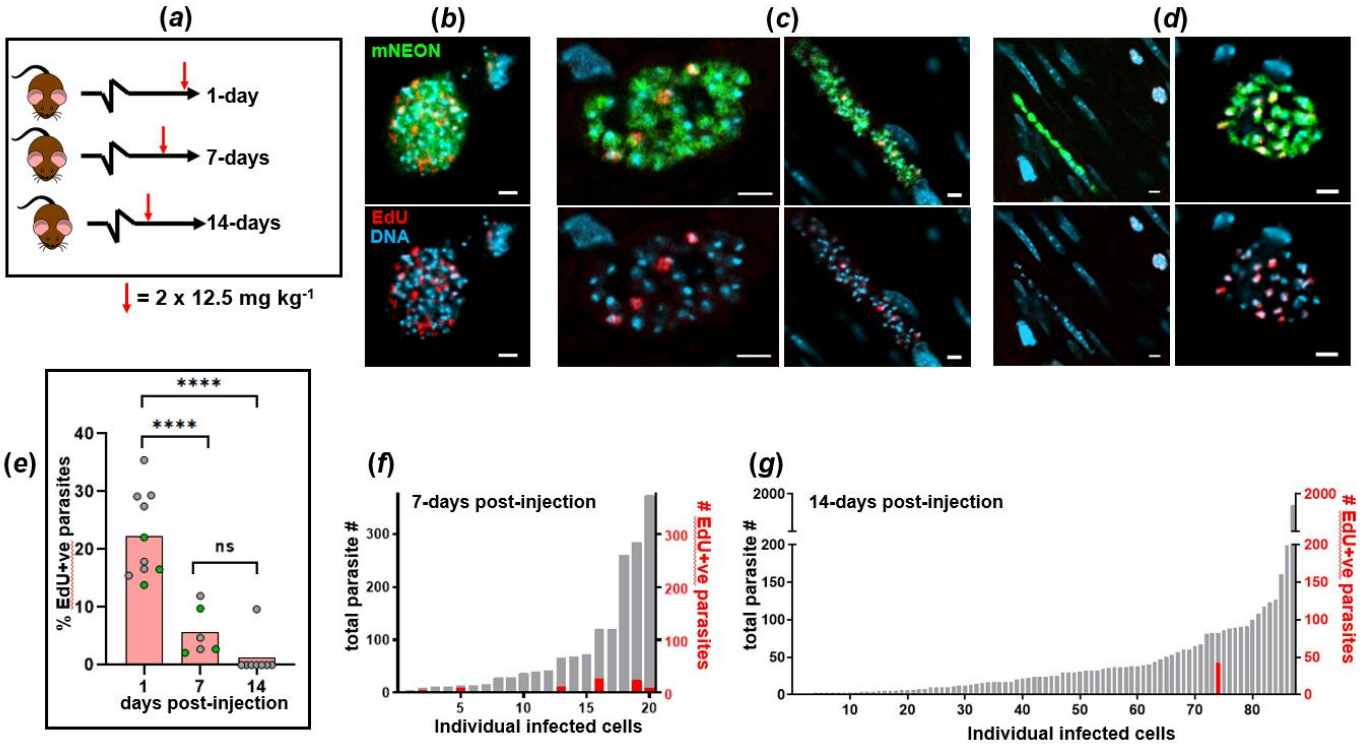

Figure 6. EdU labelling experiments reveal that parasite occupation of colonic host cells during chronic stage infections is not long-term. (*a*) Schematic of the labelling protocol. EdU was injected in two 12.5 mg kg^{-1} doses, 6 hours apart (as in figure 3*a*). After 1, 7, or 14 days, mice were sacrificed, colonic tissue excised, and infected cells detected by *ex vivo* imaging and confocal microscopy (Methods). (*b*) Representative images of parasite EdU incorporation following the 1-day labelling protocol (see also Figure 3*d*). (*c*) EdU incorporation assessed 7 days post-injection. (*d*) Left-hand image; EdU incorporation assessed 14 days post-injection. Typically, infected cells contained no EdU+ve parasites. Right-hand image; the single example of an infected host containing EdU+ve parasites after an exhaustive search of colon mounts from 8 mice. Scale bars=20 □m. (*e*) Mean % EdU+ve parasites found in infected colonic cells. Each data point represents a single mouse; 1-day post-injection, n=10; 7-days post-injection, n=6; 14-days post-injection, n=8. The total number of parasites detected, imaged and designated as EdU+ve or EdU-ve in each mouse varied from 47 to 2468, with an average of 608. The green data points indicate colons processed by standard histological sectioning, and grey data points highlight those processed through peeling away of the mucosal layer and whole mounting of the remaining colonic gut wall (Methods). Statistical analysis of treatment conditions was performed as described (Methods); **** $p \leq 0.0001$. There was no significant difference (ns) between the 7- and 14-days post-injection groups. (*f*) Percentage parasites that were EdU+ve in infected colonic cells from mice sacrificed 7-days post-injection (n=3). Grey bar indicates total parasite number in each infected cell; red

bar indicates the percentage EdU+ve. (*g*) Similar analysis of EdU positivity in infected cells found in mice 14-days post-injection (n=8).

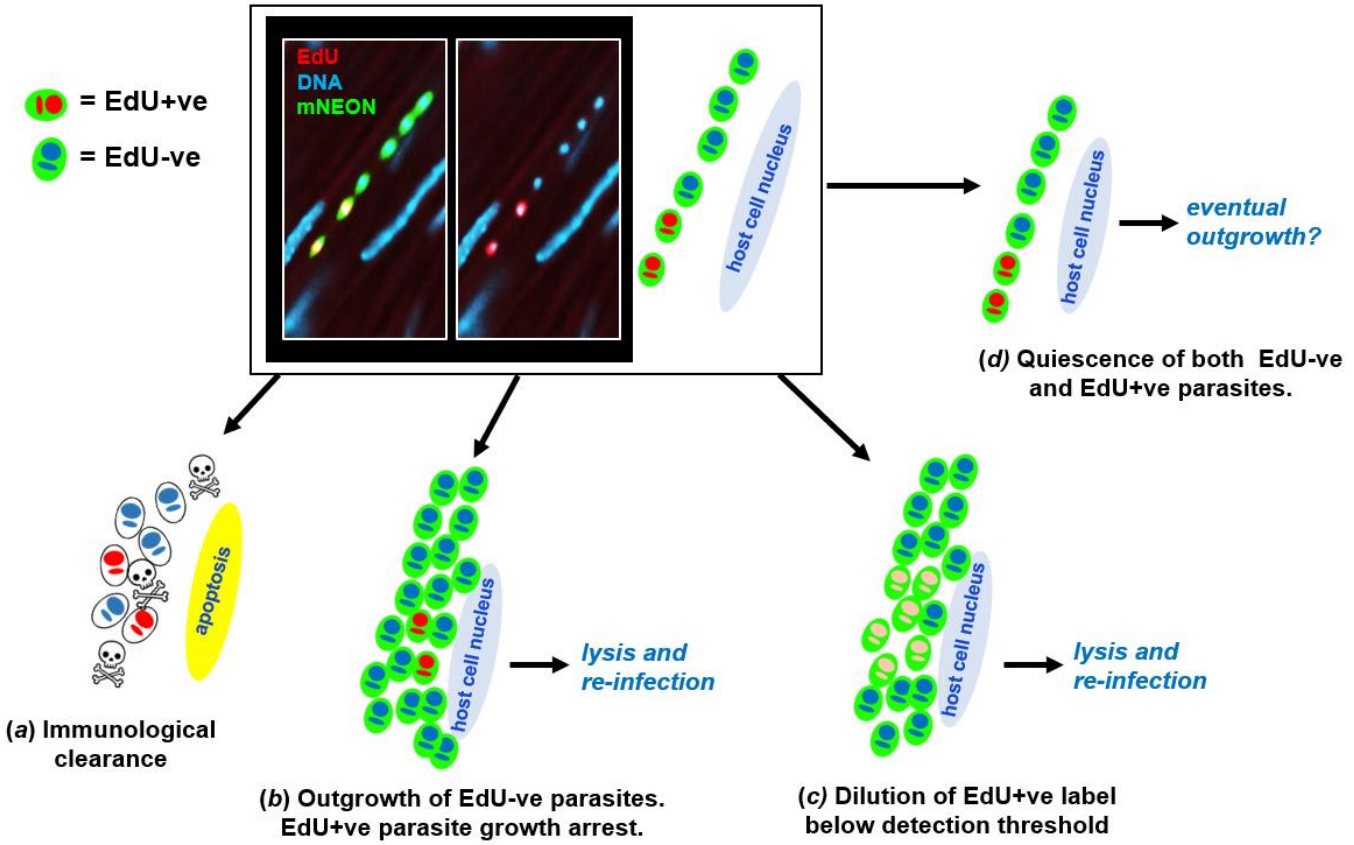

Figure 7. Schematic highlighting the possible fates of host cells and parasites following EdU labelling. The image shows a colon smooth muscle section from a chronically infected mouse following treatment with the 1-day labelling protocol (figure 3). EdU labelling (red) appears as yellow against the green background of parasite fluorescence. (*a*) Following EdU exposure, the infected cell and parasites could be cleared by the host immune response. (*b*) There could be outgrowth of EdU-ve parasites in an infected cell. The EdU+ve subset, which would have been in S-phase during exposure, might enter cell cycle arrest after incorporation. (*c*) If EdU incorporation is below the toxicity threshold for cell cycle arrest, amastigote proliferation will lead to serial dilution of the label. (*d*) After EdU incorporation by a subset of parasites, all the amastigotes in the cell might enter a slow proliferative state. This appears to be a rare event (see figure 6*d,g*).

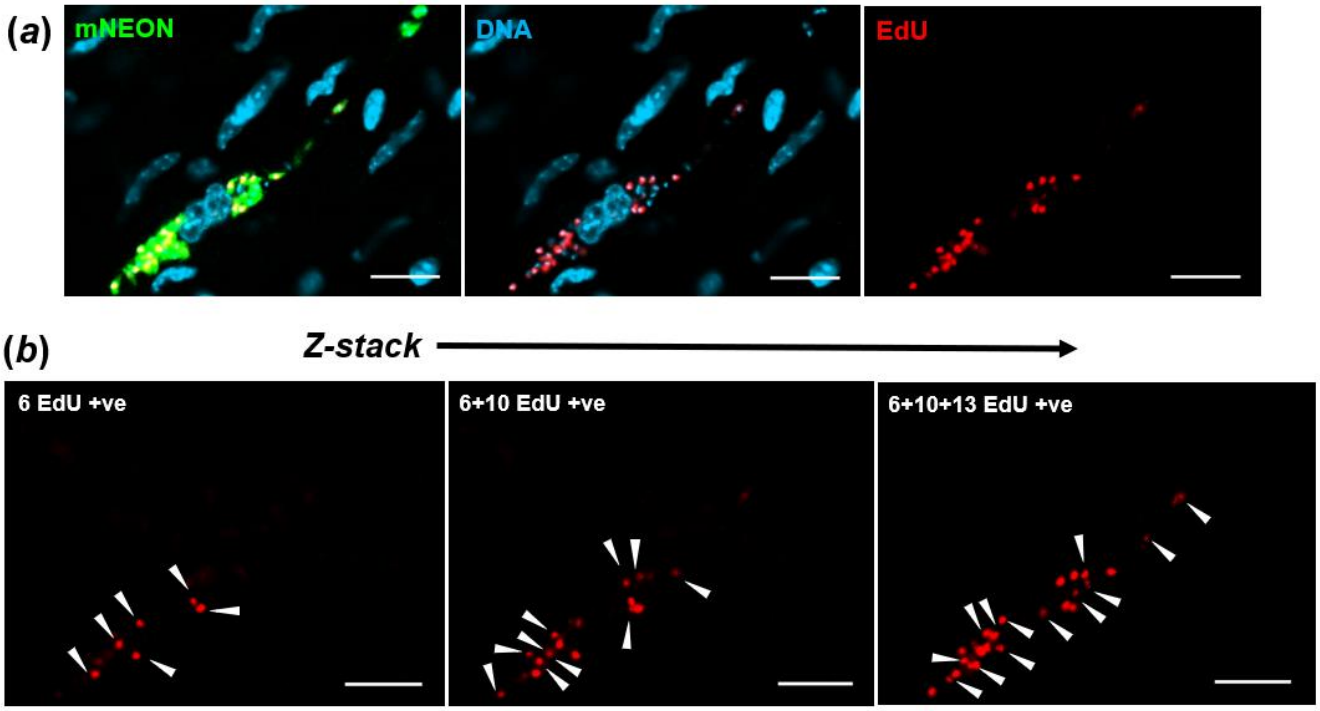

Figure S1. Determination of parasite numbers and EdU incorporation status in infected mouse cells using 3-D confocal imaging. (*a*) *T. cruzi* infected cell in the colonic gut wall of a chronic stage C3H/HeN mouse, following treatment using the standard 3.5-day EdU labelling protocol (figure 3*a*). All scale bars=20μm. (*b*) Assessment of EdU+ve parasites using a series of Z-stacked image slices from across the infected cell. 28 EdU+ve parasites were detected. The total number of parasites was determined in the same manner by visualising DAPI staining.

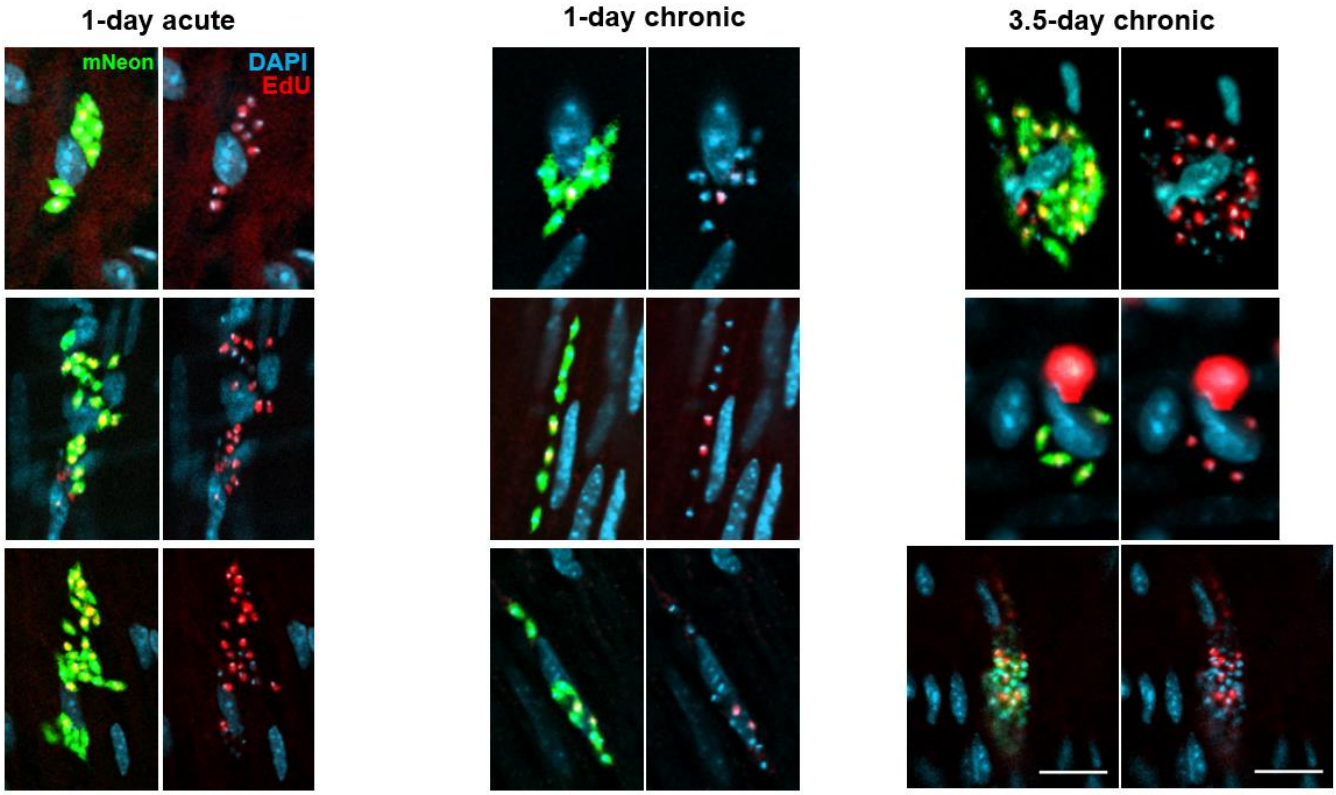

Figure S2. Further images demonstrating that, inferred from EdU incorporation, *T. cruzi* replication is slower in the chronic stage than in the acute (see also figure 3). C3H/HeN mice infected with *T. cruzi* CL-Luc::Neon were injected with EdU during the acute or chronic stage. Colonic tissue was extracted from mice 18 hours after the second injection with 12.5 mg kg^{-1} EdU (1-day treatment, acute and chronic stage) or 4 hours after the final injection (3.5-days treatment, chronic stage), and infected cells detected by *ex vivo* imaging and confocal microscopy (Methods). Labelling: parasites, green; DNA, blue (DAPI staining); EdU, red. EdU labelling on a green background appears yellow. For reference, scale bars=20 μm. These images form part of the data set collated to produce figure 3*b*.

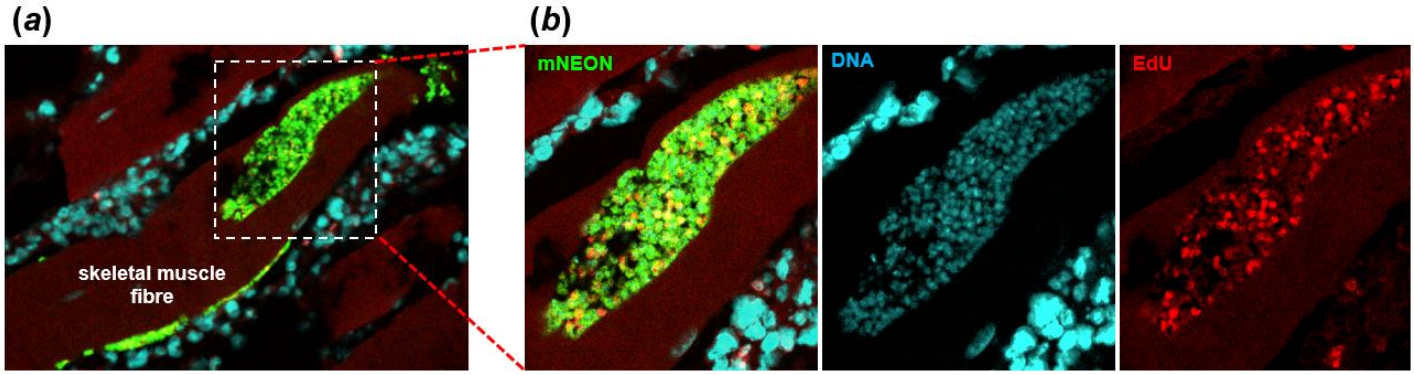

Figure S3. EdU incorporation by parasites in skeletal muscle during a chronic stage infection. (*a*) C3H/HeN mice, chronically infected with *T. cruzi* CL-Luc::Neon, were injected twice with EdU (12.5 mg kg^{-1}; 6 hours apart). Skeletal muscle was excised 18 hours later and infected cells detected by *ex vivo* imaging and confocal microscopy (Methods). (*b*) Enlarged images of nest showing fluorescent parasites (green), DNA staining (blue), and EdU incorporation (red).

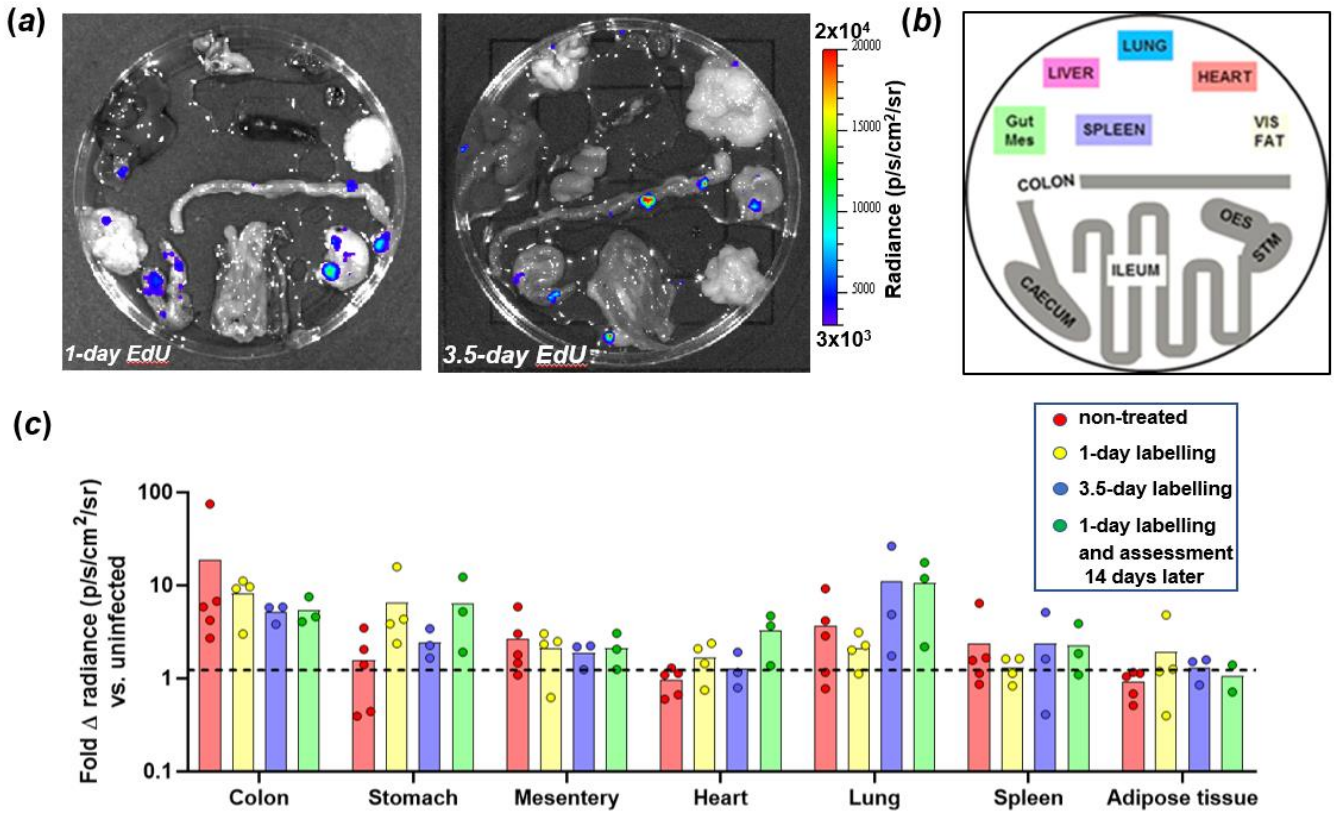

Figure S4. (*a*) *Ex vivo* bioluminescence imaging of organs and tissues from a C3H/HeN mouse chronically infected with *T. cruzi* CL-Luc::Neon, sacrificed after EdU labelling using the 1-day and 3.5-day protocol (figure 3*a*). (*b*) Schematic showing the arrangement of organs. (*c*) Comparison of the fold increase in radiance (p/s/cm^2/sr) above background associated with organs and tissues from chronically infected mice subjected to 1-day EdU labelling (n=4), 3.5-days EdU labelling (n=3), and 1-day EdU labelling, followed by assessment 14 days later (n=3) (as in figures 3 and 6). The dashed line indicates 2xSD above the background established from uninfected mice (n=4).

Table S1. Raw data which indicate increased chronic stage EdU incorporation by parasites with the 3.5-day protocol. These data were used to generate figures 5*a* and 5*c*. *Available on-line*

Supplementary Video 1. 3-D video projection and rotation after Z-stack capture of a Vero cell 5 days post-infection with *T. cruzi* CLBr-Luc::Scarlet (red) (see also figure 1*d*). Infective trypomastigotes had been pre-incubated with 10 µM CTV (Methods). The asynchronous parasite population contains amastigotes displaying different sizes and shapes suggesting variability in their cell and/or developmental cycles. Within

individual parasites, there was considerable heterogeneity in the intensity and location of CTV-staining. Similarly, in the host cell, CTV is widely dispersed (blue), frequently sequestered in vesicle-like structures that can be mistaken for amastigotes unless co-localising red fluorescence is confirmed. N=host cell nucleus. Size bars=20 µM**.** *Available on-line*

References

1. Weidner-Glunde M, Kruminis-Kaszkiel E, Savanagouder M. 2020 Herpesviral latency-common themes. *Pathogens* **9**, 125. (doi: 10.3390/pathogens9020125).
2. Dodd CE, Schlesinger LS. 2017 New concepts in understanding latent tuberculosis. *Curr. Opin. Infect. Dis.* **30**, 316-321. (doi: 10.1097/QCO.0000000000000367).
3. Barrett MP, Kyle DE, Sibley LD, Radke JB, Tarleton RL. 2019 Protozoan persister-like cells and drug treatment failure. *Nat. Rev. Microbiol.* **17**, 607-620. (doi: 10.1038/s41579-019-0238-x).
4. Pontes MH, Groisman EA. 2020 A physiological basis for nonheritable antibiotic resistance. *mBio* **11**, e00817-20. (doi: 10.1128/mBio.00817-20).
5. Mandal S, Njikan S, Kumar A, Early JV, Parish T. 2019 The relevance of persisters in tuberculosis drug discovery. *Microbiol.* **165**, 492-499. (doi: 10.1099/mic.0.000760).
6. Francisco AF, Jayawardhana S, Lewis MD, Taylor MC, Kelly JM. 2017 Biological factors that impinge on Chagas disease drug development. *Parasitol.* **144**, 1871-1880. (doi: 10.1017/S0031182017001469).
7. Cardillo F, de Pinho RT, Antas PR, Mengel J. 2015 Immunity and immune modulation in *Trypanosoma cruzi* infection. *Pathog. Dis.* **73**, ftv082. (doi: 10.1093/femspd/ftv082).
8. Tarleton RL. 2015 CD8+ T cells in *Trypanosoma cruzi* infection. *Semin. Immunopath.* **37**, 233-238. (doi: 10.1007/s00281-015-0481-9).
9. Bonney KM, Luthringer DJ, Kim SA, Garg NJ, Engman DM. 2019 Pathology and pathogenesis of Chagas heart disease. *Annu. Rev. Pathol.* **14**, 421-447. (doi: 10.1146/annurev-pathol-020117-043711).
10. Martinez SJ, Romano PS, Engman DM. 2020 Precision health for Chagas disease: Integrating parasite and host factors to predict outcome of infection and response to therapy. *Front. Cell. Infect. Microbiol.* **10**, 210. (doi: 10.3389/fcimb.2020.00210).
11. Pack AD, Collins MH, Rosenberg CS, Tarleton RL. 2018 Highly competent, non-exhausted CD8+ T cells continue to tightly control pathogen load throughout chronic *Trypanosoma cruzi* infection. *PLoS Pathog.* **14**, e1007410. (doi: 10.1371/journal.ppat.1007410).
12. Gaspar L *et al*. 2015 Current and future chemotherapy for Chagas disease. *Curr. Med. Chem.* **22**, 4293-4312. (doi: 10.2174/0929867322666151015120804).
13. Sánchez-Valdéz FJ, Padilla A, Wang W, Orr D, Tarleton RL. 2018 Spontaneous dormancy protects *Trypanosoma cruzi* during extended drug exposure. *Elife* **7**, e34039. (doi: 10.7554/eLife.34039).
14. Krishnan A *et al*. 2020 Functional and computational genomics reveal unprecedented flexibility in stage-specific *Toxoplasma* metabolism. *Cell Host Microbe* **27**, 290-306. (doi: 10.1016/j.chom.2020.01.002).
15. Fisher RA, Gollan B, Helaine S. 2017 Persistent bacterial infections and persister cells. *Nat. Rev. Microbiol.* **15**, 453-464. (doi: 10.1038/nrmicro.2017.42).
16. Gollan B, Grabe G, Michaux C, Helaine S. 2019 Bacterial persisters and infection: past, present, and progressing. *Ann. Rev. Microbiol*. **73**, 359-385. (doi: 10.1146/annurev-micro-020518-115650).
17. Waldman BS, Schwarz D, Wadsworth MH, Saeij JP, Shalek AK, Lourido S. 2020 Identification of a master regulator of differentiation in *Toxoplasma*. *Cell* **180**, 359–372.e16. (doi: 10.1016/j.cell.2019.12.013).
18. Tegazzini D, Díaz R, Aguilar F, Peña I, Presa JL, Yardley V, Martin JJ, Coteron JM, Croft SL, Cantizani J. 2016 A replicative *in vitro* assay for drug discovery against *Leishmania donovani*. *Antimicrob. Agents Chemother.* **60**, 3524-3532. (doi: 10.1128/AAC.01781-15).
19. Kloehn J, Saunders EC, O'Callaghan S, Dagley MJ, McConville MJ. 2015 Characterization of metabolically quiescent *Leishmania* parasites in murine lesions using heavy water labeling. *PLoS Pathog.* **11**, e1004683. (doi: 10.1371/journal.ppat.1004683.

20. Mandell MA, Beverley SM. 2017 Continual renewal and replication of persistent *Leishmania major* parasites in concomitantly immune hosts. *Proc. Natl. Acad. Sci. USA* **114**, E801–E810. (doi: 10.1073/pnas.1619265114).
21. Tucker MS, Mutka T, Sparks K, Patel J, Kyle DE. 2012 Phenotypic and genotypic analysis of *in vitro*-selected artemisinin-resistant progeny of *Plasmodium falciparum*. *Antimicrob. Agents Chemother.* **56**, 302–314. (doi: 10.1128/AAC.05540-11).
22. Teuscher F, Chen N, Kyle DE, Gatton ML, Cheng Q. 2012 Phenotypic changes in artemisinin-resistant *Plasmodium falciparum* lines *in vitro*: evidence for decreased sensitivity to dormancy and growth inhibition. *Antimicrob. Agents Chemother.* **56**, 428-431. (doi: 10.1128/AAC.05456-11).
23. Lanz MC, Dibitetto D, Smolka MB. 2019 DNA damage kinase signaling: Checkpoint and repair at 30 years. *EMBO J.* **38**, e101801. (doi: 10.15252/embj.2019101801).
24. Verma N, Franchitto M, Zonfrilli A, Cialfi S, Palermo R, Talora C. 2019 DNA damage stress: Cui prodest? *Int. J. Mol. Sci.* **20**, 1073. (doi: 10.3390/ijms20051073).
25. Silvester E, McWilliam KR, Matthews KR. 2017 The cytological events and molecular control of life cycle development of *Trypanosoma brucei* in the mammalian bloodstream. *Pathogens* **6**, 29. (doi: 10.3390/pathogens6030029).
26. Dumoulin PC, Burleigh BA. 2018 Stress-induced proliferation and cell cycle plasticity of intracellular *Trypanosoma cruzi* amastigotes. *mBio* **9**, e00673-18. (doi: 10.1128/mBio.00673-18).
27. Lewis MD, Fortes Francisco A, Taylor MC, Burrell-Saward H, McLatchie AP, Miles MA, Kelly JM. 2014 Bioluminescence imaging of chronic *Trypanosoma cruzi* infections reveals tissue-specific parasite dynamics and heart disease in the absence of locally persistent infection. *Cell. Microbiol.* **16**,1285-1300. (doi: 10.1111/cmi.12297).
28. Costa FC *et al*. 2018 Expanding the toolbox for *Trypanosoma cruzi*: A parasite line incorporating a bioluminescence-fluorescence dual reporter and streamlined CRISPR/Cas9 functionality for rapid *in vivo* localisation and phenotyping. *PLoS Negl. Trop. Dis.* **12**, e0006388. (doi: 10.1371/journal.pntd.0006388.
29. Ward AI, Lewis MD, Khan A, McCann CJ, Francisco AF, Jayawardhana S, Taylor MC, Kelly JM. 2020 *In vivo* analysis of *Trypanosoma cruzi* persistence foci in chronically infected mice at single cell resolution. *mBio* **11**, e01242-20. (doi: 10.1128/mBio.01242-20).
30. Lewis MD, Fortes Francisco A, Taylor MC, Jayawardhana S, Kelly JM. 2016 Host and parasite genetics shape a link between *Trypanosoma cruzi* infection dynamics and chronic cardiomyopathy. *Cell. Microbiol.* **18**, 1429-1443. (doi: 10.1111/cmi.12584).
31. Taylor MC, Ward A, Olmo F, Jayawardhana S, Francisco AF, Lewis MD, Kelly JM. 2020 Intracellular DNA replication and differentiation of *Trypanosoma cruzi* is asynchronous within individual host cells *in vivo* at all stages of infection. *PLoS Negl. Trop. Dis.* **14**, e0008007. (doi: 10.1371/journal.pntd.0008007).
32. Lewis MD, Fortes Francisco A, Taylor MC, Kelly JM. 2015 A new experimental model for assessing drug efficacy against *Trypanosoma cruzi* infection based on highly sensitive *in vivo* imaging. *J. Biomol. Screening.* **20**, 36-43. (doi: 10.1177/1087057114552623).
33. Taylor MC, Francisco AF, Jayawardhana S, Mann GS, Ward A, Olmo F, Lewis MD, Kelly JM. 2019 Exploiting genetically modified dual-reporter strains to monitor experimental *Trypanosoma cruzi* infections and host:parasite interactions. Karina Andrea Go´ mez and Carlos Andres Buscaglia (eds.), *T. cruzi* Infection: Methods and Protocols, *Methods Molec. Biol.* **1955**,147-163. (doi: 10.1007/978-1-4939-9148-8_11).
34. Filby A, Begum J, Jalal M, Day W. 2015 Appraising the suitability of succinimidyl and lipophilic fluorescent dyes to track proliferation in non-quiescent cells by dye dilution. *Methods* **82**, 29-37. (doi: 10.1016/j.ymeth.2015.02.016).
35. Lacy Kamm J, Parlane NA, Riley CB, Gee EK, Roberts JM, McIlwraith CW. 2020 CellTrace Violet™ inhibits equine lymphocyte proliferation. *Vet. Immunol. Immunopathol.* **223**, 110037. (doi: 10.1016/j.vetimm.2020.110037).
36. Kohlmeier F, Maya-Mendoza A, Jackson DA. 2013 EdU induces DNA damage response and cell death in mESC in culture. *Chromosome Res*. **21**, 87-100. (doi: 10.1007/s10577-013-9340-5).
37. Zhao H, Halicka HD, Li J, Biela E, Berniak K, Dobrucki J, Darzynkiewicz Z. 2013 DNA damage signaling, impairment of cell cycle progression, and apoptosis triggered by 5-ethynyl-2'-deoxyuridine incorporated into DNA. *Cytometry A* **83**, 979-988. (doi: 10.1002/cyto.a.22396).
38. Ligasová A, Strunin D, Friedecký D, Adam T, Koberna K. 2015 A fatal combination: a thymidylate synthase inhibitor with DNA damaging activity. *PLoS One* **10**, e0117459. (doi: 10.1371/journal.pone.0117459).

39. Pereira PD, Serra-Caetano A, Cabrita M, Bekman E, Braga J, Rino J, Santus R, Filipe PL, Sousa AE, Ferreira JA. 2017 Quantification of cell cycle kinetics by EdU (5-ethynyl-2'-deoxyuridine)-coupled-fluorescence-intensity analysis. *Oncotarget* **8**, 40514-40532. (doi: 10.18632/oncotarget.17121).
40. Sykes ML, Hilko DH, Kung LI, Poulsen SA, Avery VM. 2020 Investigation of pyrimidine nucleoside analogues as chemical probes to assess compound effects on the proliferation of *Trypanosoma cruzi* intracellular parasites. *PLoS Negl. Trop. Dis.* **14**, e0008068. (doi: 10.1371/journal.pntd.0008068).
41. Mandyam CD, Harburg GC, Eisch AJ. 2007 Determination of key aspects of precursor cell proliferation, cell cycle length and kinetics in the adult mouse subgranular zone. *Neuroscience* **146**, 108–122. (doi: 10.1016/j.neuroscience.2006.12.064).
42. Kiel MJ, He S, Ashkenazi R, Gentry SN, Teta M, Kushner JA, Jackson TL, Morrison SJ. 2007 Haematopoietic stem cells do not asymmetrically segregate chromosomes or retain BrdU. *Nature* **449**, 238-242. (doi: 10.1038/nature06115).
43. Ganusov VV, De Boer RJ. 2013 A mechanistic model for bromodeoxyuridine dilution naturally explains labelling data of self-renewing T cell populations. *J. R. Soc. Interface* **10**, 20120617. (doi: 10.1098/rsif.2012.0617).
44. Wright MC, Logan GJ, Bolock AM, Kubicki AC, Hemphill JA, Sanders TA, Maricich SM. 2017 Merkel cells are long-lived cells whose production is stimulated by skin injury. *Dev. Biol.* **422**, 4-13. (doi: 10.1016/j.ydbio.2016.12.020)**.**
45. Bielak-Zmijewska A, Mosieniak G, Sikora E. 2018 Is DNA damage indispensable for stress-induced senescence? *Mech. Ageing Dev.* **170**, 13-21. (doi: 10.1016/j.mad.2017.08.004).
46. Prokhorova EA, Egorshina AY, Zhivotovsky B, Kopeina GS. 2020 The DNA-damage response and nuclear events as regulators of nonapoptotic forms of cell death. *Oncogene* **39**, 1-16. (doi: 10.1038/s41388-019-0980-6).
47. Resende BC *et al*. 2020 The influence of recombinational processes to induce dormancy in *Trypanosoma cruzi**. Front. Cell. Infect. Microbiol.* **10**, 5. (doi: 10.3389/fcimb.2020.00005).
48. Rajão MA *et al*. 2014 Unveiling benznidazole's mechanism of action through overexpression of DNA repair proteins in *Trypanosoma cruzi*. *Environ. Mol. Mutagen.* **55**, 309-321. (doi: 10.1002/em.21839).
49. Campos MC, Phelan J, Francisco AF, Taylor MC, Lewis MD, Pain A, Clark TG, Kelly JM. 2017 Genome-wide mutagenesis and multi-drug resistance in American trypanosomes induced by the front-line drug benznidazole. *Sci. Rep.* **7**, 14407. (doi: 10.1038/s41598-017-14986-6).

Funding.

This work was supported by UK Medical Research Council (MRC) Grant MR/T015969/1 to JMK and MRC LID (DTP) Studentship MR/N013638/1 to AIW.

Author contributions.

AIW carried out laboratory work, imaging procedures and data analysis, and contributed to the design of the study and drafting of the manuscript. FO and RA carried out laboratory work and critically reviewed the manuscript. MCT contributed to study design and data analysis, and critically reviewed the manuscript. JMK contributed to study design and data analysis, and drafted the manuscript. All authors gave final approval for publication and agree to be held accountable for the work performed therein.

5.10 Chapter summary

The current debate concerning the existence of dormancy in *T. cruzi*, and its significance in clinical treatment failure, could be improved by a consensus on language. At present, the literature on this topic for the protozoal pathogens uses the terms ‘persister’, ‘dormant’ and ‘quiescent’ interchangeably. These terms are applied to the full range of slow replicative states, from sub-optimal growth due to reduced access to nutrients, to the genetic programme initiated in *T. gondii* by BFD1 leading to a near complete cell-cycle shutdown. A consensus on which terms apply in which situation is urgently required to allow clearer discussion between researchers involved in the subject across multiple human pathogens.

There are potential flaws in the interpretation of the data presented by the paper ascribing ‘spontaneous dormancy’ in *T. cruzi*. As outlined above, these relate to the growth inhibitory properties of the tracker dye CellTrace Violet (CTV) and to the cell cycle arrest that can be induced by exposing parasites to EdU at high concentrations for long periods. The collective interpretation derived from all the data published on this topic is best described as being consistent with a general slow-down in parasite growth rate post-deployment of adaptive effectors. A definitive ‘dormant’ life-cycle stage remains speculative. The contribution that this metabolic slow-down makes to treatment failure is unknown. Replication kinetics will certainly have an impact on drug treatment outcomes, although its importance remains to be determined. Despite the slower rate of parasite replication during chronic stage infection in the colon, and the potential for ‘herd-protection’ within mega-nests (Taylor *et al* 2020, see Appendix 1), it appears that infections are easier to clear in the chronic rather than acute stage (see chapter 1, Drugs and Clinical Trials). Whilst this may simply reflect parasite numbers, reaching a satisfactory answer to why this is the case will be a key next step in establishing the influence of replication kinetics on treatment outcomes. New models, in which replication status can be assessed without the incorporation of synthetic nucleotides or cytotoxic tracker dyes are essential.

Chapter 6 – A hypothesis to explain life-long persistence of *Trypanosoma cruzi* infection

6.1 Immune evasion strategies and chronicity of infection with eukaryotic pathogens

T. cruzi infection, leads to chronic, often life-long, persistence in both mice and humans. As outlined in Chapter 2, in contrast to other protozoal human pathogens (below), the mechanisms of immune evasion that allow *T. cruzi* persistence have not been well established. Here, I will briefly review progress in understanding mechanisms of infection persistence in some of the better understood examples: *Leishmania major* (in mice and humans), *Trypanosoma brucei* species (in mice and humans) and *Plasmodium falciparum* (in humans).

6.2 *Leishmania major* and the phenotype of the adaptive response

Contact with the innate immune system and occupation of the macrophage – The interaction between mice, which act as natural hosts, and *L. major* has been well investigated[1]. Inoculation of all hosts takes place via the bite of the sand fly vector into the skin. PAMP/DAMP promoted expression of inflammatory chemokines recruit circulating monocytes into the tissue[2,3]. Phagocytosis of parasites by macrophages and dendritic cells (D.C.) allows occupation of the phagolysosomal compartment by replication competent amastigotes. Down regulation of ROS/RNS producing pathways[4,5] and up-regulation of anti-oxidant defences[6] prevents parasite destruction. In SCID mice, that lack functional T-cells, *L. major* replication is uncontrolled, with animals reproducibly succumbing to disseminated infection of macrophages in the spleen, liver, lymph nodes and skin[7].

Resistance is based on deployment of IFN-γ+ CD4+ Th1 T-cells – In the majority of human infections (WHO, 2020), and those of most immunocompetent inbred mouse strains[7], parasite numbers are controlled, and the associated skin lesions are resolved. In these cases, activation of naïve CD4+ T-cells in the lymph nodes draining the skin takes place in the presence of a cocktail of cytokines generated by innate recognition, principally IL-12[8], with TNF-α, IL-1α, IL-18 and IFN-α/β important in some models[9,10]. This inflammatory environment and recognition of *L. major* antigen by clonal TCRs polarises the developing CD4+ helper cells towards the pro-inflammatory Th1 phenotype capable of high-level IFN-γ expression[11]. Deployment of these Th1 antigen-specific T-cells to the lesion[12] provides high local concentrations of IFN-γ, prompting macrophages to up-regulate the expression of ROS/NOS[4]. This overrides the modulation of the phagocytes by

L. major and results in the destruction of most parasites[13]. Backed up by human data[14], promotion of this pathway is the goal of prospective vaccine candidates[15].

Th2 T-cells and IL-10 in susceptibility – While the pathways of protective immunity have been well established, the alternative pathways that lead to susceptibility continue to be debated. Initially it was thought that susceptible mouse strains activated T cells under the polarising effect of IL-4[16]. This cytokine suppresses Th1 polarisation and promotes the antagonistic Th2 phenotype. IL-4 is secreted by naïve T-cells after relatively weak recognition of specific *L. major* antigens[17]. However, early and transient IL-4 expression also takes place in resistant animals[18]. The lack of suppression of IL-4 synthesis, rather than lack of its induction, is now considered the main determinant of poor parasite control. Differences in expression of IL-12[9], the major Th1 polarising cytokine, the kinetics of early parasite dissemination[1] and higher expression of anti-inflammatory IL-10[19] have all been suggested as mechanistic explanations. Depletion of IL-10 in resistant models has been shown to generate a sterile outcome, rather than canonical low-level persistence in the skin[20].

6.3 *Trypanosoma brucei* and perpetual antigen switching

Parasite outgrowth in the blood stream – Inoculation with *Trypanosoma brucei* occurs via the bite of the teste fly vector. Unlike most other protozoal pathogens of man, *T. brucei* exists as an extracellular parasite in the blood stream and tissue fluids of the solid organs. Non-canonical enzymatic cleavage of complement components[21] and molecular counters to innate trypanolytic factors[22], at least in the human infective species, prevent innate clearance. SCID mice universally succumb to uncontrolled infections[23].

α-VSG (variable surface glycoprotein) antibody mediated clearance of infection – The *T. brucei* genome is organised into 11 pairs of megabase chromosomes and 50-100 mini-chromosomes. The internal regions of the megabase chromosomes contain the conserved core housekeeping genes, while the subtelomeric domains and the mini-chromosomes contain ~2500 copies of the highly polymorphic, surface expressed, VSG genes and pseudogenes[24]. At any one time, a single VSG gene is expressed mono-allelically and forms a layer of ~10^7 protein molecules arranged as dimers, covering the entire plasma membrane of the trypomastigote. The most immunodominant B-cell epitopes on the intact parasite are on the hyper-variable loops at N-terminus of the VSG molecule[25]. Recognition of these leads to the production of IgM and later IgG[26] against the specific VSG type. Rapid turnover of the VSG coat, and any bound antibody, through the endocytic pathway ensures that elimination of parasites only occurs when a high concentration of anti-VSG antibody is achieved[27]. Once this threshold titre is reached, efficient

opsonisation of parasites and phagocytosis via FcγR on splenic macrophages rapidly clears infection[28]. The centrality of VSG-specific antibody in the control of *T. brucei* infection is demonstrated by the infection of B-cell deficient mice[29], which mirror the SCID model in outcome.

VSG genetic switch and chronic infection – The strict expression of only a single VSG variant and the stochastic genetic switching of this highly expressed antigen promotes *T. brucei* persistence in its host. A switch in the VSG gene expressed takes place at a frequency of 10^{-2} – 10^{-6} per generation[30], and is sufficient to outpace the generation of antibody against the new coat. This stochastic switch is accomplished through the genomic architecture of the ~15 blood stream VSG expression sites in the telomeres. Homology of the DNA sequence surrounding the VSG genes (5' 70bp repeats and conserved elements in the 3' untranslated regions) promotes homologous recombination[31]. Exchange of the VSG coding sequence results in the rapid replacement of the surface coat. In addition, during S-phase DNA replication the molecular machinery responsible for high-level expression can switch between the available expression sites providing a new VSG coat in the absence of DNA rearrangement. The precise details of how this is achieved is still being resolved[32]. Later in infection segmental recombination allows the use of information encoded in pseudogenes to generate entirely novel VSG sequences, thus ensuring the repertoire is much greater than the number of intact VSG genes in any single parasite[33].

6.4 *Plasmodium falciparum*, a complex persistent parasite

Limits of natural pre-erythrocytic immunity – Infective *P. falciparum* sporozoites are deposited in the skin during blood feeding by female *Anopheles* mosquitos. Surface expressed circumsporozoite protein (CSP) prevents complement mediated lysis[34] and, after circulatory dissemination, interacts with hepatocytes in the liver promoting cellular invasion[35]. Replication within the liver amplifies *P. falciparum* numbers ~10,000-fold per invaded hepatocyte[36], releasing merozoites into the blood stream after 6-7 days. During natural infections, these pre-erythrocytic stages are poorly immunogenic, with low numbers of infecting parasites and the relatively short time periods in which they exist extracellularly suggested as explanations[37]. The protection generated by the only licenced malaria vaccine (RTS,S) is mediated through the induction of antibodies against CSP[38]. Protection is incomplete and short lived, due to the decline in the serum titre of these antibodies over the months following vaccination[39]. Significant effort has, and continues to, go into vaccine candidates that promote antibody targeting the sporozoite, CD4+ promotion of Kupfer cell (liver resident) phagocytosis and CD8+ cytotoxicity against infected hepatocytes[40]. At present a sterilising pre-erythrocytic vaccine offering long-term protection (years) does not exist.

Suppression of blood-stage infection and natural immunity –The major target of the host response is the blood-stage infection, which is responsible for the pathology of malaria. During this stage replication via schizogony takes place in the erythrocyte, amplifying parasite numbers ~24-fold in each infected cell. Immunogenic exposure of parasite antigens expressed and exported to the erythrocyte surface takes place during the 48hrs replication cycle. Egress of merozoites and re-invasion of new host cells is rapid (seconds), briefly exposing large numbers of parasite antigens to host serum. At higher densities of blood parasite load, merozoite invasion leads to cell-cycle arrest and differentiation into the gametocyte. Up-take of this life-cycle stage by a mosquito in a blood meal completes the parasites life-cycle. Gametocyte specific antigen, even those expressed on the RBC surface are poorly immunogenic, and are increasingly the focus of transmission blocking vaccine candidates[41]. Immunity to severe disease is acquired rapidly, even after a single infection[42]. Immunity to clinical disease is usually acquired by age 5[43] and increasingly effective suppression of blood parasite density, and even sterility, are possible in older cohorts[44]. Defining the adaptive mechanisms behind this natural resistance at the molecular level remains an urgent priority[45].

Multiple strategies of immune evasion by blood-stage *P. falciparum* – Splenic *P. falciparum* specific CD4+ Th1 T-cells secreting IFN-γ activate local macrophages and are required for optimal suppression of parasite loads[46]. Preventing passage of infected erythrocytes through this organ is a major persistence promoting mechanism. Parasite encoded erythrocyte surface structures, centred on the PfEMP-1 molecule, are required for attachment to endothelial receptors in the brain, bone marrow and for a single PfEMP-1 variant, the placenta[47]. Other erythrocyte surface parasite encoded products have been confirmed to mimic the action of the immune checkpoints of the host[48], potentially accounting for the observed immunosuppression associated with malaria infection[49]. Antibodies reactive against erythrocyte surface antigens are a major focus of the host response and are required for natural immunity, with PfEMP-1 the best characterized[50]. This protein is encoded by the multicopy (~60 per nucleus) var gene family, mostly found within heterochromatin at the chromosome telomeres[51]. The stochastic expression of a single gene is strictly maintained, with transcriptional switching occurring in ~2% of parasites per generation[52]. *Var* gene polymorphism is further increased through genetic recombination events during mitosis[53] in the human host and meiosis[54] in the mosquito. Similar mechanisms vary the other erythrocyte surface exposed antigens, such as STEVORs and RIFINs[55]. Natural immunity is thought to be the result of exposure, and generation of antibodies to, the wide variety of variable antigens present in the local circulating *P. falciparum* parasites in a certain region. The limit to the diversity of these antigens is likely imposed by the structural requirements to maintain the ability to bind to host endothelial ligands. Natural immunity is not maintained on movement between geographically

distant endemic areas[56], which is hypothesised to be due to differences in circulating variable antigens between clones in these regions.

6.5 *Trypanosoma cruzi*, persistence alongside the systemic correlates of protection

Unlike experimental *L. major* infection, *T. cruzi* inoculation results in a protective Th1 response centred on CD8+ IFN-γ+ T-cells in all immunocompetent murine models analysed. A mechanism of antigenic switching analogous to *T. brucei* has not been demonstrated, and unlike *P. falciparum*, primary infection can lead to long-term immunity to secondary parasitaemia, even if the initial challenge is drug-cured[57]. The rationale for the work presented in the manuscript below was to exploit the CL Luc::mNeonGreen reporter and tissue processing methodology developed for the earlier chapters to characterise the ‘hyper-local’ immunological environment of persistent parasites. The data generated would better allow us to understand how *T. cruzi* is able to evade such an effective adaptive response to persist long-term in its host.

References

Leishmania major

1. Sacks, D. and Noben-Trauth, N. The immunology of susceptibility and resistance to *Leishmania major* in mice. *Nat. Rev. Immunol*. **2**, 845-858 (2002).
2. Matte, C. and Olivier, M. *Leishmania* – Induced cellular recruitment during the early inflammatory response: modulation of proinflammatory mediators. *J. of Infect. Dis*. **185**, 773-681 (2002).
3. de Menezes, L. P., Saraiva, E. M. and Rocha-Azevedo, B. The site of the bite: *Leishmania* interaction with macrophages, neutrophils and the extracellular matrix in the dermis. *Parasites and Vectors*. **9**, e264 (2016).
4. Horta, M. F. et al. Reactive oxygen species and nitric oxide in cutaneous leishmaniasis. *J. of Parasitol. Res*. **2012**, e203818 (2012).
5. Muxel, S. M. et al. Arginine and polyamines fate in *Leishmania* infection. *Front. Microbiol*. **8**, e2682 (2017).
6. Jasion, V. S. and Poulos, T. L. *Leishmania major* peroxidase is a cytochrome c peroxidase. *Biochemistry*. **51**, 2453-60 (2012).
7. Seydel, K. B. and Stanley, S. L. SCID mice and the study of parasitic disease. *Clinic. Microbiol. Rev*. **9**, 126-134 (1996).
8. Anderson, C. F., Mendez, S. and Sacks, D. L. Non-healing infection despite Th1 polarization produced by a strain of *Leishmania major* in C57BL/6 mice. *J. of Immunol*. **174**, 2934-2941 (2005).
9. Park, A. Y., Hondowicz, B., Kopf, M. and Scott, P. The role of IL-12 in maintaining resistance to *Leishmania major*. *J. of Immunol*. **168**, 5771-5777 (2002).
10. Stebuit, E. et al. Interleukin 1α promotes Th1 differentiation and inhibits disease progression in *Leishmania major*-susceptible BALB/ mice. *J. Exp. Med*. **198**, 191-199 (2003).
11. Rogers, K. A., Gergory, K. D., Mbow, M. L., Gillespie, R. D., Brodskyn, C. I. and Titus, R. G. Type 1 and type 2 responses to Leishmania major. *FEMS Microbiol. Letters*. **209**, 1-7 (2002).
12. Malherbe, L. et al. Selective activation and expansion of high-affinity CD4+ T-cells in resistant mice upon infection with *Leishmania major*. 13, 771-782 (2000).
13. Glennie, N. D., Volk, S. W. and Scott, P. Skin-resident CD4+ T cells protect against *Leishmania major* by recruiting and activating inflammatory monocytes. *PLOS Neg. Trop. Dis*. **13**, e1006349 (2017).

14. Mandella, A. and Beverley, S. M. Continual renewal and replication of persistent *Leishmania major* parasites in concomitantly immune hosts. *PNAS*. **2017**, e801-e810 (2017).
15. Santos, C. and Brodskyn, C. I. The role of CD4+ and CD8+ T cells in human cutaneous leishmaniasis. *Front. Public Health*. **2**, e165 (2014).
16. Biedermann, T. et al. IL-4 instructs Th1 responses and resistance to Leishmania major in susceptible BALB/c mice. *Nat. Immunol*. **2**, 1054-60 (2001).
17. Fernandez, L. et al. Antigenicity of *Leishmania*-activated C-kinase antigen (LACK) in human peripheral blood mononuclear cells, and protective effect of prime-booth vaccination with pCl-neo-LACK plus attenuated LACK-expressing *vaccina* viruses in hamsters. *Front. Immunol*. **9**, e843 (2018).
18. Scott, P., Eaton, A., Gause, W. C., Zhou, X. and Hondowicz, B. Early IL-4 production does not predict susceptibility to *Leishmania major*. *Exp. Parasitol*. **84**, 178-87 (1996).
19. Kane, M. M. and Mosser, D. M. The role of IL-10 in promoting disease progression in leishmaniasis. *J. Immunol*. **166**, 1141-7 (2001).
20. Belkaid, Y. et al. The role of Interleukin (IL-)-10 in the persistence of *Leishmania major* in the skin after healing and therapeutic potential of anti-IL-10 receptor antibody for sterile cure. *J. Exp. Med*. **184**, 1497-1506 (2001).

***Trypanosoma brucei* species**

21. Macleod, O. J. et al. A receptor for the complement regulator factor H increases transmission of trypanosomes to tsetse flies. *Nat. commun*. **11**, e1326 (2020).
22. Thomson, R. and Finkelstein, A. Human trypanolytic factor APOL1 forms pH-gated cation-selective channels in planar lipid bilayers: relevance to trypanosome lysis. *PNAS*. **112**, 2894-2899 (2015).
23. Inoue, N., Narumi, D., Mbati, P. A., Hirumi, K., Situakibanza, N. T. and Hirumi, H. Susceptibility of severe combined immune-deficient (SCID) mice to *Trypanosoma brucei gambiense* and *T. b. rhodesiense*. *Trop. Med. Int. Health*. **3**, 408-12 (1998).
24. Berriman, M. et al. The genome of the African trypanosome *Trypanosoma brucei*. *Science*. **309**, 416-22 (2005).
25. Schwede, A., Macleod, O. J., MacGregor, P. and Carrington, M. How does the VSG coat of bloodstream from African trypanosomes interact with external proteins? *PLOS Path*. **11**, e1005259 (2015).
26. Magez, S. et al. The role of B-cells and IgM antibodies in parasitaemia, anaemia, and VSG switching in *Trypanosoma brucei*-infected mice. *PLOS Path*. **8**, e1000122 (2008).

27. Pinger, J., Chowdhury, S. and Papavasiliou, F. N. Variant surface glycoprotein density defines an immune evasion threshold for African trypanosomes undergoing antigenic variation. *Nat. Commun*. **8**, e828 (2017).
28. Ponte-Sucre, A. An overview of *Trypanosoma brucei* infection: an intense host-parasite interaction. *Front. Microbiol*. **7**, e2126 (2016).
29. Campbell, G. H. and Weinbaum, F. I. *Trypanosoma rhodesiense* infection in B-cell-deficient mice. *mBio*. **18**, 434-438 (1977).
30. McWilliams, K. R. et al. Developmental competence and antigen switch frequency can be uncoupled in *Trypanosoma brucei*. *PNAS*. **116**, 22774–22782 (2019).
31. Berriman, M. et al. The architecture of variant surface glycoprotein gene expression sites in *Trypanosoma brucei*. *Mol. Biochem. Parasitol*. **122**, 131-40 (2002).
32. Faria, J., Glover, L., Hutchinson, S., Boehm, C., Field, M. C. and Horn, D. Monoallelic expression and epigenetic inheritance sustained by a *Trypanosoma brucei* variant surface glycoprotein exclusion complex. *Nat. Coummun*. **10**, e2023 (2019).
33. Pereira, S. S. et al. Variant antigen diversity in *Trypanosoma vivax* is not driven by recombination. *Nat. commun*. **11**, e844 (2020).

Plasmodium falciparum

34. Kiyuka, P. K., Meri, S. and Khattab, A. Complement in malaria: immune evasion strategies and role in protective immunity. *FEBS Lett*. **594**, 2502-2517 (2020).
35. Vacca, I. New insights into *Plasmodium* hepatocyte entry*. Nat. Rev. Microbiol*. **15**, e382 (2017).
36. Matthews, H., Duffy, C. W. and Merrick, C. J. Checks and balances? DNA replication and the cell cycle in *Plasmodium*. *Parasit. Vectors*. **11**, e216 (2018).
37. Gomes, P. S., Bhardwai, J., Rivera-Correa, J., Freire-de-Lima, C. Morrot, A. Immune escape strategies of malaria parasites. *Front. Microbiol*. **7**, e1617 (2016).
38. RTS,S randomised controlled trial. *Lancet* https://doi.org/10.1016/S0140-6736(15)60721-8
39. Sanchez, L. et al. Antibody responses to the RTS,S/AS01 vaccine and *Plasmodium falciparum* antigens after a booster dose within the phase 3 trial in Mozambique. *NPJ vaccines*. **5**, e46 (2020).
40. Molina-Franky, J. et al. *Plasmodium falciparum* pre-erythrocytic stage vaccine development. *Malaria J*. **19**, e56 (2020).

41. Acquah, F. K., Kim, J. A., Williamson, K. C. and Amoah, L. E. Transmission-blocking vaccines: old friends and new prospects. *mBio*. **87**, e00775-18 (2019).
42. Griffin, J. T. et al. Gradual acquisition of immunity to severe malaria with increasing exposure. *Proc. Biol. Sci*. **282**, 2014-2657 (2015).
43. Doolan, D. L., Dobano, C. and Baird, J. K. Acquired immunity to malaria. *Clin. Microbiol*. **22**, 13-36 (2009).
44. Ashley, E. A. and White, N. J. The duration of *Plasmodium falciparum* infections. *Malar. J*. **13**, e500 (2014).
45. Moormann, A. M. and Stewart, V. A. The hunt for protective correlates of immunity to *Plasmodium falciparum* malaria. *BMC Med*. **12**, e134 (2014).
46. Kurup, S. P., Bulter, N. S. and Harty, J. T. T cell mediated immunity to malaria. *Nat. Rev. Immunol*. **19**, 457-471 (2019).
47. Jean-Bernard, L. D. et al. Sequestration of *Plasmodium falciparum*-infected erythrocytes to chondroitin sulfate A, a receptor for maternal malaria: monoclonal antibodies Against the native parasite ligand reveal pan-reactive epitopes in placental isolates. *Blood*. 100, 1478-1483 (2002).
48. Saito, F. et al. Immune evasion of Plasmodium falciparum by RIFIN via inhibitory receptors. Nature. 552, 101-105 (2017).
49. Pradhani, V and Ghosh, K. Immunological imbalances associated with malaria infection. J. Parasit. Dis. 37, 11-15 (2013).
50. Ademolue, T. W. and Awandare, G. A. Evaluating anti-disease immunity to malaria and implications for vaccine design. *Immunology*. **153**, 423-434 (2018).
51. Bunnik, E. M. et al. Comparative 3D genome organization in apicomplexan parasites. *PNAS*. **116**, 3183-3192 (2019).
52. Guizetti, J. and Scherf, A. Silence, activate, poise and switch! Mechanisms of antigenic variation in *Plasmodium falciparum*. *Cell Microbiol*. **15**, 718-726 (2013).
53. Claessens, A. et al. Generation of antigenic diversity in *Plasmodium falciparum* by structured rearrangement of Var genes during mitosis. *PLOS Genet*. **10**, e1004812 (2014).
54. Kyes. S. A., Kraemer, S. M. and Smith, J. D. Antigenic variation in *Plasmodium falciparum*: gene organization and regulation of the *var* multigene family. *mBio*. **6**, 1511–1520 (2007).
55. Araujo, R. B. et al. Independent regulation of *Plasmodium falciparum* rif gene promotors. *Sci. Reports*. **8**, e9332 (2018).
56. Kraemer, S. M. et al. Patterns of gene recombination shape var gene repertoires in *Plasmodium falciparum*: comparisons of geographically diverse isolates. *BMC Genomics*. **8**, e45 (2007).

57. Gurdip, S. M. et al. Drug-cured experimental *Trypanosoma cruzi* infections confer long-lasting and cross-strain protection. *PLOS Neg. Trop. Dis*. **14**, e0007717 (2020).

6.6 –

London School of Hygiene & Tropical Medicine
Keppel Street, London WC1E 7HT

T: +44 (0)20 7299 4646
F: +44 (0)20 7299 4656
www.lshtm.ac.uk

RESEARCH PAPER COVER SHEET

Please note that a cover sheet must be completed for each research paper included within a thesis.

SECTION A – Student Details

Student ID Number	lsh1406159	**Title**	Mr
First Name(s)	Alexander		
Surname/Family Name	Ward		
Thesis Title	Trypanosoma cruzi: Where is it? Does it ever sleep? and why are infections almost always life-long?		
Primary Supervisor	John Kelly		

If the Research Paper has previously been published please complete Section B, if not please move to Section C.

SECTION B – Paper already published

Where was the work published?			
When was the work published?			
If the work was published prior to registration for your research degree, give a brief rationale for its inclusion			
Have you retained the copyright for the work?*	Choose an item.	Was the work subject to academic peer review?	Choose an item.

*If yes, please attach evidence of retention. If no, or if the work is being included in its published format, please attach evidence of permission from the copyright holder (publisher or other author) to include this work.

SECTION C – Prepared for publication, but not yet published

Where is the work intended to be published?	Nature Communications
Please list the paper's authors in the intended authorship order:	Alexander I. Ward., Micheal D. Lewis., Martin C. Taylor and John M. Kelly
Stage of publication	**Submitted**

SECTION D – Multi-authored work

For multi-authored work, give full details of your role in the research included in the paper and in the preparation of the paper. (Attach a further sheet if necessary)	I completed collection of all the data in this manuscript and provided the first draft to John Kelly, who completed the final edit.

SECTION E

Student Signature	Alexander Ward
Date	11/09/2020

Supervisor Signature	John Kelly
Date	27/10/2020

See ** for the on-line version on (bioRxiv).

Incomplete recruitment of protective T-cells facilitates *Trypanosoma cruzi* persistence in the mouse colon

Alexander I. Ward, Michael D. Lewis, Martin C. Taylor and John M. Kelly*

Department of Infection Biology,

London School of Hygiene and Tropical Medicine,

London, UK.

*For correspondence john.kelly@lshtm.ac.uk

Abstract

Trypanosoma cruzi is the etiological agent of Chagas disease. Following T-cell mediated suppression of the acute phase infection, this intracellular eukaryotic pathogen persists in a limited sub-set of tissues at extremely low-levels. The reasons for this tissue-specific chronicity are not understood. Using a dual bioluminescent:fluorescent reporter strain, which allows experimental infections to be imaged at single-cell resolution, we have characterised the 'hyper-local' immunological microenvironment of rare parasitized cells in the mouse colon, a key site of persistence. We demonstrate that incomplete recruitment of T-cells to infection foci permits repeated cycles of intracellular parasite replication and differentiation to motile trypomastigotes to occur at a frequency sufficient to perpetuate chronic infections. The life-long persistence of parasites in this immunotolerant site continues despite the presence, at a systemic level, of a highly effective T-cell response. Overcoming this low-level dynamic equilibrium between host and parasite represents a major challenge for vaccine development.

Indroduction

The insect-transmitted protozoan parasite *Trypanosoma cruzi* is the causative agent of Chagas disease, and infects 5-7 million people in Latin America[1]. Despite decades of effort, only limited progress has been made in developing a vaccine, and doubts remain about the feasibility of vaccination as a method of disease control[2,3]. In humans, *T. cruzi* infection passes through an acute stage that lasts 2-8 weeks, during which parasitaemia is readily detectable, although symptoms are generally mild and non-specific. With the induction of the adaptive immune response, in which $CD8^+$ IFN-γ^+ T-cells play a key role[4,5], there is a significant reduction in the parasite burden. However, sterile clearance is not achieved and parasites persist as a chronic life-long infection. One-third of those infected with *T. cruzi* eventually develop Chagasic pathology, although symptoms can take decades to become apparent. Cardiomyopathy is the most common clinical outcome[6-8], followed by digestive tract megasyndromes, which are reported in about 10% of infected individuals, often in parallel with cardiac disease.

Although the innate immune system is able to detect the parasite[9,10], there is a delay in the subsequent induction of an adaptive response relative to other pathogens[5,11]. This, together with a rapid rate of parasite division[12], allows *T. cruzi* to disseminate widely during the acute stage, with most organs and tissues becoming highly infected[13]. The $CD8^+$ T-cell response generated, which predominantly targets a sub-set of immunodominant epitopes in members of the *trans*-sialidase surface antigen family[14,15], is critical for controlling the infection in mice. The parasite burden is reduced by 2-3 orders of magnitude as the disease transitions to a chronic dynamic equilibrium[13]. Understanding why the immune system then fails to eliminate the remaining parasites is a central question in Chagas disease research. This information is crucial to underpin rational vaccine design and immunotherapeutic interventions.

Because of the complexity and long-term nature of Chagas disease in humans, mice have been important experimental models for research on interactions between parasite and host. They display

a similar infection profile to humans, exhibit chronic cardiac pathology, and are widely used in drug and vaccine development[16]. Imaging studies have revealed that the GI tract is a major parasite reservoir during chronic infections and that the degree of containment to this region is determined by both host and parasite genetics[13,17]. Parasites are also frequently detectable in the skin, and in some mouse models, skeletal muscle can be an additional site of persistence[4,18]. In the colon, the most frequently infected cells are myocytes located in the gut wall. However, the extent of infection is low, and in most cases, this entire organ contains only a few hundred parasites, concentrated in a small number of host cells[18]. After transition to the chronic stage, *T. cruzi* also exhibits a reduced proliferation rate at this site, although the cycle of replication, host cell lysis and re-infection appears to continue, with little evidence for wide-spread parasite dormancy[12].

Multiple studies have shown that experimental *T. cruzi* vaccines have protective efficacy and can reduce both parasitaemia and disease severity[19-24]. However, unambiguous evidence of complete parasite elimination after challenge, is lacking. In contrast, drug-cured infections can confer sterile long-lasting protection against re-challenge with a homologous parasite strain[3], although this level of protection was only achieved in ~50% of animals. Re-challenge with a heterologous strain did not result in sterile protection, although there was >99% reduction in the parasite burden. All unprotected animals that displayed re-infection, transitioned to the canonical chronic stage equilibrium and organ distribution, without passing through an elevated acute stage parasitaemia. Once established in permissive sites, such as the GI tract, parasites appear to survive the systemic *T. cruzi*-specific IFN-γ^+ T-cell response generated by the primary challenge. In the absence of information on the immunological micro-environment of these persistent parasites, the reasons for this are unclear. Resolving this question will have a major strategic impact on the development of an effective vaccine.

Progress in this area has been limited by technical difficulties in locating and analysing the rare infection foci in permissive tissue sites, such as the colon. Here, we describe the application of a *T.*

cruzi bioluminescent:fluorescent dual reporter strain and enhanced imaging procedures that have allowed us to show that incomplete 'hyper-local' homing of T-cells to foci of intracellular infection is associated with the ability of the parasite to persist in the colon.

Results

$CD4^+$ and $CD8^+$ T-cells have non-redundant roles in suppression of the colonic parasite load during chronic *T. cruzi* infection. Myocytes in the colonic gut wall are an important site of *T. cruzi* persistence in murine models of chronic Chagas disease. However, infected host cells are extremely rare and unevenly distributed[18]. To assess the role of the cellular immune response in controlling infection in this tissue compartment, we infected C3H/HeN mice with *T. cruzi* CL Luc::mNeon, a parasite line that constitutively expresses a bioluminescent:fluorescent fusion protein[25]. This reporter strain can be used in combination with *ex vivo* imaging and confocal microscopy of peeled whole colonic wall mounts to detect persistent infection foci at single cell resolution (Methods). When infections had reached the chronic stage (>100 days post-infection), one cohort of mice was immunosuppressed with cyclophosphamide, an alkylating agent that is generally suppressive of the lymphocyte population[26], and which has been widely used to drive the relapse of low-level *T. cruzi* infections[27,28]. Treatment led to a reduction in peripheral blood mononuclear cells (PBMCs) close to basal levels within 5-10 days (Fig. 1a, b). In parallel, other groups of mice were subjected to antibody-mediated depletion of the circulating $CD4^+$ or $CD8^+$ T-cell populations. This was achieved, with high specificity, on a similar time-scale (Fig. 1c; Supplementary Fig. 1). Circulating anti-*T. cruzi* serum antibody levels were not significantly altered by cyclophosphamide treatment, or by depletion of the $CD4^+$ or $CD8^+$ T-cell subtypes (Fig. 1d).

Examination of mouse colons by *ex vivo* bioluminescence imaging >12 days after the initiation of treatment, revealed that cyclophosphamide-induced immunosuppression had resulted in wider dissemination and intensity of the infection (Fig. 2a). Further analysis of peeled external gut walls by confocal microscopy (Methods), which allows the full length of the longitudinal and circular

smooth muscle layers of the colon to be assessed at a 3-dimensional level[18], confirmed that there had been a substantial increase in the number of infected cells (Fig. 2b, c, d). Therefore, reduction of the PMBC population perturbs the ability of the immune system to control the proliferation of persistent parasites within the colon. However, specific depletion of either the $CD4^+$ or the $CD8^+$ T-cell repertoires by themselves, did not have a significant effect (Fig. 2d). Furthermore, in the absence of PBMCs, it is implicit from the resulting parasite dissemination that the circulating serum antibodies are unable to suppress the infection during the chronic stage (Fig. 1d).

Parasites persisting in the colon can induce effective hyper-local T-cell recruitment. At any one time, the majority of the parasite population that persists in the colon is found in a small number of 'mega-nests', infected cells that typically contain several hundred replicating amastigotes, or occasionally, differentiated non-dividing trypomastigotes[12]. The remainder of the population is more widely distributed, with considerably lower numbers of parasites per infected cell. To better understand the process of long-term parasite survival, we investigated the cellular microenvironment of persistent infection foci. When infections had advanced to the chronic stage, peeled whole colonic wall mounts were examined by confocal microscopy (Methods), and compared to those of naïve age-matched mice. In non-infected tissue, using DAPI staining to highlight nuclei, an average of 55 host cells were identified in 200 μM diameter circles positioned around randomly selected nuclei within the whole mounted gut wall (Fig. 3a). Most cells had elongated nuclei typical of smooth muscle myocytes. In the infected group, parasitized cells were identified by green fluorescence (Methods). Scanning revealed that total cellularity in the immediate locality of infection foci was similar in most cases to that in non-infected colon tissue; 95% were within 3 x S.D. of the background mean, compared with 98% around randomly selected cells from naïve control regions (Fig. 3a, b). However, in other instances, there was evidence of highly localised cellular infiltration, with 3.4% of infection foci surrounded by a local cellularity that was >4 x S.D. above the background mean. Within these intense infiltrates, host cells with more rounded nuclei predominated. In contrast to the majority of parasitized cells that had not triggered a major response (Fig. 3c), amastigotes in these infiltrates

frequently displayed a morphology that suggested immune-mediated damage, as judged by the diffuse pattern of green fluorescence (compare Fig. 3c, d and e).

We investigated the nature of these cellular infiltrates, by staining whole colon sections from chronically infected mice with specific immune cell markers (Methods). This revealed that leukocytes (as identified by anti-CD45 antibodies) constituted close to 100% of the infiltrate population (Fig. 4a). A major proportion of the recruited cells were also positive when stained with anti-CD3 antibodies, specific markers for the T-cell receptor complex (Fig. 4b, c), with both $CD4^+$ and $CD8^+$ T-cells represented within this population (Fig. 4d). To assess the local density of stained immune cells, we examined 200 μM diameter circular tissue sections centred on each infection focus using Z-stack confocal microscopy. A series of imaged sections starting 5 μm above and 5 μm below the centre of the parasite nest (a total volume of 314 μm^3) were generated, and the number of stained cells in the infection microenvironment determined in 3-dimensions (Supplementary Fig. 2). In sections of colonic smooth muscle from non-infected mice, leukocytes were dispersed and rare, with an average of ~1 CD45+ve cell per 314 μm^3, although they were more numerous in the sub-mucosal tissue (Supplementary Fig. 3). Using a cut-off value of 3 x S.D. above the respective background level, 40 - 45% of infection foci displayed evidence of leukocyte infiltration (Fig. 4e). Therefore, despite being a site of parasite persistence, dynamic hyper-local homing of T-cells to the sites of infection in the murine colon is a characteristic of chronic stage disease, although at any one point in time, not all parasite nests will have triggered this type of recruitment response. Given the 'snapshot' nature of imaging, our data therefore suggest that in the majority of cases, the most likely outcome of colonic cell invasion will be infiltration of leukocytes, and the presumptive destruction of the parasites (Fig. 3d, e).

Incomplete homing of protective T-cells allows a subset of intracellular colonic infections to complete their replication cycle. Evidence indicates that *T. cruzi* rarely occupies individual colonic myocytes for extended periods (>2 weeks)[12], implying that parasites are either efficiently eliminated

by the immune response, or that they complete a cycle of replication and host cell lysis within this period. In addition, there is considerable diversity in the level of infection within individual colonic cells, with parasite numbers that can range from 1 to >1000[12]. We therefore investigated whether the immune response induced against infected cells increased in line with the intra-cellular parasite burden. When the levels of infiltrating leukocytes in the local environment of infected cells were compared with the number of intracellular *T. cruzi* parasites, we found no apparent correlation (Fig. 5a-c). This was the case irrespective of whether anti-CD45, anti-CD4 or anti-CD8 antibodies were used to assess the nature of the cellular infiltrate. It is implicit therefore, that the time-length of an individual intracellular infection, as inferred from the extent of parasite proliferation, is not a determinant of the likelihood of detection and targeting by the host immune system.

Of 237 infected colonic cells detected in 13 animals, only 4 (~1.7%) contained parasites that had clearly differentiated into flagellated trypomastigotes, the life-cycle stage that disseminates the infection by re-invasion of other host cells, or via transmission to the blood-sucking triatomine vector. Three of the infected cells contained very large numbers of parasites (>1,000), while the fourth contained 128. In each case, the leukocyte densities in the local microenvironment were within a range similar to host cells where the infection was less advanced, as judged by the number of intracellular parasites and the lack of differentiation into trypomastigotes. In the example shown (Fig. 6a, b), Z-stack imaging was used to serially section a mega-nest containing >1000 parasites, and shows mature trypomastigotes in the act of egress, despite the recruitment of a small number of $CD45^+$ leukocytes, including $CD8^+$ T-cells (Fig. 6c, d). Although the precise signals that trigger differentiation to the trypomastigote stage are unknown, it can be inferred from our data that the differentiation process itself, does not act to promote rapid infiltration of leukocytes to the site of infection, at least in the colon. Therefore, in a proportion of cases, the host immune system is either not triggered by an infection, is too slow to respond, or is in some way blocked. As a result, at least in the colon, the entire cycle of parasite proliferation, differentiation and egress can occur in the

absence of intervention by a cellular immune response, leading to the invasion of new host cells and prolongation of the chronic infection.

Discussion

Despite the generation of a vigorous and specific $CD8^+$ T-cell response[4,14,29,30], *T. cruzi* infections in mice are rarely cleared to sterility, even in vaccinated animals. Instead, the parasite persists in a small number of immunotolerant tissue sites, typically for the life-time of the host[10]. Intermittent dissemination from these locations to less permissive organs, such as the heart, may promote repeated episodes of infection, resulting in localised inflammatory responses that contribute to disease pathology in a cumulative manner[31]. Understanding why the immune system fails to eliminate *T. cruzi* infections is one of the key challenges in Chagas disease research. Here, using techniques that allow the immunological microenvironment of infection sites to be assessed at single cell resolution, we demonstrate that both $CD4^+$ and $CD8^+$ T-cells are frequently recruited to chronic infection foci in the colon, and that parasites in this site of persistence are subject to immune-mediated destruction. However, for a sub-set of infected cells, recruitment is not efficiently executed, and the intracellular cycle of parasite proliferation and differentiation to the trypomastigote stage can be completed (Fig. 6). Thus, chronic *T. cruzi* infections in the colon are not characterised by a generalised tissue-specific latency, but by a dynamic equilibrium between host and pathogen.

T-cell recruitment during *T. cruzi* infection is driven by secretion of chemokines from infected cells. For example, the CXCR3 ligands CXCL9 and CXCL10 have been implicated in cardiac infiltration[32]. IFN-γ and TNF-α expression by antigen specific $CD8^+$ T cells[4], and subsequent iNOS expression[33-35], potentially from recruited innate monocytes or from somatic cells of the infected tissue, then increases the local concentration of reactive nitrogen species. In Chagas disease, the resulting inflammatory environment tightly controls the number of infected cells, but can also act as the key driver of chronic immunopathology[7, 14, 36, 37]. An important observation from our study is that the likelihood of T-cell recruitment is not linked with the maturity of individual infections, as judged by

the intracellular parasite load (Fig. 5). In addition, the process of differentiation to the flagellated trypomastigote form, which occurs in highly parasitized cells, does not appear to be a key trigger that enhances infiltration of leukocytes, including $CD8^+$ cells, to the site of infection (Fig. 6).

The reasons why protective T-cells are not recruited to a small set of infection foci are unclear. Hypothesised mechanisms to account for *T. cruzi* immune evasion include a general absence of pathogen associated molecular patterns (PAMPs)[38], the extensive antigenic diversity expressed by the large families of trans-sialidase and mucin genes[39-41], stress-induced cell-cycle arrest and dormancy[42]. However, none of these explanations obviously correspond with our observation that there is a lack of association between the extent or longevity of an individual infection and the magnitude of hyper-local leukocyte recruitment (Fig. 5). Some highly infected mega-nests appear to be invisible to the immune system, whereas other low-level infections trigger massive cellular infiltration. In the majority of cases, infections are detected, presumably through innate detection pathways, as yet poorly defined, or through the generation of damage associated molecular patterns (DAMPs). Despite a diverse and complex antigenic repertoire, induction of the T-cell response in draining lymph nodes is known to be highly focussed[40], and once T-cell recruitment has been triggered, parasite destruction can be initiated (Fig. 3d and e). Widespread parasite dormancy was not evident in colonic tissue, and did not appear to be necessary for immune evasion.

Success or failure of the immune system in eliminating the rare chronic infection foci may be a largely stochastic process resulting from the dynamic interplay between the host and pathogen at a single cell level. If parasites were able to universally suppress innate detection pathways, with concomitant reduction in localised chemokine output, this would have a negative impact on both host survival and long-term *T. cruzi* transmission. Conversely, if infections were always detected by the immune system before completion of the replication cycle, the parasite would risk host-wide elimination. The ability of *T. cruzi* to persist in some organs/tissues, may therefore be dependent on the propensity, or otherwise, of these tissues to amplify the low-level chemokine signals triggered

by infection of an individual host cell. In mice, there are strain-specific differences in the extent of such tissue-restriction during chronic infections. This could have parallels in humans, and account for the heterogeneous profile of disease progression.

T. cruzi infection induces a high titre polyclonal B-cell/antibody response during the acute stage of infection, which although delayed[43], does contribute to parasite control and can protect against virulent infections. In the chronic stage, a role for the humoral response in suppressing the dissemination of persistent parasites has not been well defined[10], and the general consensus is that B-cells are not key components. In line with this, we show that in the absence of PBMCs, circulating antibodies are unable to maintain tissue-specific repression of the parasite burden (Fig. 1d, 2d). If the humoral response has a significant protective role during the chronic stage, for example, involving opsonisation of the parasite through FcR-antibody binding, then this function is lost on depletion of key cellular effectors. The central role of $CD8^+$ T-cells in controlling *T. cruzi* infections is well established, and in various parasite:mouse strain combinations, depletion of circulating $CD8^+$ T-cells leads to partial recrudescence, at least in skeletal muscle and adipose tissue[4,5,15,30]. When we examined the effect of $CD8^+$ T-cell depletion at a cellular level in colonic tissue, we found no significant increase in the number of infected cells, in contrast to the major rebound observed with cyclophosphamide-mediated reduction of the entire PMBC population (Fig. 1, 2). A non-redundant function for $CD4^+$ T-cells is less well established in murine models of Chagas disease[44-46], although in humans with untreated HIV co-infections, parasitaemia becomes easily detectable in the bloodstream[47]. Since depletion of either $CD4^+$ or $CD8^+$ T-cells by themselves did not promote the level of relapse observed with cyclophosphamide treatment (Fig. 2), our results therefore suggest that both lymphocyte sub-types contribute to the suppression of chronic stage infections, at least in the colon. Furthermore, innate leukocytes, which are unable to control the infection alone, could also be required to mediate and enhance T cell effector functions.

Our findings have important implications for anti-*T.cruzi* vaccine development. Vaccines protect by presenting non-tolerised antigens in the correct immunological context, to expand small numbers of naïve T and B cells. The expanded memory populations then allow more rapid deployment of adaptive effectors on future contact with the pathogen. However, *T. cruzi* is able to persist indefinitely in hosts that already have expansive systemic populations of effective T-cells. Unless vaccines can prevent parasites from accessing sites of persistence after the initial infection, or they are able to enhance successful homing of adaptive effector cells, it will be difficult to achieve sterilising immunity. Drug-cured infections can confer complete protection against re-challenge with a homologous strain, but with heterologous strains, despite the prevention of an acute stage peak, the infection proceeds directly to a status that is analogous to the chronic stage in terms of parasite burden and tissue distribution[3]. Therefore, it seems that successful anti-*T. cruzi* vaccines will require an ability to eliminate parasites at the initial site of infection during the first intracellular replication cycle. This will be a considerable challenge.

Methods

Mice and parasites. All experiments were performed using female C3H/HeN mice, purchased from Charles River (UK). They were maintained in individually ventilated cages, under specific pathogen-free conditions, with a 12-hour light/dark cycle, and provided with food and water *ad libitum.* Research was carried out under UK Home Office project licenses PPL 70/8207 and P9AEE04E4, with approval of the LSHTM Animal Welfare and Ethical Review Board, and in accordance with the UK Animals (Scientific Procedures) Act 1986 (ASPA). The *T. cruzi* line CL Luc::mNeon, a derivative of the CL Brener strain (discrete typing unit VI), was used in all experiments. It had been genetically modified to express a bioluminescent:fluorescent fusion protein containing red-shifted luciferase and mNeonGreen fluorescent domains[25,48]. For infections, C3H/HeN mice, aged 6-8 weeks, were inoculated i.p. with $1x10^3$ bloodstream trypomastigotes obtained from immunodeficient CB17-SCID mice, as described previously[28]. Mice were then monitored by *in vivo* bioluminescence imaging[17]

which indicated that they had transitioned to the chronic stage by 50-60 days post-infection. Experiments were performed when on mice that had been infected for at least 100 days.

Suppression of the murine immune response. General immunosuppression was achieved by injecting mice i.p. with cyclophosphamide (200 mg/kg) at 4-day intervals, up to a maximum of 3 injections, in accordance with animal welfare[17,28]. Circulating $CD8^+$ T-cells were depleted by i.p. injection of 400 μg of the YTS 169.4 monoclonal anti-CD8α (2BScientific), diluted in PBS, at 4-day intervals, up to a maximum of 4 times. The same regimen was applied for depletion of $CD4^+$ T-cells, using the GK1.5 monoclonal antibody (2BScientific).

Tissue processing and imaging. When mice were sacrificed, organs and tissues were removed and examined by *ex vivo* bioluminescence imaging using the IVIS Spectrum system (Caliper Life Science) and the LivingImage 4.7.2 software[49]. Colonic gut walls were peeled, whole mounted as described previously[18], and then exhaustively searched for parasites (green fluorescence) with a Zeiss LSM880 confocal microscope. Small tissue sections (~5 mm^2) around parasite nests were excised from the whole mount by scalpel, washed twice in PBS and incubated for 2 days in 1:300 primary antibody diluted in 5% PBS / 5% fetal calf serum / 1% Triton-X at 4ºC. Following 2 further washes in PBS, secondary antibody diluted in 1:500 in the same blocking/permeabilising solution was added to the tissue sections, and incubated for 3 hours at room temperature. Sections were then mounted in Vectashield, containing the DNA stain DAPI, and imaged by confocal microscopy. Colonic gut walls from naïve aged-matched mice were similarly prepared as controls, with and without the primary antibody.

For accurate determination of intracellular parasite and surrounding host cell numbers, tissue samples were imaged in 3-dimensions (Z-stacking), with the appropriate scan zoom setting[18]. The Image Browser overlay function was used to add scale bars, and images were exported as .TIF files to generate figures. Primary antibodies used were as follows: anti-luciferase (G7451, Promega),

CD45 (Tonbo Biosciences, 30-F11), CD3 (Abcam, ab11089), CD4 (Abcam, ab25475), CD8 (Abcam, ab25478). The secondary antibodies were Invitrogen A-11055, Invitrogen A-21434, Invitrogen A-11007.

Flow cytometry. At each time-point, mice were placed in a "hot box" and left at 38^{o}C for 10 minutes. They were then placed in a restrainer and the lateral tail vein punctured using a 0.5M EDTA (pH 7.4) soaked 21G needle. A single drop of blood was transferred to a 2 ml Eppendorf tube and 10µl 0.5M EDTA added to prevent clotting. Each sample was then mixed with 400 µl ice-cold PBS and placed onto 300 µl Histopaque 1083 (Sigma-Aldrich), and spun at 400 *g* for 30 minutes in a microcentrifuge. The separated monocytic layer was aspirated using a pipette, mixed with 1 ml ice-cold PBS, pelleted and resuspended in 200 µl flow cytometry buffer (PBS, 5% fetal bovine serum, 0.05% sodium azide), and 1 µl of the cocktail of conjugated antibodies added (1:200 dilution in each case). After 1 hour incubation in the dark, cells were pelleted and re-suspended in 2% paraformaldehyde in PBS, followed by a further 45 minutes incubation in the dark. The stained/fixed cells were then pelleted, re-suspended in filtered flow cytometry buffer and transferred to standard flow cytometry tubes. Samples were analysed using a BD Bioscience LSRII flow cytometer, with plots created and analysed in FlowJo V.10.6.1. The following antibodies were used: CD45 (ThermoFisher, 30-F11, Super Bright 600), CD3 (ThermoFisher, 17A2, FITC), CD4 (ThermoFisher, RM4-5, eFluor 450), and CD8 (ThermoFisher, SK1, Alexa Fluor 780).

α-*T. cruzi* antibody ELISA. 96-well plates were coated with sonicated *T. cruzi* CL Luc::mNeon trypomastigote lysate; 100 µl (0.5 µg) per well diluted in 15 mM Na_2CO_3, 34.8 mM $NaHCO_3$. The plates were incubated at 4^{o}C overnight to allow antigen binding, washed 3x with PBS / 0.05% Tween 20, and then blocked with PBS / 2% milk powder. Diluted murine serum samples, collected from each Histopaque separation, were further diluted to 1:1600. These were aliquoted in triplicate (100 µl per well) and incubated for 1 hour at 37^{o}C. Horse radish peroxidase (HRP) conjugated anti-mouse IgG secondary antibody (Abcam, ab99774) was then added (1:5000; 100 µl per well), and the plates

incubated for a further 1 hour. After the addition of HRP substrate (80 μl per well) (Stabilised TMB, Life Technologies), the plates were incubated at room temperature in the dark for 5 minutes and read using a FLUOstar Omega plate reader (BMG LABTECH), after the addition of 40 μl 1M HCl.

Statistics. Analyses were performed in GraphPad PRISM v8.0. S.D. Background cellularity and CD45+, CD4+ and CD8+ cut-offs were set as mean + 3 x S.D. Data sets were compared using a 2-sample t-test with Welch correction. If data were not normally distributed, as assessed using a Shapiro-Wilk test, a Mann-Whitney rank sum test was used.

References

1. Bern, C. Chagas' disease. *N. Eng. J. Med*. **373**, 456-466 (2015).
2. Bustamante, J. & Tarleton, R. Reaching for the Holy Grail: insights from infection/cure models on the prospects for vaccines for *Trypanosoma cruzi* infection. *Mem. Inst. Oswaldo Cruz* **110**, 445-451 (2015).
3. Mann, G. S. et al. Drug-cured experimental *Trypanosoma cruzi* infections confer long-lasting and cross-strain protection. *PLoS Negl. Trop. Dis.* **14**, e0007717 (2020).
4. Pack, A. D., Collins, M. H., Rosenberg, C. S. & Tarleton, R. L. Highly competent, non-exhausted CD8+ T cells continue to tightly control pathogen load throughout chronic *Trypanosoma cruzi* infection. *PLoS Path.* **14**, e1007410 (2018).
5. Pack, A. P., Bustamante, J. M & Tarleton, R. L. CD8+ T cells in *Trypanosoma cruzi* infection. *Semin. Immunopathol.* **37**, 233-238 (2015).
6. Ribeiro A. L., Nunes, M. P., Teixeira, M. M. & Rocha, M. O. Diagnosis and management of Chagas disease and cardiomyopathy. *Nat. Rev. Cardiol*. **9**, 576-589 (2012).
7. Cunha-Neto, E. & Chevillard, C. Chagas disease cardiomyopathy: immunopathology and genetics. *Mediat. Inflamm*. **2014**, 683230 (2014).
8. Bonney, K. M., Luthringer, D. J., Kim, S. A, Garg, N. J. & Engman, D. M. Pathology and pathogenesis of Chagas heart disease. *Annu. Rev. Pathol.* **14**, 421-447 (2019).

9. Kayama, H. & Takeda, K. The innate immune response to *Trypanosoma cruzi* infection. *Microbes Infect*. **12**, 511–517 (2010).

10. Pérez-Mazliah, D., Ward, A. I. & Lewis, M. D. Host-parasite dynamics in Chagas disease from systemic to hyper-local scales. *Parasite Immunology*. **00**, e12786 (2020).

11. Padilla, A. M., Simpson, L. J. & Tarleton, R. L. Insufficient TLR activation contributes to the slow development of CD8+ T cell responses in *Trypanosoma cruzi* infection. *J. Immunol.* **183**, 1245-1252 (2009).

12. Ward A. I., Olmo, F., Atherton, R. L., Taylor, M. C. & Kelly, J. M. *Trypanosoma cruzi* amastigotes that persist in the colon during chronic stage murine infections have a reduced replication rate. *Open Biol*. **10**, 200261 (2020)

13. Lewis M. D. et al. Bioluminescence imaging of chronic *Trypanosoma cruzi* infections reveals tissue-specific parasite dynamics and heart disease in the absence of locally persistent infection. *Cell. Microbiol.* **16**, 1285-1300 (2014).

14. Martin D. L. et al. CD8+ T-Cell responses to *Trypanosoma cruzi* are highly focused on strain-variant trans-sialidase epitopes. *PLoS Path.* **2**, e77 (2006).

15. Rodriguez, E. A., Furlan, C. A., Vernengo, F. F, Montes, C. L. & Gruppi, A. Understanding CD8+ T cell immunity to *Trypanosoma cruzi* and how to improve it. *Trends Parasitol*. **35**, 899-917 (2019).

16. Chatelain, E. & Scandale, I. Animal models of Chagas disease and their translational value to drug development. *Expert Opin. Drug Discov*. **15**, 1381-1402 (2020).

17. Lewis M. D., Francisco, A. F., Taylor, M. C., Jayawardhana, S. & Kelly, J. M. Host and parasite genetics shape a link between *Trypanosoma cruzi* infection dynamics and chronic cardiomyopathy. *Cell. Microbiol.* **18**, 1429-1443 (2016).

18. Ward A. I. et al. *In vivo* analysis of *Trypanosoma cruzi* persistence foci in chronically infected mice at single cell resolution. *mBio* **11**, e01242-20 (2020).

19. Rodríguez-Morales, O. et al. Experimental vaccines against Chagas Disease: A journey through history. *J. Immunol. Res.* **2015**, 489758 (2015).

20. Luhrs K. A., Fouts, D. L. & Manning, J. E. Immunization with recombinant paraflagellar rod protein induces protective immunity against *Trypanosoma cruzi* infection. *Vaccine.* **21**, 3058-3069 (2003).

21. Gupta, S. & Garg, N. J. TcVac3 induced control of *Trypanosoma cruzi* infection and chronic myocarditis in mice. *PLoS ONE*. **8**, e59434 (2013).

22. Arce-Fonseca, M., Rios-Castro, M., Carrillo-Sánchez, S. Martinéz-Cruz, M. & Rodrígeuz-Morales, O. Prophylactic and therapeutic DNA vaccines against Chagas disease. *Parasit. Vectors* **8**, 121 (2015).

23. Barry, M. A. et al. A therapeutic vaccine prototype induces protective immunity and reduces cardiac fibrosis in a mouse model of chronic *Trypanosoma cruzi* infection. *PLoS Negl. Trop. Dis*. **13**, e0007413 (2019).

24. de la Cruz, J. J. et al. Production of recombinant TSA-1 and evaluation of its potential for the immuno-therapeutic control of *Trypanosoma cruzi* infection in mice. *Hum. Vaccine Immunother*. **15**, 210-219 (2019).

25. Costa, F. C. et al. Expanding the toolbox for *Trypanosoma cruzi*: A parasite line incorporating a bioluminescence-fluorescence dual reporter and streamlined CRISPR/Cas9 functionality for rapid *in vivo* localisation and phenotyping. *PLoS Negl. Trop. Dis.* **12**, e0006388 (2018).

26. Feng, L. et al. Optimized animal model of cyclophosphamide-induced bone marrow suppression. *Basic Clin. Pharmacol. Toxicol.* **119**, 428-435 (2016).

27. Bustamante, J. M., Craft, J. M., Crowe, B. D., Ketchie, S. A. & Tarleton, R. L. New, combined, and reduced dosing treatment protocols cure *Trypanosoma cruzi* infection in mice *J. Infect. Dis.* **209**, 150-62 (2014).

28. Lewis, M. D., Francisco, A. F., Taylor, M. C. & Kelly, J. M. A new experimental model for assessing drug efficacy against *Trypanosoma cruzi* infection based on highly sensitive *in vivo* imaging. *J. Biomolec. Screen*. **20**, 36-43 (2015).

29. Rosenburg, C. S., Martin, D. L. & Tarleton, R. L. CD8+ T cells specific for immunodominant trans-sialidase epitopes contribute to control of *Trypanosoma cruzi* infection but are not required for resistance. *J. Immunol*. **185**, 560-568 (2010).

30. Martin, D. & Tarleton, R. Generation, specificity, and function of CD8+ T cells in *Trypanosoma cruzi* infection. *Immunol. Rev.* **201**, 304-17 (2004).

31. Lewis, M. D. & Kelly, J. M. Putting infection dynamics into the heart of Chagas disease. *Trends Parasitol*. **32**, 899-911 (2016).

32. Ferreira, C. P. et al. CXCR3 chemokine receptor guides *Trypanosoma cruzi*-specific T-cells triggered by DNA/adenovirus ASP2 vaccine to heart tissue after challenge. *PLOS Neg. Trop. Dis.* **13**, e0007597 (2019).

33. Vespa G. N., Cunha F. Q. & Silva J. S. Nitric oxide is involved in control of *Trypanosoma cruzi*-induced parasitemia and directly kills the parasite in vitro. *Infect. Immun*. **62**, 5177–5182 (1994).

34. Hölscher, C. et al. Defective nitric oxide effector functions lead to extreme susceptibility of *Trypanosoma cruzi*-infected mice deficient in gamma interferon receptor or inducible nitric oxide synthase. *J. Immunol*. **66**, 1208-1215 (1998).

35. Carbajosa S. et al. L-arginine supplementation reduces mortality and improves disease outcome in mice infected with *Trypanosoma cruzi*. *PLoS Negl. Trop.* Dis.**12**, e0006179 (2018).

36. Roffe, E. et al. *Trypanosoma cruzi* causes paralyzing systemic necrotizing vasculitis driven by pathogen-specific type I immunity in mice. *Infect. Immun*. **84**, 1123-1136 (2016).

37. Weaver, J. D., Hoffham, V. J., Roffe, E. & Murphy, M. Low-level parasite persistence drive vasculitis and myosistis in skeletal muscle of mice chronically infected with *Trypanosoma cruzi. mBio*. **87**, e00081-19 (2019).

38. Kurup, S. P. & Tarleton, R. L. Perpetual expression of PAMPs necessary for optimal control and clearance of a persistent pathogen. *Nat. Commun.* **4**, 2616 (2013).

39. Mucci, J., Lantos, A. B., Buscaglia, C. A., Leguizamón, M. S. & Campetella, O.

The *Trypanosoma cruzi* surface, a nanoscale patchwork quilt. *Trends Parasitol.* **33**, 102-112 (2017).

40. Martin D.L. et al. CD8+ T-Cell responses to *Trypanosoma cruzi* are highly focused on strain-variant trans-sialidase epitopes. *PLoS Pathog.* **2**, e77 (2006).

41. Weatherly, D. B., Peng, D. & Tarleton R. L. Recombination-driven generation of the largest pathogen repository of antigen variants in the protozoan *Trypanosoma cruzi. BMC Genomics*. **17**, 729 (2016).

42. Sánchez-Valdéz F.J., Padilla, A., Wang, W., Orr, D. & Tarleton, R. L. Spontaneous dormancy protects *Trypanosoma cruzi* during extended drug exposure. *Elife* **7**, e34039.

43. Bermejo, D. A. et al. *Trypanosoma cruzi* infection induces a massive extrafollicular and follicular splenic B-cell response which is a high source of non-parasite-specific antibodies. *Immunology*. **132**, 123-33 (2011).

44. Hoft, D. F., Schnapp, A. R., Eickhoff, C. S. & Roodman S. T. Involvement of CD4+ Th1 cells in systemic immunity protective against primary and secondary challenges with *Trypanosoma cruzi*. *Infect. Immun*. **68**,197-204 (2000).

45. Padilla, A., Xu, D., Martin, D. & Tarleton, R. Limited role for CD4+ T-cell help in the initial priming of *Trypanosoma cruzi*-specific CD8+ T cells. *Infect. Immun.* **75**, 231-235 (2007)

46. Flávia Nardy, A., Freire-de-Lima, C. G. & Morrot, A. Immune evasion strategies of *Trypanosoma cruzi J. Immunol. Res.* **2015**, 178947 (2015).

47. de Almeida, E., Ramos, A. N., Correia, D. & Shikanai-Yasuda, A. Co-infection *Trypanosoma cruzi*/HIV: systematic review (1980-2010). *Rev. Soc. Bras. Med. Trop*. **44**, 762-70 (2011).

48. Branchini, B. R. et al. Red-emitting luciferases for bioluminescence reporter and imaging applications. *Anal. Biochem*. **396**, 290-297 (2010).

49. Taylor, M. C. et al. Exploiting genetically modified dual-reporter strains to monitor experimental *Trypanosoma cruzi* infections and host:parasite interactions. Karina Andrea Go´mez and Carlos Andres Buscaglia (eds.), *T. cruzi* Infection: Methods and Protocols, *Methods Molec. Biol.* **1955**,147-163 (2019).

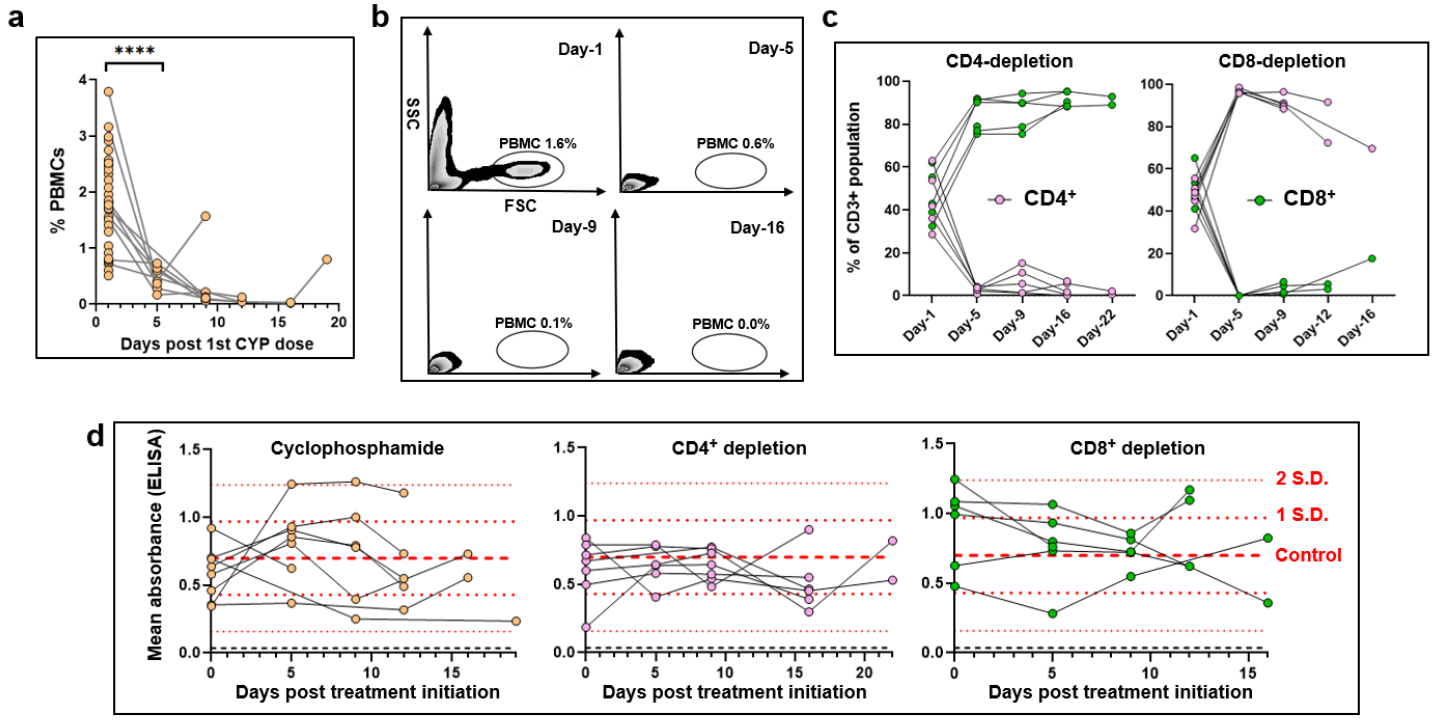

Fig. 1.

Fig. 1 Suppression of cellular immunity in mice chronically infected with *T. cruzi.* **a** C3H/HeN mice chronically infected (>100 days) with *T. cruzi* CL Luc::mNeon (n=6) were immunosuppressed by i.p. inoculation with cyclophosphamide (200 mg/kg) at 4-day intervals, up to a maximum of 3 injections (Methods). The % events recorded as peripheral blood mononuclear cells (PBMCs) at different time points after the initiation of treatment for individual mice are shown (Methods). Also included in the day 1 values are additional data points (n=24) from immunocompetent chronically infected mice. **b** Flow cytometry plots showing the loss of detectable events in the PBMC gate (black oval) over the course of cyclophosphamide treatment (see also Supplementary Fig. 1) PBMCs were identified based on the spectral forward (FFC) and side (SSC) scatter. **c** Effective depletion of T-cell subsets by treatment of mice with specific anti-CD4 or anti-CD8 antibodies (Methods). The graphs show the $CD4^+$ and $CD8^+$ flow cytometry events of individual mice as a % of the total $CD3^+$ population over the treatment periods. **d** ELISA mean absorbance readings for chronically infected mice treated with cyclophosphamide at different time-points after treatment initiation, or treated with anti-CD4 or anti-CD8 antibodies. Microtitre plates containing *T. cruzi* lysates were prepared as described (Methods). Dashed red lines identify the mean, 1 x S.D. and 2 x S.D. values, determined

from immunocompetent chronic stage controls (n=28). One of the anti-CD8 antibody treated mice died between day 5 and 9.

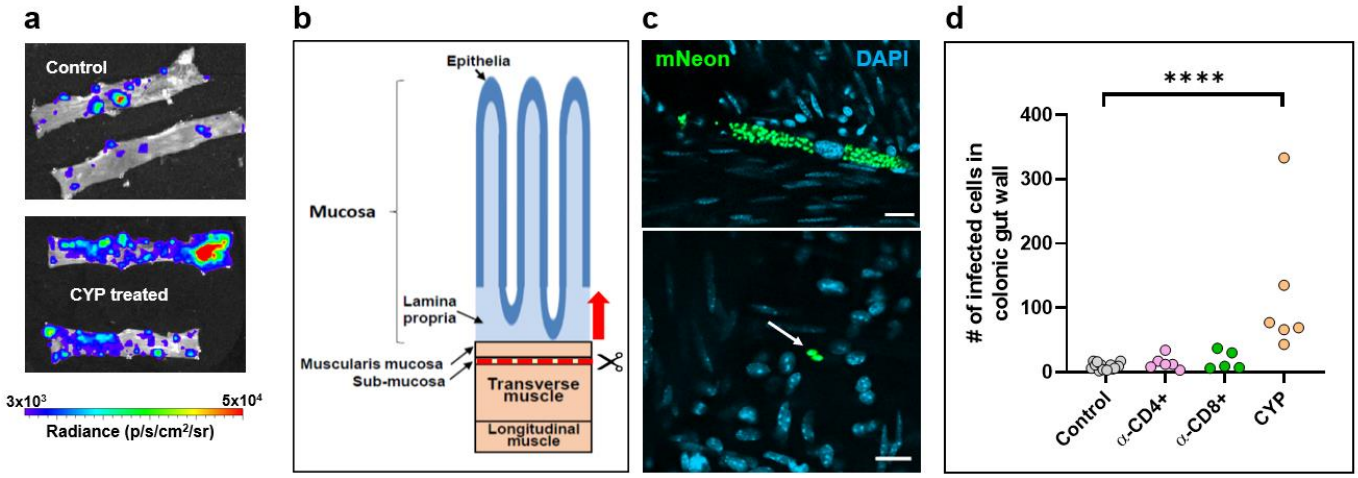

Fig. 2

Fig. 2 Control of persistent parasites in the colon of chronically infected mice is lost on suppression of cellular immunity, with CD8⁺ and CD4⁺ T-cells playing non-redundant roles. **a** Colon sections from C3H/HeN mice chronically infected with *T. cruzi* CL-Luc::mNeon were pinned luminal side up and examined by e*x vivo* bioluminescence imaging. Radiance (p/s/cm^2/sr) is on a linear-scale pseudo-colour heat map. Upper inset, colonic sections from non-treated infected mice; lower inset, section from mice immunosuppressed by cyclophosphamide treatment (Methods). **b** Schematic highlighting the distinct layers of the GI tract. The dashed red line and arrow indicate the position above which tissue can be peeled off to leave the external colonic wall layers[18]. **c** External gut wall mounts were examined in their entirety at a 3-dimensional level by confocal microscopy. Examples of parasite infected cells and their locations, detected by green fluorescence (mNeon). DAPI staining (blue) identifies host cell nuclei. Scale bars=20μm. **d** The total number of parasitized cells counted in each whole mounted colonic gut wall for the control and the immune-depleted groups. Each dot represents a single mouse, with the colons examined >12 days post treatment initiation. **** = p≤0.0001. Differences between control values and those obtained from mice that had been treated with anti-CD4 and anti-CD8 antibodies were non-significant.

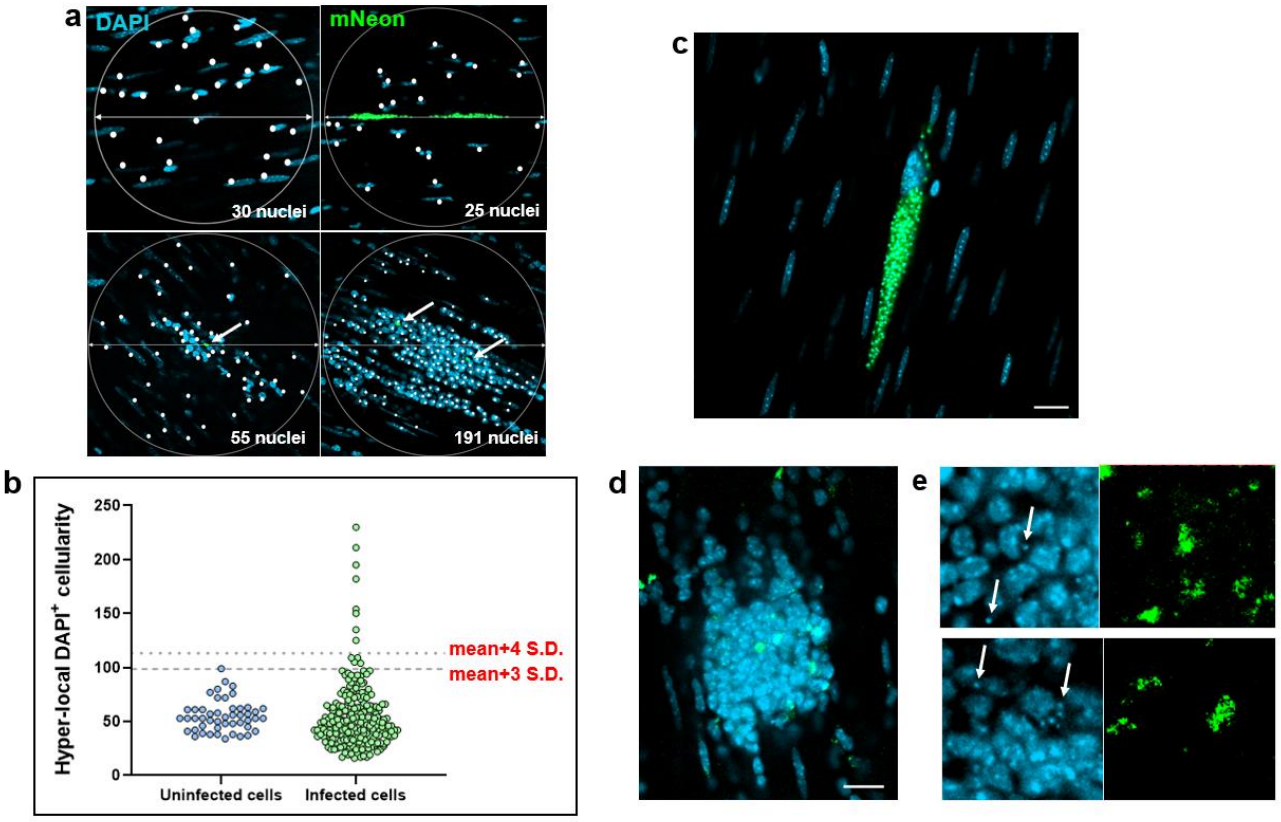

Fig. 3

Fig. 3 Defining the hyper-local cellularity of *T. cruzi* infected host cells in the colonic gut wall.

a Images of whole mounted colonic gut wall from C3H/HeN mice chronically infected with *T. cruzi* CL-Luc::mNeon (Methods). When infection foci were identified, 200 μM diameter circles were drawn centred on each parasite cluster or 'nest'. Circles were placed by centering on randomly selected cells in the case of non-infected age-matched controls (top left). DAPI-stained nuclei (blue) that fell within this disc (highlighted by white dots) were counted as a measure of cellularity. Intracellular parasites can be identified by green fluorescence. These are indicated by white arrows in the lower images. **b** Background cellularity around randomly selected cells (n=48) on whole mounted colonic gut walls from naïve age-matched C3H/HeN mice was established as above. With tissue from chronically infected mice, hyper-local cellularity was calculated using circles centred on parasite foci (green) (n=247). Individual values are indicated by blue (non-infected) and green (infected) dots. The dashed lines indicate 3 x S.D. and 4 x S.D. above the background mean. **c** An infected myocyte where the local cellularity is equivalent to the background level and the intracellular amastigotes (green) are structurally intact. Scale bar=20 μm. **d** Image of an intense cellular infiltrate (nuclei, blue)

in which the *T. cruzi* parasites (green) display a diffuse morphology. **e** Zoomed-in views of two regions of the same cellular infiltrate. Many discrete disc-like kDNA structures (the parasite mitochondrial genome network) are detectable by DAPI-staining throughout this inflammatory focus (examples indicated by white arrows). They often co-localise with diffuse green fluorescence of parasite origin (right-hand images).

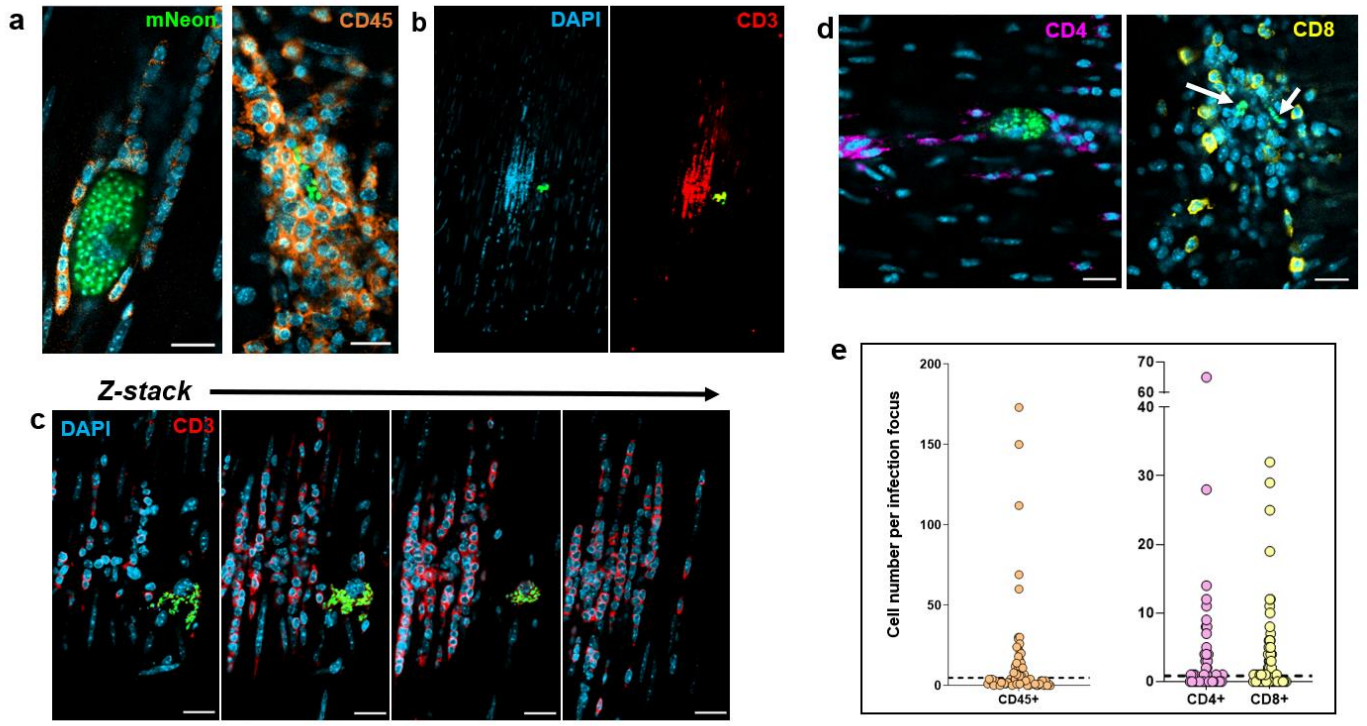

Fig. 4

Fig. 4 T-cells are major constituents of the leukocyte population recruited to chronic stage infection foci. a Confocal images of colonic gut wall sections from chronically infected mice (Methods). Rare infection foci were identified by mNeonGreen fluorescence (parasites) after exhaustive searching of whole mounted gut walls. Staining with anti-CD45 (orange) reveals that hematopoietic cells constitute the vast majority of the infiltrate population. Host cell nuclei were identified by DAPI staining (blue). **b** Anti-CD3 staining of cellular infiltrates shows that T-cells constitute a majority of the population. Blue, host cell nuclei; red, CD3 staining; green, parasite fluorescence. **c** Serial Z-stack imaging (Methods) through the same cellular infiltrate as in b, showing selected sections through the infiltrate. **d** Histological sections containing cellular infiltrates and associated infection foci (parasites, green; indicated by white arrows in right-hand image) stained

with either anti-CD4 (purple) or anti-CD8 (yellow) antibodies. Scale bars=20 μm. **e** Whole mounts containing infection foci were stained with anti-CD45, anti-CD4, or anti-CD8 antibodies and the number of positive host cells in the immediate vicinity (314 μm^3 volume) was determined by serial Z-stack confocal imaging (see also Fig. 2). Each dot corresponds to a single infection focus. The horizontal dashed line is 3 x above the S.D. of the mean background level in non-infected tissue. In the case of anti-CD45 staining, none of the 50 tissue sections examined from non-infected mice contained CD45+ve positive cell numbers above this value. 41%, 45% and 42% of infection foci identified by CD45, CD4 and CD8 staining, respectively, were above this cut-off.

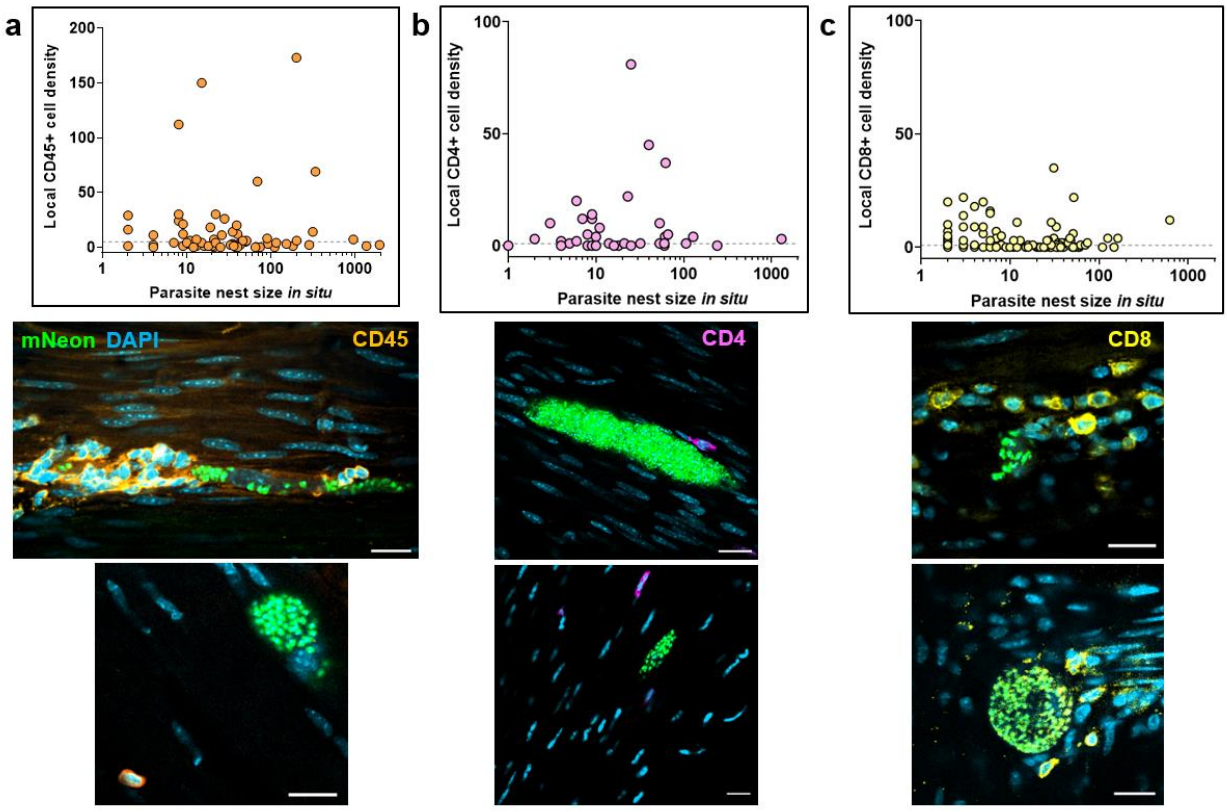

Fig. 5

Fig. 5 Lack of correlation between intracellular parasite load and hyper-local T-cell infiltration during chronic infections. a Comparison of the parasite numbers in infected colonic gut wall cells with the local leukocyte cell density. Infection foci were identified in whole mounts of colonic tissue, which were then stained with anti-CD45 antibody (Methods). The parasite and cell numbers in a tissue volume of 314 μm^3 were determined using serial Z-stack imaging, with leukocytes identified by orange staining and parasites by green fluorescence. The horizontal dashed line is 3 x above

the SD of the mean background level in non-infected tissue. Each dot identifies a single infection focus, with tissue samples derived from 6 mice (71 infection foci). The confocal images show representative infection foci used to generate the data, and illustrate the varying extents of leukocyte infiltration. **b** Similar analysis of infection foci using anti-CD4 staining (purple). Tissue samples were derived from 3 mice (54 infection foci). **c** Analysis of infection foci using anti-CD8 staining (yellow). Tissue derived from 4 mice (116 infection foci).

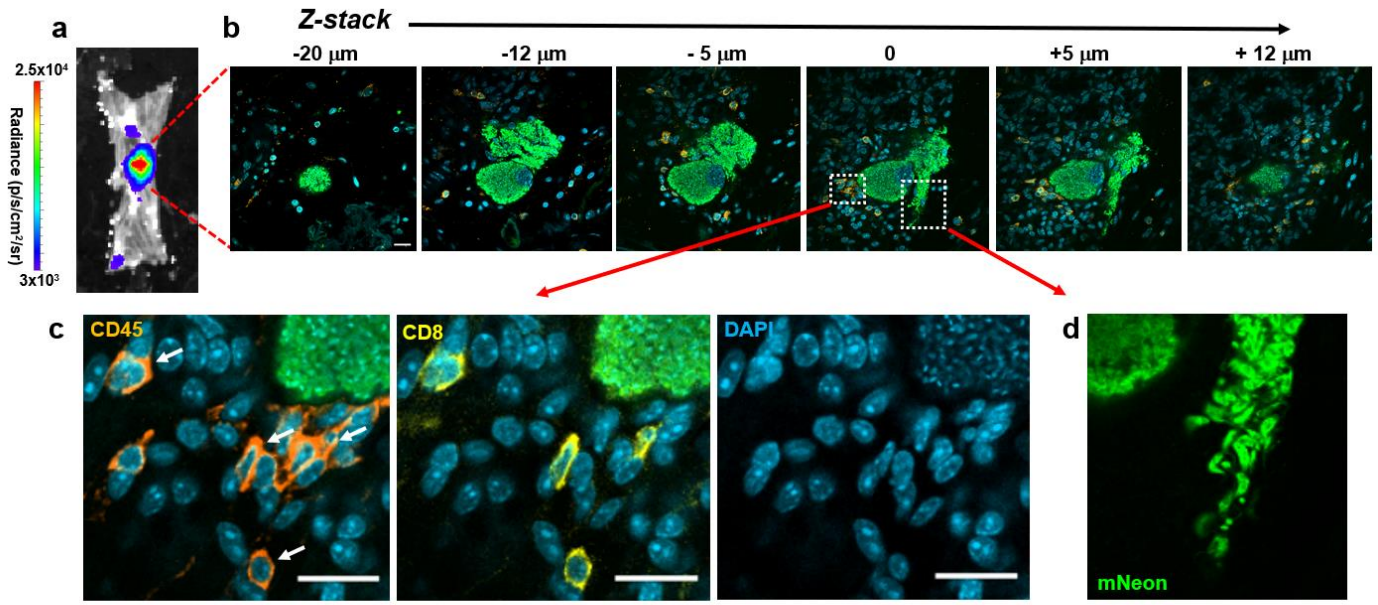

Fig. 6

Fig. 6 Incomplete recruitment of leukocytes allows progression of *T. cruzi* through the full intracellular infection cycle. a An intense bioluminescent focus in a chronic stage distal colon viewed by *ex vivo* imaging (Methods). Radiance (p/s/cm^2/sr) is on a linear-scale pseudocolour heatmap. **b** Confocal imaging of the corresponding parasite mega-nest showing representative serial Z-stack images taken along the depth of the infected cell. The Z-axis position relative to the centre of the nest is indicated above each of the images. Parasite numbers >1000 were determined from green fluorescence and the characteristic DAPI staining of the parasite kinetoplast DNA (the mitochondrial genome)[18] (blue). Infiltrating leukocytes (orange) were identified by staining with anti-CD45 antibodies (Methods). Scale bar=20 μm. **c** Enlarged images of a small cluster of infiltrating CD45$^+$ (orange) and CD8$^+$ (yellow) cells in close vicinity to the nest. White arrows indicate leukocytes

corresponding to CD8$^+$ T-cells. **d** Egress of differentiated trypomastigotes into the extracellular environment.

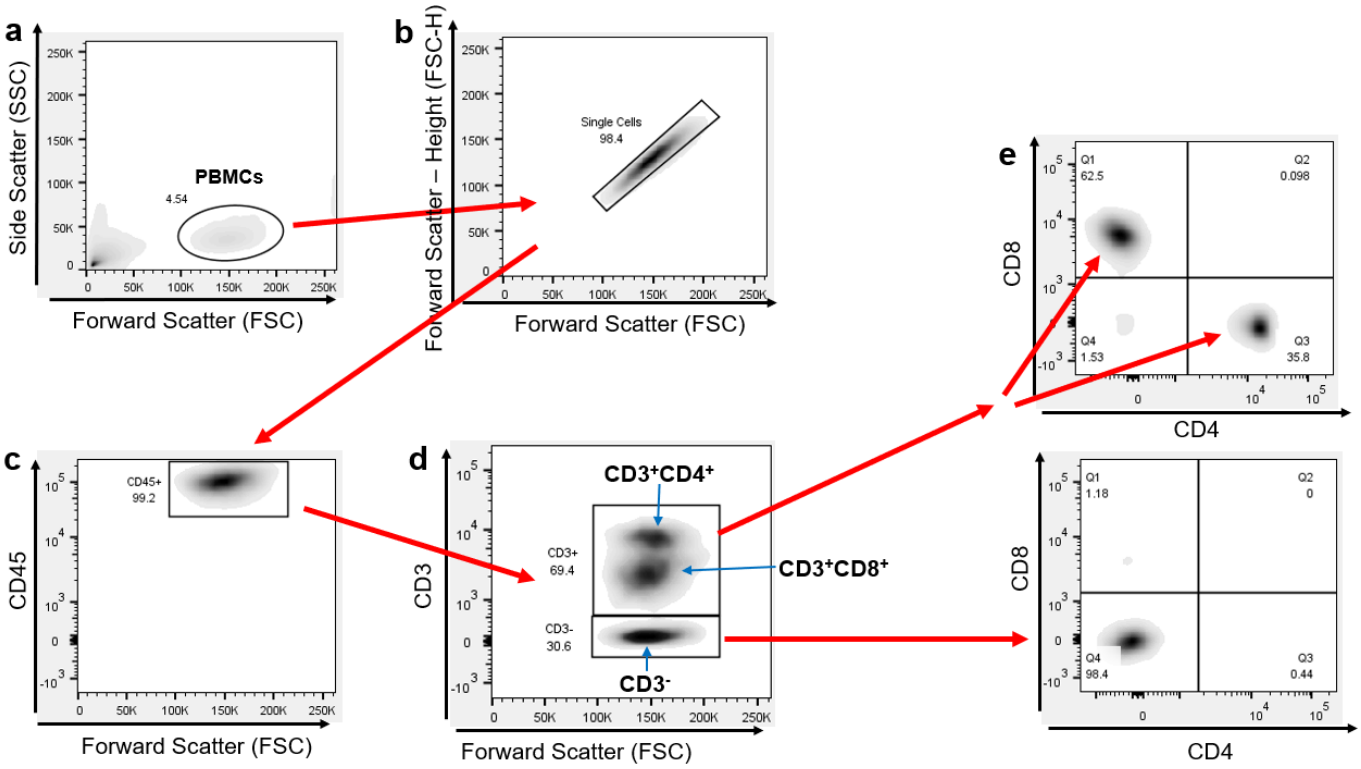

Supplementary Fig. 1

Supplementary Fig. 1 Flow cytometry gating strategy. a PBMCs isolated in the black oval based on forward (FSC) and side (SSC) scatter spectral properties. **b** Singlets isolated. **c** Population staining +ve with anti-CD45 antibody. **d** CD45$^+$ population separated by CD3 positivity. **e** Both CD3$^+$ and CD3$^-$ populations separated by CD4 and CD8 markers

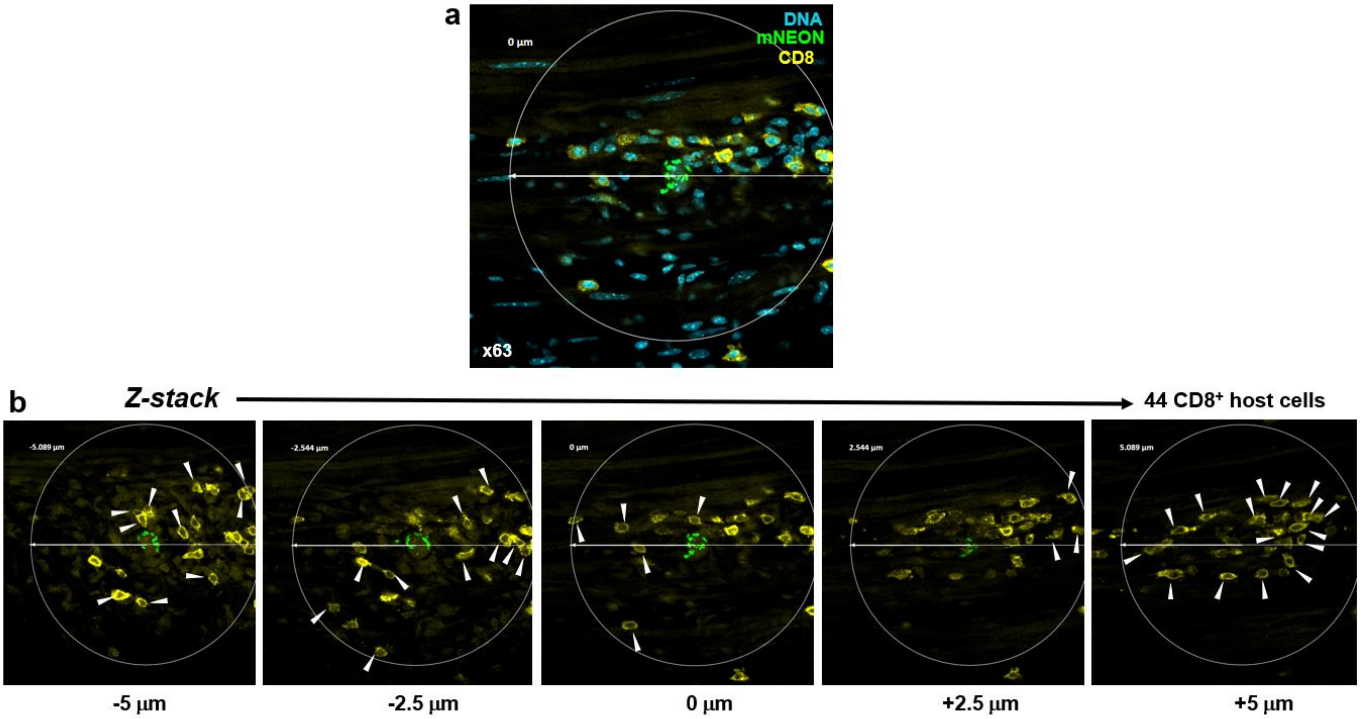

Supplementary Fig. 2

Supplementary Fig. 2 Establishing the extent of CD8$^+$ T-cell recruitment to infection foci using 3-dimensional serial Z-stack confocal imaging. a A parasite nest detected in the whole mounted colonic gut wall of a mouse chronically infected with *T. cruzi* CL Luc::mNeon (Methods). Parasites, green; DNA, blue (DAPI); CD8$^+$ T-cells, yellow (stained with antibody prior to mounting). The area selected for Z-stack imaging is identified by a 200 µm diameter circle, centred on the parasite nest. **b** The local density of CD8$^+$ host cells was determined by counting the number of stained cells (yellow) in a series of Z-stack images acquired with a Zeiss LSM880 confocal microscope from 5 µm above and below the centre of the parasite nest on the Z-axis, a cylinder volume of 314 µm^3. Any cells that fell within the 200 µm diameter circle were included. The number of hyper-local CD8$^+$ T-cells was calculated to be 44.

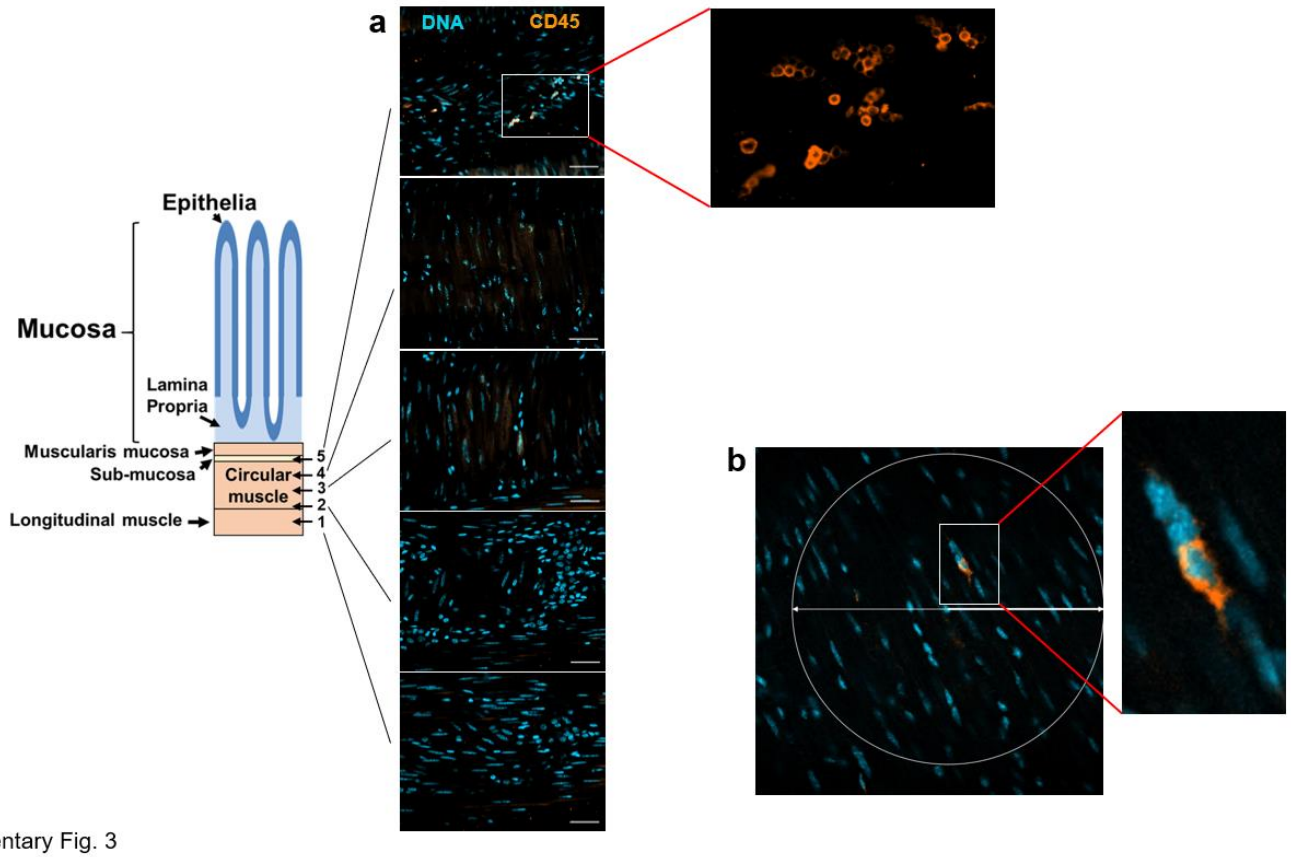

Supplementary Fig. 3

Supplementary Fig. 3 The longitudinal and transverse smooth muscle layers of the colon are largely devoid of CD45⁺ leukocytes in non-infected C3H/HeN mice. a Serial Z-stack images of a whole mounted colonic gut wall from an age-matched non-infected C3H/HeN mouse. DNA, blue (DAPI); CD45⁺ (a pan-leukocyte marker), orange. Scale bars=20 μm. The images correspond to the cross-sectional regions of the colon indicated in the schematic (1-5). CD45⁺ can be readily detected in the sub-mucosal layer (inset). **b** Rare example of a CD45⁺ cell within the longitudinal and transverse smooth muscle layers. A 200 μm diameter circle is superimposed on the image.

6.5 Chapter summary

Relative to the other parasitic infections described in the introduction, post-acute stage *T. cruzi* appears to be unable to survive contact with the systemic immune system. Instead, as outlined in the above manuscript, the pathogen is a ‘true evader’, able to invade, differentiate, replicate and re-differentiate within specific host cells at specific tissue sites, in the local absence of T cells. These host myocytes represent a single-cell level immune-permissive niche, which appear unable to signal effectively for external cellular help. If such a mechanism of immune evasion is in operation in humans, the prospects for a sterilizing vaccine are poor. Since the systemic adaptive response is already highly effective, there might be little to be gained from further boosting.

Chapter 7 – General discussion, future work and concluding remarks

7.1 General Discussion

T. cruzi infection remains a major threat to human health in Latin America, and is a rising concern for health systems in other regions. At present, a practical vaccine does not exist and vector control measures have not eliminated transmission, despite significant effort. Three major research questions currently impede progress towards better drugs and management of *T. cruzi* infection and associated symptomatic Chagas disease.

1. **Why do only ~30% of human infections result in clinically observable pathology?**
2. **Why are the outcomes of current chemotherapeutic treatments so variable?**
3. **Is an effective Chagas disease vaccine theoretically achievable?**

In this thesis, highly-sensitive bioluminescent-fluorescent parasite reporters[1] were employed in mouse models to better understand these questions. As a first aim, we sought to better clarify the tissues and host cell types that harbour rare infection foci at late infection time-points. This information is of great value in ensuring drug candidates reach threshold bioavailability at the sites at which *T. cruzi* persists. In addition, as recently established[2,3], the chronic stage distribution of parasites and the dynamics of persistence in different tissues can be predictive of cardiac fibrosis. The hypothesis stated in Lewis and Kelly, 2016[4] suggests that development of cardiac pathology correlates with the ability, or otherwise, of the host immune response to restrict infection foci to specific ‘sites of persistence’. Parasite genetics also determine propensity to disseminate, with the interaction between the two responsible for the progression of cardiac pathology. Whether human infections that result in pathology are of the more ‘disseminated’ type is currently unknown.

Here, for the first time, we demonstrate that the smooth muscle cells of the gastrointestinal tract (GIT) are a key reservoir of chronic infection in two mouse strains. Outside the GIT, the skin is also routinely infected in both models, while the skeletal muscle is an additional site of particularly high parasite load in the C3H/HeN model. These findings support the previously suggested propensity for *T. cruzi* to persist in muscle cells[5], and suggest that good bioavailability of anti-chagasic compounds in these cells is a requirement for a curative outcome.

The role of the ‘persister’ state in treatment failure of *T. cruzi* infections has been hotly debated, but a clear link has yet to be established. Here, we report an absence of evidence to support the recently reported hypothesis that rare *T. cruzi* amastigotes stochastically enter a definitively ‘dormant’ state in the absence of drug treatment[6], at least in chronic stage infections of the colon. This hypothesis suggests that parasites in this state *in vivo* are resistant to drug treatment but remain replication competent. Using the best current experimental methodology available, *in vivo* injection of the thymidine analogue EdU, we show that there is a ~3-fold slow-down in parasite replication after the generation and deployment of the adaptive immune response. We stop short of describing this state as ‘dormant’ since even at late infection time-points, regular cycles of intracellular growth, host cell lysis and reinfection are ongoing. Its currently unknown if this inferred slow-down in replication impacts the dynamics of drug treatment.

Despite decades of effort[7,8,9,10], the prospect of an anti-*T. cruzi* vaccine in the near future is remote. This feeds into the broader debate over why eukaryotic pathogens have been so intractable to vaccination as a method of infection control. This is in sharp contrast to many viral[11] and prokaryotic[12] pathogens. Certainly, one explanation is that the basic biology and immunology of complex parasitic organisms has been poorly characterised, making rational design of vaccine candidates and adjuvants challenging. Another is that these organisms are capable of long-term persistence in immunocompetent hosts, meaning a successful vaccine would have to out-perform a natural infection. Whether this is possible, will determine if creating a sterilizing *T. cruzi* vaccine is a realistic goal.

The final part of this thesis sought to exploit the optimization of the reporter systems and the technical progress described in the first two papers to generate data that would help answer this question. We were able to assemble a large catalogue of images of chronic infection foci and to characterize their immunological context. We used these data to generate a new hypothesis explaining *T. cruzi* persistence. This states that of the population of host cells infected during the chronic stage, the majority will become the target of intra-tissue T-cells. However, a minority are permitted to complete multiple cycles of intracellular replication, followed by differentiation and dissemination, without obvious recruitment of immune effectors. If this hypothesis holds for human infections, it is difficult to envisage what advantage further boosting of the adaptive effectors, T cells and antibody, would have for infection outcomes.

7.2 Future work and concluding remarks

Here I provide comment on the future directions that the research presented in this thesis should take for maximum front-line benefit. These comments are ordered to correspond to the above chapter order.

1. **Infection dynamics and Chagasic pathology (Chapter 4)**
2. **Towards a mechanistic understanding of drug treatment failure (Chapter 5)**
3. **Prospects for a sterilising Chagas disease vaccine (Chapter 6)**

Infection dynamics and Chagas pathology – Work aimed at further clarifying the chronic stage localisation and infection dynamics of *T. cruzi* infection is crucial to underpin the rest of our biological and immunological understanding of this important persistent parasite. Why only a minority of infected humans develop clinical pathologies is not understood, with a clear answer required to better target current and future drugs to patients who will develop pathology. The hypothesis proposed in Lewis and Kelly, 2016[4], that cardiac damage is dependent on the frequency of periodic invasion from more permissive sites, followed by local inflammation, is supported by robust data from murine models. The next step will be to characterise the mechanistic basis of trypomastigote dissemination from immune-permissive sites. Crucially, this will involve identification of polymorphisms in immunological genes of the host, and those in the genome of the parasite, associated with the dissemination of infection and increased cardiac damage. Identifying these in the outbred human populations at the highest risk will be a significant undertaking, but could offer a novel approach to targeting even poor-quality drugs for maximum benefit.

Towards a mechanistic understanding of drug treatment failure – With the prospects of a sterilising or disease limiting vaccine remote in the short/medium term, accelerating progress towards less toxic and more efficacious drugs is paramount. Improvements, that could be introduced in the short-term, may include altered dosing regimens of current front-line compounds, either reducing the toxicity of side-effects or increasing cure rate. To better inform both efforts, the mechanics of drug treatment success and failure need to be better understood at the cellular and molecular level. The fierce debate around whether a dormant life-cycle stage exists in natural *T. cruzi* infection has intrigued researchers in the field, and has implications for chemotherapeutic outcomes. The Bustamante *et al* 2020[13] study suggests that more infrequent higher dosing of BZ, relative to current guidance, is more effective at curing infections in mice. The suggested mechanism is that short-term exposure to high BZ concentrations overcomes the ability of the

parasite to survive in a dormant or persister metabolic state. In light of the data presented here, an alternative explanation could be that short-sharp drug treatment maybe more effective against slowly replicating chronic stage parasites. If confirmed in humans, this altered regimen could offer better curative outcomes. It would still however, leave clinicians with the difficult choice of treating potentially benign infections with high doses of a toxic drug. Further information on why current frontline drugs often fail to cure human infections is essential to accelerate progress in Chagas disease management and the development of better candidate compounds.

Prospects for a sterilising Chagas disease vaccine – In my view, *T. cruzi* represents a zoonotic parasitic threat that will exist in endemic countries indefinitely, due to its successful parasitization of most mammals and unlikely elimination of the vector species. International migration is likely to increase in future decades, resulting in increased presentation of Chagas disease cases in non-endemic countries. *Triatomine* species are widespread across the tropics, giving potential for new foci of endemicity in previously non-endemic nations. Vector control remains incomplete and requires continued investment to maintain high standards of housing stock and regular spraying. An effective and practical vaccine, able to prevent infection or prevent the development of pathology in those vaccinated and subsequently infected, would be of great value. If the results presented in chapter 6 hold as a major mechanism of immune evasion in humans, as well as mice, the prospects for such a vaccine are poor. Preventing infectious metacyclic trypomastigotes from initiating the acute phase parasitaemia could prevent parasite access to the sites in which they can best avoid immunological destruction. The obstacles to this are highlighted by the large-scale trial of the anti-malaria RTS,S vaccine[14]. Antibodies targeting the short-lived infective stage sporozoites offer a measure of short-term protection from clinical disease, but this wanes rapidly over time as serum titres fall. Similar problems can be expected in candidates designed to eliminate *T. cruzi* metacyclic trypomastigotes soon after inoculation. Arguably, the most important question in *T. cruzi* vaccine research is what impact inflammatory damage has during the acute stage, and whether this is linked to future chronic pathologies. The development of vaccine candidates that significantly reduce acute phase parasite load, is at present outpacing progress towards establishing whether they can be used to improve outcomes for those who become infected. Due to the long-time spans between infection and Chagas disease pathology in humans, murine models offer a practical platform to investigate this.

References

1. Costa, F. C. et al. Expanding the toolbox for *Trypanosoma cruzi*: a parasite line incorporating a bioluminescent-flourescent dual reporter and streamlines CRISPR/Cas9 functionality for rapid *in vivo* localisation and phenotyping. *PLOS Neg. Trop. Dis*. **12**, e0006388 (2018).
2. Lewis, M. D. et al. Bioluminescence imaging of chronic *Trypanosoma cruzi* infections reveals tissue-specific parasite dynamics and heart disease in the absence of locally persistent infection. *Cell Microbiol*. **16**, 1285-300 (2014).
3. Lewis, M. D., Fransisco, A. F., Taylor, M. C., Jayawardhana, S. and Kelly, J. M. Host and parasite genetics shape a link between *Trypanosoma cruzi* infection dynamics and chronic cardiomyopathy. Cell Microbiol. 18, 1429-1443 (2016).
4. Lewis, M. D. and Kelly, J. M. Putting infection dynamics into the heart of Chagas disease. *Trends in Parasitology*. 32, 899-911 (2016).
5. Maldonado, I. R., Ferreira, M. L. Camargos, E. R., Chiari, E. and Machado, C. R. Skeletal muscle regeneration and *Trypanosoma cruzi*-induced myositis in rats. *Histol. Histopathol*. **19**, 85-93 (2004).
6. Sanchez-Valdez, F. J., Padilla, A., Wang, W., Orr, D. and Tarleton, R. L. Spontaneous dormancy protects *Trypanosoma cruzi* during extended drug exposure. *eLife*. **7**, e34039 (2018).
7. Rodríguez-Morales, O. et al. Experimental vaccines against Chagas Disease: A journey through history. *J. Immunol. Res.* **2015**, 489758 (2015).
8. Luhrs K. A., Fouts, D. L. & Manning, J. E. Immunization with recombinant paraflagellar rod protein induces protective immunity against *Trypanosoma cruzi* infection. *Vaccine.* **21**, 3058-3069 (2003).
9. Gupta, S. & Garg, N. J. TcVac3 induced control of *Trypanosoma cruzi* infection and chronic myocarditis in mice. *PLoS ONE*. **8**, e59434 (2013).
10. Arce-Fonseca, M., Rios-Castro, M., Carrillo-Sánchez, S. Martinéz-Cruz, M. & Rodrígeuz-Morales, O. Prophylactic and therapeutic DNA vaccines against Chagas disease. *Parasit. Vectors* **8**, 121 (2015).
11. Hawken, J. and Troy, S. B. Adjuvants and inactivated polio vaccine: a systematic review. *Vaccine*. **30**, 1-9 (2012).
12. Hutchinson, E. Typhoid vaccine effective. *Nature Reviews Gastoenterology and Hepatology*. **6**, 563 (2009).

13. Bustamante, J. M., Sanchez-Valdez, F., Padilla, A. M., White, B., Wang, W. Tarleton, R. L. A modified drug regimen clears active and dormant trypanosomes in mouse models of Chagas disease. *Sci. Transl. Med*. **12**, e7656 (2020).
14. Tinto, H *et al*. Long-term incidence of severe malaria following RTS,S/AS01 vaccination in children and infants in Africa: an open-label 3-year extension study of a phase 3 randomised controlled trial. *Lancet*. **19**, 821-832 (2019).

Appendix

London School of Hygiene & Tropical Medicine
Keppel Street, London WC1E 7HT
T: +44 (0)20 7299 4646
F: +44 (0)20 7299 4656
www.lshtm.ac.uk

RESEARCH PAPER COVER SHEET

Please note that a cover sheet must be completed for each research paper included within a thesis.

SECTION A – Student Details

Student ID Number	lsh1406159	**Title**	Mr
First Name(s)	Alexander		
Surname/Family Name	Ward		
Thesis Title	Trypanosoma cruzi: Where is it? Does it ever sleep? Why is a sterile outcome rarely achieved?		
Primary Supervisor	John Kelly		

If the Research Paper has previously been published please complete Section B, if not please move to Section C.

SECTION B – Paper already published

Where was the work published?	PLOS Neglected Trop. Diseases		
When was the work published?	March 2020		
If the work was published prior to registration for your research degree, give a brief rationale for its inclusion			
Have you retained the copyright for the work?*	**Yes**	Was the work subject to academic peer review?	**Yes**

*If yes, please attach evidence of retention. If no, or if the work is being included in its published format, please attach evidence of permission from the copyright holder (publisher or other author) to include this work.

SECTION C – Prepared for publication, but not yet published

Where is the work intended to be published?	
Please list the paper's authors in the intended authorship order:	
Stage of publication	Choose an item.

SECTION D – Multi-authored work

For multi-authored work, give full details of your role in the research included in the paper and in the preparation of the paper. (Attach a further sheet if necessary)	I am joint first author on this paper. My contribution was in the development of the methods involving EdU labelling and generation and interpretation of the data presented in Figures 4, 5 and 6. I provided the first draft of the corresponding parts of the paper. Final edit was done John Kelly and Martin Taylor.

SECTION E

Student Signature	Alexander Ward
Date	09/07/2020

Supervisor Signature	John Kelly
Date	10/07/2020

See https://journals.plos.org/plosntds/article?id=10.1371/journal.pntd.0008007 for the on-line version.

Intracellular DNA replication and differentiation of *Trypanosoma cruzi* is asynchronous within individual host cells *in vivo* at all stages of infection

Martin. C. Taylor*+, Alexander Ward+, Francisco Olmo+, Shiromani Jayawardhana+ Amanda F. Francisco, Michael D. Lewis and John M. Kelly

Faculty of Infectious and Tropical Diseases, London School of Hygiene and Tropical Medicine, London, UK

*Corresponding author: martin.taylor@lshtm.ac.uk (MCT)

+ Contributed equally to the work

Short title: Replication and differentiation of *T. cruzi in vivo*

ABSTRACT

Investigations into intracellular replication and differentiation of *Trypanosoma cruzi* within the mammalian host have been restricted by limitations in our ability to detect parasitized cells throughout the course of infection. We have overcome this problem by generating genetically modified parasites that express a bioluminescent/fluorescent fusion protein. By combining *in vivo* imaging and confocal microscopy, this has enabled us to routinely visualise murine infections at the level of individual host cells. These studies reveal that intracellular parasite replication is an asynchronous process, irrespective of tissue location or disease stage. Furthermore, using TUNEL assays and EdU labelling, we demonstrate that within individual infected cells, replication of both mitochondrial (kDNA) and nuclear genomes is not co-ordinated within the parasite population, and that replicating amastigotes and non-replicating trypomastigotes can co-exist in the same cell. Finally, we report the presence of distinct non-canonical morphological forms of *T. cruzi* in the mammalian host. These appear to represent transitional forms in the amastigote to trypomastigote differentiation process. Therefore, the intracellular life-cycle of *T. cruzi in vivo* is more complex than previously realised, with potential implications for our understanding of disease pathogenesis, immune evasion and drug development. Dissecting the mechanisms involved will be an important experimental challenge.

AUTHOR SUMMARY

Chagas disease, caused by the protozoan parasite T*rypanosoma cruzi,* is becoming an emerging threat in non-endemic countries and establishing new foci in endemic countries. The treatment available has not changed significantly in over 40 years. Therefore, there is an urgent need for a greater understanding of parasite biology and disease pathogenesis to identify new therapeutic targets and to maximise the efficient use of existing drugs. We have used genetically modified strains of *T. cruzi* carrying a bioluminescence/fluorescence dual reporter fusion gene to monitor parasite replication *in vivo* during both acute and chronic infections in a mouse model. Utilising TUNEL assays for mitochondrial DNA replication and EdU incorporation for total DNA replication, we have found that parasite division within infected cells is asynchronous in all phases of infection. Differentiation also appears to be uncoordinated, with replicating amastigotes co-existing with non-dividing trypomastigotes in the same host cell.

INTRODUCTION

The obligate intracellular parasite *Trypanosoma cruzi* is responsible for Chagas disease, a debilitating infection that is widespread in Latin America. There are an estimated 6-7 million people infected [1]. In addition, due to migration, cases are increasingly being detected outside endemic regions [2, 3]. *T. cruzi* is spread by blood-sucking triatomine bugs, although oral transmission via contaminated food or drink, and the congenital route are also important. The parasite has a wide mammalian host range and can infect most nucleated cells. During its life-cycle, the major features of which were established more than a century ago [4], *T. cruzi* passes through a number of differentiation stages involving both replicative and non-replicative forms. Infections are initiated by insect transmitted metacyclic trypomastigotes, which are flagellated and non-replicating. Once these have invaded host cells, they escape from the parasitophorous vacuole into the cytosol, differentiate into ovoid non-motile amastigotes, and divide by binary fission. After a period of approximately 4-7 days, by which time parasite numbers can have reached several hundred per infected cell, they differentiate into non-replicating flagellated motile trypomastigotes. This eventually promotes host cell lysis, and the released parasites then invade other cells, spread systemically through blood and tissue fluids, or can be taken up by triatomine bugs during a bloodmeal. Within the insect vector, they differentiate into replicating epimastigotes, and finally metacyclic trypomastigotes, to complete the cycle.

More recently, *in vitro* studies have suggested that the parasite life-cycle may be more complex than outlined above. These reports include the identification of an intracellular epimastigote-like form [5], and amastigote-like forms with short flagella, termed sphaeromastigotes [6]. Whether these parasite forms represent intermediate transitional types, or correspond to intracellular stages with a specific role, remains to be determined. Adding to the complexity, trypomastigotes can also differentiate into an epimastigote-like stage, via an amastigote-like transitional form [7]. These recently differentiated epimastigotes have a distinct proteomic profile, display complement-resistance, can invade phagocytic and cardiac cells, and are infectious to mice. In addition, it has been reported that when bloodstream trypomastigotes invade mammalian cells, they can undergo a differentiation step in which asymmetric cell division results in the generation of an amastigote, together with a second, defective parasite cell termed a zoid, which contains a kinetoplast, but lacks a nucleus [8]. This has not, as yet, been demonstrated for the metacyclic trypomastigote which initiates natural mammalian infection. Most recently, it has been observed that infrequent spontaneous dormancy can

occur in intracellular amastigotes, a phenomenon that may be linked to increased drug tolerance [9]. These non-proliferating intracellular amastigotes, which have been identified both *in vivo* and *in vitro,* retain the ability to differentiate into trypomastigotes. Their metabolic status is unknown. To date, a lack of sufficiently sensitive *in vivo* parasite detection methods has meant that it has not been possible to investigate the biological role of these and the other non-classical parasite forms during either acute or chronic stage infections.

There are three distinct stages to Chagas disease. In humans, the acute stage occurs in the first 4-6 weeks, and is characterised by a widely disseminated infection, together with patent parasitemia. This results in the induction of a robust $CD8^+$ T cell-mediated response [10], with infected individuals then progressing to the asymptomatic chronic stage, where the parasite burden is extremely low and difficult to detect. Around 30-40% of those infected eventually develop chronic disease pathology, predominantly cardiomyopathy and/or digestive tract megasyndromes [11, 12]. In humans, infections with *T. cruzi* are considered to be life-long, however our understanding of parasite biology and tropism during the chronic stage, and their relationship to disease outcome are limited [13]. To address these issues, we developed an experimental murine model based on highly sensitive bioluminescence imaging of *T. cruzi* genetically modified to express a red-shifted luciferase [14, 15]. This system allows chronic infections to be followed in real time for periods of longer than a year, and enables endpoint assessment of parasite location by *ex vivo* imaging. In this mouse model, the infection is pan-tropic during the acute stage and parasites are readily detectable in almost all organs and tissues. During the chronic stage however, the parasite burden is very low and restricted mainly to the colon and/or stomach, with other organs/tissues infected only sporadically [14, 16].

Although bioluminescence can be widely used for *in vivo* testing of drugs and vaccines, and as a technique for exploring infection kinetics and dynamics, it does not easily allow the identification or study of single parasites at a cellular level [16-19]. To overcome this limitation, we re-engineered the *T. cruzi* strain to express a bioluminescent/fluorescent fusion protein [20]. The aim was to enable infection dynamics to be monitored at a whole animal level using bioluminescence, followed by investigation of host-parasite interactions at a single cell level using fluorescence. With this approach, we have been able to routinely image individual parasites in murine tissues during chronic stage infections. This has allowed us to readily

visualise parasites residing within individual host cells in chronically infected animals. Here, we describe the exploitation of this dual imaging procedure to gain new insights into parasite biology in experimental models of acute and chronic Chagas disease.

METHODS

Parasite culture

T. cruzi CL-Luc::Neon epimastigotes were cultured in supplemented RPMI-1640 as described previously [21]. Genetically manipulated lines were routinely maintained on their selective agent (hygromycin, 150 µg ml^{-1}; puromycin, 5 µg ml^{-1}; blasticidin, 10 µg ml^{-1}; G418, 100 µg ml^{-1}). MA-104 (fetal African green monkey kidney epithelial) cells (ATCC CRL-2378.1) were cultivated to 95–100% confluency in Minimum Essential Medium Eagle (MEM, Sigma.), supplemented with 5 % Foetal Bovine Serum (FBS), 100 U/ml of penicillin, and 100 µg ml^{-1} streptomycin at 37°C and 5% CO_2. Tissue culture trypomastigotes (TCTs) were derived by infecting MA104 cells with stationary phase metacyclic trypomastigotes. Cell cultures were infected for 18 hours. External parasites were then removed by washing in Hank's Balanced Salt Solution (Sigma-Aldrich), and the flasks incubated with fresh medium (Minimum Essential Medium (Sigma-Aldrich) supplemented with 5% FBS) for a further 5-7 days. Extracellular TCTs were isolated by centrifugation at 1600 *g*. Pellets were re-suspended in Dulbecco's PBS and motile trypomastigotes counted using a haemocytometer. *In vitro* infections for microscopy were carried out as above, but on coverslips incubated in 24-well plates using an MOI of 5:1 (host cell:parasite). Coverslips were fixed with 2% paraformaldehyde at 72 hours post infection. Cells were then labelled with TUNEL (section 4.6).

Ethics statement

All animal work was performed under UK Home Office licence 70/8207 and approved by the London School of Hygiene and Tropical Medicine Animal Welfare and Ethical Review Board. All protocols and procedures were conducted in accordance with the UK Animals (Scientific Procedures) Act 1986.

Mouse infection and necropsy

Mice were maintained under specific pathogen-free conditions in individually ventilated cages. They experienced a 12 hour light/dark cycle and had access to food and water *ad libitum*. Female mice aged 8-12

weeks were used. CB17 SCID mice were infected with $1x10^4$ tissue culture trypomastigotes, and monitored by bioluminescence imaging (BLI), as previously reported [14]. At the peak of the bioluminescence signal, when trypomastigotes were visible in the bloodstream, the mouse was culled by an overdose of pentobarbital sodium, and the infected blood obtained by exsanguination. The trypomastigotes were washed in Dulbecco's PBS and diluted to $5x10^3$ ml^{-1}. $1x10^3$ trypomastigotes were injected i.p. into each mouse (BALB/c or C3H/HeN) and the course of infection followed by BLI. At specific time-points, the mice were euthanised by an overdose of pentobarbital sodium and necropsied (for detailed description of the necropsy method, see Taylor *et al*., 2019). Their organs were subject to *post mortem* BLI. We excised those segments that were bioluminescence-positive and placed them into histology cassettes. BLI images from living animals and *post-mortem* tissues were analysed using Living Image 4.5.4 (PerkinElmer Inc.)

Tissue embedding and sectioning

Tissue sections were produced as described previously [20, 22]. Briefly, excised tissue was fixed in pre-chilled 95% ethanol for 20-24 hours in histology cassettes. The tissues were dehydrated in 100% ethanol, cleared in xylene, and then embedded in paraffin at 56°C. Sections were cut with a microtome and mounted on glass slides, then dried overnight. Slides were stored in the dark at room temperature until required.

TUNEL assay for kDNA replication

For *in vitro* studies, logarithmically growing epimastigotes and infected mammalian cells on coverslips were fixed with 2% paraformaldehyde in PBS. Fixed epimastigotes were air-dried onto glass 8-well slides. Cells were washed once in PBS and permeabilized in 0.1% TritonX-100/PBS for 5 min and washed 3 times with PBS. 20 µL TUNEL reaction mixture (In situ Cell Death Detection Kit, TMR-red, Roche) was added to each well or coverslip and the reaction incubated for 1 hour at 37°C. For tissue sections, slides were deparaffinised in 2 changes (30 s each) of xylene, 3 changes (1 min each) of pre-chilled 95% ethanol, and 3 changes (1 min each) of pre-chilled Tris-buffered saline (TBS). Sections were outlined with a hydrophobic pen then permeabilized in 0.1% TritonX-100/PBS for 5 min and washed 3 times with PBS. 20 µL TUNEL reaction mixture was added to each section and the slide was overlaid with a coverslip to ensure that the reaction mix was evenly distributed. The reaction was incubated for 20 min to 2 hours at 37°C. Coverslips and slides were

mounted in VECTASHIELD® with DAPI (Vector Laboratories, Inc.) before observation on a Zeiss Axioplan LSM510 confocal microscope.

EdU assay for DNA replication

Mice were injected intraperitoneally with 12.5 mg kg^{-1} EdU (Sigma-Aldrich) in PBS at specific time points (as detailed in Results) prior to euthanasia. Tissues were fixed and sectioned as above. Labelling of the incorporated EdU was carried out using the Click-iT Plus EdU AlexaFluor 555 Imaging kit (Invitrogen), following a similar method as used for TUNEL labelling, but substituting the Click-iT reagent for the TUNEL reaction mix. For sections which had been in paraffin for extended time periods (> 6 months), the slides were immersed in 100 mM EDTA for 16 hours (on manufacturer's recommendation), then washed extensively with TBS prior to the Click-iT reaction.

Confocal microscopy

Slides and sections were examined using a Zeiss LSM510 Axioplan confocal laser scanning microscope. Cells containing multiple parasites were imaged in three dimensions to allow precise counting of amastigotes (using the 63x or 100x objectives with appropriate scan zoom for the particular cell/number of parasites). Phase images were obtained at lower magnification (40x) to allow orientation of the tissue section and identification of specific layers/structures. All images were acquired using Zeiss LSM510 software. Scale bars were added using the Zeiss LSM Image Browser overlay function and the images were then exported as .TIF files to generate the figures.

Live imaging of infected cells.

Videos were acquired using an inverted Nikon Eclipse microscope. The chamber containing the specimen was moved in the x-y plane through the 580 nm LED illumination. Images were collected using a 16-bit, 1-megapixel Pike AVT (F-100B) CCD camera set in the detector plane. An Olympus LMPlanFLN 20x/0.40 objective was used to collect the exit wave leaving the specimen. Time-lapse imaging was performed by placing the chamber slide on the microscope surrounded by an environmental chamber (Solent Scientific Limited, UK) maintaining the cells and the microscope at 37°C / 5% CO_2. Time-lapse video sequences were created using the deconvolution app in the Nikon imaging software.

RESULTS

Parasite kinetoplast DNA replication is not synchronised within individual infected cells.

The text book view of the *T. cruzi* intracellular cycle is that invading trypomastigotes differentiate into amastigotes, which then begin to divide by binary fission within the cytoplasm of the host cell. These then differentiate into trypomastigotes and the host cell lyses releasing the trypanosomes, see for example Figure 1a in [23]. However, the degree to which amastigote division and differentiation are co-ordinated within single cells, and the potential for this to be influenced by host cell type and/or tissue-specific location are poorly understood.

During trypanosomatid cell division there are two distinct DNA replication events that result in duplication of the mitochondrial (kinetoplast or kDNA) and then the nuclear genomes. However, at early stages of kDNA or nuclear DNA replication, it is not feasible to assign parasites to a particular cell-cycle phase by morphology or total DNA staining, as many parasites appear similar. To identify the replication status of the mitochondrial genome in intracellular amastigotes we took advantage of the TUNEL assay (terminal deoxynucleotidyl transferase dUTP nick end labelling), a procedure normally used to quantify apoptotic cell death in mammalian cells [24]. In *T. cruzi*, this assay can be utilised to monitor kDNA replication [20], a genome that consists of thousands of catenated circular double-stranded DNA molecules. The majority of these are the mini-circles that encode the guide RNAs that mediate RNA editing [25]. To maintain functional RNA editing, daughter cells must each inherit copies of the entire mini-circle repertoire. During replication, mini-circles are first detached from the catenated network and the new strands are then synthesised. However, some of the single-strand breaks that result from removal of RNA primers in the newly synthesised DNA are maintained until the whole mini-circle network has been replicated. This enables newly duplicated circles to be distinguished from non-replicated circles and ensure each daughter network is complete [26, 27]. Therefore, during the S-phase of kDNA replication, the free 3’ hydroxyl groups at the nicks on the newly synthesised strands can be labelled with a fluorescent analogue by terminal uridylyl transferase [20, 26, 28]. This means that the TUNEL assay enables specific labelling of parasites that have commenced cell division.

We first applied TUNEL assays to asynchronous, exponentially growing epimastigote cultures to confirm that this method was applicable to *T. cruzi*. Parasites in the early phase of kDNA synthesis displayed TUNEL

positivity in antipodal sites on either side of the kDNA disk, indicative of the two replication factories (Figure 1a). Later in replication, the entire disk was labelled (Figure 1b). Nuclear DNA did not exhibit a positive signal at any stage (Figure 1a and b).

To quantify the replication of kDNA in intracellular amastigotes, the parasites in 200 infected cells were assessed for TUNEL positivity *in vitro* 72 hours post-infection. These cultures were infected with a low multiplicity of infection (1 parasite per 5 host cells) to minimise the chance of individual cells being infected twice. It was apparent that kDNA replication within single infected cells was largely asynchronous, since most infected cells contained both TUNEL+ve and –ve amastigotes (Figure 1c and d). Most TUNEL+ve parasites displayed antipodal staining, indicative of early phase replication (see examples in Figure 1c). The number of amastigotes displaying whole disk staining was low suggesting that kDNA nick repair may occur more rapidly than in epimastigotes. The few amastigotes that displayed a 2K1N morphology showed no TUNEL staining on either kinetoplast, indicating that nicks are repaired prior to segregation, as expected (example shown in Figure S1) [26].

Total amastigote numbers within infected cells were also consistent with asynchronous replication; they did not follow a geometric progression as would be expected if growth was co-ordinated (Figure 1d, red line). There were no cases where a specific number of amastigotes within a cell was always associated with 100% TUNEL labelling (Figure S2). Intracellular populations of 2, 4 or 8 amastigotes were equally as likely to be asynchronous as populations containing non-geometric numbers (Figure 1d, black bars, Figure S2). In the minority of infected cells where every amastigote was TUNEL+ve (14.5% of cells that contained more than one parasite), there were differences in the degree of labelling between the parasites in 24% of the host cells (Figure 1c inset, for example, white arrows indicate faint TUNEL labelling of one amastigote in earlier phase of kDNA replication). Collectively, these results therefore show that within a single infected cell *in vitro*, amastigote kDNA replication is not synchronised within the population.

We then applied the TUNEL assay to mouse tissues obtained from acute experimental infections with the dual bioluminescent/fluorescent *T. cruzi* cell line CL-Luc::Neon [20]. The acute phase in mice is characterised by widespread dissemination of infection with amastigotes in diverse cell and tissue types. We sampled a

range of organs and tissues (Figure 2; Figure S3). This revealed that within any given infected host cell, the extent of kDNA labelling varied between parasites. We quantified the frequency of TUNEL positivity amongst amastigotes in sections from various organs in a single mouse (Figure 3). The majority of amastigotes in the acute phase had TUNEL+ve kDNA, showing that they were undergoing replication. However, there was no evidence for programmed synchronicity, and in each tissue, individual cells could contain both TUNEL+ve and TUNEL-ve parasites. Moreover, all of the different organs that were analysed showed similar profiles with respect to parasite replication states (Figure 3).

Replication of parasite nuclear DNA is not synchronised within individual infected host cells.

TUNEL assays identify parasites where kDNA replication has initiated, but do not provide information on those where it has terminated and the parasite has progressed to nuclear DNA synthesis. To get a more quantitative picture of both nuclear and kinetoplast replication, we injected *T. cruzi*-infected mice with the nucleoside analogue 5-ethynyl-2'-deoxyuridine (EdU) at specific time points prior to necropsy [29]. We chose EdU rather than BrdU, since this analogue can be fluorescently labelled directly in double stranded DNA and does not require harsh denaturing conditions. This preserves the mNeonGreen fluorescence used to locate *T. cruzi in situ*. EdU is incorporated into newly synthesised DNA molecules and identifies parasites undergoing nuclear or kDNA replication during the time period of the EdU pulse. It also labels mammalian cells that enter S-phase during this period. EdU distribution in murine tissues is extensive and incorporation is stable. For example, Merkel cells from mice whose mothers were injected with EdU during pregnancy remain labelled nine months after birth, suggesting that the analogue is not removed during DNA repair [30-32]. Labelling of replicating host cells within a given tissue section can therefore be used as an internal control for EdU tissue penetration to sites of *T. cruzi* infection. Fixed tissue sections containing host cells and/or parasites that incorporate EdU are fluorescently labelled by click chemistry and can be examined by confocal microscopy [33] (Experimental procedures).

We assessed a range of bioluminescence positive tissues excised from mice in the acute stage of infection (Figure 4). In cardiac sections, there was negligible labelling of host cell nuclei, as expected, since heart muscle consists predominantly of terminally differentiated non-replicative cells. However, labelled intracellular parasites were easily detected. Within host cells containing multiple parasites, EdU labelling was

heterogeneous across the population and many parasites had not incorporated EdU (Figure 4a) during the time of exposure. Similarly, in adipose tissue, parasites within the same infected cells displayed a wide range of EdU specific fluorescence intensity (Figure 4b). This heterogeneity was dispersed throughout the infected cell, with replicating and non-replicating organisms being interspersed.

In gut sections obtained from chronically infected mice, EdU labelling of host cells in the mucosal epithelium was readily apparent, since these cells are continually shed into the gut lumen and replaced from stem cells (Figure 4c, white arrowheads). As in the acute stage, the labelling pattern within amastigote "nests" was consistent with asynchronous replication of nuclear DNA, with many parasites showing no detectable EdU incorporation (Figure 4c; Figure S4a and b). We also analysed sections taken from tissue samples that contained all of the detectable bioluminescent foci in the gastrointestinal tract of three individual chronically infected C3H/HeN mice (M275-17, M277-17 and M279-17). We injected these animals with two pulses of EdU at 18 and 28 hours before euthanasia. The number of parasites and infected cells was consistent with the strength of the bioluminescent signal visible on *ex-vivo* organ sections (Figure 5a). Some of the nests were very large ("mega-nests"), containing hundreds of parasites, and in some cases, they clearly extended beyond the limits of the tissue section (indicated by asterisks, Figure 5b, c). However, examination of serial sections of a single large nest indicated that the asynchronous nature of EdU incorporation was sustained throughout the nest (Figure 6), since in each section there were both EdU+ve and Edu-ve amastigotes. The extent of EdU labelling within amastigotes in an infected cell was variable as had been observed with the TUNEL assay. This would be expected if parasites were sampled at different stages within S-phase. It was clear that many parasites had not replicated during the period of EdU exposure because most amastigotes (77% in the GI tract, 62% in the peritoneal muscle) were negative for EdU labelling in either kinetoplast or nucleus. Therefore, both TUNEL assays and EdU incorporation demonstrate that *in vivo*, the timing of DNA replication is autonomous to individual parasites within an infected host cell, with no evident synchronisation of the process between different amastigotes.

Both replicating and differentiating parasites co-exist in the same host cell

The final step in the intracellular development of *T. cruzi* is differentiation of replicating amastigotes into non-dividing flagellated trypomastigotes, prior to their escape from the host cell. The mechanisms that regulate

this process *in vivo,* from a temporal and organisational perspective, are unknown. In mammalian cell monolayers infected *in vitro*, we observed that amastigotes could be detected in the same cells as differentiated trypomastigotes (Figure 7a). We used the TUNEL assay to examine whether amastigotes in this environment were undergoing replication or were about to differentiate. Antipodal TUNEL staining was observed in the kinetoplasts of some amastigotes present in cells with trypomastigotes indicating ongoing kDNA replication (Figure 7b). Co-existence of replicating parasites with trypomastigotes was confirmed by live-cell imaging of infected cells *in vitro* (Figure S5, Movie S1). This suggested asynchronicity in the process of both differentiation and cell division. Amastigotes can therefore initiate a new replicative phase while in the same host cell as parasites that have differentiated to trypomastigotes as judged by morphology and flagellar position. It remains possible that some amastigotes initiate replication but then "pause", leading to TUNEL+ve parasites co-existing with flagellated trypomastigotes.

Multiple morphological forms of *T. cruzi* are present in deep tissues of infected mice

Classically, the *T. cruzi* life-cycle in mammals involves two distinct morphological stages, the intracellular replicative amastigote, which lacks an external flagellum, and the non-replicating extracellular flagellated trypomastigote. However, other forms of the parasite have been observed under *in vitro* conditions (for review, [34]). These observations normally involve only one host cell type, and lack environmental signals and a tissue milieu. Therefore, it has not been possible to be assess if these non-classical forms are physiologically relevant during host infections, or whether they are artefacts of *in vitro* culture.

We observed a number of distinct *T. cruzi* morphological forms during murine infections that do not conform to the standard amastigote/trypomastigote dichotomy. In both acute and chronic infections, we frequently visualised amastigote-like forms with a protruding flagellum (Figure 8). This flagellum extended from the anterior of the parasite, based on the relative position of the kinetoplast and nucleus (Figure 8a-c). The kinetoplast and nucleus displayed the forms associated with the replicative stages of the parasite. The length of the visible flagellum was highly variable with the majority of amastigotes having no protruding flagellum. (Figure 8d). The length of the amastigote cell body varied between 3 and 7 µm (mean 4.2 ± 0.8 µm) with the flagellar length being independent of cell body length (Figure 8c and e). The flagellated amastigote-like

parasites have similarities to sphaeromastigotes (Tyler & Engman, 2001), a form that has been observed *in vitro*.

In addition to the flagellated amastigote-like parasites, we also observed a second non-standard form that displays an epimastigote-like morphology (Figure 8c, orange box and inset). Similar forms have been reported once before in a very early stage of infection (day 8) [35]. These epimastigote-like forms, which we detected repeatedly in tissue samples, often co-existed with dividing amastigotes and differentiating trypomastigotes in the same infected cell, and could be observed by live cell imaging *in vitro* (Figure S5). Whether these forms are simply morphological intermediates, or have a distinct role in infection or transmission remains unknown.

DISCUSSION

The broad outline of *T. cruzi* replication and stage-specific differentiation during mammalian infection has been known for more than a century. However, it is clear that this part of the life-cycle is more complex than previously described, with possible implications for our understanding of pathogenesis, immune evasion and transmission [34]. Unravelling the biology of *T. cruzi* within the host is also crucial from a drug development perspective, since some life-cycle stages may be less sensitive to treatment [9], and the ability of the parasite to reside in metabolically distinct tissue compartments may have significant effects on drug exposure and pharmacodynamics. To date, most research on *T. cruzi* replication and differentiation has utilised *in vitro* systems. Although these are informative, they may not capture the full developmental range, and could give rise to artefactual observations that are not relevant to these processes within the mammalian host. In addition, *in vitro* cultures often use immortalised mammalian cell lines, whereas *in vivo T. cruzi* is usually found in non-replicating terminally differentiated cells such as muscle fibres.

One of the major unknowns in *T. cruzi* biology is the extent to which parasite growth is co-ordinated within individual host cells during a mammalian infection, and how it is influenced by tissue/organ location and disease status. This issue has been highlighted by recent reports of spontaneous dormancy during intracellular infection (Sánchez-Valdéz et al., 2018). Here, using a bioluminescent/fluorescent dual reporter strain that significantly enhances our ability to identify and visualise infected host cells *in vivo*, we provide

evidence that intracellular replication is largely asynchronous. From observation, it is apparent that the number of parasites per host cell does not follow a predictable or tightly regulated pattern *in vitro* (Figure 1, Figure S2), or *in vivo*, at any phase of the infection, or in any specific tissues (Figures 2-6). Consistent with this, two separate assays indicate that, within individual infected cells, DNA replication is not synchronised between parasites at either nuclear or kinetoplast genome levels (Figures 2-6, S3, S4). In the case of EdU labelling, this was not a reflection of differential tissue penetration, since replicating amastigotes were interspersed with non-labelled parasites in a wide range of tissues types, during both acute and chronic infections. TUNEL labelling is not dependent on incorporation of nucleoside analogues in a living mouse and is therefore an orthogonal assay for mitochondrial DNA replication.

The finding that extremely large nests of asynchronously dividing or differentiating parasites can exist in chronically infected animals (Figure 6 and Figure S4) could have therapeutic implications. Infected cells such as these may contain parasites in a range of metabolic states (including dormancy) that exhibit heterogeneity in terms of drug susceptibility. In addition, the possibility that these *in vivo* mega-nests could result in some form of intracellular “herd-protection” may give rise to an environment that is difficult to replicate in the standard *in vitro* assays used in the drug development pipeline.

Single infected cells can contain both replicating amastigotes and non-replicating, differentiated trypomastigotes (Figure 7). Therefore, whatever the signal(s) that trigger differentiation and/or replication, they are not perceived and/or acted on in concert by every parasite within the nest. This contrasts with the related extracellular parasite *T. brucei* in which a well-characterised quorum sensing pathway initiates differentiation from the replicative long slender bloodstream form to the non-replicating short stumpy form, preadapted for transmission to the tsetse fly vector [36-39]. The lack of synchrony in differentiation between amastigote, intracellular “epimastigote” and trypomastigote, during *T. cruzi* infection, indicates that either a ubiquitous quorum sensing mechanism of this kind does not operate within single infected host cells, or that some parasites remain refractory to the trigger signal, as exemplified by the quiescent amastigotes identified recently [9].

The dual reporter parasite strain also enabled us to identify a number of non-standard parasite forms in tissues of infected mice, sometimes co-existing within the same host cell (Figure 5, Figure S5). The role of the intracellular and extracellular epimastigote-like, and flagellated amastigote-like forms in the parasite life-cycle remains to be determined. Their relative scarcity suggests that they could be transient forms which occur during the differentiation from amastigote to trypomastigote. Importantly, detection of these morphological forms *in vivo* excludes the possibility that they represent laboratory culture artefacts. Intriguingly, in this context, it has been established that in the opossum, an ancient natural host of *T. cruzi*, there is an insect stage-like epimastigote cycle within the anal glands. This appears to exist independently of the intracellular pathogenic cycle found in other tissues [40]. It has also been demonstrated that trypomastigotes can exist in two distinct populations (TS+ and TS-, referring to *trans*-sialidase surface expression). TS- parasites are poorly infective to mammalian cells and significantly less virulent in mice [41]. This suggests that the two populations may have distinct roles, one perhaps preadapted for invasion of the insect vector, and the other for propagation of infection within the mammalian host, analogous to the slender and stumpy forms of *T. brucei.*

In conclusion, this study reports the first detailed analysis of *T. cruzi* replication in animals at the level of single infected cells within a range of tissue types. The data reveal the complexity of parasite replication and differentiation cycles, and confirm the existence *in vivo* of parasites with a non-classical morphology. The presence of even transient non-canonical forms in infected animals highlights important questions about their susceptibility to trypanocidal drugs, compared with standard amastigotes. Similarly, it is unknown whether these forms express the same surface protein repertoire as amastigotes and/or trypomastigotes, if they are equally targeted by anti-parasite antibodies in the bloodstream and tissue fluids, or if they retain the ability to infect other cells and disseminate the infection. It will now be important to develop procedures to isolate these non-classical parasite types in sufficient numbers to allow their biochemical and biological characterisation.

References

1. WHO. Chagas disease (American Trypanosomiasis) 2019. Available from: www.who.int/news-room/fact-sheets/detail/chagas-disease-(american-trypanosomiasis).
2. Bern C, Kjos S, Yabsley MJ, Montgomery SP. Trypanosoma cruzi and Chagas' Disease in the United States. Clin Microbiol Rev. 2011;24(4):655-81.

3. Requena-Mendez A, Aldasoro E, de Lazzari E, Sicuri E, Brown M, Moore DA, et al. Prevalence of Chagas disease in Latin-American migrants living in Europe: a systematic review and meta-analysis. PLoS Negl Trop Dis. 2015;9(2):e0003540.
4. Chagas C. Nova tripanozomiaze humana: estudos sobre a morfolojia e o ciclo evolutivo do Schizotrypanum cruzi n. gen., n. sp., ajente etiolojico de nova entidade morbida do homem. Memorias do Instituto Oswaldo Cruz. 1909;1(2):159-218.
5. Almeida-de-Faria M, Freymuller E, Colli W, Alves MJ. Trypanosoma cruzi: characterization of an intracellular epimastigote-like form. Exp Parasitol. 1999;92(4):263-74.
6. Tyler KM, Engman DM. The life cycle of Trypanosoma cruzi revisited. Int J Parasitol. 2001;31(5-6):472-81.
7. Kessler RL, Contreras VT, Marliere NP, Aparecida Guarneri A, Villamizar Silva LH, Mazzarotto G, et al. Recently differentiated epimastigotes from Trypanosoma cruzi are infective to the mammalian host. Mol Microbiol. 2017;104(5):712-36.
8. Kurup SP, Tarleton RL. The Trypanosoma cruzi flagellum is discarded via asymmetric cell division following invasion and provides early targets for protective CD8(+) T cells. Cell Host Microbe. 2014;16(4):439-49.
9. Sanchez-Valdez FJ, Padilla A, Wang W, Orr D, Tarleton RL. Spontaneous dormancy protects Trypanosoma cruzi during extended drug exposure. Elife. 2018;7.
10. Tarleton RL. CD8+ T cells in Trypanosoma cruzi infection. Semin Immunopathol. 2015;37(3):233-8.
11. Ribeiro AL, Nunes MP, Teixeira MM, Rocha MO. Diagnosis and management of Chagas disease and cardiomyopathy. Nat Rev Cardiol. 2012;9(10):576-89.
12. Cunha-Neto E, Chevillard C. Chagas disease cardiomyopathy: immunopathology and genetics. Mediators Inflamm. 2014;2014:683230.
13. Lewis MD, Kelly JM. Putting Infection Dynamics at the Heart of Chagas Disease. Trends Parasitol. 2016;32(11):899-911.
14. Lewis MD, Fortes Francisco A, Taylor MC, Burrell-Saward H, McLatchie AP, Miles MA, et al. Bioluminescence imaging of chronic Trypanosoma cruzi infections reveals tissue-specific parasite dynamics and heart disease in the absence of locally persistent infection. Cell Microbiol. 2014;16(9):1285-300.
15. Lewis MD, Francisco AF, Taylor MC, Kelly JM. A new experimental model for assessing drug efficacy against Trypanosoma cruzi infection based on highly sensitive in vivo imaging. J Biomol Screen. 2015;20(1):36-43.
16. Lewis MD, Francisco AF, Taylor MC, Jayawardhana S, Kelly JM. Host and parasite genetics shape a link between Trypanosoma cruzi infection dynamics and chronic cardiomyopathy. Cell Microbiol. 2016;18(10):1429-43.
17. Francisco AF, Jayawardhana S, Lewis MD, White KL, Shackleford DM, Chen G, et al. Nitroheterocyclic drugs cure experimental Trypanosoma cruzi infections more effectively in the chronic stage than in the acute stage. Sci Rep. 2016;6:35351.
18. Francisco AF, Lewis MD, Jayawardhana S, Taylor MC, Chatelain E, Kelly JM. Limited Ability of Posaconazole To Cure both Acute and Chronic Trypanosoma cruzi Infections Revealed by Highly Sensitive In Vivo Imaging. Antimicrob Agents Chemother. 2015;59(8):4653-61.
19. Taylor MC, Lewis MD, Fortes Francisco A, Wilkinson SR, Kelly JM. The Trypanosoma cruzi vitamin C dependent peroxidase confers protection against oxidative stress but is not a determinant of virulence. PLoS Negl Trop Dis. 2015;9(4):e0003707.
20. Costa FC, Francisco AF, Jayawardhana S, Calderano SG, Lewis MD, Olmo F, et al. Expanding the toolbox for Trypanosoma cruzi: A parasite line incorporating a bioluminescence-fluorescence dual reporter and streamlined CRISPR/Cas9 functionality for rapid in vivo localisation and phenotyping. PLoS Negl Trop Dis. 2018;12(4):e0006388.
21. Kendall G, Wilderspin AF, Ashall F, Miles MA, Kelly JM. Trypanosoma cruzi glycosomal glyceraldehyde-3-phosphate dehydrogenase does not conform to the 'hotspot' topogenic signal model. EMBO J. 1990;9(9):2751-8.
22. Taylor MC, Francisco AF, Jayawardhana S, Mann GS, Ward AI, Olmo F, et al. Exploiting Genetically Modified Dual-Reporter Strains to Monitor Experimental Trypanosoma cruzi Infections and Host-Parasite Interactions. Methods Mol Biol. 2019;1955:147-63.
23. Dumoulin PC, Burleigh BA. Stress-Induced Proliferation and Cell Cycle Plasticity of Intracellular Trypanosoma cruzi Amastigotes. MBio. 2018;9(4).
24. Gavrieli Y, Sherman Y, Ben-Sasson SA. Identification of programmed cell death in situ via specific labeling of nuclear DNA fragmentation. J Cell Biol. 1992;119(3):493-501.

25. Sturm NR, Simpson L. Kinetoplast DNA minicircles encode guide RNAs for editing of cytochrome oxidase subunit III mRNA. Cell. 1990;61(5):879-84.
26. Guilbride DL, Englund PT. The replication mechanism of kinetoplast DNA networks in several trypanosomatid species. J Cell Sci. 1998;111 (Pt 6):675-9.
27. Liu B, Liu Y, Motyka SA, Agbo EE, Englund PT. Fellowship of the rings: the replication of kinetoplast DNA. Trends Parasitol. 2005;21(8):363-9.
28. Mandell MA, Beverley SM. Continual renewal and replication of persistent Leishmania major parasites in concomitantly immune hosts. Proc Natl Acad Sci U S A. 2017;114(5):E801-E10.
29. Salic A, Mitchison TJ. A chemical method for fast and sensitive detection of DNA synthesis in vivo. Proc Natl Acad Sci U S A. 2008;105(7):2415-20.
30. Wright MC, Logan GJ, Bolock AM, Kubicki AC, Hemphill JA, Sanders TA, et al. Merkel cells are long-lived cells whose production is stimulated by skin injury. Dev Biol. 2017;422(1):4-13.
31. Bordiuk OL, Smith K, Morin PJ, Semenov MV. Cell proliferation and neurogenesis in adult mouse brain. PLoS One. 2014;9(11):e111453.
32. King JB, von Furstenberg RJ, Smith BJ, McNaughton KK, Galanko JA, Henning SJ. CD24 can be used to isolate Lgr5+ putative colonic epithelial stem cells in mice. Am J Physiol Gastrointest Liver Physiol. 2012;303(4):G443-52.
33. Mead TJ, Lefebvre V. Proliferation assays (BrdU and EdU) on skeletal tissue sections. Methods Mol Biol. 2014;1130:233-43.
34. Francisco AF, Jayawardhana S, Lewis MD, Taylor MC, Kelly JM. Biological factors that impinge on Chagas disease drug development. Parasitology. 2017:1-10.
35. Ferreira BL, Orikaza CM, Cordero EM, Mortara RA. Trypanosoma cruzi: single cell live imaging inside infected tissues. Cell Microbiol. 2016;18(6):779-83.
36. Mony BM, Matthews KR. Assembling the components of the quorum sensing pathway in African trypanosomes. Mol Microbiol. 2015;96(2):220-32.
37. Reuner B, Vassella E, Yutzy B, Boshart M. Cell density triggers slender to stumpy differentiation of Trypanosoma brucei bloodstream forms in culture. Mol Biochem Parasitol. 1997;90(1):269-80.
38. Rojas F, Silvester E, Young J, Milne R, Tettey M, Houston DR, et al. Oligopeptide Signaling through TbGPR89 Drives Trypanosome Quorum Sensing. Cell. 2019;176(1-2):306-17 e16.
39. Vassella E, Reuner B, Yutzy B, Boshart M. Differentiation of African trypanosomes is controlled by a density sensing mechanism which signals cell cycle arrest via the cAMP pathway. J Cell Sci. 1997;110 (Pt 21):2661-71.
40. Jansen AM, Madeira F, Carreira JC, Medina-Acosta E, Deane MP. Trypanosoma cruzi in the opossum Didelphis marsupialis: a study of the correlations and kinetics of the systemic and scent gland infections in naturally and experimentally infected animals. Exp Parasitol. 1997;86(1):37-44.
41. Pereira ME, Zhang K, Gong Y, Herrera EM, Ming M. Invasive phenotype of Trypanosoma cruzi restricted to a population expressing trans-sialidase. Infect Immun. 1996;64(9):3884-92.

Figure Legends

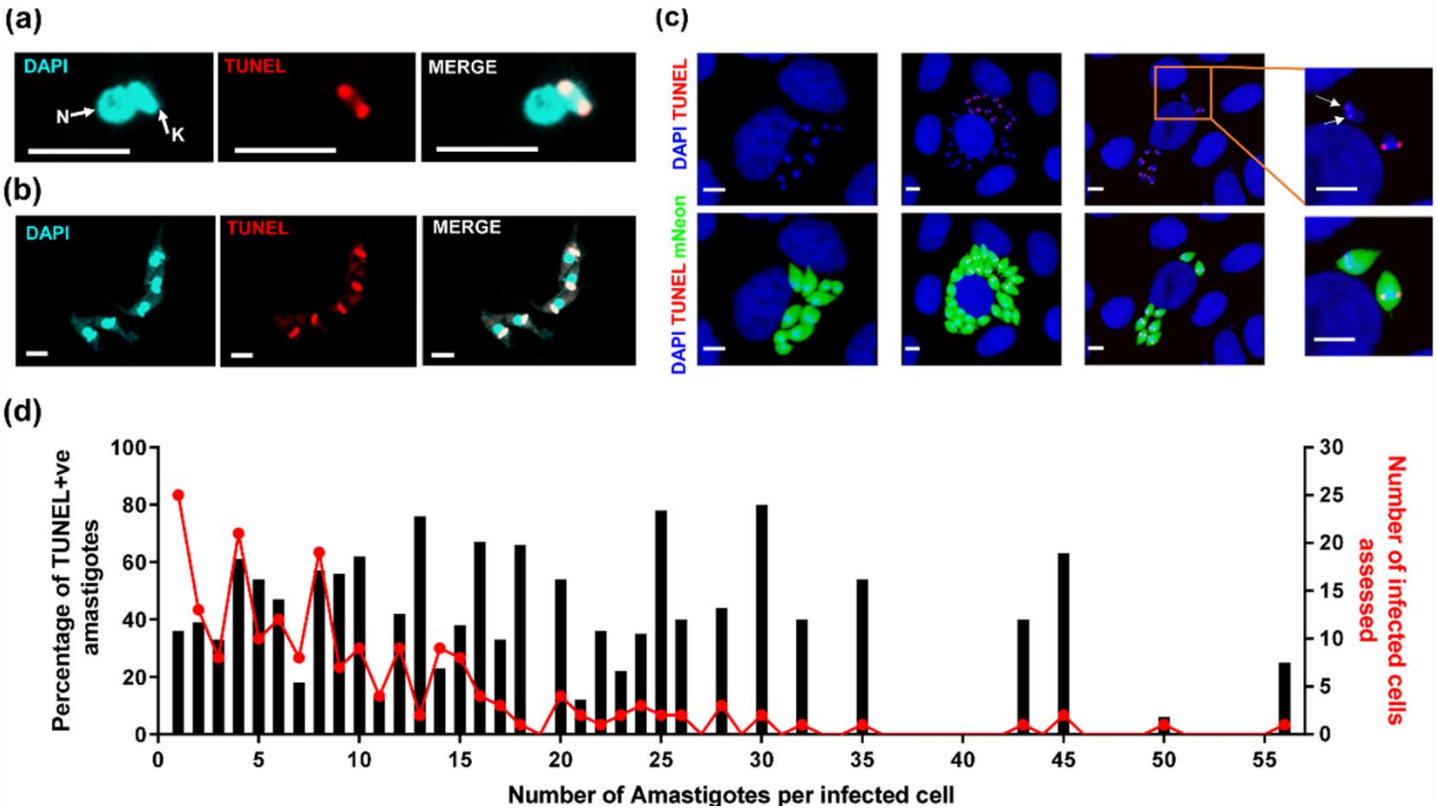

FIGURE 1 Kinetoplast replication of *T. cruzi* amastigotes is asynchronous *in vitro*. (a) Epimastigote at early stage of kDNA replication with TUNEL labelling of antipodal sites. (b) Epimastigotes at late stage of kDNA replication showing TUNEL labelling of entire kDNA disk. (c) MA104 cells infected with *T. cruzi* CL-Luc::Neon amastigotes for 72 hours then fixed and labelled with the TUNEL reagent. Left hand panel: cell containing 11 amastigotes with non-replicating kDNA (all TUNEL-ve); central panel: cell with parasites in which kDNA replication is asynchronous (mix of TUNEL+ve and TUNEL-ve); right hand panel: cell where all amastigotes are TUNEL+ve, but at different stages of kDNA replication (7 of 8 amastigotes display bright antipodal staining, the eighth is faintly TUNEL+ve, as shown by white arrows in the inset). (d) TUNEL data from 200 infected cells pooled from 3 replicate wells. The red line represents the number of infected cells assessed that contained the specified number of resident amastigotes. The black bars represent the percentage of amastigotes per cell that label as TUNEL+ve. Bar = 5 μm.

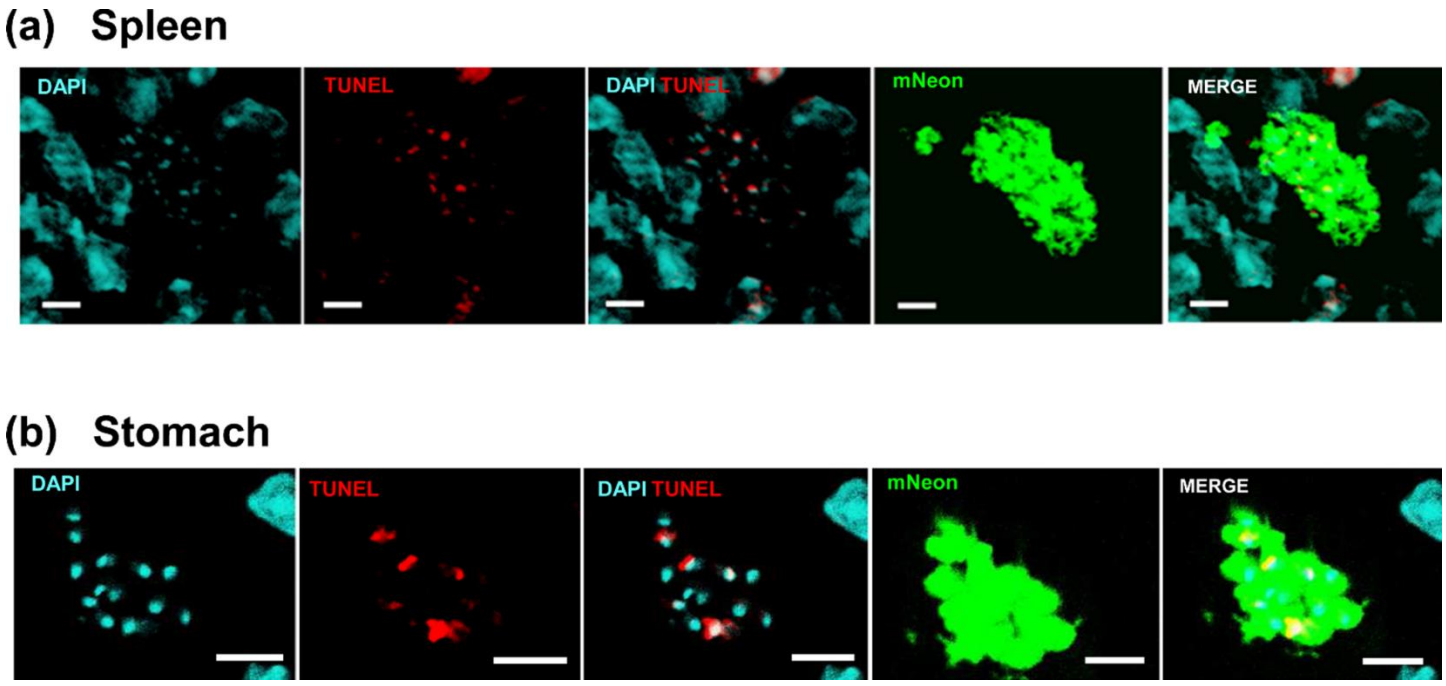

FIGURE 2 Asynchronous replication of parasite mitochondrial DNA within single infected host cells *in vivo* revealed by TUNEL assays. (a) Asynchronous replication of kDNA in intracellular parasites infecting mouse spleen cells during an acute stage infection (day 19). BALB/c mice were infected with *T. cruzi* CL-Luc::Neon and histological sections prepared from bioluminescent tissue (Experimental procedures). Parasites were detected by green fluorescence (mNeon), and the tissue sections subjected to TUNEL assays to highlight replicating kDNA (red). (b) Asynchronous replication of kDNA in an amastigote nest detected in the smooth muscle layer of stomach tissue during a chronic stage infection (day 117). Bar = 10 μm.

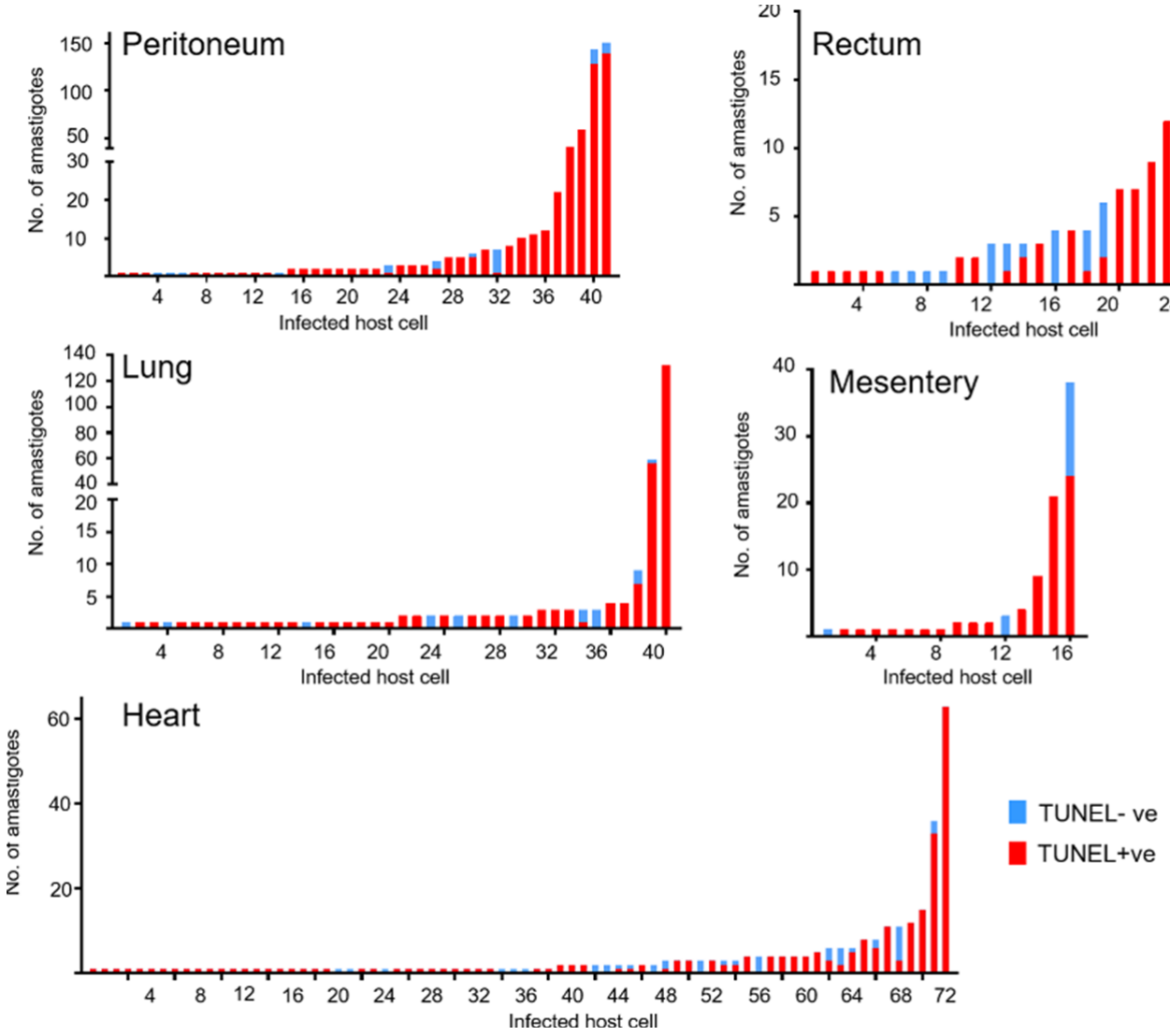

FIGURE 3 Quantification of TUNEL in BALB/c mice during the acute stage of infection with *T. cruzi* CL-Luc::Neon. Tissue sections from mice sacrificed on day 19 post-infection were processed for imaging and subjected to TUNEL staining (Experimental procedures). The graphs show the number of amastigotes that were TUNEL+ve (red) or TUNEL-ve (blue) in individual infected cells within the specified tissues. The x-axis refers to individual host cells. Bars containing both TUNEL-ve and +ve amastigotes were present in all tissues examined. Note that the level of TUNEL signal may vary between amastigotes within a given cell, so even bars that are red only may represent parasites at different stages of kDNA replication (c.f. differential levels of TUNEL staining in Figure 2a and b, DAPI/TUNEL panels).

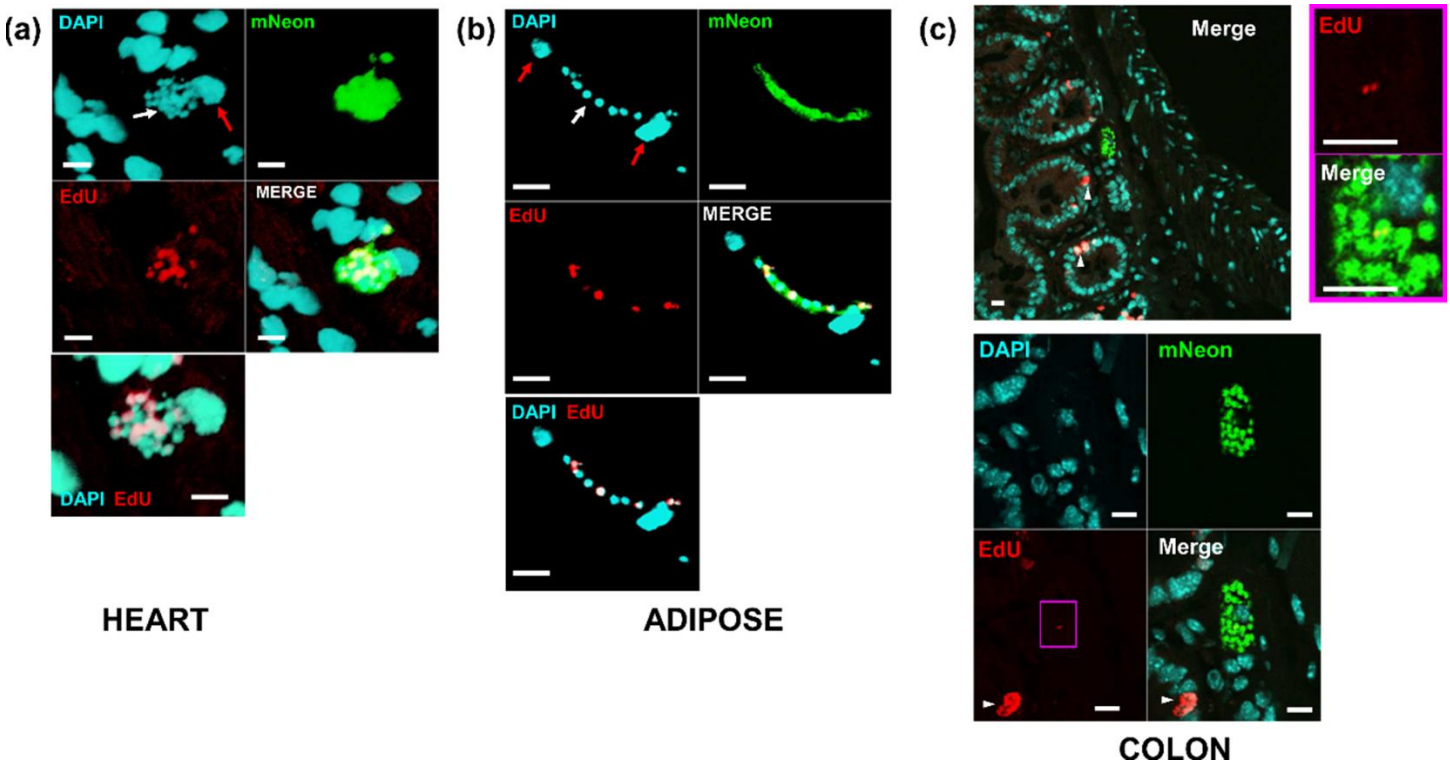

FIGURE 4 Asynchronous parasite DNA replication within single infected host cells *in vivo* revealed by EdU-labelling. Replication of parasite DNA within mice infected by *T. cruzi* clone CL-Luc::Neon was assessed after inoculating EdU (for (a) and (b), one pulse 6 hours prior to tissue sampling; for (c), two pulses 18 and 28 hours prior to tissue sampling (Experimental procedures). Parasite location in histological sections was detected by green fluorescence (mNeon). (a) DNA replication (EdU, red) in a parasite nest during an acute stage infection (heart tissue, day 15 post-infection). In the DAPI stained image, the white arrow indicates parasite nest, and red arrow the host cell nucleus. The merged DAPI/EdU image, bottom left, illustrates the heterogeneity in the DNA replication status of parasites within the nest. (b) DNA replication in parasites within adipose tissue (day 15 post-infection). Red and white arrows in the DAPI image identify host and parasite DNA, respectively. Combined EdU and DAPI image shows replicating parasites interspersed with non-replicating parasites. (c) Section from GI tract of mouse, upper panel shows image at low magnification – note the presence of some EdU+ve mammalian cells within the mucosal layer due to epithelial cell replacement (indicated by white arrowheads). Lower panels show magnified view of parasite nest. EdU signal in magenta box is shown in higher magnification to the right; note a single amastigote with EdU labelling at antipodal sites of kDNA replication. All other parasites in this nest are negative. Bars = 10 μm.

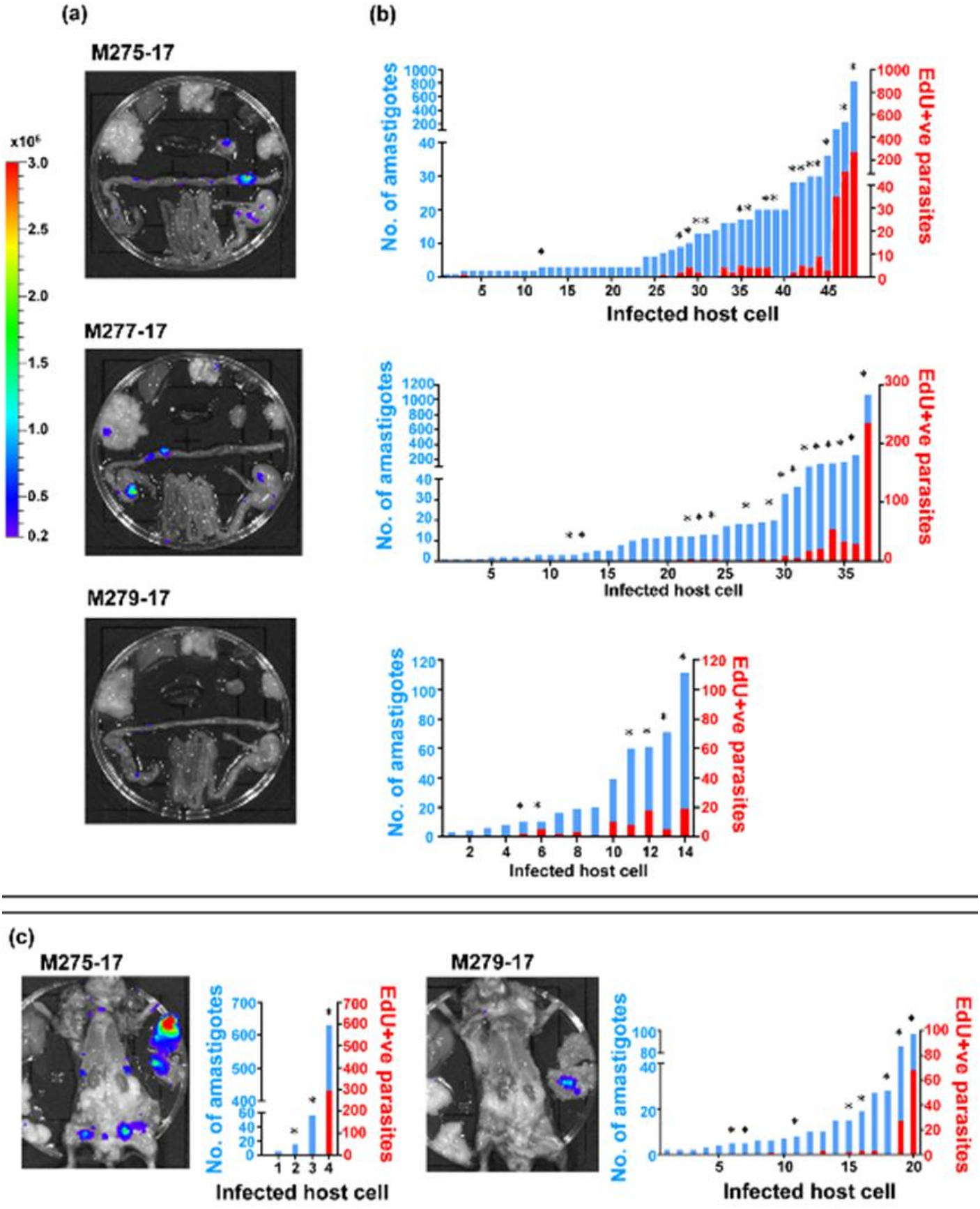
(a)
M275-17
x10⁶
3.0
2.5
2.0
1.5
1.0
0.5
0.2
M277-17
M279-17
(b)
No. of amastigotes
EdU+ve parasites
Infected host cell
(c)
M275-17
M279-17
No. of amastigotes
EdU+ve parasites
Infected host cell

FIGURE 5 EdU labelling reveals that cells infected with small numbers of amastigotes have a lower percentage of actively replicating parasites in a chronic infection. (a) *Ex vivo* imaging of organs. Bioluminescent foci were removed from the GI tract of three chronically infected C3H/HeN mice (day 211 post-infection) that had been injected with two pulses of EdU 18 and 28 hours prior to necropsy (Experimental procedures). (b) Each infected cell in the GI tract foci was imaged and the number of amastigotes that were positive or negative for EdU incorporation was quantified. The graphs show the total number of amastigotes in each cell (blue bars) and the number that were labelled with EdU (red bars). (c) Bioluminescent foci from the peritoneal muscle were also dissected, stained for EdU and quantified as above. Asterisks above bars indicate cells were the number of parasites represents a minimum due to the infected nest being larger than the z-dimension of the section.

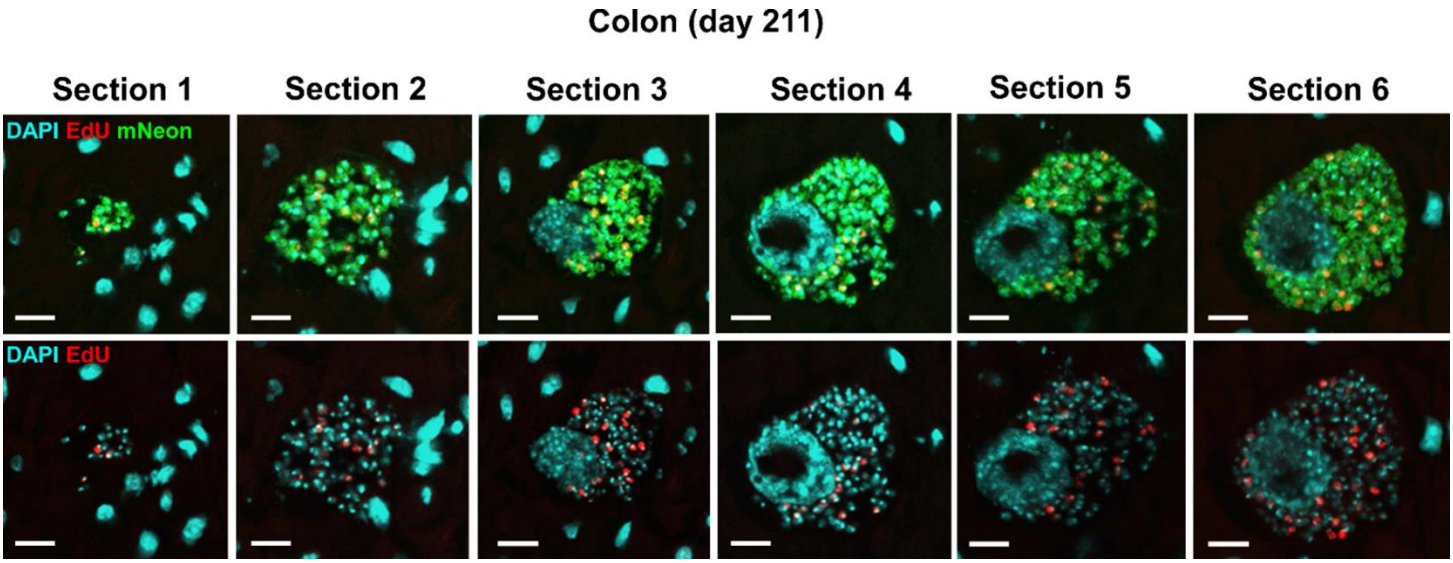

FIGURE 6 Large nests are present in the chronic stage of infection (C3H/HeN mouse, day 211) and show asynchronous EdU incorporation throughout. Images of the same nest taken from different sections through the tissue. The top row shows DAPI, EdU and mNeonGreen merged channels, whilst the lower row shows DAPI and EdU channels (for clarity). Bar = 10 μm. Note that sections are from the same infection focus but not all sections of this nest are included due to loss in processing.

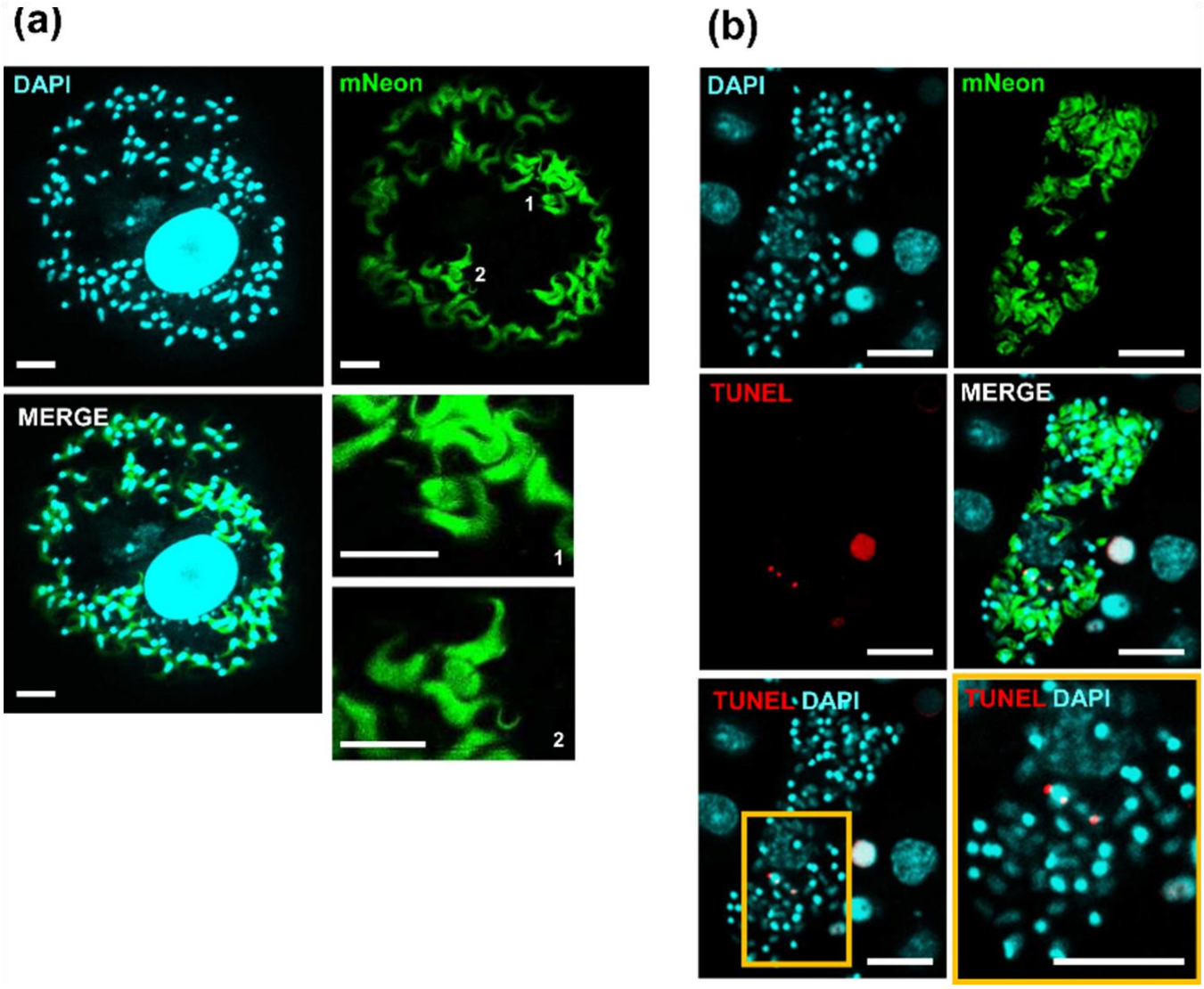

FIGURE 7 TUNEL assays indicate that amastigote replication and amastigote-to-trypomastigote differentiation can occur concurrently within single infected host cells *in vitro* and *in vivo*. (a) MA104 cells infected *in vitro* with *T. cruzi*. Two amastigotes (1 and 2) are visible within a cell full of trypomastigotes. The two lower right-hand panels show the two amastigotes at a higher magnification for clarity. (b) MA104 cells infected *in vitro* with *T. cruzi*. The cells were fixed 72 hours post-infection and subjected to a TUNEL assay. Two replicating amastigotes can be identified by antipodal TUNEL labelling on the kinetoplast, amongst a population of differentiated trypomastigotes. Bar = 10 μm.

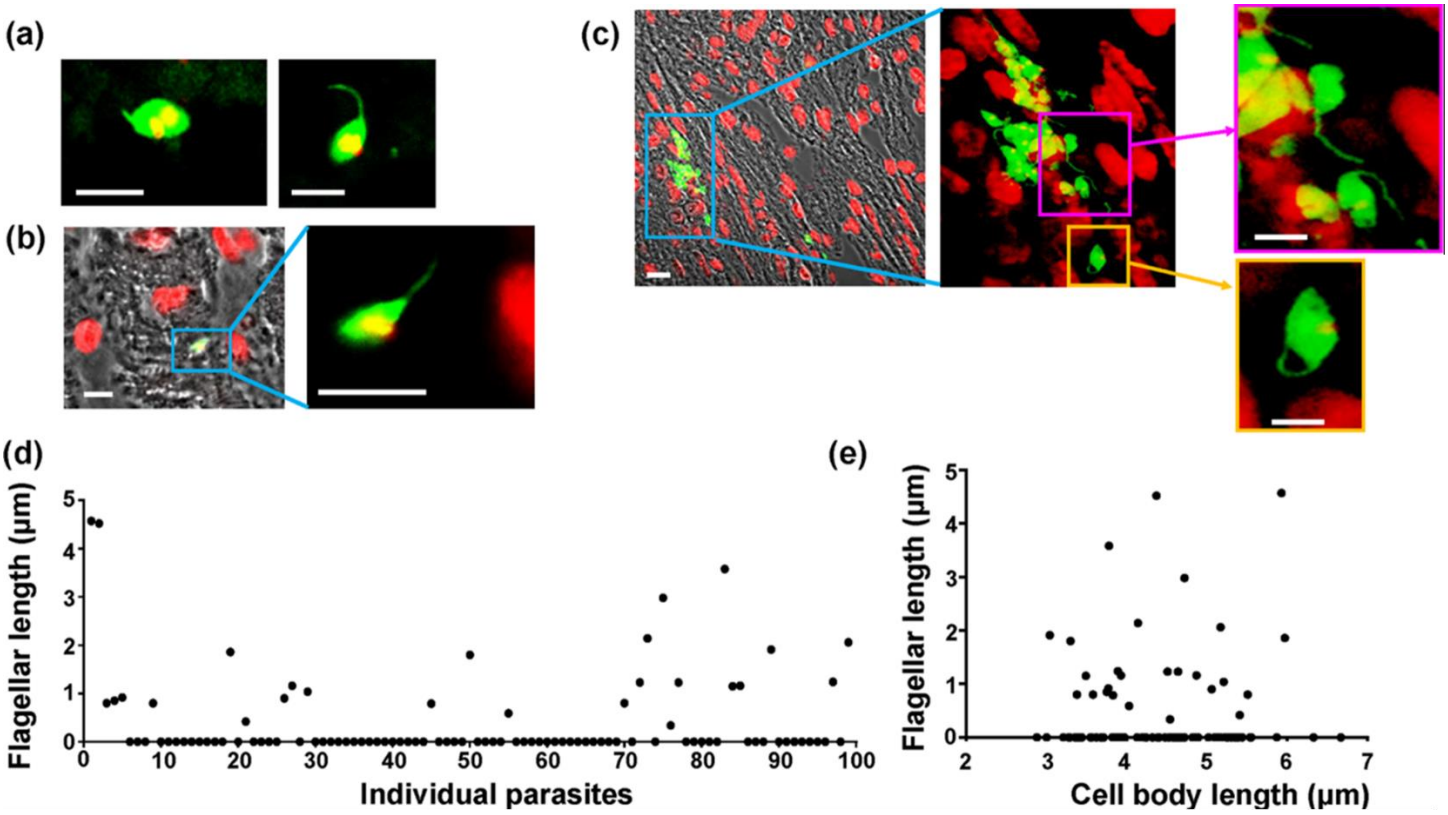

FIGURE 8 *T. cruzi* parasites display a wide range of morphologies during murine infections. BALB/c mice were inoculated with parasites expressing a fluorescent/bioluminescent fusion protein and infected tissues identified by *in vivo* bioluminescence imaging (Experimental procedures). Fluorescent (green) flagellated "amastigote" forms detected in (a) adipose tissue (day 13 post-infection) (DNA stained red – appears yellow where mNeon fluorescence overlaps DNA), and (b) cardiac tissue (day 19 post-infection). (c) Parasite nests in the rectum (day 19 post-infection) containing a variety of morphological forms. Note that none of the flagellated forms displays the posterior rounded kinetoplast characteristic of trypomastigotes. Bar = 5 µm. (d and e) The flagellar length was measured in 100 amastigote-like cells from various tissue sites, where parasites were distinct enough to measure both flagellum and cell body. (d) Graph showing the flagellar length (µm) measured in each individual amastigote. (e) Graph showing the flagellar length (µm) plotted against parasite body length (µm).

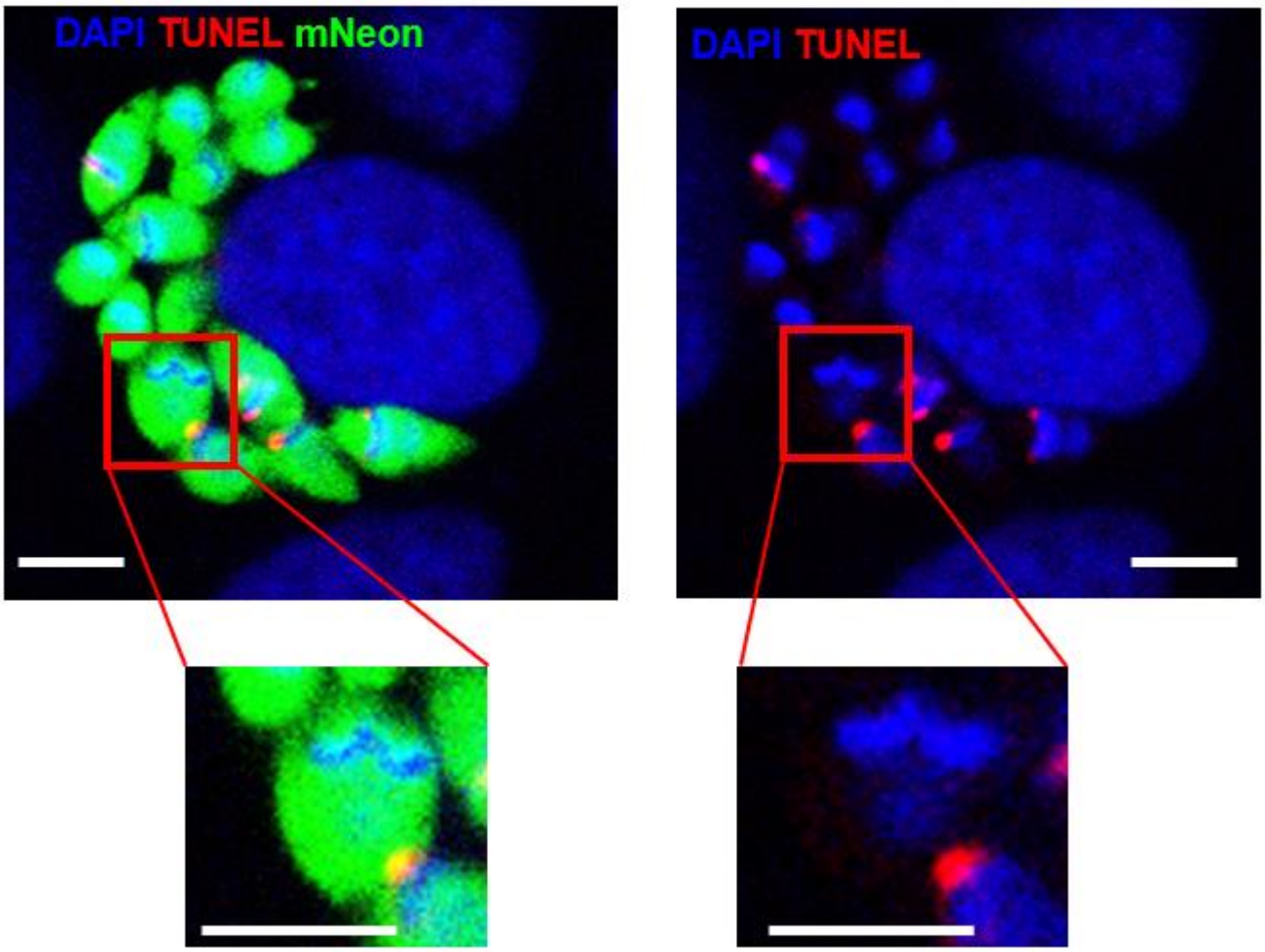

Figure S1 MA104 cells infected with *T. cruzi* CL-Luc::Neon amastigotes for 72 hours, fixed, then labelled with the TUNEL reagent. The parasite in the red box has completed kDNA replication and segregation, but not nuclear replication, and clearly shows that the segregated kinetoplasts no longer display TUNEL positivity.

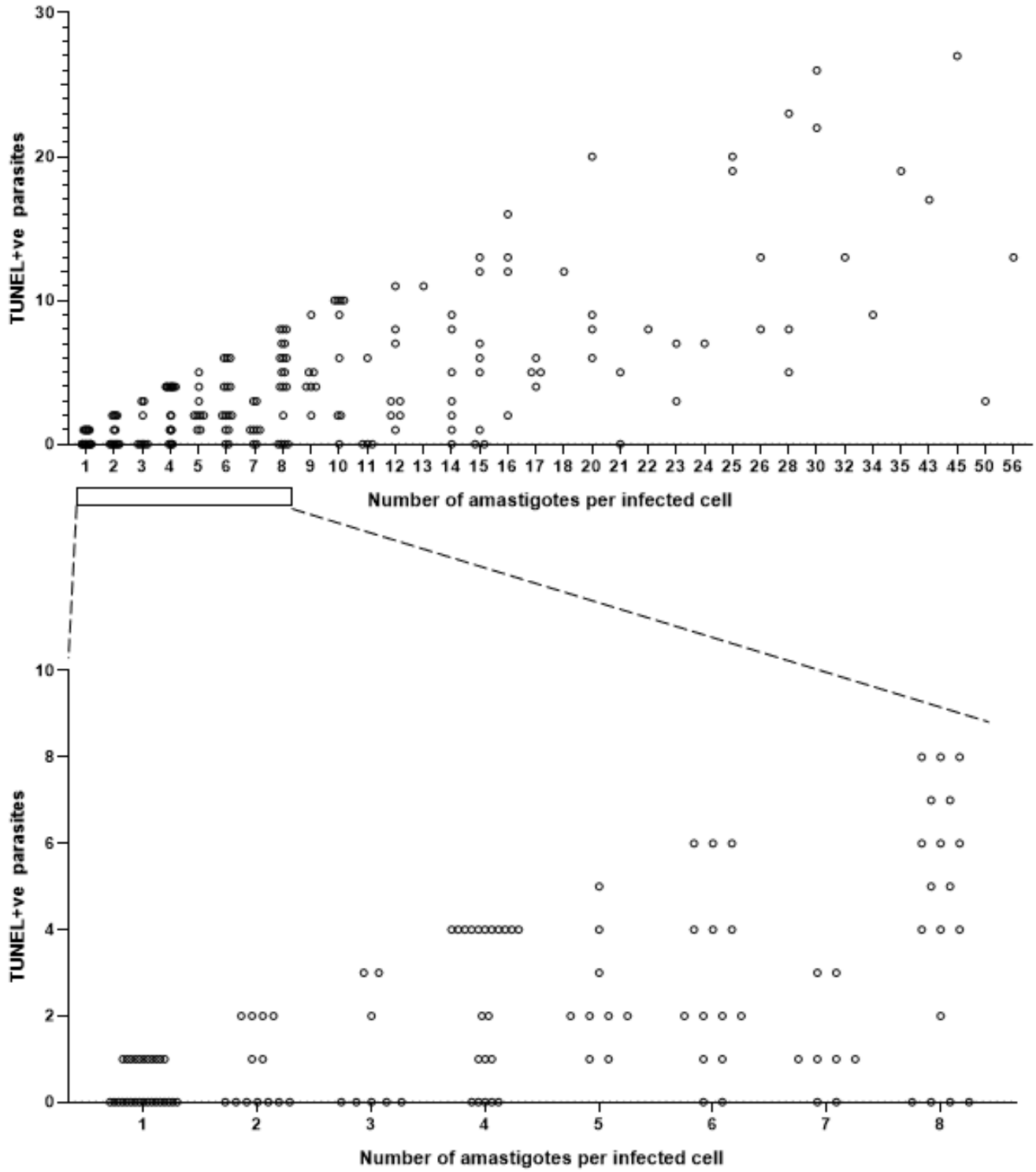

Figure S2 Plot of TUNEL+ve amastigote numbers as a function of total amastigotes present in an infected cell, for each infected cell used to derive Figure 1d. Each circle represents a single infected host cell. (a) All 200 infected cells from Figure 1d. (b) An expanded view of the area indicated by the box to allow clear visualisation of the host cell numbers. For cells infected with 1 amastigote, n=28.

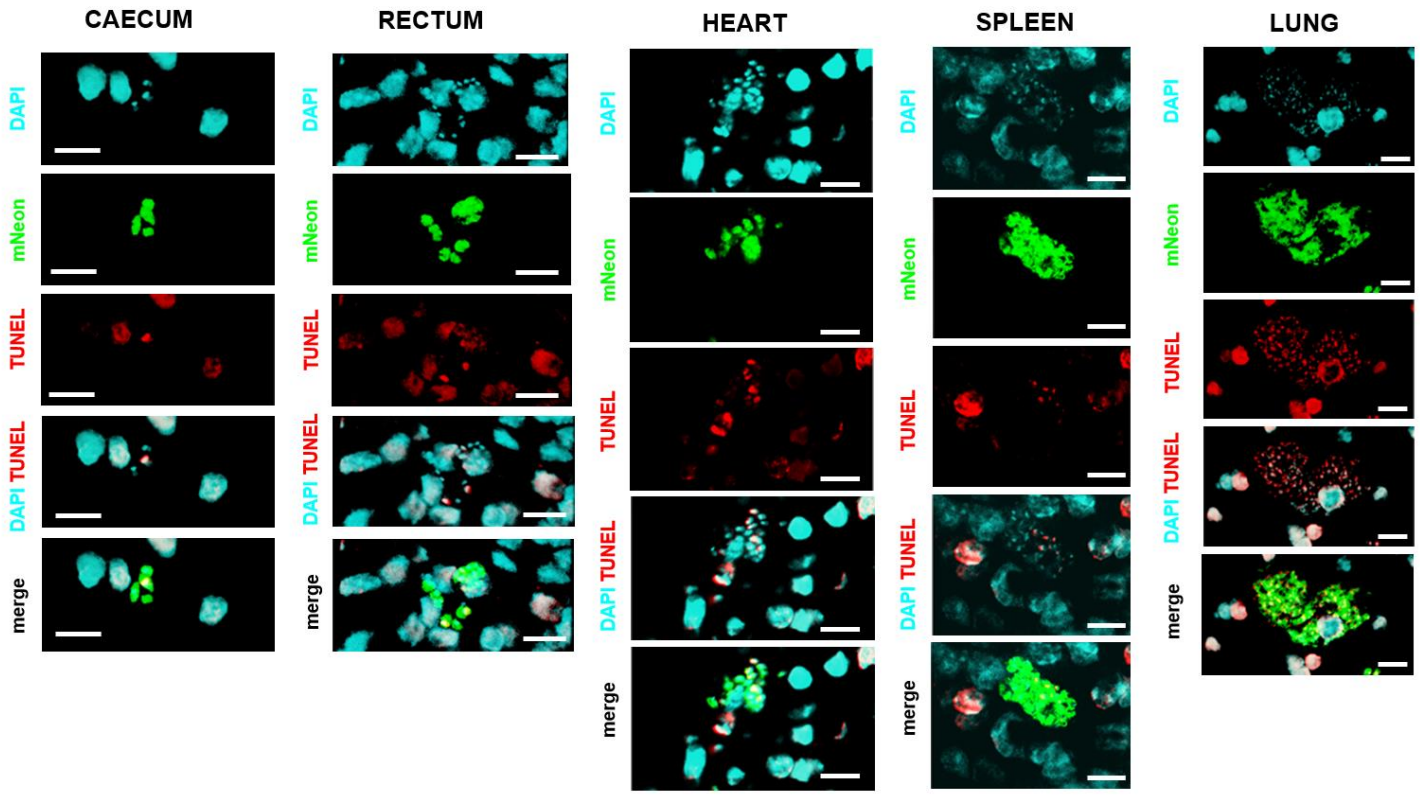

Figure S3 Asynchronous parasite kDNA replication within single infected host cells *in vivo* in acutely infected (19 days post infection) BALB/c mice revealed by TUNEL reactivity. (a) caecum, (b) rectum, (c) heart, (d) spleen and (e) lung. Images are from two individual mice. Bar = 10 μm

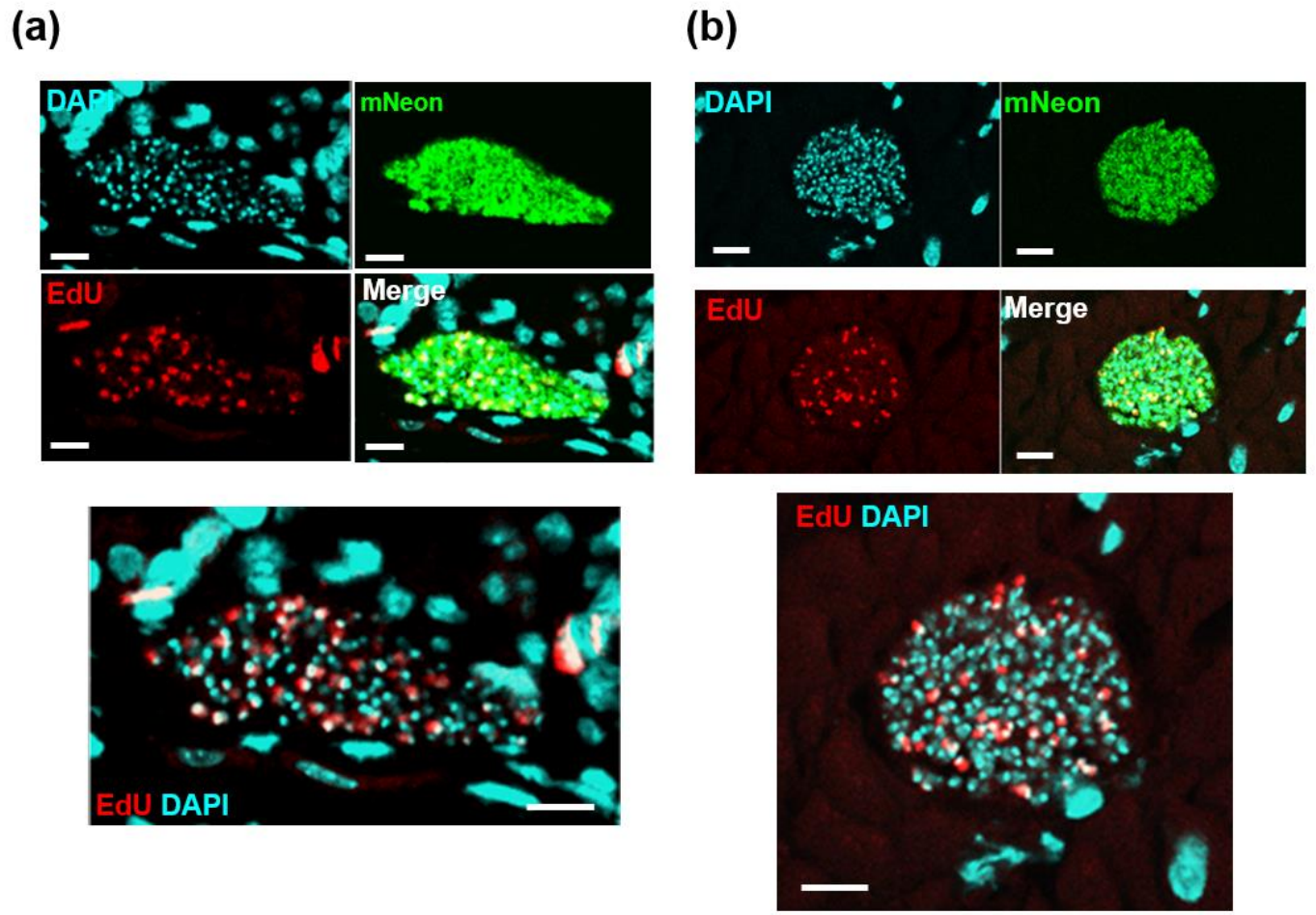

Figure S4 Asynchronous parasite DNA replication within single infected host cells in chronically infected (211 days post infection) C3H/HeN mice revealed by EdU-labelling. Replication of parasite DNA within mice infected by *T. cruzi* clone CL-Luc::Neon (Costa et al., 2018) was assessed after inoculating two EdU pulses 18 and 28 hours prior to tissue sampling (Experimental procedures). Parasites were located in histological sections by fluorescence (mNeon, green). a) DNA replication (red) in a chronic phase parasite nest (colon). The combined DAPI/EdU image illustrates the heterogeneity of parasite replication within the nest. Bar = 10 μm. b) Section from colon of mouse showing parasite nest. Upper panels show individual channels and a merged image. The lower panel shows DAPI and EdU channels only, allowing visualisation of the interspersed nature of EdU+ve amongst EdU-ve parasites. (a) and (b) are from different mice. Bars indicate 10 μm.

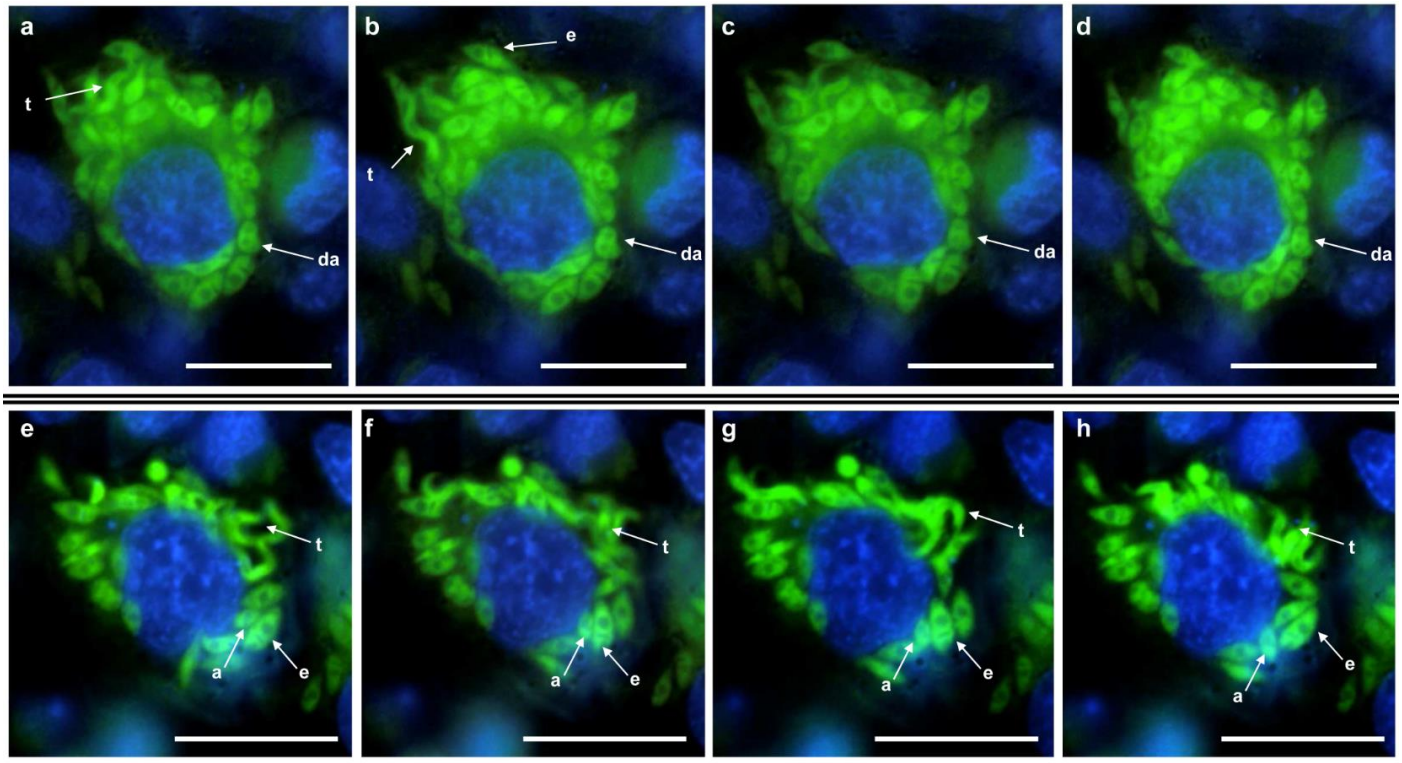

Fig S5 Multiple morphological forms within single infected cells. Each image shows an M104 cell (blue, nucleus) 6 days after infection with T. cruzi (green) showing dividing amastigotes (arrow a), epimastigote-like forms (arrow e) and trypomastigotes (arrow t) within the same cell. (a-d) sequential still images from Movie S1, (e-h) sequential still images from Movie S2

Movie S1 Multiple morphological forms within a single infected cell. Live cell imaging of an M104 cell 6 days after infection with *T. cruzi* showing dividing amastigotes, epimastigote-like forms and differentiating trypomastigotes within the same cell. See Figure S5 for locations of representative parasites for each morphotype. *Available on-line*

Movie S2 Multiple morphological forms within a single infected cell. Live cell imaging of an M104 cell 6 days after infection with *T. cruzi* showing dividing amastigotes, epimastigote-like forms and differentiating trypomastigotes within the same cell. See Figure S5 e-h for locations of representative parasites for each morphotype. *Available on-line*